



Climate Trends and Farmers' Perceptions in the Eastern Province of Rwanda

By

Rwema Michel

A Thesis submitted in fulfillment of the requirements for the degree of:
Doctor of Philosophy in Physics (Atmospheric and Climate Science)

Department of Physics
School of Science
College of Science and Technology
University of Rwanda

September 2025

Copyright

©2025 Rwema Michel

All rights reserved. No part of this publication may be produced, stored in a retrieval system or transmitted, in any form or by any means, electronic, mechanical, photocopying, recording or otherwise without prior permission from the author.

Declaration

I declare that this dissertation contains my work except where acknowledged, and it has been passed through the anti-plagiarism system and found to be compliant and this is the approved version of the PhD Thesis: *Climate Trends and Farmers' Perceptions in the Eastern Province of Rwanda*.



Rwema Michel, Reg N°:220018884

Date: 10/10/2025

Name, Registration Number and signature of the PhD candidate

The PhD Thesis Supervisory Team of Mr. Rwema Michel



Dr. Mouhamadou Bamba Sylla

Date: 10/10/2025

Name and signature of the Main Supervisor



Prof. Bonfils Safari

Date: 10/10/2025

Name and signature of the Co-supervisor

Dedication

This dissertation is dedicated to my wife, Naome, whose constant encouragement and steadfast support have been my deepest source of motivation. I also dedicate this work to my children, Meghan and Reagan, whose joyful spirit and inquisitive nature inspire me daily. Your patience and love have made this achievement possible, and I am endlessly thankful.

Acknowledgement

This research was conducted between 2021 and 2025, with key activities carried out at the University of Rwanda and during my visit to Lappeenranta-Lahti University of Technology (LUT) in Finland. I am deeply grateful to my primary supervisor, Dr. Mouhamadou Bamba Sylla, and my co-supervisor, Professor Safari Bonfils, for their dedicated guidance, insightful advice, and unwavering support throughout my doctoral journey. I also sincerely thank Professors Lassi Roininen and Marko Laine for their valuable supervision and collaboration during my time at LUT, as well as for their contributions as co-authors of my publications.

I extend my appreciation to the esteemed members of my dissertation committee, whose constructive feedback and thoughtful critiques have significantly enhanced the quality of my research. My gratitude also goes to the administrative and academic staff at the University of Rwanda for their reliable assistance that ensured a smooth and well-organized research experience.

I am thankful to my colleagues and friends across the University of Rwanda, the African Institute for Mathematical Sciences (AIMS), and the LUT for their encouragement and camaraderie throughout this journey. A special thanks to Dr. Charles Mberi Kimpolo for his inspirational mentorship and support.

I acknowledge the financial and institutional support provided by AIMS, LUT, and the Research Council of Finland, which were instrumental in facilitating my research activities and access to necessary resources.

Above all, I am profoundly grateful to my family for their unconditional love and encouragement. My deepest thanks go to my wife, Naome, and our children, Meghan and Reagan, whose patience, motivation, and understanding have been my greatest strength throughout this endeavor.

This work was funded by a grant from the African Institute for Mathematical Sciences, www.nexteinstein.org, with financial support from the Government of Canada provided through Global Affairs Canada (www.international.gc.ca), and the International Development Research Centre (www.idrc.ca): IDRC Grant No: 108246-001. LR and ML were funded by the Research Council of Finland (project numbers 353083, 353095, 321890).

Abstract

This dissertation presents a comprehensive assessment of climate trends and farmers' perceptions in Rwanda's Eastern Province by analyzing meteorological data from 1981 to 2021 alongside local knowledge gathered from farmer surveys. Employing robust statistical methods, the study investigates spatial and temporal variations in precipitation and temperature, characterizes drought dynamics, and examines smallholder farmers' awareness and adaptation strategies in response to ongoing climatic changes. Analyses of precipitation trends across 56 meteorological stations reveal a complex seasonal variability. During the March–May (MAM) season, 39 stations recorded declining rainfall trends, with eight stations in the southern part showing statistically significant decreases. Conversely, in the September–December (SOND) season, 31 stations exhibited declining rainfall, but with only one significant station, while increasing rainfall trends were observed at 25 stations in SOND, with one significant. Regionally, MAM rainfall trends showed a non-significant decrease, whereas SOND demonstrated a slight but non-significant increase. Notably, season duration expanded in SOND across 43 stations, attributed primarily to earlier onset dates, which showed significant decreasing trends at 41 stations. The timing of trend change points generally clustered between 2000 and 2020, coinciding with critical shifts in regional agroclimatic conditions that have influenced cropping practices and heightened crop failure risks. Concurrently, temperature trend analysis highlights substantial warming, especially in minimum and mean temperatures. The annual minimum temperature increased significantly by 2.95 °C (95% CI: 1.64–4.45 °C), with the June–August season showing the greatest rise of 3.37 °C (1.75–4.81 °C). Mean temperature rose by 1.87 °C regionally (0.61–3.19 °C), while maximum temperature changes were not statistically significant. Temporal trends exhibited non-linear behavior, with a plateau in warming from 1990 to 2010, followed by accelerated increases post-2010. Among the identified climatic zones, Northwestern, Central, and Southeastern, the Northwestern zone experienced the most pronounced temperature rise, particularly in seasonal minimum temperatures, underscoring its heightened vulnerability to climate-related stressors. Drought analyses

reveal an intensification of frequency, duration, and severity since 2010, with geographic variability intimating complex underlying environmental drivers. The Central zone exhibited the highest drought frequency, whereas the Northwestern and Southeastern zones displayed distinct patterns of short- and long-term drought extremes. Complementing the climatic assessment, a socio-environmental inquiry involving 204 farmers across five districts of the Eastern Province examined perceptions, indigenous knowledge, and adaptive responses. The majority (85%) acknowledged the reality of climate change, with over half observing rising temperatures (54%) and nearly 40% noting decreased rainfall.

These perceptions are closely aligned with observed meteorological data, reinforcing the reliability of local knowledge systems. Farmers attributed climate change primarily to deforestation, linking it to adverse outcomes such as crop failures, yield reduction, and food shortages. Adaptation strategies employed were diverse, including agroforestry, crop varietal changes, and fertilizer use; however, financial constraints, lack of access to information, and limited availability of inputs present major obstacles to widespread adoption. Importantly, indigenous forecasting methods based on meteorological indicators remain a vital resource for many, enhancing decision-making despite limited formal education among respondents. This integrated analysis elucidates the multifaceted nature of climate change impacts in Eastern Rwanda, revealing significant shifts in climate drivers alongside tangible effects on vulnerable farming communities. The findings emphasize the importance of incorporating localized indigenous knowledge into adaptation planning and underscore the need for supportive policies that address both environmental changes and socioeconomic barriers. Together, these results provide an essential foundation for developing targeted resilience-building initiatives that foster sustainable agricultural practices and improve livelihoods amid evolving climatic challenges.

Keywords: Climate change, Climate trends, Farmer perception, Adaptation strategies, Eastern Rwanda

List of symbols, acronyms and abbreviations

ACF: Autocorrelation Function

CHIRPS: Climate Hazards Group InfraRed Rainfall and Stations

CPC: Climate Prediction Centre

CRU: Climatic Research Unit

DLM: Dynamic Linear Model

EA: East Africa

ENACTS: Enhancing National Climate Services

ENSO: El Niño-Southern Oscillation

GDP: Gross Domestic Product.

GIS: Geographic Information Systems

IOD: Indian Ocean Dipole

ITCZ: Inter-tropical Convergence Zone

JF: January-February

JJA: June-July-August

LM: Linear Model

MAE: Mean Absolute Error

MAM: March-April-May (MAM)

METEO-RWANDA: Rwanda Meteorology Agency

MCMC: Markov chain Monte Carlo

MK: Mann–Kendall

NOAA: National Oceanic and Atmospheric Administration

ODK: Open Data Kit

PET: Potential Evapotranspiration

PhD: Doctor of Philosophy

r: Pearson correlation coefficient

REMA: Rwanda Environment Management Authority

RKT: Regional Kendall test

RMSE: Root Mean Square Error

SI: Supporting Information

SMKRS: Sequential Mann-Kendall Rank Statistic

SOND: September-October-November-December

SPI: Standardised Precipitation Index

SPSS: Statistical Package for Social Sciences

T: Mean temperature

T_n: Minimum temperature

T_x: Maximum temperature

°C: Degree Celsius

°C/decade: Degree Celsius per decade

mm: Milimeter

mm·day⁻¹: Milimeter per day

mm/decade: Milimeter per decade

R^2 : R-squared

σ^2 : variance

X^2 : Chi-squared

Table of Content

Copyright	i
Declaration	ii
Dedication	iii
Acknowledgement.....	iv
Abstract	v
List of symbols, acronyms and abbreviations	vii
Table of Content	ix
List of figures	xiii
List of tables	xvi
List of publications	xvii
Chapter 1 General introduction and thesis outline	1
1.1 Introduction	1
1.2 Status of Rainfall Variability and Trends in Rwanda.....	1
1.3 Temperature Trends and Microclimatic Diversity.....	2
1.4 Drought Incidence, Distribution, and Evolution	2
1.5 Farmers' Perceptions, Knowledge, and Adaptation Strategies.....	3
1.6 Methodological Approaches in Climate Trend Analysis.....	3
1.7 Statement of the Research Problem.....	5
1.8 Motivation and Significance of the Research.....	5
1.9 Objectives of the research.....	6
1.10 Outline of the thesis	7
1.11 Reference	7
Chapter 2 Trend analysis and change point detection in precipitation time series over the Eastern Province of Rwanda during 1981-2021	13
2.1 Introduction	13
2.2 Data and Methodology	15

2.2.1 Study area and data.....	15
2.2.2 Method for data analysis.....	17
a. Variables considered	17
b. Trends calculation	19
c. Trend magnitude	19
d. Change point identification	20
2.3 Results and Discussion	21
2.3.1 Trends Analysis.....	21
a. Regional scale trends.....	21
b. Rainfall amount and number of rainy days at station level	25
c. Seasonal rainfall event classes.....	29
d. Onset and cessation dates of the season and season duration.....	34
2.3.2 Change points of significant trends.....	38
2.4 Conclusion	43
References	44
Chapter 3 Trends and Variability of Temperatures in the Eastern Province of Rwanda	56
3.1 Introduction	56
3.2 Data and Methods.....	59
3.2.1 Study area and data.....	59
3.2.2 Methods	61
a. Microclimatic zone identification.....	61
b. The dynamic linear model for trend analysis	63
c. Goodness-of-Fit Test.....	66
3.3 Results	67
3.3.1 Spatial Distributions of Long-Term Mean Temperature and Rainfall	67
3.3.2 K-means clustering.....	69
3.3.3 Near Homogeneous zones	72
3.3.4 Goodness-of-Fit.....	73
3.3.5 Trends and Variability in Temperatures	74
3.4 Discussion	79

3.5 Conclusion	82
1 Goodness-of-Fit	85
References	120
Chapter 4 Climate-induced drought characteristic estimate in the Eastern region of Rwanda	136
4.1 Introduction	136
4.2 Methodology	137
4.2.1 Drought index calculation with SPI	137
4.3 Results	138
4.3.1. Incidence and Categories of Drought Events	138
4.3.2. Drought Episodes, Duration, and Severity	138
4.3.3. Temporal Distribution and Evolution of Droughts	139
4.3.4 Comparison of First and Last 21 Years	140
4.4 Discussion	141
References	142
Chapter 5 Understanding Farmers’ Knowledge, Perceptions, and Adaptation Strategies to Climate Change in Eastern Rwanda	145
5.1 Introduction	145
5.2 Materials and Methods	147
5.2.1. Study Area	147
5.2.2. Sample(s)	149
5.2.3. Data Type and Data Collection Approach	151
a. Climate Data Analysis.....	154
b. Farmers’ Field Data Analysis.....	154
5.3. Results	156
5.3.1. Changes in Temperature and Rainfall Events in Eastern Province	156
5.3.2. Socioeconomic Characteristics of Respondent Farmers	157
5.3.3. Farmers’ Knowledge of Weather and Climate Change	160
5.3.4. Respondent Farmers’ Perceptions of Climate Change	162
5.3.5. Respondent Farmers’ Perceptions of the Impacts of Climate Change	164

5.3.6. Climate Change Adaptation Strategies	165
5.3.7. Barrier to the Effective Adaptation to Climate Change	166
5.3.8. Socioeconomic Factors Influencing Farmers' Choice of Adaptation Strategies...	166
5.4. Discussion	170
5.5. Conclusions	175
References	182
Chapter 6 Conclusion and Future Directions	193

List of figures

Figure 2.1 Rwanda Map with Eastern province boundary highlighted with solid black line (a) and Eastern Province with locations of meteorological stations highlighted in red (b).....	17
Figure 2.2 Time series of rainfall for MAM (a) and SOND (b), Onset for MAM (c) and SOND (d), and Cessation for MAM (e) and SOND (f) seasons at the Eastern regional scale from 1981-2021.....	23
Figure 2.3 Spatial distribution of trends' slope (mm/day/year) for MAM rainfall (a), and SOND rainfall (b) for the period of 1981 to 2021. The black circles on the maps show the locations of stations with significant trends (at $\alpha=0.05$) from the Mann-Kendall and Sen's Slope tests.	27
Figure 2.4 Spatial distribution of trends' slope for MAM (a) and SOND (b) number of rainy days for the period of 1981 to 2021. The black circles on the maps show the locations of stations with significant trends (at $\alpha=0.05$) from the Mann-Kendall and Sen's Slope tests.....	29
Figure 2.5 Spatial distribution of trends' slope for MAM Light rainy days (a), MAM Moderate rainy days (b), and MAM Heavy rainy days (c) for the period of 1981 to 2021. The black circles on the maps show the locations of stations with significant trends (at $\alpha=0.05$) from the Mann-Kendall and Sen's Slope tests.	31
Figure 2.6 Spatial distribution of trends' slope for SOND Light rainy days (a), SOND Moderate rainy days (b), and SOND Heavy rainy days (c) for the period of 1981 to 2021. The black circles on the maps show the locations of stations with significant trends (at $\alpha=0.05$) from the Mann-Kendall and Sen's Slope tests.	33
Figure 2.7 Spatial distribution of trends' slope for MAM (a) and SOND (b) onset days for the period of 1981 to 2021. The black circles on the maps show the locations of stations with significant trends (at $\alpha=0.05$) from the Mann-Kendall and Sen's Slope tests.....	35
Figure 2.8 Spatial distribution of trends' slope for MAM (a) and SOND (b) cessation days for the period of 1981 to 2021. The black circles on the maps show the locations of stations with significant trends (at $\alpha=0.05$) from the Mann-Kendall and Sen's Slope tests.....	36
Figure 2.9 Spatial distribution of trends' slope for MAM (a) and SOND (b) season duration for the period of 1981 to 2021. The black circles on the maps show the locations of stations with significant trends (at $\alpha=0.05$) from the Mann-Kendall and Sen's Slope tests.....	37

Figure 3.1 Geographical location of the study area. Panel (a) displays the study area highlighted in grey on the map of Rwanda, while panel (b) features a topographic map illustrating the area's elevation and terrain. 60

Figure 3.2 Spatial distribution of the long-term mean of Temperature ($^{\circ}\text{C}$) over Eastern Rwanda for January-February (JF) (a), March-April-May (MAM) (b), June-July-August (JJA) (c), September-October-November-December (SOND) (d), and Annual (e) during the period of 1983–2021 (Source of data: Rwanda Meteorology Agency). 69

Figure 3.3 The Elbow plot shows the optimal cluster number with the vertical dotted line showing the Elbow joint corresponding to the chosen number of clusters ($k=3$). 70

Figure 3.4 Maps of clustered zones by number of clusters (k). This figure shows the partition of Eastern Province for different cluster counts: (a) $k=2$, (b) $k=3$, (c) $k=4$, and (d) $k=5$. It demonstrates how the regional partitioning changes as the number of clusters increases, revealing patterns of spatial organisation and cluster stability. 71

Figure 3.5 Climatic zone classification of the Eastern Province based on temperature and rainfall data for 1983-2021. The identified three near-homogeneous zones named Zone1: Northwestern, Zone2: Central, and Zone3: Southeastern are highlighted in green, yellow, and magenta, respectively. 73

Figure 3.6 DLM fit for yearly average temperature during 1983-2021. The observed yearly average temperature (black dots) is displayed together with the background mean level μt (black solid line). The smooth black solid line represents the estimated temperature trend together with a 95 % probability envelope. The dashed blue line is the linear trend. The Z1, Z2, and Z3, respectively, stand for the Northwestern, Central, and Southeastern zones. The bottom panel in each column indicates the results obtained from the east. 78

Figure 4.1 Temporal variation of the Standardized Precipitation Index (SPI-3) from 1981 to 2021 across three micro-climate zones in the Eastern Province of Rwanda: (a) Northwestern zone: Zone 1 SPI-3, (b) Central zone: Zone 2 SPI-3, and (c) Southeastern zone: Zone 3 SPI-3. Red bars indicate periods of drought, while blue bars represent wet conditions. 140

Figure 4.2 Temporal variation of the Standardized Precipitation Index (SPI-6) from 1981 to 2021 across three micro-climate zones in the Eastern Province of Rwanda: (a) Northwestern zone: Zone 1 SPI-6, (b) Central zone: Zone 2 SPI-6, and (c) Southeastern zone: Zone 3 SPI-6. Red bars indicate periods of drought, while blue bars represent wet conditions. 140

Figure 4.3 Comparison of drought characteristics (episode, duration (in the month), and severity) of the periods 1981-2001 and 2001-2021 using the Standardized Precipitation Index (SPI-3 and SPI-6) across three micro-climate zones in the Eastern Province of Rwanda: (a–b) Zone 1, (c–d) Zone 2, and (e–f) Zone 3. Black bars represent data from the period 2001–2021, while the white bars indicate the period from 1981–2001.....	141
Figure 5.1 Eastern Province map with the surveyed participants’ location highlighted with purple dots.	149
Figure 5.2 Conceptual framework illustrating the process of farmers’ climate change adaptation. The framework shows how socioeconomic characteristics and knowledge of weather and climate change influence farmers’ perceptions and observed impacts, which in turn shape adaptation strategies. Barriers to adaptation are also depicted as factors that constrain or modify the effectiveness of these strategies.	154
Figure 5.3 Farmers’ knowledge about causes or reasons for climate change ($n = 204$).	162
Figure 5.4 Respondent farmers’ perception of change in temperature and drought pattern ($n = 204$).....	163
Figure 5.5 Respondent farmers’ perceptions of change in the MAM season rainfall pattern...	164
Figure 5.6 Respondent farmers’ perceptions of change in the SON/D season rainfall pattern. .	164
Figure 5.7 Percentage (%) of respondent farmers who perceived the impacts of climate change ($n = 204$).....	165

List of tables

Table 2.1 Variables considered and their definitions	18
Table 2.2 Identified trends' slope values at the Eastern regional scale	25
Table 2.3 Identified significant change points in climate variables at the Eastern regional scale	25
Table 2.4 Identified change points for significant trends	41
Table 3.1 Changes (in °C) and standard deviations of the averaged seasonal and annual mean of Tx, Tn, and T in Northwestern, Central, and Southeastern zones and the whole Eastern Province of Rwanda during the period 1983-2021	75
Table 4.1 Frequency of different drought categories in 3-month and 6-month SPI from 1981-2021 in three micro-climate zones of the Eastern Province.	138
Table 4.2 Drought quantities for the 1981–2021 period.....	139
Table 5.1 Farmers' distribution in districts, sectors, and cells.	151
Table 5.2 Displays changes (in °C/decade) with a 95% confidence interval in brackets [] for the averaged seasonal and annual means of Tx, Tn, and T in the Eastern Province of Rwanda from 1983 to 2021.....	157
Table 5.3 Slope value of identified trends for rainfall events at the Eastern regional scale. The * in the results indicates that significant regional trends are observed at a 95% confidence level.	157
Table 5.4 Socioeconomic characteristics of respondents ($n = 204$).	158
Table 5.5 Climate indicators associated with farmers' knowledge about rainy season onset and cessation ($n = 204$).	161
Table 5.6 Climate change adaptation strategies adopted by respondent farmers ($n = 204$).	165
Table 5.7 Barriers to the effective adaptation of climate change by respondent farmers ($n = 204$).	166
Table 5.8 Analysis of the models' significance and goodness of fit.	167
Table 5.9 Logistic regression results: odds ratio (OR) and 95% confidence interval showing socioeconomic factors influencing farmers' choice of selected adaptation strategies.	169

List of publications

This dissertation is article-based and comprises three published journal articles and one draft manuscript. Details about these publications and their contributions to the respective chapters of the dissertation are outlined below.

1. Published article: Rwema, M., Sylla, M.B., Safari, B., Roininen, L., & Laine, M. (2025). Trend analysis and change point detection in precipitation time series over the Eastern Province of Rwanda during 1981-2021, *Theoretical and Applied Climatology*. 156, 98. <https://doi.org/10.1007/s00704-024-05317-7> (Chapter 2)
2. Published article: Rwema, M., Safari, B., Laine, M., Sylla, M.B., & Roininen, L. (2025). Trends and Variability of Temperatures in the Eastern Province of Rwanda, *International Journal of Climatology*. 45, e8793. <https://doi.org/10.1002/joc.8793> (Chapter 3)
3. Drafted manuscript: Rwema, M., Sylla, M.B., Safari, B., Roininen, L., & Laine, M. Climate-induced drought characteristic estimate in the Eastern region of Rwanda (Chapter 4)
4. Published article: Rwema, M., Safari, B., Sylla, M.B., Roininen, L., & Laine, M. (2025). Understanding Farmers' Knowledge, Perceptions, and Adaptation Strategies to Climate Change in Eastern Rwanda. *Sustainability*. 17, 6721. <https://doi.org/10.3390/su17156721> (Chapter 5)

Chapter 1 General introduction and thesis outline

1.1 Introduction

Climate change has become a central issue of global concern, with its impacts increasingly evident across diverse regions and sectors. Since the pre-industrial era, the concentration of greenhouse gases in the atmosphere has risen sharply, primarily due to anthropogenic activities such as fossil fuel combustion and deforestation, leading to significant changes in climate variables worldwide (IPCC 2023a). These changes are manifested through shifts in temperature and precipitation patterns, increased frequency and intensity of extreme weather events, and widespread effects on ecosystems and human livelihoods (IPCC 2023b).

Globally, agriculture and water resources are among the sectors most vulnerable to climate variability and change (IPCC 2023b). This vulnerability is particularly pronounced in the Global South, where agriculture is predominantly rain-fed and forms the backbone of many economies (Adger et al. 2003). In sub-Saharan Africa, and especially in Eastern Africa, the combination of high climate variability, limited adaptive capacity, and the predominance of smallholder agriculture heightens vulnerability to climate-related hazards (Adger et al. 2003; Kew et al. 2021; Thornton et al. 2014). In addition, high dependence on ecosystem goods for livelihoods intensifies the continent's susceptibility to climate change impacts (IPCC 2023b; WMO 2019). Rwanda, situated in this region, exemplifies these challenges: agriculture accounts for a significant share of the country's GDP. It provides employment for the majority of the population, with smallholder farmers contributing around 75% of total production (NISR 2023).

1.2 Status of Rainfall Variability and Trends in Rwanda

In regions where agriculture heavily depends on rainfall, such as Rwanda, the timing, intensity, and duration of rainy seasons are critical determinants of agricultural productivity. Any shifts in these rainfall characteristics can significantly impact crop yields and food security. Variations in total precipitation, seasonal distribution, and inter-annual variability pose considerable risks to rain-fed agriculture, underscoring the importance of understanding and monitoring these patterns. Given that the majority of smallholder farmers in Rwanda rely on rain-fed systems, evolving rainfall variability and trends carry direct socio-economic consequences and play a vital role in shaping effective adaptation strategies.

Climate studies in Rwanda have often focused on broad national or regional scales, producing mixed findings regarding rainfall trends. For example, Ntirenganya (2018), analyzing data from 15 meteorological stations across the country, found no statistically significant national rainfall trend. However, more localized investigations, such as the study by Sebaziga et al. (2020), which examined nine stations from 1981 to 2016, revealed a significant decline in rainfall during the March–April–May (MAM) season specifically in the Eastern Province. Likewise, Rwanyiziri and Rugema (2013) reported decreasing annual rainfall and increased rainfall variability in the Bugesera district using data from a single station. Similar challenges have been documented in neighboring Uganda, which shares a border with Rwanda’s Eastern Province; studies there have noted increasing rainfall variability and related adverse effects on smallholder agriculture (Mubiru et al. 2018). These regional parallels highlight the critical importance of localized climate analyses, such as the present study focusing on Eastern Rwanda, to support targeted and context-specific adaptation strategies.

1.3 Temperature Trends and Microclimatic Diversity

Temperature trends in Rwanda have generally shown an increase in mean, minimum, and maximum values, with regional differences driven by topography (Safari and Sebaziga 2023). Recent studies have consistently reported significant warming trends across Rwanda. Using data from five meteorological stations, Safari (Safari 2012) found an increasing trend in annual mean temperature since 1977, with Kigali city exhibiting the highest rate at 0.045 °C per year. Mohammed et al. (2016), analyzing six stations nationwide for the period 1964–2010, also identified a marked rise in air temperatures. More recently, gridded analyses for 1983–2022 have shown a continued rise in minimum temperatures and a greater frequency of warm nights and days across the country (Safari and Sebaziga 2023). Sebaziga et al. (Safari and Sebaziga 2023) highlighted the importance of microclimate conditions in explaining spatial and temporal variability, underscoring the need for more granular studies in the region (Rwema et al. 2025a).

1.4 Drought Incidence, Distribution, and Evolution

Drought is commonly defined as a prolonged period of abnormally low precipitation that leads to a water shortage affecting natural ecosystems, agriculture, and human activities (Wilhite and Glantz 1985). It is a complex and multifaceted hazard that varies in intensity, duration, and spatial extent, often classified into meteorological, agricultural, hydrological, and socio-economic droughts depending on its impacts (Mishra and Singh 2010). Understanding the

incidence and behavior of droughts, including the distribution of dry and wet events and how these patterns evolve over time, is essential for effective risk management and adaptation planning. Across Africa, numerous studies have documented an increase in both the frequency and severity of drought events under climate change (IPCC 2023b; Seneviratne et al. 2012). In particular, recent research focusing on East Africa indicates that rising temperatures, coupled with changing precipitation regimes, are intensifying drought trends in the region, thereby exacerbating vulnerabilities in agricultural productivity and water resource availability (Kew et al. 2021).

In Eastern Rwanda, drought constitutes a recurrent hazard with significant adverse effects on water availability, crop production, and food security (Sarkodie et al. 2016; Uwimbabazi et al. 2022). Given the region's reliance on rainfed agriculture and limited water infrastructure, understanding local drought patterns and their evolution is critical to formulating targeted strategies that can enhance resilience and adaptive capacity.

1.5 Farmers' Perceptions, Knowledge, and Adaptation Strategies

The consequences of climate change are not limited to biophysical impacts; they also shape the perceptions, knowledge, and adaptive strategies of farming communities. Farmers' perceptions and adaptive responses are strongly influenced by their direct experiences with climate extremes, making these perceptions critical for the success of adaptation interventions (Messner and Meyer 2006). Studies in similar contexts by Mertz et al. (2009) and Below et al. (2012) show that local perceptions can both inform and sometimes diverge from scientific observations, affecting the uptake of adaptation strategies (Rwema et al. 2025b). Farmers in Eastern Rwanda, whose livelihoods are closely tied to climate-sensitive activities, are directly affected by shifts in rainfall onset and cessation, temperature extremes, and the increasing unpredictability of weather patterns (Rwema et al. 2025c; Uwimbabazi et al. 2022). Their perceptions and responses are crucial for the development of locally appropriate adaptation strategies and for informing policy interventions aimed at building resilience.

1.6 Methodological Approaches in Climate Trend Analysis

A trend in climate refers to a long-term directional change or systematic pattern observed in climate variables, such as temperature, precipitation, or atmospheric pressure, over an extended period of time. Detecting and quantifying these trends is critical for understanding the evolving

climate system, assessing impacts, and informing adaptation and mitigation strategies (Wilks 2011; IPCC 2023a). Trends may be linear or nonlinear, monotonic or non-monotonic, and can vary spatially and temporally, reflecting both natural variability and anthropogenic influences.

In climate trend analysis, a diverse array of methodological approaches is employed to rigorously detect and quantify changes in climate variables. Statistical and parametric methods, including linear regression, polynomial fits, and ARIMA models, are widely utilized to estimate trends, forecast climatic variables, and identify change points, typically relying on underlying statistical assumptions to ensure robust inference (Box et al. 2015; Wilks 2011). In contrast, non-parametric methods such as the Mann–Kendall test, Sen’s slope estimator, and Spearman’s Rho provide flexible alternatives that do not require strict distributional assumptions, making them particularly suitable for climate datasets that may violate normality or exhibit outliers (Hirsch et al. 1982; Kendall 1975; Sen 1968). Advancing beyond these foundational techniques, advanced analytics, encompassing Bayesian inference (Beven and Binley 1992), ensemble modeling (Knutti et al. 2010), and wavelet or spectral analysis (Torrence and Compo 1998), allow for the exploration of complex, nonlinear behaviors and rigorous quantification of uncertainty, thereby offering a more nuanced and multifaceted perspective on trend characterization and climate projections.

In the context of Rwanda, climate trend analyses have predominantly relied on classical statistical approaches, particularly the non-parametric Mann–Kendall test (Rwema et al. 2025c; Safari 2012; Safari and Sebaziga 2023). While effective in identifying monotonic trends, these methods may not fully capture the inherent complexity and dynamic nature of climate variability, especially nonlinear and time-varying patterns that are increasingly recognized as critical in contemporary climate research (Mikkonen et al. 2015; Mohorji and Şen 2020). Advanced computational techniques, such as dynamic linear state-space models, have demonstrated enhanced capability for detecting intricate climate signals elsewhere (Mikkonen et al. 2015), highlighting their potential to enrich climate analyses in Rwanda. Integrating these advanced methodologies with established classical methods can provide a more comprehensive and robust understanding of climate trends and their implications. Building on this integration, the present study employs both classical and advanced statistical techniques to generate deeper insights into climate variability and its impacts in Eastern Rwanda.

1.7 Statement of the Research Problem

Despite the growing global and regional recognition of climate change and its profound impacts on agriculture, there remains a significant gap in understanding how these changes are experienced and perceived at the local level, particularly among smallholder farmers in Eastern Rwanda. While numerous studies have documented rising temperatures and erratic rainfall patterns in Rwanda, most have focused on national or broad regional scales, often overlooking the microclimatic and topographical distinctions that characterize the Eastern Province (Safari 2012; Sebaziga et al. 2023). This has led to a limited understanding of spatial and temporal climate variability within this agriculturally critical region. Moreover, previous research has largely centered on quantifying changes in total rainfall, rainy days, and temperature trends, with insufficient attention to intra-seasonal dynamics such as rainfall onset, cessation, and season duration, factors that are essential for agricultural planning and food security (Ntirenganya 2018; Rwanyiziri and Rugema 2013; Sebaziga et al. 2020). The lack of high-resolution, long-term climate data in earlier studies further constrained the ability to draw robust conclusions about local climate trends and their implications for farming communities.

At the same time, there is a paucity of research exploring how farmers perceive these climate changes, how their perceptions align with observed climate data, and how these perceptions influence their adaptation strategies. Given that farmers' knowledge and responses are pivotal for the development of effective and context-specific adaptation measures, this gap undermines efforts to build resilience and ensure sustainable livelihoods in the region. Therefore, the core research problem addressed in this study is the insufficient understanding of both the physical manifestations of climate change and the perceptions and adaptive responses of farmers in Eastern Rwanda. This dual gap limits the effectiveness of policy interventions and adaptation strategies aimed at mitigating vulnerability and enhancing resilience in one of Rwanda's most climate-sensitive and agriculturally important regions (MoE 2019; Warner et al. 2015).

1.8 Motivation and Significance of the Research

The motivation for this study stems from the urgent need to address the growing challenges posed by climate change to agriculture and rural livelihoods in Eastern Rwanda. Agriculture remains the backbone of Rwanda's economy, contributing significantly to GDP and employing the majority of the population, with smallholder farmers playing a central role (NISR 2023). However, the sector is highly vulnerable to climate variability, particularly changes in rainfall

and temperature patterns, which directly threaten food security and economic stability (Adger et al. 2003; IPCC 2023b). Despite recognition of these risks, previous studies in Rwanda have primarily focused on national or broad regional analyses, often overlooking the microclimatic and topographical diversity within the Eastern Province (Ndakize Joseph et al. 2022). This has resulted in a lack of localized understanding of how climate change is affecting farming communities at the grassroots level. Moreover, earlier research has been constrained by limited data availability, short observation periods, or insufficient spatial coverage, further impeding the development of effective adaptation strategies (Ntirenganya 2018; Rwanyiziri and Rugema 2013; Sebaziga et al. 2020).

Recent advancements, such as the availability of high-resolution climate datasets from the Rwanda Meteorological Agency (Meteo Rwanda 2024), now provide an unprecedented opportunity to conduct robust, localized analyses of climate trends and variability¹. This enables a more accurate assessment of how specific climate parameters, such as rainfall onset, cessation, and season duration, are changing in the Eastern Province, information that is crucial for agricultural planning and risk management (Rwema et al. 2025c; Uwimbabazi et al. 2022). Equally important is understanding farmers' perceptions, knowledge, and adaptive responses to climate change. Farmers are not only the most affected by climate shocks but also possess valuable experiential knowledge that can inform the design of context-specific adaptation measures. However, there is a notable gap in research exploring how farmers perceive and respond to climate variability in Eastern Rwanda, and how these perceptions align with observed climate data. By bridging these gaps, this study aims to provide evidence-based insights that can support policymakers, development practitioners, and local communities in crafting targeted interventions to enhance resilience, mitigate vulnerability, and promote sustainable agricultural development in Eastern Rwanda. Ultimately, the study's findings will contribute to the broader discourse on climate adaptation in sub-Saharan Africa and inform efforts to achieve food security and sustainable livelihoods under changing climatic conditions.

1.9 Objectives of the research

The primary objective of this study is to comprehensively assess climate trends and their influence on farmers' perceptions and adaptation strategies in the Eastern Province of Rwanda. This involves analyzing long-term changes in precipitation and temperature patterns, characterizing drought events, and integrating farmers' local knowledge and experiences to

better understand and support effective climate adaptation in the region. To accomplish this main objective, the study is guided by the following specific objectives:

- To analyze long-term trends and change points in seasonal precipitation and rainfall characteristics (including onset, cessation, and duration) in Eastern Rwanda.
- To assess temporal trends and variability of temperature events across microclimatic zones in the Eastern Province.
- To evaluate the frequency, distribution, and temporal evolution of drought events in Eastern Rwanda.
- To evaluate farmers' knowledge, perceptions, and experiences regarding climate change and climate extremes, particularly droughts, in Eastern Rwanda.
- To document and analyze the adaptation strategies employed by farmers in response to observed and perceived climate change impacts in the region.

1.10 Outline of the thesis

This thesis is organized into six detailed chapters, each focusing on a key aspect of the research. The first chapter provides a general introduction to the topic. The second chapter analyzes trend analysis and change point detection in precipitation time series for the Eastern Province of Rwanda. The third chapter examines trends and variability of temperatures in the Eastern Province of Rwanda. The fourth chapter assesses the characteristics of climate-induced drought in the Eastern Region of Rwanda. The fifth chapter investigates farmers' knowledge, perceptions, and adaptation strategies in response to climate change in Eastern Rwanda. Finally, the sixth chapter presents conclusions and future research directions.

1.11 Reference

Adger, W.N., Huq, S., Brown, K., Conway, D., Hulme, M., (2003). Adaptation to climate change in the developing world. *Prog. Dev. Stud.* 3, 179–195. <https://doi.org/10.1191/1464993403ps060oa>.

Below, T.B., Mutabazi, K.D., Kirschke, D., Franke, C., Sieber, S., Siebert, R., Tscherning, K., (2012). Can farmers' adaptation to climate change be explained by socio-economic household-level variables? *Glob. Environ. Change* 22, 223–235. <https://doi.org/10.1016/j.gloenvcha.2011.11.012>.

Beven, K. J., Binley, A. M., (1992). The future of distributed models: Model calibration and uncertainty prediction. *Hydrological Processes*, 6(3), 279–298. <https://doi.org/10.1002/hyp.3360060305>.

Box, G.E., Jenkins, G.M., Reinsel, G.C. and Ljung, G.M., (2015). *Time series analysis: forecasting and control*. John Wiley & Sons.

Hirsch, R. M., Slack, J. R., & Smith, R. A., (1982). Techniques of trend analysis for monthly water quality data. *Water Resources Research*, 18(1), 107–121. <https://doi.org/10.1029/WR018i001p00107>.

IPCC, (2023a). *Climate Change 2021 – The Physical Science Basis: Working Group I Contribution to the Sixth Assessment Report of the Intergovernmental Panel on Climate Change*, 1st ed. Cambridge University Press. <https://doi.org/10.1017/9781009157896>.

IPCC, (2023b). *Climate Change 2022 – Impacts, Adaptation and Vulnerability: Working Group II Contribution to the Sixth Assessment Report of the Intergovernmental Panel on Climate Change*, 1st ed. Cambridge University Press. <https://doi.org/10.1017/9781009325844>.

Kendall, M.G., (1975). *Rank correlation methods*, 4th edn. Charles Griffin Co. Ltd.

Kew, S.F., Philip, S.Y., Hauser, M., Hobbins, M., Wanders, N., Van Oldenborgh, G.J., Van Der Wiel, K., Veldkamp, T.I.E., Kimutai, J., Funk, C., Otto, F.E.L., (2021). Impact of precipitation and increasing temperatures on drought trends in eastern Africa. *Earth Syst. Dyn.* 12, 17–35. <https://doi.org/10.5194/esd-12-17-2021>.

Knutti, R., Abramowitz, G., Collins, M., Eyring, V., Hawkins, E., Mace, G., Sanderson, B. M., (2010). *Good Practice Guidance Paper on Assessing and Combining Multi Model Climate Projections*. IPCC Expert Meeting on Assessing and Combining Multi Model Climate

Projections. Retrieved from
https://www.ipcc.ch/site/assets/uploads/2018/05/pcmdi_guidance_2010.pdf.

Sarkodie, S., Rufangura, P., Herath MPC Jayaweera, Owusu, P.A., (2016). Situational Analysis of Flood and Drought in Rwanda 1773839 Bytes.
<https://doi.org/10.6084/M9.FIGSHARE.3381463.V1>.

Sebaziga, N.J., Ntirenganya, F., Tuyisenge, A., Iyakaremye, V., (2020). A Statistical Analysis of the Historical Rainfall Data Over Eastern Province in Rwanda. *East Afr J Sc Technol* 10, 33–52.

Sen, P. K., (1968). Estimates of the regression coefficient based on Kendall's tau. *Journal of the American Statistical Association*, 63(324), 1379–1389.
<https://doi.org/10.1080/01621459.1968.10480934>.

Seneviratne, S.I., Nicholls, N., Easterling, D., Goodess, C.M., Kanae, S., Kossin, J., Luo, Y., Marengo, J., McInnes, K., Rahimi, M., Reichstein, M., Sorteberg, A., Vera, C., Zhang, X., Rusticucci, M., Semenov, V., Alexander, L.V., Allen, S., Benito, G., Cavazos, T., Clague, J., Conway, D., Della-Marta, P.M., Gerber, M., Gong, S., Goswami, B.N., Hemer, M., Huggel, C., Van Den Hurk, B., Kharin, V.V., Kitoh, A., Tank, A.M.G.K., Li, G., Mason, S., McGuire, W., Van Oldenborgh, G.J., Orłowsky, B., Smith, S., Thiaw, W., Velegrakis, A., Yiou, P., Zhang, T., Zhou, T., Zwiers, F.W., (2012). Changes in Climate Extremes and their Impacts on the Natural Physical Environment, in: Field, C.B., Barros, V., Stocker, T.F., Dahe, Q. (Eds.), *Managing the Risks of Extreme Events and Disasters to Advance Climate Change Adaptation*. Cambridge University Press, pp. 109–230. <https://doi.org/10.1017/CBO9781139177245.006>.

Torrence, C., Compo, G. P., (1998). A practical guide to wavelet analysis. *Bulletin of the American Meteorological Society*, 79(1), 61–78. [https://doi.org/10.1175/1520-0477\(1998\)079](https://doi.org/10.1175/1520-0477(1998)079).

Mertz, O., Mbow, C., Reenberg, A., Diouf, A., (2009). Farmers' Perceptions of Climate Change and Agricultural Adaptation Strategies in Rural Sahel. *Environ. Manage.* 43, 804–816.
<https://doi.org/10.1007/s00267-008-9197-0>.

Messner, F., Meyer, V., (2006). Flood damage, vulnerability and risk perception - challenges for flood damage research, in: Schanze, J., Zeman, E., Marsalek, J. (Eds.), *Flood Risk*

Management: Hazards, Vulnerability and Mitigation Measures. Springer Netherlands, Dordrecht, pp. 149–167. https://doi.org/10.1007/978-1-4020-4598-1_13.

Meteo Rwanda (2024) Dataset Documentation. Rwanda Meteorology Agency. Available at: <http://maproom.meteorwanda.gov.rw/maproom/Summary/index.html#tabs-2>. (Accessed: 31 July 2024).

Mikkonen, S., Laine, M., Mäkelä, H. M., Gregow, H., Tuomenvirta, H., Lahtinen, M. and Laaksonen, A. (2014) Trends in the average temperature in Finland, 1847–2013. *Stochastic Environmental Research and Risk Assessment*, 29, 1521-1529. <https://doi.org/10.1007/s00477-014-0992-2>.

Mishra, A. K., Singh, V. P., (2010). A review of drought concepts. *Journal of Hydrology*, 391(1-2), 202–216. <https://doi.org/10.1016/j.jhydrol.2010.07.012>.

MoE, M. of environment, (2019). National Environment and Climate Policy [WWW Document]. Minist. Environ. URL <https://www.environment.gov.rw/> (accessed 6.22.21).

Mohammed, H., Jean, C.K., Ahmad, W.A., (2016). Projections of precipitation, air temperature and potential evapotranspiration in Rwanda under changing climate conditions. *Afr. J. Environ. Sci. Technol.* 10, 18–33. <https://doi.org/10.5897/AJEST2015.1997>.

Mohorji, A. M., Şen, Z., (2020). Trend Analyses Methodologies in Hydro-meteorological Records. *Earth Systems and Environment*, 4(3), 713–725. <https://doi.org/10.1007/s41748-020-00159-8>.

Mubiru, D.N., Radeny, M., Kyazze, F.B., Zziwa, A., Lwasa, J., Kinyangi, J., Mungai, C., (2018). Climate trends, risks and coping strategies in smallholder farming systems in Uganda. *Clim. Risk Manag.* 22, 4–21. <https://doi.org/10.1016/j.crm.2018.08.004>.

Ndakize Joseph, S., Safari, B., Ndiwa Joshua, N., Didier, N., Bethwel Kipkoech, M., Safari, A., Rwema, M., (2022). Rainfall variability and trends over Rwanda. *J. Clim. Change Sustain.* 4, 26–34. <https://doi.org/10.20987/jccs.04.06.2022>.

NISR, (2023). GDP-National Accounts (Fiscal Year 2022/23) [WWW Document]. Natl. Inst. Stat. Rwand. URL <https://www.statistics.gov.rw/publication/2017> (accessed 8.19.24).

Ntirenganya, F., (2018). Analysis of Rainfall Variability in Rwanda for Small-scale Farmers Coping Strategies to Climate Variability. *East Afr. J Sci Technol* 8, 75–96.

Rwanyiziri, G., Rugema, J., 2013. Climate Change Effects on Food Security in Rwanda: Case Study of Wetland Rice Production in Bugesera District. *Rwanda J Agric Sc* 1, 35–51.

Rwema, M., Safari, B., Laine, M., Sylla, M.B., & Roininen, L. (2025a). Trends and Variability of Temperatures in the Eastern Province of Rwanda, *International Journal of Climatology*. 45, e8793. <https://doi.org/10.1002/joc.8793>.

Rwema, M., Safari, B., Sylla, M.B., Roininen, L., Laine, M., (2025b). Understanding Farmers' Knowledge, Perceptions, and Adaptation Strategies to Climate Change in Eastern Rwanda. *Sustainability*.17,6721. <https://doi.org/10.3390/su17156721>.

Rwema, M., Sylla, M.B., Safari, B., Roininen, L., Laine, M., (2025c). Trend analysis and change point detection in precipitation time series over the Eastern Province of Rwanda during 1981–2021. *Theor. Appl. Climatol*. 156, 98. <https://doi.org/10.1007/s00704-024-05317-7>.

Safari, B., (2012). Trend Analysis of the Mean Annual Temperature in Rwanda during the Last Fifty Two Years. *J. Environ. Prot.* 3, 538–551. <https://doi.org/10.4236/jep.2012.36065>.

Safari, B., Sebaziga, J.N., (2023). Trends and Variability in Temperature and Related Extreme Indices in Rwanda during the Past Four Decades. *Atmosphere* 14, 1449. <https://doi.org/10.3390/atmos14091449>.

Thornton, P.K., Ericksen, P.J., Herrero, M., Challinor, A.J., (2014). Climate variability and vulnerability to climate change: a review. *Glob. Change Biol.* 20, 3313–3328. <https://doi.org/10.1111/gcb.12581>.

Uwimbabazi, J., Jing, Y., Iyakaremye, V., Ullah, I., Ayugi, B., (2022). Observed Changes in Meteorological Drought Events during 1981–2020 over Rwanda, East Africa. *Sustainability* 14, 1519. <https://doi.org/10.3390/su14031519>.

Warner, K., Van de Logt, P., Brouwer, M., Van Bodegom, A.J., Satijn, B., Galema, F.M., Buit, G.L., 2015. *Climate change Profile: Rwanda*.

Wilhite, D. A., Glantz, M. H., (1985). Understanding the drought phenomenon: The role of definitions. *Water International*, 10(3), 111–120. <https://doi.org/10.1080/02508068508686328>.

Wilks, D.S., (2011). *Statistical methods in the atmospheric sciences (Vol. 100)*. Academic press.

WMO, W.M., (2019). *State of the Climate in Africa 2019 [WWW Document]*. URL <https://library.wmo.int/records/item/57196-state-of-the-climate-in-africa-2019> (accessed 6.29.22).

Chapter 2 Trend analysis and change point detection in precipitation time series over the Eastern Province of Rwanda during 1981-2021

This Chapter reproduces the content of our published paper (<https://doi.org/10.1007/s00704-024-05317-7>)

2.1 Introduction

The issue of climate change has received considerable attention worldwide. After the pre-industrial period, there has been a large increase in greenhouse gas (GHG) concentration in the atmosphere, and anthropogenic activities remain the major contributors (IPCC 2018; IPCC 2021). This rapid increase has led to a change in precipitation patterns (Nelson et al. 2009; Zwiers et al. 2013; Sylla et al. 2016), impacting human activities (Opoku et al. 2021; Sintayehu 2018). The agriculture and water resources sectors are adversely affected (Adger et al. 2003; IPCC 2013, 2021). In the global south, countries where most agriculture practices are rain-fed, changing seasonal features is a challenging issue (Index Mundi 2013; FAO 2014). Agriculture is an important component of the economy and plays a key role in the development of many African countries, including Rwanda in Eastern Africa. In Rwanda, agriculture is a key sector in Gross Domestic Product (GDP) growth and job creation for the majority of the population. In recent years, this sector has contributed around 26% of Rwanda's GDP (NISR 2023) and around 75% of the production from smallholder farmers (RDB 2021).

Over the past few years, there has been an increasing interest in understanding climate change in the country because the observed changes experienced through temperature and precipitation since 1970 have been unprecedented. Temperature trends were increasing (REMA 2011; Safari 2012), while rainfall trends were erratically mixed depending on geographical differences (Warner et al. 2015; MoE 2019). However, in most parts of the country, the negative effects of climate change are evident (MIDIMAR 2015).

Although some climate research has been carried out in the country, most studies in this field have only focused on occurring changes in total rainfall, the number of rainy days, and temperature at the country level. However, these studies were limited by either the short length of the period, the small number of stations used, or the annual/seasonal values instead of the intra-seasonal aspects, which are essential for agriculture. For example, Rwanyirizi and Rugema (2013) examined trends in annual rainfall totals and mean temperature in Bugesera,

an Eastern district, using only one closest meteorological station (Kanombe Airport) from 1980 through 2012. In another study, Ntirenganya (2018) analysed rainfall data to investigate variability and trends in total rainfall and dry spells over the whole country but using only 15 meteorological stations where differences in station's data length and presence of missing values were the major challenge in the study. The starts of some records were in the 1930s (at six stations), 1950s (at three stations), the 1970s (five stations), and the 1990s (at one station), while the end of records was in the 1990s (at five stations) and 2013 (at ten stations). More recently, Sebaziga et al. (2020) studied trends in annual total rainfall, annual total rainy days, and seasonal total rain in the Eastern province; however, only nine meteorological stations were used, and the study covered only the period from 1981 to 2016.

The Rwandan Meteorological Agency (Meteo Rwanda) recently made a large dataset available as a goal of the Enhanced National Climate Services (ENACTS) project (Meteo Rwanda 2024). Thus, this allows for statistically more significant and representative ground-borne studies, such as trend analysis of seasonal rainfall amounts. Trend analysis provides essential information on the change and variability in the climate variables (Hussain et al. 2022). It helps to monitor climate variables and understand whether they are increasing or decreasing, which allows better resource management and disaster prevention and mitigation (Şen 2012; Zhang and Liang 2020). The trend magnitude serves to determine the extent to which the changes are happening and how the situation tends to be while enabling informed decision-making to increase adaptation. The trend analysis has been employed in several studies in different parts of the world (Safari 2012; Gitau et al. 2018; Bosire 2019; Margaritidis 2021; Ngarukiyimana et al. 2021; Hussain et al. 2022). Furthermore, the exploitation of change points in these trends helps to localise the occurrence of significant abrupt change during the study period (Dipak et al. 2014; Chakraborty et al. 2017).

Rainfall amount and its distribution within the season are one of the most important climate parameters to track for a better understanding of occurring impacts due to its high sensitivity to the effects of climate change (Usman and Reason 2004). Because this variable significantly impacts crop yields (Prichard and Verdegaal 2001; Malheiro et al. 2010; Araujo et al. 2014; Kazora et al. 2021). A decreasing or increasing trend provides valuable information that can enhance water management strategies for sustainable adaptation in the agricultural sector. The excess rainfall during the growing season can cause water logging and several crop diseases, while scarcity of rainfall, together with an increase in other climate parameters such as

temperature, can result in low soil moisture and drought, reducing productivity (Cahill et al. 2007; Prichard and Verdegaal 2001; Araujo et al. 2014; Olumuyiwa and Masengo 2018).

Other crucial parameters for rain-fed agriculture are the onset and the cessation of the rainy season. This information assists the farmers in scheduling their planting dates and selecting the appropriate crop type and variety (Mugalavai et al. 2008; Olumuyiwa and Masengo 2018). Trend analysis in both onset and cessation also helps understand whether the rainy season is shifting backward or forward and to determine whether the season is expanding or shortening in a given period. Different definitions of rainfall onset and cessation were developed (Stern et al. 1981; Fasheun 1983; Omotosho et al. 2000) and adopted in several studies (Mugalavai et al. 2008; Dunning et al. 2016; Nkrumah et al. 2022).

Based on these premises, this paper aims to estimate the observed trends in seasonal precipitation events and identify significant change points in the Eastern Province of Rwanda, a region characterised by intensive agricultural practices. In particular, we aim first to investigate long-term trends of six variables (seasonal rainfall, number of rainy days, intensity of rainy days, onset and cessation days, and season duration) and second, ascertain significant change points from precipitation events of March-April-May (MAM) and September-October-November-December (SOND) rain seasons. We use data reconstructed through Enhanced National Climate Services (ENACTS) from 56 stations' locations in the Eastern province of Rwanda for the period ranging from 1981 to 2021. A combination of quantitative approaches is used in the data analysis to contribute to a deeper understanding of climate change in the Eastern province.

Understanding the information related to these variables effectively plays a critical role in decision-making to increase adaptation in a sustainable manner. This helps suggest reliable and justifiable approaches for mitigating vulnerability and increasing resilience (Hansen 2002).

2.2 Data and Methodology

2.2.1 Study area and data

We select the Eastern province for two main reasons:

First, it is the largest farming area in Rwanda, and hence, the area plays an important role in the production of main cultivated crops, including common/bush bean, maize, sorghum,

groundnut, soybean, and banana (GCF 2021). The region is also renowned for livestock, which plays a pivotal role in Rwanda's milk and meat production. Second, it is an area used to experience frequent climate-related hazards such as drought and famine which have become persistent challenges for agriculture and livestock production in the past years (Warner et al. 2015; GCF 2021). The region's less mountainous terrain, characterised by lowlands with altitudes below 1500 m altitudes, partially explains its suitability for agricultural and livestock practices. Rainfall is distributed over the whole region, with a gradual decrease from Central West to Southeast for both MAM and SOND, as shown in the supplementary material (Figure S1). This map also indicates that the North-western part receives less rainfall during the MAM season.

Current research investigates trends and change points in precipitation events from 1981 to 2021. The Rwanda Meteorology Agency (Meteo Rwanda) provided the data utilized in our study. This dataset is gridded with a grid resolution of 0.0375 (~4km), and the grid at locations of 56 existing weather stations (see Figure 2.1b) across Eastern Rwanda was considered in this study. Specifically, these existing stations include three synoptic stations and fifty-three climatological stations. A list of the stations and their coordinates is provided in supplementary material as Table S1. The obtained data were reconstructed at Meteo Rwanda using the methodologies outlined by Dinku et al. (2014), Siebert et al. (2019), and Meteo Rwanda (2024). The quality of these data was managed through rigorous quality control measures, including verifying station coordinates, detecting outliers, and checking for time series homogeneity (Meteo Rwanda 2024). To address gaps and missing values, especially due to a 15-year gap in observations, a modified ENACTS approach was used (Meteo Rwanda 2024). This involved combining station observations with the CHIRP satellite product, adjusting for mean climatological biases based on data from 1981 to 1993. Interpolation and standard merging techniques were applied when station data were available, ensuring a robust and reliable dataset for further climatic analysis. At the country level and eastern region level, this data has been used in previous studies such as Sebaziga et al. (2020), Uwimbabazi et al. (2022), Sebaziga et al. (2022), Safari and Sebaziga (2023), and Sebaziga et al. (2023).

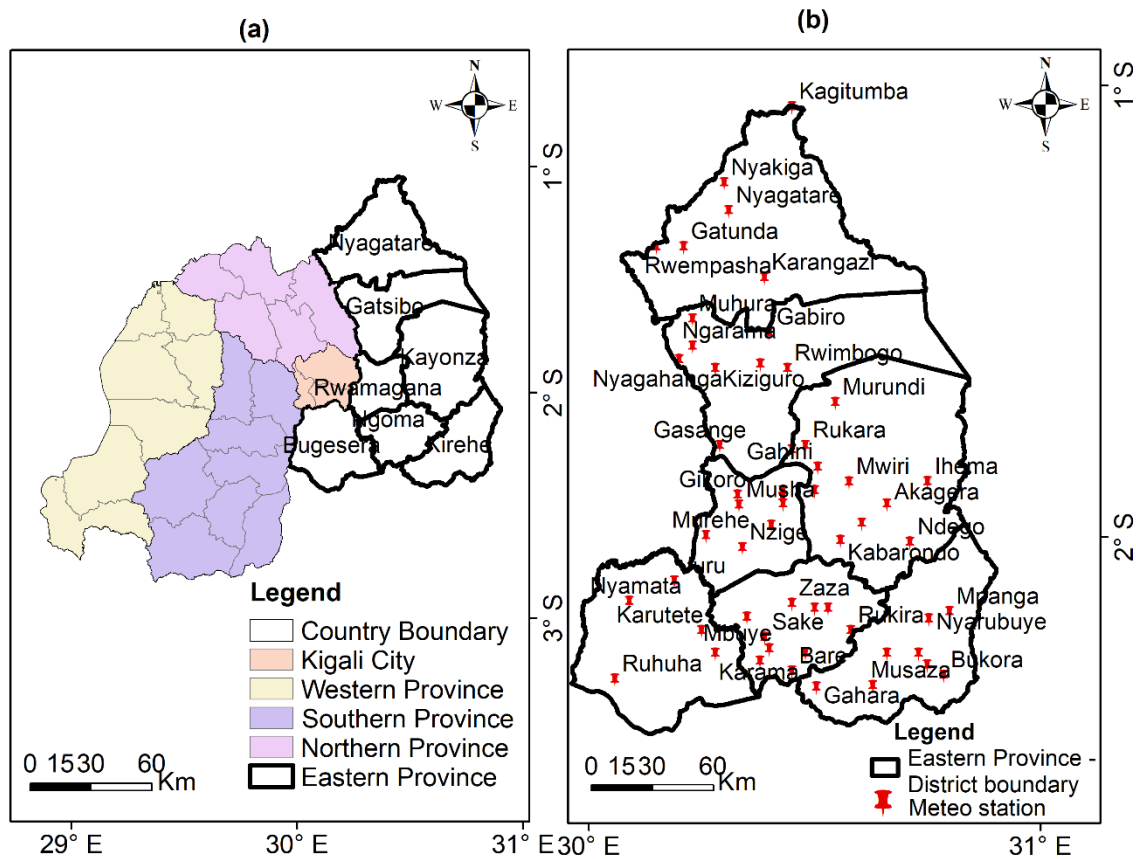


Figure 2.1 Rwanda Map with Eastern province boundary highlighted with solid black line (a) and Eastern Province with locations of meteorological stations highlighted in red (b).

2.2.2 Method for data analysis

a. Variables considered

Table 2.1 illustrates the characteristics of the variables we used in this study. Those include definitions for a rainy day, rainy season, number of rainy days, onset, cessation, season duration, and rainfall intensity. These variables are computed based on the definitions in the table and by considering all the days of the two rainy seasons: Season A, known as SOND (September, October, November, and December), and Season B, known as MAM (March, April, and May).

Table 2.1 Variables considered and their definitions

Variables	Definitions	References
Rainy and dry day	A day with rainfall ≥ 1 mm and < 1 mm respectively.	Meteo Rwanda 2020; Meteo Rwanda 2022;
Number of rainy days	A total number of days with rainfall ≥ 1 mm.	Stern et al. 1981; Olumuyiwa and Masengo 2018; Offoro and Lubango 2018; Edoga 2007; Omotosho et al. 2000
Onset of rain	Occurrence of total rainfall of 20 mm over 5 days with at least 3 consecutive rain days and dry spell not exceeding 7 days in the next 21 days.	
Cessation of rain	Accumulated 10 days of precipitation with less than 0.5 of the evapotranspiration.	
Season duration	The difference between the cessation date and the onset date of the rainy season.	
Rainfall intensity	Based on the threshold values of daily rainfall in mm as < 1 mm (Trace rain), 1– 4.9 mm (Light rain), 5 – 19.9 mm (Moderate rain), 20 – 50 mm (Heavy rain), and > 50 mm (Very heavy rain).	

b. Trends calculation

We applied the non-parametric Mann-Kendall test (Mann 1954; Kendall 1975) in trend analysis, along with its regional counterpart, the Regional Kendall test (Helsel and Frans 2006), which are the common approaches for identifying whether there is an increasing or decreasing trend over time in environmental and climatic data. The choice of the Mann-Kendall test was driven by its robustness against non-normal distributions and its ability to handle missing data and outliers well (Partal and Kahya 2006; Taotao et al. 2016), making it particularly useful for long-term climate analysis. The Mann-Kendall test works by comparing each pair of data points in the time series to determine if there's a general upward or downward trend. For detailed information on the Mann-Kendall formulas and methodology, readers can refer to studies such as Safari (2012), Narayanan et al. (2013), Kahsay et al. (2019), Rizwan et al. (2019), Mallick et al. (2020), Sebaziga et al. (2020), Citakoglu and Minarecioglu (2021), and Quenum et al. (2021), among others. The Regional Kendall test extends the functionality of the Mann-Kendall test by allowing the simultaneous analysis of trends across multiple locations, accounting for spatial correlation between datasets. This enhanced capacity makes it possible to identify region-wide patterns and trends while considering the interrelationship of different monitoring stations or regions. The Regional Kendall Test has been extensively employed in trend analysis, with further information available in works by Dietz and Killen (1981), Taotao et al. (2016), and Margaritidis (2021). To address the negative effects of autocorrelation on trend estimates (Kumar et al. 2014; Ullah et al. 2018), we first investigated the presence of lag-one autocorrelation in the time series data. When autocorrelation was identified, it was removed using the pre-whitening approach (Hamed 2009; Taotao et al. 2016; Hussain et al. 2022) before applying the Mann-Kendall test.

c. Trend magnitude

In addition to detecting trends, we estimated their magnitude using a non-parametric approach, Sen's Slope estimator. This method was selected because it's reliable and not easily affected by outliers (Xu et al. 2003). It calculates the rate of change by finding the median of all possible slopes between data points. The known formula of this approach is

$$Q_i = \frac{X_j - X_k}{j - k}, \quad (2.1)$$

for pair values (X_j and X_k) of a time series, with $j > k$. Sen's estimator is obtained as the median of ranked observed Q_i in ascending order, which takes the form

$$Q_{\frac{N+1}{2}} \text{ if } N \text{ is odd and } \frac{1}{2} [Q_{\frac{N}{2}} + Q_{\frac{N+2}{2}}] \text{ if } N \text{ is even.}$$

The N is obtained from n values of the original time series as $N = n(n-1)/2$ and is the number of Q_i . The Sen's Slope gives us a straightforward measurement of how much the variable increases or decreases over time, which is crucial for understanding the extent of climate change. The technique was used in different studies to quantify trends' magnitude (Narayanan et al. 2013; Taotao et al. 2016; Kahsay et al. 2019; Rizwan et al. 2019; Fathian et al. 2020; Sebaziga et al. 2020). The combination of the Mann-Kendall test and Sen's Slope estimator is well-suited for providing a comprehensive understanding of the direction and magnitude of trends in climate data. While the Mann-Kendall test detects the existence of a significant trend, the Sen's Slope estimator quantifies the trend's rate of change, offering a transparent and interpretable measure of climatic shifts.

d. Change point identification

To identify shifts in the time series data, we used the change point detection method, which is an essential tool for detecting abrupt changes or transitions in climate variables over time. This method helps pinpoint specific times when a significant shift in the data occurs, which is crucial for understanding sudden changes in climate patterns. We employed the Sequential Mann-Kendall Rank Statistic (SMKRS) to detect these change points because it is compatible with climate data where trends and shifts are not always linear (Dipak et al. 2014). This approach allowed us to identify when the most significant changes took place within the study period, providing deeper insights into periods of potential climate anomalies or transitions. Starting with the initial time series, the technique consists of the development of the prograde $u(t_i)$ and retrograde $u'(t_i)$ series through the following steps:

1. From a given ranked time series $x_i (i = 1, 2, \dots, n)$, generates the series $x_j (j = 1, 2, \dots, i - 1)$.
2. Compare the values x_i and x_j . At each comparison, the cases where $x_i > x_j$ are counted and indicated by n_i .
3. Compute the test statistic t_i as

$$t_i = \sum_{j=1}^i n_j. \quad (2.2)$$

4. As defined, the mean and variance of t_i are obtained through

$$E(t_i) = \frac{i(i-1)}{4}, \quad (2.3)$$

$$Var(t_i) = \frac{i(i-1)(2i+5)}{72}.$$

5. The retrograde sequential values $u(t_i)$ are calculated as

$$u(t_i) = \frac{t_i - E(t_i)}{\sqrt{Var(t_i)}}. \quad (2.4)$$

For the prograde sequential values $u'(t_i)$, steps 1 to 5 are carried out on the same time series starting from the end of the series. The graphical representation of $u(t_i)$ and $u'(t_i)$ indicate significant change points only when they cross each other and then diverge and exceed specific threshold values, which are ± 1.96 ($\alpha = 0.05$) in our case. The method is linked to the previous tests because detecting the presence of a trend (using Mann-Kendall) and determining the change points (using SMKRS) provide complementary insights: the trend test highlights general behavior over time, while the change point analysis helps to identify when significant changes occurred, further explaining any observed trends. Together, they allow for a more robust analysis, capturing gradual trends and abrupt shifts in the data. The approach was widely used by researchers, including Dipak et al. (2014), Zhao et al. (2015), and Taotao et al. (2016).

2.3 Results and Discussion

2.3.1 Trends Analysis

a. Regional scale trends

The results of the Regional Kendall test (RKT) applied to seasonal rainfall for the period 1981-2021 for MAM and SOND seasons for the Eastern province are shown in Table 2.2. Significant decreasing trends are observed on heavy rainy days with a slope of $-0.02 (\pm 0.004)$ days/year during MAM. No trend is detected for MAM rainy days, light rainy days, moderate rainy days, and cessation days. The decreasing non-significant trends are observed in rainfall amount with a slope of $-0.01 (\pm 0.002)$ mm/day/year and in Onset days with a slope of $-0.21 (\pm 0.041)$ days/year. The MAM season duration indicates a non-significant increasing trend with a slope of $0.21 (\pm 0.045)$. The SOND season indicates a significant decreasing trend in Onset with a

slope of $-0.21 (\pm 0.041)$ days/year and a significant increase in season duration with a slope of $0.23(\pm 0.035)$. We observed non-significant positive trends in rainy days with a slope of $0.06 (\pm 0.024)$ days/year, $0.03 (\pm 0.015)$ days/year in light rainy days, and $0.06 (\pm 0.012)$ days/year in moderate rainy days. Given that MAM rainfall indicates a decline over the region, it is worth noting the high influence of heavy rain, which revealed a significant decrease in its frequency over the whole area. On the other side, with the SOND season, no trend in rainfall is observed, while moderate rain is spotted as it indicates a high slope value in the frequency of moderate rainy days. Furthermore, it is also essential to emphasize the observed significant increase in season duration of the SOND season, where the observed negative significant trend in onset implies early Onset has contributed to expanding the rainy season by starting earlier than before. Seasonal rainfall variations in Rwanda are largely influenced by factors such as the El Niño–Southern Oscillation (ENSO) and the Indian Ocean Dipole (IOD) (Safari et al. 2022; Sebaziga et al. 2024). Additionally, topography plays a significant role in shaping rainfall's spatial and temporal distribution (Ntwali 2016; Siebert et al. 2019). Previous studies in Rwanda by Uwimbabazi et al. (2022) noted a non-significant decreasing trend in MAM rainfall with a slope of -3.4 mm/decade and an increase in SOND rainfall with a slope of 4.5 mm/decade, which agrees with our findings. A study by Kazora et al. (2021) also revealed a decreasing trend in MAM rainfall and an increasing trend in the SOND rainy season over Rwanda. This is in line with our findings in Eastern Rwanda.

These weak trends' magnitude in many characteristics at the regional level highlights the small-scale nature of rainfall events in Eastern Rwanda and the need to consider the station level for a more robust and detailed study. In the following sections, we thus focus on trends in rainfall characteristics at the station level.

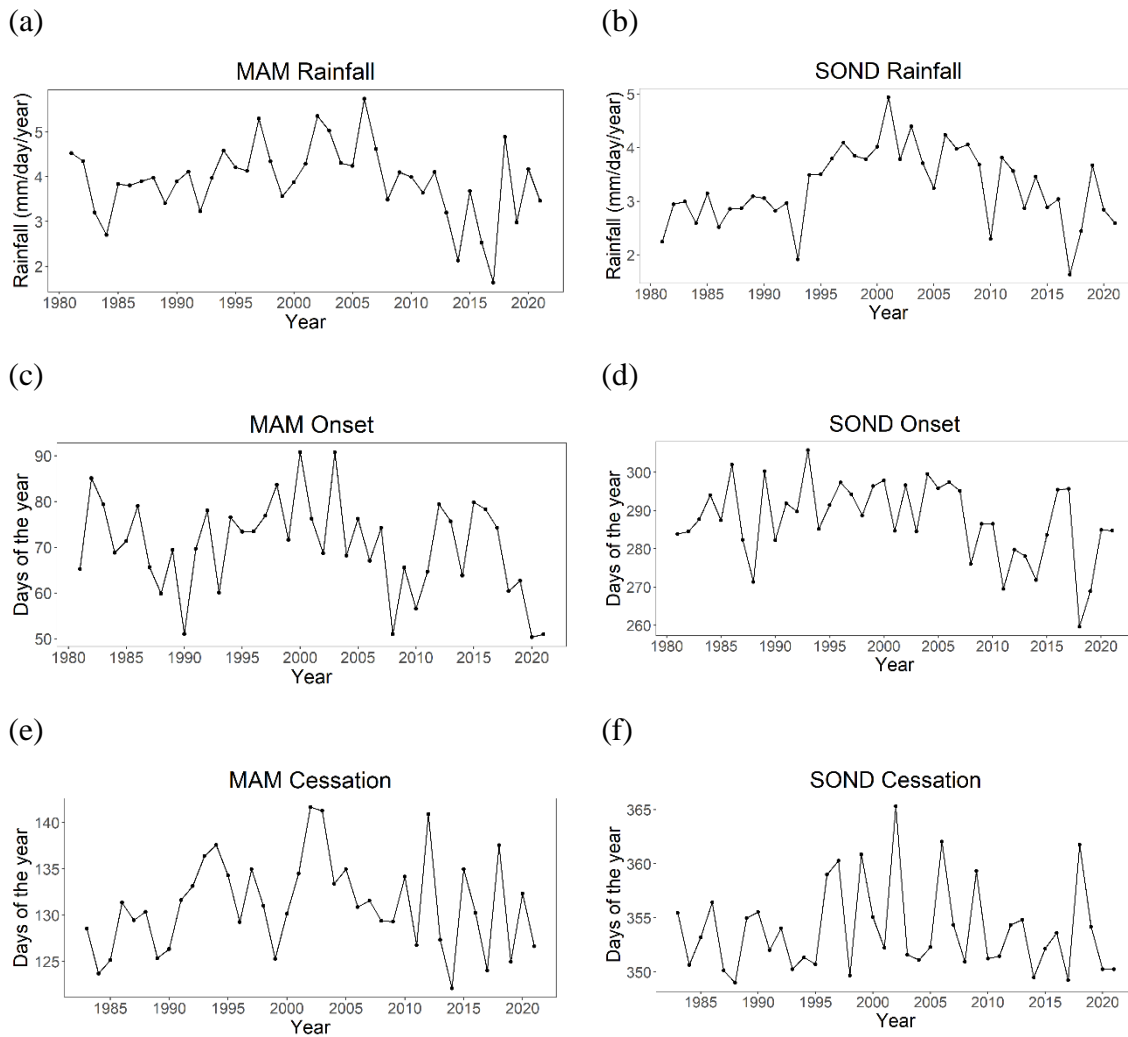


Figure 2.2 Time series of rainfall for MAM (a) and SOND (b), Onset for MAM (c) and SOND (d), and Cessation for MAM (e) and SOND (f) seasons at the Eastern regional scale from 1981-2021.

An illustration time series for the Eastern region level displaying rainfall, onset, and cessation variables for both MAM and SOND is provided in Figure 2.2. In MAM rainfall (Figure 2.2a), there is a noticeable increase between 1981 and 2006, which is followed by a decreasing trend between 2006 and 2017. This figure shows the wettest year was 2006, with an average of 5.73 mm/day/year, and 2017 became the driest with 1.64 mm/day/year during the study period. In the MAM Onset time series (Figure 2.2c), we observe an irregular variation in onset days characterised by a period of decreasing trend between 1981 and 1990. It is followed by a period of increasing trend from 1990-2000, a period of decreasing trend from 2000-2008, then rising during 2008-2015, and a decrease in the last period, 2015-2021. The years 1990, 2008, 2020, and 2021 indicate the earlier onset days around the 51st day of the year, while 2000 and 2003

recorded the latter Onset day at the 91st day of the year. In MAM (Figure 2.2e) cessation days, an increasing trend was observed between 1983 and 2006, followed by a decreasing trend between 2006 and 2021. The year with the latest cessation was 2002 (142nd day of the year), while the earliest cessation was recorded in 2014 (122nd day). In SOND rainfall (Figure 2.2b), the period from 1981 to 2010 indicates an increasing trend followed by a decreasing trend between 2010 and 2021. We noticed an overall increasing trend for the study period, and the year 2017 received low-season rainfall with an average of 1.63 mm/day/year, while 2001 recorded high-season rain with an average of 4.94 mm/day/year. In SOND onset day (Figure 2.2d), an increasing trend is observed between 1981 and 1993, which is followed by a period of decreasing trend between 1993 and 2021. The year 2018 indicates the earliest onset day (on the 260th day of the year) in the time series. In SOND (Figure 2.2f) cessation days, we also observe an increasing trend in 1981-2006, followed by a decreasing trend in 2006-2021.

In general, we observed that in both seasons, a period of rapid increase followed by a period of decrease trend, which implies the absence of linear trends in rainfall events. Despite the observed irregularity in onset days in all seasons, the overall decreasing trend is evident, which indicates the tendency for earlier onset days in the region. There is high variability in season cessation days over the area and a tendency for earlier cessation between 2006-2021. The variability in cessation days and the trend observed from 1981-2006 can be attributed to several factors. The increasing trend in cessation days during the 1981-2006 period may be linked to the intensification of global warming, which contributed to prolonged rainy seasons. Additionally, regional climatic phenomena such as the El Niño–Southern Oscillation (ENSO) and Indian Ocean Dipole (IOD) might have played a significant role during this period, affecting the timing of rainfall cessation. However, the subsequent decrease in cessation days after 2006 could be due to a combination of factors, including changing land use patterns, such as deforestation and agricultural expansion, which alter local microclimates and water cycles. These human-induced changes and regional climatic variability may have contributed to the earlier cessation of rainfall in recent years. In Eastern Rwanda, such shifts could be further influenced by topographical effects, as the region’s varied terrain has been shown to modulate rainfall patterns and intensities.

Table 2.2 Identified trends' slope values at the Eastern regional scale

1981-2021								
Time scale	Rainfall amount	Rainy days	Light Rain	Moderate Rain	Heavy Rain	Onset	Cessation	Season Duration
MAM	-0.01	0.00	0.00	0.00	-0.02*	-0.21	0.00	0.21
SOND	0.00	0.06	0.03	0.06	0.00	-0.21*	0.00	0.23*

the * in the results denotes that significant regional trends are detected at a 95% confidence level.

Table 2.3 presents the detected change points in rainfall events at the regional level in Eastern Rwanda. In the MAM season, significant shifts were identified in 1987 for total rainfall, 1982 for rainy days, 1982 for light rainy days, and 1985 for heavy rainy days. Onset and cessation dates showed significant changes in 1991 and 1986, respectively, while the season duration displayed a notable shift in 1987. For the SOND season, significant change points were observed in 1982 for total rainfall, 1983 for rainy days, 1983 for light rainy days, 1986 for moderate rainy days, and 2008 for season duration. No significant changes were found in the onset (2011) and cessation (1984) dates. Both MAM and SOND seasons revealed that most variables experienced change points during the 1980s, likely associated with early climate shifts and changes in regional land use. A study by Ongoma and Chen (2016) of rainfall trends in the East African region noted non-significant change points in 1953 and 1980.

Table 2.3 Identified significant change points in climate variables at the Eastern regional scale

1981-2021								
Time scale	Rainfall amount	Rainy days	Light Rain	Moderate Rain	Heavy Rain	Onset	Cessation	Season Duration
MAM	1987	1982	1982	2020 n.s	1985	1991	1986	1987
SOND	1982	1983	1983	1986	-	2011 n.s	1984 n.s,	2008

n.s: non-significant

b. Rainfall amount and number of rainy days at station level

Spatial maps (Figure 2.3) present the magnitude of rainfall trends obtained using Sen's Slope test for the MAM and SOND seasons during 1981-2021. During 1981-2021, the magnitude of

the slope of the MAM rainfall trends (in Figure 2.3a) ranges from -0.038 to 0.042 (± 0.002) mm/day/year. The uncertainties in the parentheses (i.e., ± 0.002) are given as standard error values. Of the 56 stations covering the whole Eastern Province, 39 reveal decreasing trends, and eight are statistically significant and located in the Southern region. The statistically significant decreasing trends indicate an average slope of -0.035 (± 0.002) mm/day/year. A significant increasing trend with a slope of 0.042 (± 0.002) mm/day/year is recorded at only one station in the Northern region (i.e., Gatsibo district) among the 17 out of 56 stations, indicating positive trends.

For the SOND rainfall amount trend analysis, Figure 2.3b reveals that the extreme Northern part shows a decreasing trend, while the Southwest shows an increasing trend. The decreasing trends are recorded at 31 stations, one of which is significant with a slope of -0.021(± 0.002) mm/day/year located in the Southeast in the Kirehe district. The increasing trends are recorded in 25 stations, and one of them located in the Northeastern part (i.e., in Kayonza district) is significant with a slope of 0.025 (± 0.002) mm/day/year. Overall, for the SOND season, rainfall amount trends range from -0.024 to 0.025 (± 0.002) mm/day/year.

MAM and SOND show similar features of a predominant increasing trend in a large part of the Northern regions. In addition, decreasing trends are primarily located in the Southern part, with the most significant decrease identified in Kirehe district. This indicates consistency in seasonal rainfall reduction since 1981, which has become more pronounced in the last 21 years over the South as visualised in the time series Figure 2.2. The same variation in stations results of decreasing and increasing trend in seasonal rainfall was also revealed over Eastern Rwanda (Sebaziga et al. 2020). Sebaziga et al. (2020) conducted a station-specific trends analysis with nine stations from the Eastern province. In his findings, during the MAM rainy season, 3 out of 9 stations indicated a decreasing trend, and one station indicated a significant trend. During SOND, he revealed that 2 out of 9 stations indicated a significant increasing trend and a non-significant trend at 7 out of 9 stations. These results agreed with our observations, with some minor differences primarily attributed to different lengths of rainfall time series (used period 1981-2016). The variability in seasonal rainfall amount affected farmers' activities adversely as it increased the probability of drought occurrence in recent decades (Sarkodie et al. 2015; Uwimbabazi et al. 2022).

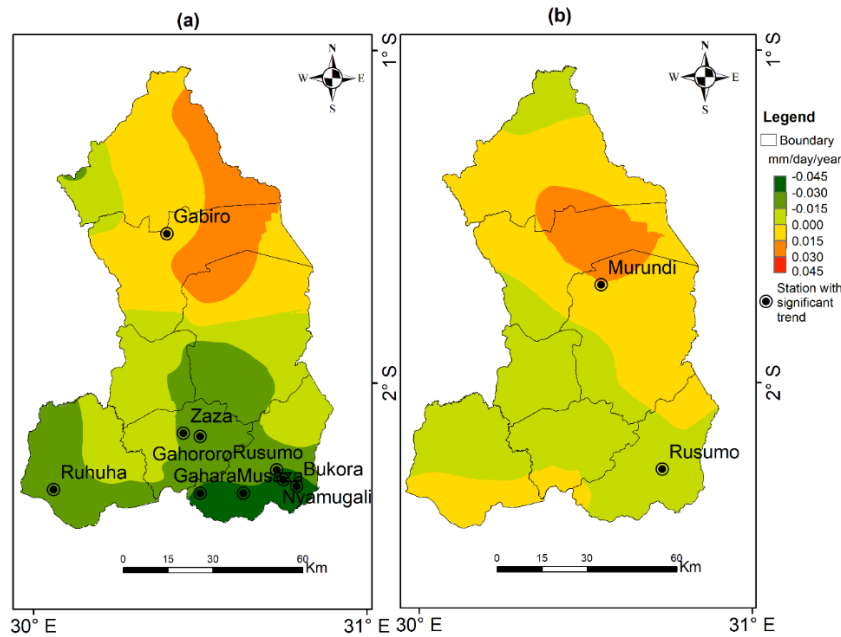


Figure 2.3 Spatial distribution of trends' slope (mm/day/year) for MAM rainfall (a), and SOND rainfall (b) for the period of 1981 to 2021. The black circles on the maps show the locations of stations with significant trends (at $\alpha=0.05$) from the Mann-Kendall and Sen's Slope tests.

Trend analysis of the seasonal number of rainy days is presented spatially in Figure 2.4. In MAM (i.e., Figure 2.4a), Central and Southwest regions indicate negative slope values in the number of seasonal rainy days. The decreasing trends are detected at 34 out of 56 stations. However, only one station with a slope of $-0.38 (\pm 0.021)$ day/year in the Southwest is significant. Except for a small part in the Northwest, the Northern part and some areas in the South show generally an increasing trend detected in 22 stations. Statistically significant increases are only recorded at 4 stations, of which three are located in the South with an average slope of $0.27 (\pm 0.021)$ days/year and one in the North with $0.40 (\pm 0.021)$ days/year. Generally, the results show that slope values range from -0.38 to $0.40 (\pm 0.021)$ days/year, where the highest decrease and increase trends are recorded respectively at Juru station (in the Southwest) and Gabiro station (in the North).

In SOND, the number of rainy days undergoes positive trends from the North to the Southeast (i.e., Figure 2.4b). The positive slopes are identified at 34 stations, mainly found in the North and the Southeastern part of the region. Among them, seven are significant, three of which are located in the North with an average slope of $0.31 (\pm 0.024)$ days/year and another three in the Southeast with an average slope of $0.34 (\pm 0.024)$ days/year. Akagera

station (in Central East) shows the highest positive slope value (0.43 ± 0.024 days/year), followed by Karangazi (in North) and Murehe (in Southeast) stations with $0.42 (\pm 0.024)$ and $0.41 (\pm 0.024)$ days/year, respectively. In contrast, the negative slope values are recorded at 22 stations among the 56 stations across the Eastern province. Most of them are located in the Southwestern part, and only one station in Central (i.e., Kayonza) is statistically significant with the highest slope of $-0.39 (\pm 0.024)$ days/year.

Thus, both seasons (i.e., MAM and SOND) show similar features of a predominant increasing trend in a large part of the North and Southeastern regions. Overall, in the Southeast, positive trends in the number of rainfall events and negative trends in the rainfall amount indicate that precipitation events have become less intense. In addition, the decreasing trend in rainfall over the Southwest is probably due to less frequent precipitation events. Finally, in most parts of the North, the increasing trend of rainfall amount is consistent with more frequent precipitation events. These trends have influenced the type and variety of crops that farmers grow in their respective regions because different crops require different quantities of water within a given number of days (Todorovic 2005; Fischer 2007). These considerations indicate substantial differences in the occurrences of rainfall event classes.

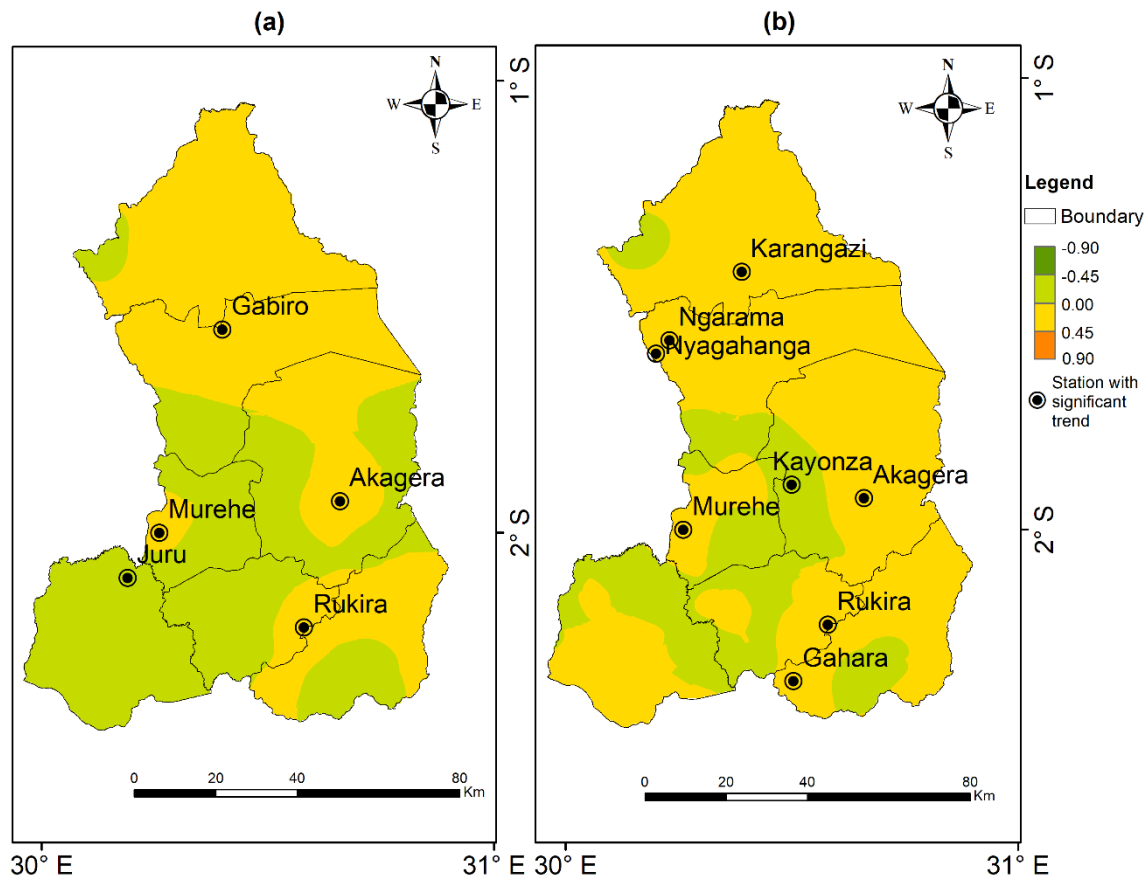


Figure 2.4 Spatial distribution of trends' slope for MAM (a) and SOND (b) number of rainy days for the period of 1981 to 2021. The black circles on the maps show the locations of stations with significant trends (at $\alpha=0.05$) from the Mann-Kendall and Sen's Slope tests.

c. Seasonal rainfall event classes

The slope of trends for different rainfall classes during the 1981-2021 period is shown in Figure 2.5. The number of light rainy days for MAM indicates negative slope values in the Central and Southern parts (Figure 2.5a). In 33 stations showing decreasing trends, only one, located in the Western part of the region (i.e., at Gasange station), exhibits a significant trend with $-0.25 (\pm 0.013)$ days/year. Increasing trends are observed at 23 stations, with three stations (two in the North and one in the South) revealing a significant increase, and one with the highest increasing slope value was $0.25 (\pm 0.013)$ days/year recorded at Murehe station in the South.

Negative trends in MAM's moderate rain events during 1981-2021 are more confined to the southern part of the region (Figure 2.5b). More specifically, decreasing trends are found at 26 stations, and significant trends are detected at two stations with an average slope of -0.2

(± 0.012) days/year. The highest slope value is $-0.20 (\pm 0.012)$ days/year, observed at two stations, Gahororo and Juru, in the Southwest. Increasing trends are observed in the Northern and large areas of the Central part. Increasing trends are found at 29 stations, of which five stations located in the North indicate a significant trend with an average slope of $0.20 (\pm 0.012)$ days/year. The highest slope values are $0.25 (\pm 0.012)$ days/year recorded at Rwimbogo station (in the Northwest). No trend is recorded at one station. As presented in Figure 2.5c, the number of heavy rainy days shows negative slopes in the central and southern parts. In fact, 48 stations have recorded decreasing trends, 9 (19%) of which are significant and concentrated in the southern part with an average slope of $-0.07 (\pm 0.004)$ days/year. Increasing trends are observed at eight stations in the North, but they are not significant. Generally, the observed slope values range from -0.09 to $0.08 (\pm 0.004)$ days/year.

Generally, the observed decrease in total rainfall of the MAM season is also easily observed in the reduction of the frequency of all rainfall categories, including the light, moderate, and heavy rainy days in a large part of eastern Rwanda, mainly in the central and southern parts. The same decreasing trend in MAM rainfall was also recorded in the previous studies over the eastern province (Sebaziga et al. 2020) and Rwanda (Kazora et al. 2021; Sebaziga et al. 2022; Uwimbabazi et al. 2022). Our findings also agree with the studies in the neighboring countries (Makula and Zhou 2021) and over the eastern African region (Ongoma and Chen 2016, Gebrechorkos et al. 2020), which showed a decay in MAM rainfall in recent decades, leading to severe and frequent disaster events. A significant change in the frequency of heavy rainfall was also recorded over the East African region (Ojara et al. 2021, Gebrechorkos et al. 2020), where the variability is primarily associated with natural internal factors like the El Niño–Southern Oscillation (ENSO) and Indian Ocean Dipole (IOD) (Safari et al. 2022; Sebaziga et al. 2024)

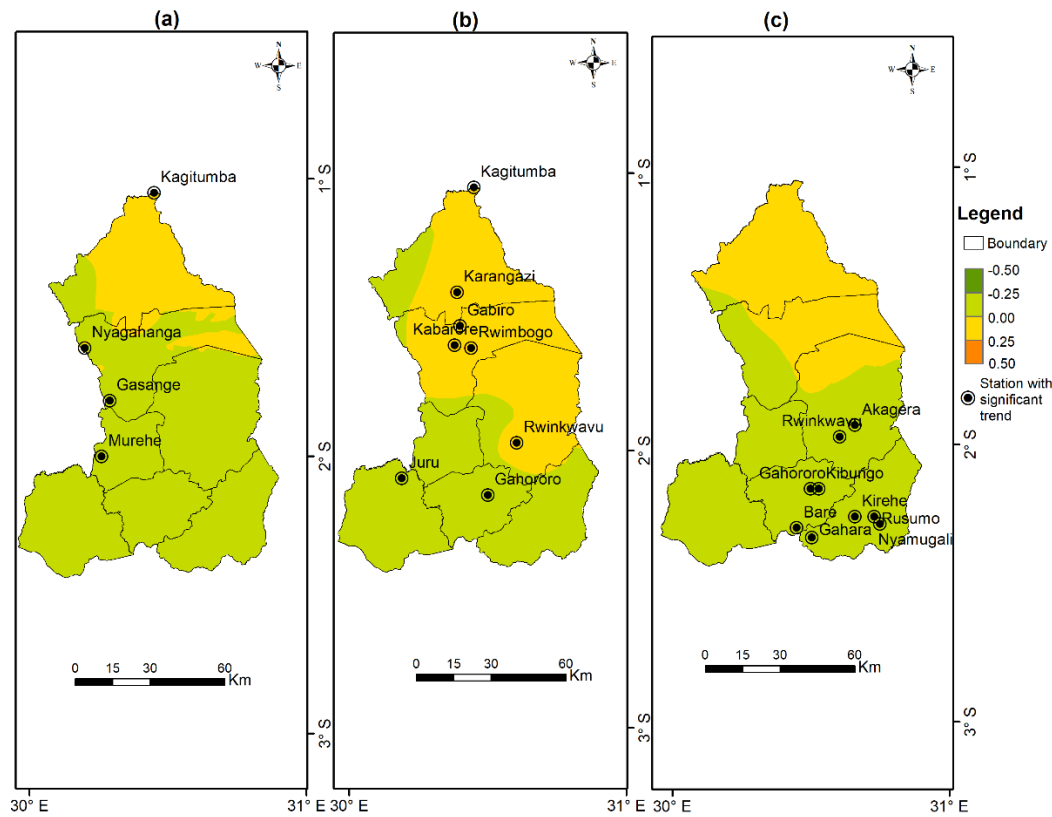


Figure 2.5 Spatial distribution of trends' slope for MAM Light rainy days (a), MAM Moderate rainy days (b), and MAM Heavy rainy days (c) for the period of 1981 to 2021. The black circles on the maps show the locations of stations with significant trends (at $\alpha=0.05$) from the Mann-Kendall and Sen's Slope tests.

Figure 2.6 shows the magnitudes of the trend in the SOND rainfall categories. In the Northwest, a small area in the Central and Southwestern parts, light rainy days (Figure 2.6a) indicate negative slope values influenced by 20 stations. Among the stations undergoing a decreasing trend, only one located in the Northwest, shows significance with a slope of $-0.23 (\pm 0.015)$ days/year. The highest slope value for the decreasing trend is observed at Rwempasha station with $-0.23 (\pm 0.015)$ days/year in the Northern region. Increasing trends of light rainy days occur at 35 stations, mainly located over the North and the South. The trend at four stations is significant, two of which are located in the North with an average slope of $0.27 (\pm 0.015)$ days/year, and two are found in the South with an average slope of $0.21 (\pm 0.015)$ days/year. The highest slope values for the increase are detected at Kagitumba (0.40 ± 0.015) in the Northern. No trend was recorded at one station (i.e., Kiziguro) in the North.

For the moderate rainy days (i.e., Figure 2.6b), the decreasing trends are recorded at 14 stations, mainly found in the Southern and Northern parts, with no significance detected. The Central, Southwest, and Northeast parts exhibited positive slope values. At 42 stations, there was an increasing trend, 10 of which were statistically significant. These significances are mainly located in the Central and Northeastern parts of the study region, with an average slope of $0.19 (\pm 0.012)$ days/year and a maximum slope value of $0.23 (\pm 0.012)$ days/year recorded at Rukara station. The slope of SOND heavy rainy days presented in Figure 2.6c shows a prevalence of decreasing trends in the Central and Southern parts. The decreasing trends recorded at 42 stations, of which Kiziguro station in the Central part is found to be significant with a slope of $-0.06 (\pm 0.004)$ days/year. Increasing trends are observed in the Northern parts of the Eastern Province. The increasing trends are found at 13 stations, with two of them (Gatunda and Gabiro) significant and located in the Northern part of the region. No trend was observed at one station in the Southwest. The maximum positive slope value is $0.07 (\pm 0.004)$ days/year and is recorded at Gabiro (in North) stations.

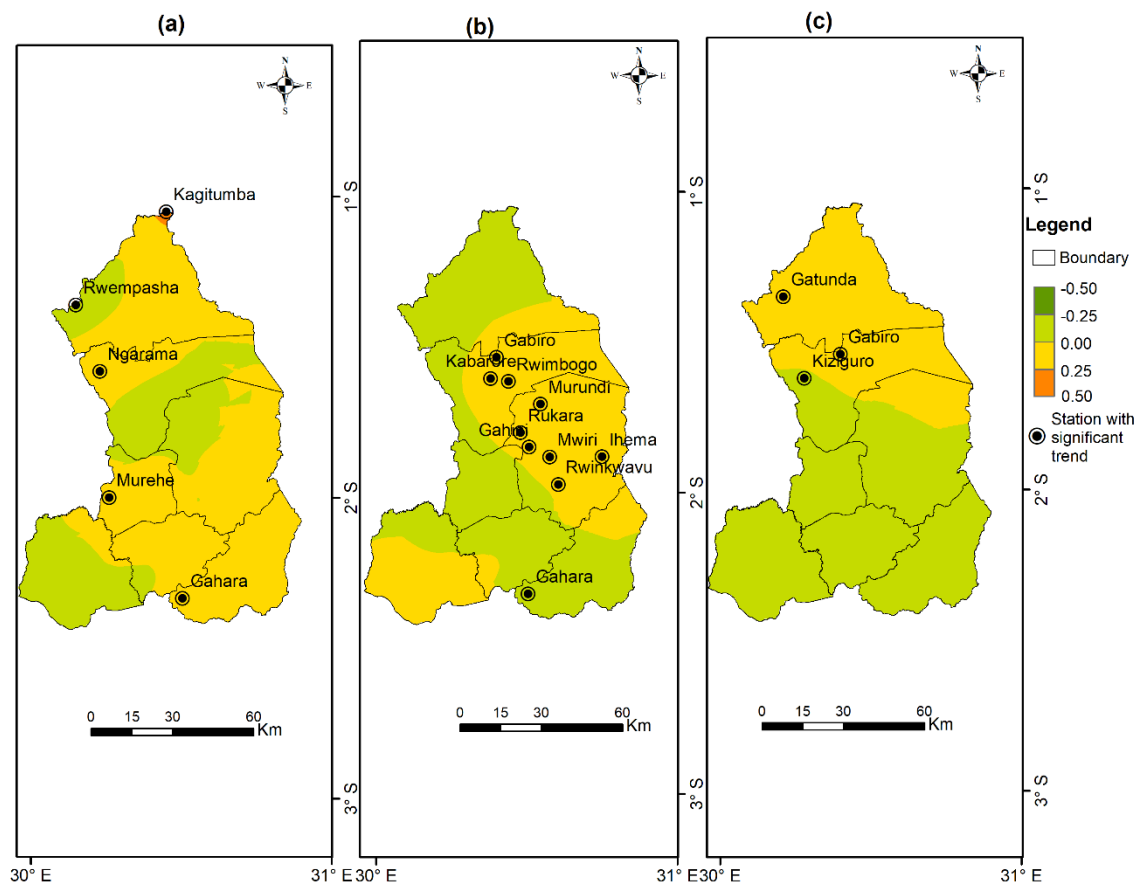


Figure 2.6 Spatial distribution of trends' slope for SOND Light rainy days (a), SOND Moderate rainy days (b), and SOND Heavy rainy days (c) for the period of 1981 to 2021. The black circles on the maps show the locations of stations with significant trends (at $\alpha=0.05$) from the Mann-Kendall and Sen's Slope tests.

Overall, it is found that the contribution of heavy rain in the observed increase of SOND rainfall amounts is low compared to the observed increase in the frequency of light and moderate rain. Moderate rain tends to significantly influence the SOND rain increase, where 75% of the stations revealed an increasing trend. This was statistically significant at 25% of these stations, mainly located in the central part of the eastern province of Rwanda. The previous study which considered OND also noted an increase in OND rainfall amount over Rwanda (Kazora et al. 2021; Uwimbabazi et al. 2022) and the Eastern African region (Gebrechorkos et al. 2020, Ongoma and Chen 2016, Makula and Zhou 2021) and noted a higher fluctuation in the OND season than MAM. This agrees with our results. It was revealed that the SOND rainfall highly correlated with the Indian Ocean Dipole (IOD) over Rwanda (Gebrechorkos et al. 2020; Safari et al. 2022; Sebaziga et al. 2024).

d. Onset and cessation dates of the season and season duration

The trends in seasonal onset dates for MAM and SOND during 1981-2021 are shown spatially in Figure 2.7. A decreasing trend (i.e., negative slope) indicates a tendency towards the occurrences of early onsets, while an increasing trend (i.e., positive slope values) indicates the occurrences of late onsets. In the MAM season (Figure 2.7a), the tendency towards an early onset date is observed in most of the eastern region from North to South, except for a few areas in the extreme Southeast and Central west, where later onset dates are observed. Decreasing trends are identified at 41 stations, where 12 of them are mainly located in the North and Southwest and are statistically significant with an average slope of $-0.62 (\pm 0.041)$ days/year. The maximum negative slope value is at $-0.80 (\pm 0.041)$ at Gabiro (in the North) stations. In contrast, the increasing trends are found at 15 stations distributed in the Central west and extreme Southeast, one of which is statistically significant with a slope of $0.62 (\pm 0.041)$ days/year recorded at Musaza station (in the Southeast).

For the SOND (Figure 2.7b), the spatial distribution of the trends in onset date exhibits a negative slope across the entire northern and parts of the central and southern areas of the eastern region. Out of 56 stations across the whole Eastern region, 41 show decreasing trends, 12 of which are located mainly in the North and Southwest, which are statistically significant with an average slope of $-0.63 (\pm 0.041)$ days/year. The steepest decreasing trend ($-0.83 (\pm 0.042)$ days/year) is recorded at Rukira (in the South) stations. Conversely, a positive slope is observed in small parts of the central western region and the southwest in the extreme north of the Bugesera district. None of the 15 stations with increasing trends are statistically significant.

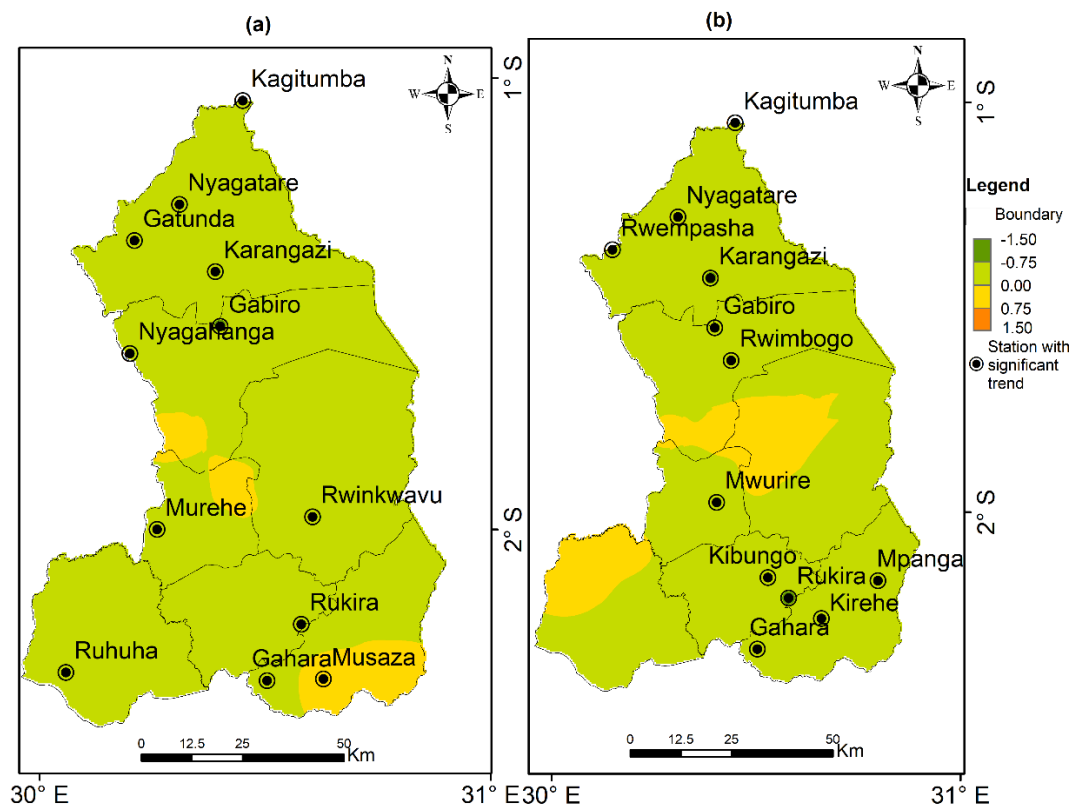


Figure 2.7 Spatial distribution of trends' slope for MAM (a) and SON (b) onset days for the period of 1981 to 2021. The black circles on the maps show the locations of stations with significant trends (at $\alpha=0.05$) from the Mann-Kendall and Sen's Slope tests.

The Cessation dates (Figure 2.8a) during MAM present the dominance of decreasing trends mainly in the South and extreme Northwest and increases elsewhere. However, one station in the South of Ngoma district (i.e., Bare) shows significant patterns. In SON (Figure 2.8b), increasing trends prevail everywhere except in the Northwest, where significant decreasing trends are recorded at Kiziguro and Nyagahanga in the Gatsibo district with an average slope of $-0.12 (\pm 0.004)$ days/year. These increasing patterns in both seasons, mainly in the North, indicate the tendency of season expansion in a large part of the eastern province.

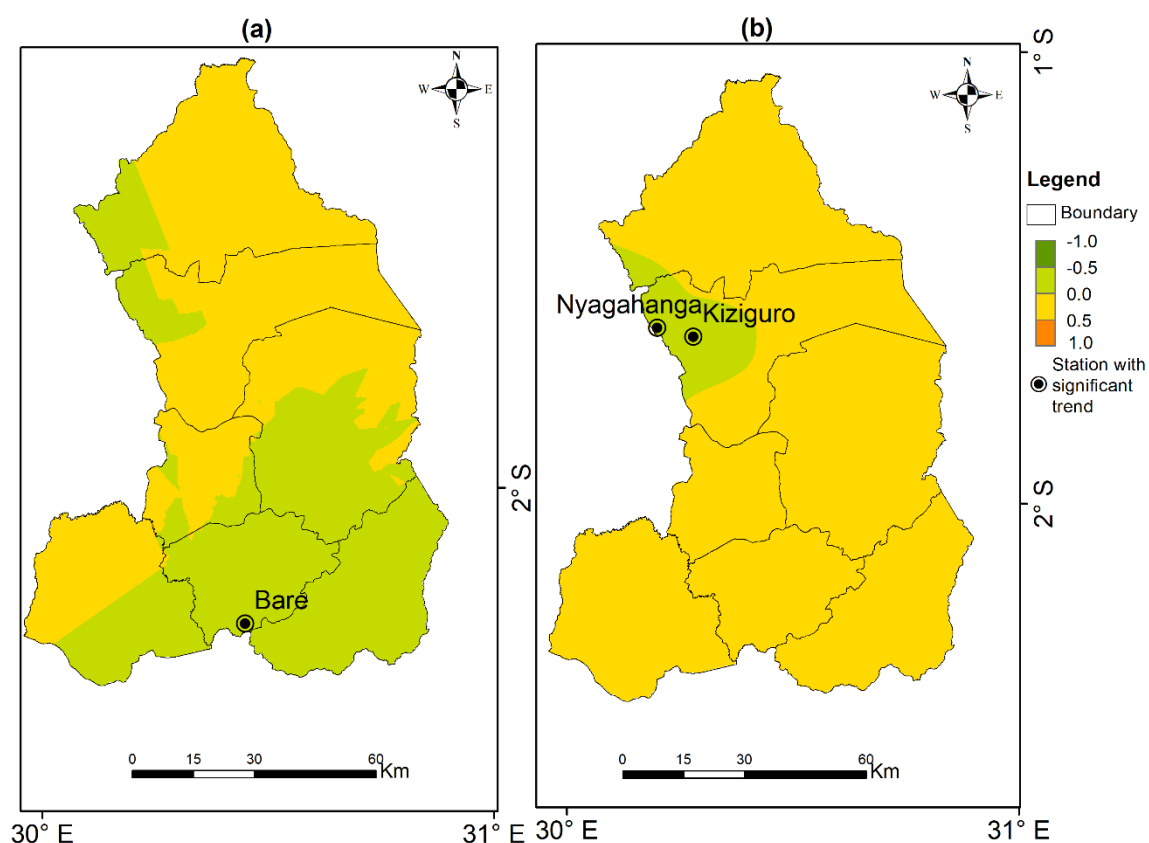


Figure 2.8 Spatial distribution of trends' slope for MAM (a) and SON (b) cessation days for the period of 1981 to 2021. The black circles on the maps show the locations of stations with significant trends (at $\alpha=0.05$) from the Mann-Kendall and Sen's Slope tests.

Figure 2.9 presents the analysis of the season duration (i.e., the difference between cessation and onset dates) for both the MAM and SON seasons. In MAM, the season duration exhibited an increasing trend at 43 out of 56 meteorological stations, with 5 stations being statistically significant and mainly located in the North (Figure 2.9a). On average, these increasing trends had a slope of $0.35 (\pm 0.045)$ days/year. Thirteen stations showed a decreasing trend with an average slope of $-0.29 (\pm 0.045)$ days/year; however, none of these trends were statistically significant.

For the season duration in SON, Figure 2.9b reveals that the part extending from the North, central east, to the south shows an increasing trend. The rising trends are recorded at 48 stations, six of which are statistically significant and mainly located in the southeast. The average of the rising trends was $0.31 (\pm 0.035)$ days/year. The small part in Central and Southwest shows a decreasing trend. The decreasing trend is recorded at eight stations, with

none of them being statistically significant. On average, decreasing trends were $-0.22 (\pm 0.035)$ days/year.

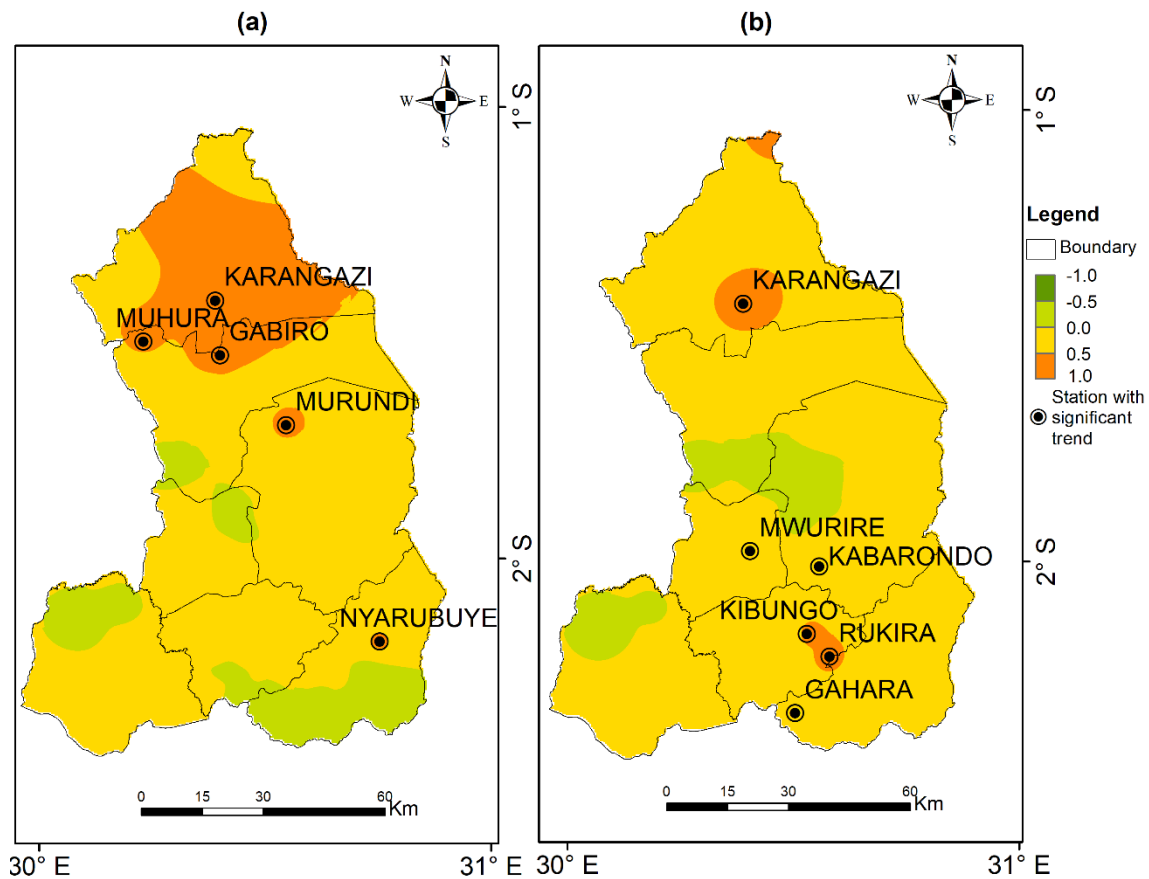


Figure 2.9 Spatial distribution of trends' slope for MAM (a) and SON (b) season duration for the period of 1981 to 2021. The black circles on the maps show the locations of stations with significant trends (at $\alpha=0.05$) from the Mann-Kendall and Sen's Slope tests.

Basically, it is clear that the duration of rainy seasons has lengthened in large areas in both seasons, where a high significance in MAM is spotted in the northern while SON is spotted in the southeast. This is further explained by observed occurrences of early onsets and late cessation over these areas. In contrast, late-onset and earlier cessation have shortened the rainy season in small areas like the extreme Southeast regions.

These rainfall patterns provide a clear picture of the characteristics of the rainy seasons in the different parts of the Eastern Province of Rwanda. For example, in the North, the tendency towards lengthening the rainy seasons during SON has generally increased the

number of rainy days in moderate and/or heavy rainfall events, as many stations' locations indicate significant trends favouring an elevated amount. The next section analyses when the change points, i.e., abrupt variations in these time series, occur.

2.3.2 Change points of significant trends

Table 2.4 presents the obtained results for the change points of the significant trends in all variables discussed. First, the change points in rainfall amount and number of rainy days for the stations showing a significant trend over Eastern Rwanda are analysed. For MAM rainfall amount, the significant change points for stations undergoing decreasing trends, located mainly in the Central and Southern parts, were detected after 2000. On the other hand, the change points of increasing trends recorded mainly for the stations located in the Northeast were captured in the 1980s. For SOND, where only two stations present significant trends, their abrupt change occurred in 2009 and 1990, respectively, for decreasing and increasing trends.

The analysis of change points in the MAM number of rainy days is presented in Table 2.4. Except for one station in the north (i.e., Gabiro), which shows an abrupt change in 1985, the records for change points where increasing trends are observed primarily lie in the period from 2009 to 2016 for the stations located in the Southern part. The only significant decreasing trend in MAM rainy days (at Juru in the Southwest) has a change point in 1989. For SOND rainy days (Table 2.4) at all stations with positive significant trends from north to south, the abrupt change occurred after 2000. However, for the station in the central region (i.e., Kayonza) experiencing a significant decreasing trend, an abrupt change was recorded in 1991.

The abrupt shift in seasonal light rainy days for MAM and SOND from 1981 to 2021 is shown in Table 2.4. In the Centralwest (at Gasange), the observed change point for the station revealed a significant decreasing trend in MAM light rainy days found in 1984. On the contrary, the stations with significant increasing trends, mainly located in the North, show an abrupt change later between 1992 and 2007. For SOND light rainy days, the only station with a significant decreasing trend in the Northwest (i.e., Rwempasha) has an abrupt change in 1992. For the stations with significant positive trends in SOND light rainy days, mainly located in the Northwest and South, change points were observed after 2002.

For the MAM moderate rainy days (Table 2.4) exhibiting significant decreasing trends, mainly in the two stations located in the South, the changed points are recorded in the 1990s. Similarly, in the Northern part, which shows increasing trends in MAM moderate rainy days, the change points are detected in the 1990s. During the SOND rainy season, moderate rainy days, the observed change points of significant increasing trends (i.e., stations accumulated in the Central west) are in the 2010s.

The analysis of change points in MAM heavy rainy days is presented in Table 2.4. Nine stations exhibit significant decreasing trends in the southern part, and the change points identified at these stations are mainly in the 2010s. For SOND heavy rainy days, the station that indicates a significant decreasing trend in the North (i.e., Kiziguro) reveals the change point in 2019. Abrupt change of MAM onset dates during the 1981-2021 period is shown in Table 2.4. In the North and Southwestern regions, a significant abrupt shift occurs after 2002 at stations undergoing a significant decreasing trend. Additionally, the SOND season experienced change points after 2005 for most stations in the North and Southeast, with a significant decreasing trend. Table 2.4 also shows the observed change points for MAM cessation dates. The only station (Bare) that shows a significant declining trend in the Southern region displays a sudden change in 2006. In SOND, abrupt variation is shown in 1998 and 2009, respectively, at two sites in the Northwest (i.e., Kiziguro and Nyagahanga), with significant decreasing trends. Generally, the stations with decreasing trends show a change point in the last two decades.

The analysis of change points in season duration for MAM is presented in Table 2.4. Except for one station in the north (i.e., Muhura), which had its first abrupt change in late 2007, the records for change points where increasing significant trends are observed primarily indicate more than one change point. The earliest lies in the period from 1986 to 1993, and the latter after 2000 for the stations located in the North and Southern parts. For SOND, at most stations with positive significant trends from north to south, the abrupt change occurred after 2000. The only station that indicates an earlier change point is Mwurire (1995) in the central west. The trends after the change point in both MAM and SOND at all stations agree with the results of the MK test, which indicates a significant increasing trend.

It is thus clear that stations with decreasing trends are generally associated with change points that occurred in the most recent decades (that is, after 2000). This is generally the case in rainfall amounts, heavy rainy days, and moderate rainy days in both rainy seasons.

However, for the number of rainy days and light rain days, it is the opposite. The recent change points likely reflect the intensified impact of global warming, particularly in the most recent decades. At the same time, earlier shifts may be due to initial climatic adjustments and regional land use changes.

The significant trends in precipitation observed in Rwanda, particularly in the Eastern Province, can be attributed to a combination of factors within the climate system. Global climate change plays a crucial role, with rising temperatures and altered ocean temperatures, such as those from the Indian Ocean, affecting atmospheric moisture and precipitation patterns. Regional phenomena like the Indian Ocean Dipole (IOD) and the El Niño-Southern Oscillation (ENSO) also significantly influence rainfall variability, with positive IOD and El Niño events generally associated with increased precipitation in the region (Safari et al. 2022; Sebaziga et al. 2024). Additionally, local geographical features, including orographic effects from the area's varied topography and influences from large lakes, contribute to spatial variations in rainfall. Changes in land use, such as deforestation and urbanization, may further impact local climates by altering evapotranspiration rates and surface characteristics (Sahin and Cigizoglu 2010). These factors, coupled with natural climate variability, collectively shape the observed precipitation trends in the Eastern Province of Rwanda.

The early or recent change points in precipitation events detected in our study align with other studies of different regions in Africa or elsewhere. The change-point of rainfall events and temperature caused by ENSO and La Niña events, or urbanization, was also detected in Malaysia in 1997/98 and 2001/02 (Suhaila and Yusop 2018). Rainfall and temperature shifts due to ENSO were also observed around 2001/02 in India and Nigeria (Bisai et al. 2014; Dibal et al. 2017). Previous studies in Rwanda have shown that seasonal rainfall variations are influenced by phenomena like El Niño–Southern Oscillation (ENSO) and Indian Ocean Dipole (IOD) (Safari et al. 2022; Sebaziga et al. 2024), and the impact of topography on the spatial and temporal distribution of rainfall has been confirmed (Ntwali 2016; Siebert et al. 2019).

Table 2.4 Identified change points for significant trends

MAM			SOND		
Rainfall amount					
Station	Year	Trend	Station	Year	Trend
Gahara	2013	Decreasing	Rusumo	2009	Decreasing
Rusumo	2004		Murundi	1990	Increasing
Musaza	2008				
Nyamugali	2008				
Bukora	2013				
Gahororo	2010				
Zaza	2008				
Ruhuha	2007				
Gabiro	1989	Increasing			
Rainy days					
Juru	1989	Decreasing	Kayonza	1991	Decreasing
Murehe	2009	Increasing	Murehe	2006	Increasing
Gabiro	1985		Karangazi	2001	
Akagera	2016		Ngarama	2019	
Rukira	2011		Nyagahanga	2019	
			Akagera	2008	
		Gahara	2007		
		Rukira	2000		
Light rain					
Gasange	1984	Decreasing	Rwempasha	1992	Decreasing
Murehe	2007	Increasing	Murehe	2002	Increasing
Kagitumba	1992		Kagitumba	1997	
Nyagahanga	2002		Ngarama	2018	
			Gahara	2004	
Moderate rain					
Gahororo	1992	Decreasing	Kabarore	2018	Increasing

Juru	1994		Gabiro	2011	
Kagitumba	1993		Rwimbogo	2018	
Karangazi	1993		Gahini	2014	
Gabiro	1990	Increasing	Murundi	2016	
Kabarore	2004		Ihema	2013	
Rwimbogo	2004		Mwiri	2018	
Rwinkwavu	2020		Rukara	2011	
			Rwinkwavu	2018	
			Gahara	2018	
Heavy rain					
Rwinkwavu	1997		Kiziguro	2019	Decreasing
Akagera	2019		Gabiro	1994	Increasing
Gahara	2017		Gatunda	2006	
Rusumo	2015				
Kirehe	2009				
Nyamugali	2012	Decreasing			
Gahororo	2014				
Kibungo	2013				
Bare	2011				
Onset day					
Murehe	2007		Mwurire	2016	
Gatunda	2016		Kagitumba	1994	
Kagitumba	2016		Nyagatare	1989	
Nyagatare	2018		Rwempasha	1998	
Karangazi	2018		Karangazi	2007	
Nyagahanga	2002	Decreasing	Gabiro	2010	Decreasing
Gabiro	2007		Rwimbogo	2006	
Rwinkwavu	2017		Gahara	1994	
Gahara	2004		Kirehe	2007	
Rukira	2009		Mpanga	2005	
Karutete	2013		Nyarubuye	2016	
Ruhuha	2004		Kibungo	2013	

Musaza	1997	Increasing	Rukira	2007	
Cessation day					
Bare	2006	Decreasing	Kiziguro	1998	Decreasing
			Nyagahanga	2009	
Season Duration					
Karangazi	1988		Karangazi	2007	
Muhura	2007		Mwurire	1995	
Gabiro	1986	Increasing	Kabarondo	2017	Increasing
Murundi	1992		Kibungo	2014	
Nyarubuye	1988		Rukira	2007	
			Gahara	2002	

2.4 Conclusion

In this study, a detailed analysis was conducted to investigate the trends and ascertain the change points of the significant trends in precipitation events of rainy seasons from 1981 to 2021. Trend analysis was performed over 56 meteorological stations distributed across the Eastern Province of Rwanda using Mann-Kendall and Regional Kendall tests, Sen's Slope, and Sequential Mann-Kendall Rank Statistic tests. Six variables critical for agriculture practices, namely seasonal rainfall amount, number of rainy days, rainfall classes (light, moderate, and heavy rainy days), as well as onset and cessation dates, and season duration for March-May and September-December seasons, were considered. The negative trends in seasonal rainfall amounts were recorded in a large area in the Southern part of the Eastern Province in MAM. And the regional trend in MAM rainfall indicated a non-significant decreasing trend. In contrast, the SOND season indicated an increasing trend in a large part of the eastern province and also showed a very weak but positive trend in rainfall at the regional level. At the regional level, we observed a significant increase in season duration of the SOND season, where the observed significant negative trend in onset implies that early Onset has contributed to expanding the rainy season by starting earlier than before. The change points analysis indicated that, for the majority of the variables, stations undergoing decreasing trends have generally experienced an abrupt change in the last two decades.

These results will help develop adequate adaptation strategies that sustainably respond to the needs of the vulnerable group. They will also be a research tool for future studies assessing the impacts of trends that occurred in the Eastern Province of Rwanda. The reduction in station data during the 1994 to 2010 period could potentially impact the identification of change points in our study, given the increased reliance on satellite estimates during this time. Given that many (almost 50%) of the change points identified in this study fall within the 1994 - 2010 period, to further strengthen the findings and reaffirm the reliability of the identified change points, additional steps could include cross-validation with other independent datasets and comparison with alternative methods. This would help ensure that the change points identified are genuinely reflective of climatic trends and not artifacts of data limitations. Future studies could also extend the time series analysis beyond this period to enhance robustness.

References

Adger WN, Huq S, Brown K, Conway D, Hulme M (2003) Adaptation to climate change in the developing world. *Progress in Development Studies* 3(3):179-195. <http://dx.doi.org/10.1191/1464993403ps060oa>.

Anyamba A, Small JL, Britch SC, Tucker CJ, Pak EW, Reynolds CA et al (2014) Recent weather extremes and impacts on agricultural production and vector-borne disease outbreak patterns. *PLoS ONE* 9(3): e92538. <http://dx.doi.org/10.1371/journal.pone.0092538>.

Araujo JA, Babatunde JA, Crespo O (2014) Impacts of drought on grape yields in Western Cape, South Africa. *Theoretical and Applied Climatology* 123:117-130. <https://dx.doi.org/10.1007/s00704-014-1336-3>.

Bisai D, Chatterjee S, Khan ABN (2014) Statistical analysis of trend and change-point in surface air temperature time series for midnapore weather observatory, West Bengal, India. *J. Waste Water Treat. Anal.* 5 (2). [http://refhub.elsevier.com/S2405-8440\(21\)02127-7/sref9](http://refhub.elsevier.com/S2405-8440(21)02127-7/sref9).

Bosire EN (2019) Simulating Impacts of Climate Change on Sorghum Production in the Semi- arid Environment of Katumani in Machakos County, Kenya. University of Nairobi Web. <http://erepository.uonbi.ac.ke/handle/11295/106681>. Accessed 1 August 2024.

Cahill KN, Lobell DB, Christopher B, Bonfils C, Hayhoe K (2007) Modelling climate change impacts on wine grape yields and quality in California. Proceedings of the conference ‘Global Warming, Which Potential Impacts on the Vineyards?’, Dijon, France, March 2007. https://chaireunesco-vinetculture.u-bourgogne.fr/colloques/actes_clima/Actes/Article_Pdf/Cahill.pdf.

Chakraborty D, Saha S, Singh RK, Sethy BK, Kumar A, Saikia US, Das SK, Makdoh B, Borah TR, Nomita Chanu, A, Walling I, Rolling Anal PS, Chowdhury S, Daschadhuri D (2017) Spatio-temporal trends and change point detection in rainfall in different parts of North-eastern Indian states. *Journal of Agrometeorology* 19(2):160-163. <https://journal.agrimetassociation.org/index.php/jam/article/download/713/605>.

Citakoglu H., Minarecioglu N (2021) Trend analysis and change point determination for hydrometeorological and groundwater data of Kizilirmak basin. *Theoretical and Applied Climatology* 145:1275–1292. <https://doi.org/10.1007/s00704-021-03696-9>.

Dibal NP, Mustapha MMAT, Yahaya AM (2017) Statistical change-point Analysis in air temperature and rainfall time series for cocoa research institute of Nigeria, ibadan, Oyo state, Nigeria. *Int. J. Appl. Math. Theor. Phys.* 3 (4): 92. [http://refhub.elsevier.com/S2405-8440\(21\)02127-7/sref16](http://refhub.elsevier.com/S2405-8440(21)02127-7/sref16).

Dipak B, Chatterjee S, Khan A, Barman N (2014) Application of Sequential Mann-Kendall Test for Detection of Approximate Significant Change Point in Surface Air Temperature for Kolkata Weather Observatory, West Bengal, India. *International Journal of Current Research* 6(2):5319-5324. https://www.researchgate.net/publication/272678623_Application_of_Sequential_Mann-Kendall_Test_for_Detection_of_Approximate_Significant_Change_Point_in_Surface_Air_Temperature_for_Kolkata_Weather_Observatory_West_Bengal_India.

Dunning CM, Black ECL, Allan RP (2016) The onset and cessation of seasonal rainfall over Africa. *Journal of Geophysical Research: Atmospheres* 121(19): 11,405-11,424. <http://dx.doi.org/10.1002/2016JD025428>.

Dietz EJ, Killeen JT (1981) A Nonparametric Multivariate Test for Monotone Trend with Pharmaceutical Applications. *Journal of the American Statistical Association* 76(373):169-174. <http://www.tandfonline.com/action/showCitFormats?doi=10.1080/01621459.1981.10477624>.

Dinku T, Hailemariam K, Maidment R, Tarnavsky E, Connor S (2014) Combined use of satellite estimates and rain gauge observations to generate high-quality historical rainfall time series over Ethiopia. *International Journal of Climatology* 34: 2489–2504. <https://doi.org/10.1002/joc.3855>.

FAO (2014) Rwanda at a glance. Food and Agriculture Organisation Web. <http://www.fao.org/rwanda/our-office-in-rwanda/rwanda-at-a-glance/en/>. Accessed 8 July 2021.

Fasheun A (1983) Modeling of daily rainfall sequence for farm operations planning in Ibadan. *Nigerian Meteorological Journal* 1: 102-109.

GCF (2021) Transforming Eastern province through adaptation. Green Climate Fund Web. <http://www.greenclimate.fund/project/fp167>. Accessed 1 October 2021.

Gebrechorkos SH, Hülsmanna S, Bernhofer C (2020) Analysis of climate variability and droughts in East Africa using high-resolution climate. *Global and Planetary Change* 186 (2020) 103130. <https://doi.org/10.1016/j.gloplacha.2020.103130>.

Getahun YS, Ming-Hsu L, Iam-Fei P (2021) Trend and change-point detection analyses of rainfall and temperature over the Awash River basin of Ethiopia. *Heliyon* 7(2021):e08024 <https://doi.org/10.1016/j.heliyon.2021.e08024>.

Gitau W, Camberlin P, Ogallo L, Bosire E (2018) Trends of intraseasonal descriptors of wet and dry spells over. *International Journal of Climatology* 38:1189–1200. <https://doi.org/10.1002/joc.5234>.

Fathian F, Ghadami M, Haghghi P, Amini M, Naderi S, Ghaedi Z (2020) Assessment of changes in climate extremes of temperature and precipitation over Iran. *Theoretical and Applied Climatology*. <https://doi.org/10.1007/s00704-020-03269-2>.

Fischer G, Tubiello F, Velthuis H, Wiberg D (2007) Climate change impacts on irrigation water requirements: Effects of mitigation, 1990-2080. *Technological Forecasting and Social Change* 74:1083-1107. <http://10.1016/j.techfore.2006.05.021>.

Hamed KH (2009) Enhancing the effectiveness of pre-whitening in trend analysis of hydrologic data. *Journal of Hydrology* 368(1-4):143-155. <https://dx.doi.org/10.1016/j.jhydrol.2009.01.040>.

Hansen JW (2002) Realizing the potential benefits of climate prediction to agriculture: issues, approaches, challenges. *Agricultural Systems* 74(3):309-330. [https://doi.org/10.1016/S0308-521X\(02\)00043-4](https://doi.org/10.1016/S0308-521X(02)00043-4).

Helsel DR, Frans LM (2006) Regional Kendall Test for Trend. *Environmental Science and Technology* 40(13):4066-4073. <https://doi.org/10.1021/es051650b>.

Hussain A, Cao J, Ali S, Muhammad S, Ullah W, Hussain I, Akhtar M, Wu X, Guan Y, Zhou J (2022) Observed trends and variability of seasonal and annual precipitation in Pakistan during 1960–2016. *International Journal of Climatology* 42(16): 8313-8332. <https://doi.org/10.1002/joc.7709>.

Index Mundi (2013) Rwanda Economy Profile 2013. Index MundiWeb. http://www.indexmundi.com/rwanda/economy_profile.html. Accessed 23 June 2022.

IPCC (2013) Summary for the Policymakers. In: *Climate Change 2013: The Physical Science Basis*. Stocker TF, Qin D, Plattner GK, Tignor M, Allen SK, Boschung J, Nauels A, Xia Y, Bex V and Midgley PM (Eds.), Contribution of Working Group I to the Fifth Assessment Report of the Intergovernmental Panel on Climate Change. Cambridge University Press, Cambridge <http://dx.doi.org/10.1017/CBO9781107415324>.

IPCC (2018) Impacts of 1.5°C Global Warming on Natural and Human Systems. In: *Global Warming of 1.5°C. An IPCC Special Report on the impacts of global warming of 1.5°C above pre-industrial levels and related global greenhouse gas emission pathways, in the*

context of strengthening the global response to the threat of climate change, sustainable development, and efforts to eradicate poverty. [Masson-Delmotte V, Zhai P, Pörtner HO, Roberts D, Skea J, Shukla PR, Pirani A, Moufouma-Okia, W, Péan C, Pidcock R, Connors S, Matthews JBR, Chen Y, Zhou X, Gomis MI, Lonnoy E, Maycock T, Tignor M, Waterfield T (eds.)]. Cambridge University Press, Cambridge, pp. 175-312. <https://doi.org/10.1017/9781009157940.005>.

IPCC (2021) Summary for Policymakers. In: Climate Change 2021: The Physical Science Basis. Masson-Delmotte V, Zhai P, Pirani A, Connors SL, Pean C, Berger S, Caud N, Chen Y, Yelekeci LO, Yu R and Zhou B (eds), Contribution of Working Group I to the Sixth Assessment Report of the Intergovernmental Panel on Climate Change. Cambridge University Press, Cambridge <https://www.ipcc.ch/report/sixth-assessment-report-working-group-i/>.

Kahsay HT, Guta DD, Birhanu BS, Gidey TG (2019) Farmers' Perceptions of climate change trends and adaptation strategies in semiarid highlands of Eastern Tigray, Northern Ethiopia. *Advances in Meteorology* 2:1-13. <https://doi.org/10.1155/2019/3849210>.

Kazora J, Wen W, Shahid S, Ali AMd, Bilal M, Habtemicheal BA, Iyakaremye V, Qiu Z, Almazroui M, Wang Y, Sebaziga NJ, Tiwari P (2021) Spatiotemporal variability of rainfall trends and influencing factors in Rwanda. *Journal of Atmospheric and Solar-Terrestrial Physics* 219(2021):105631. <https://doi.org/10.1016/j.jastp.2021.105631>.

Kendall MG (1975) Rank correlation methods, 4th edn. Charles Griffin & Company Limited, London. [http://refhub.elsevier.com/S1364-6826\(21\)00091-2/opt98UiiitOxCu](http://refhub.elsevier.com/S1364-6826(21)00091-2/opt98UiiitOxCu).

Kumar R, Singh S, Randhawa SS, Singh KK, Rana JC (2014) Temperature trend analysis in the glacier region of Naradu Valley, Himachal Himalaya, India. *Comptes Rendus Geoscience* 346(9-10):213-222. <https://doi.org/10.1016/j.crte.2014.09.001>.

Makula EK, Zhou B. (2021) Changes in March to May rainfall over Tanzania during 1978–2017. *Int J Climatol*. 1–13. <https://doi.org/10.1002/joc.7146>.

Malheiro AC, Santos JA, Fraga H, Pinto JG (2010) Climate change scenarios applied to viticultural zoning in Europe. *Climate Research* 43(3):163-177. <http://dx.doi.org/10.3354/cr00918>.

Mallick J, Talukdar S, Alsubih M, Salam R, Ahmed M, Kahla NB, Shamimuzzaman Md (2020) Analysing the trend of rainfall in Asir region of Saudi Arabia using the family of Mann-Kendall tests, innovative trend analysis, and detrended fluctuation analysis. *Theoretical and Applied Climatology* <https://doi.org/10.1007/s00704-020-03448-1>.

Mann HB (1945) Nonparametric tests against trend. *Econometrica: Journal of the econometric society* 13: 245-259. <https://doi.org/10.2307/1907187>.

Margaritidis AK (2021) Site and Regional Trend Analysis of Precipitation in Central Macedonia, Greece. *Computational Water, Energy, and Environmental Engineering* 10(2): 49-70. <https://doi.org/10.4236/cweee.2021.102004>.

Meteo Rwanda (2020) Climate Summary for Local Governments. Rwanda Meteorology AgencyWeb. <https://www.maproom.meteorwanda.gov.rw/maproom/Summary/index.html>. Accessed 25 January 2021.

Meteo Rwanda (2022) Maproom. Rwanda Meteorology AgencyWeb. <https://www.maproom.meteorwanda.gov.rw/maproom/Summary/>. Accessed 25 June 2022.

Meteo Rwanda (2024) Dataset Documentation. Rwanda Meteorology AgencyWeb. <http://maproom.meteorwanda.gov.rw/maproom/Summary/index.html#tabs-2>. Accessed 31 July 2024.

MoE (2019) National Environment and Climate Policy. Ministry of EnvironmentWeb. <https://www.environment.gov.rw>. Accessed 20 June 2021.

MIDIMAR (2015) The National Risk Atlas of Rwanda. Ministry of Disaster Management and Refugee AffairsWeb. <http://midimar.gov.rw>. Accessed 25 June 2022.

Mugalavai EM, Kipkorir EC, Raes D, Rao MS (2008) Analysis of rainfall onset, cessation and length of the growing season for western Kenya. *Agricultural and forest meteorology* 148(6-7):1123-1135. <http://dx.doi.org/10.1016/j.agrformet.2008.02.013>.

Narayanan P, Basistha A, Sarkar S, Sachdeva K (2013) Trend analysis and ARIMA modeling of pre-monsoon rainfall data for western India. *Comptes Rendus Geoscience* 345(1):22-27. <http://doi.org/10.1016/j.crte.2012.12.001>.

Nelson GC, Rosegrant MW, Koo J, Robertson R, Sulser T, Zhu T, Ringler C, Msangi S, Palazzo A, Batka M, Magalhaes M, Valmonte-Santos R, Ewing M, Lee D (2009) Food Policy Report: Climate Change: Impact on Agriculture and Costs of Adaptation. International Food Policy Research Institute Washington 21:1-19. <http://dx.doi.org/10.2499/0896295354>.

Ngarukiyimana JP, Fu Y, Sindikubwabo C, Nkurunziza IF, Ogou FK, Vuguziga F, Ogwang BA, Yang Y (2021) Climate Change in Rwanda: The Observed Changes in Daily Maximum and Minimum Surface Air Temperatures during 1961–2014. *Frontiers in Earth Science* 9(2021). <https://doi.org/10.3389/feart.2021.619512>.

Nicholson SE (1996) A review of climate dynamics and climate variability in eastern Africa. In: Johnson, T.C. and Odada, E.O (Eds.) *The Limnology, Climatology, and Paleoclimatology of the East African Lakes*, 1st edn. CRC Press: Dordrecht, The Netherlands, pp. 25 - 56. <https://doi.org/10.1201/9780203748978-2>.

NISR (2023) GDP-National Accounts (Fiscal Year 2022/23). National Institute of Statistics of RwandaWeb. <https://www.statistics.gov.rw/publication/2017> Accessed 29 August 2024.

Nkrumah F, Quagraine KA, Quagraine KT, Wainwright C, Quenum GMLD, Amankwah A, Klutse NAB (2022) Performance of CMIP6 HighResMIP on the Representation of Onset and Cessation of Seasonal Rainfall in Southern West Africa. *Atmosphere* 13(7): 999. <https://doi.org/10.3390/atmos13070999>.

Ntirenganya F (2018) Analysis of Rainfall Variability in Rwanda for Small-scale Farmers Coping Strategies to Climate Variability. *East African Journal of Science and Technology* 8(1):75-96.

https://www.researchgate.net/publication/329416464_Analysis_of_Rainfall_Variability_in_Rwanda_for_Small-scale_farmers_Coping_Strategies_to_Climate_Variability.

Ntwali D, Ogwang BA, Ongoma V (2016) The impacts of topography on spatial and temporal rainfall distribution over Rwanda based on WRF model. *Atmos. Clim. Sci.* 6:145–157. [http://refhub.elsevier.com/S2405-8440\(21\)02127-7/sref49](http://refhub.elsevier.com/S2405-8440(21)02127-7/sref49).

Ojara MA, Yunsheng L, Babaousmail H, Wasswa P (2021) Trends and zonal variability of extreme rainfall events over East Africa during 1960–2017. *Natural Hazards*, 109(1):33-61. <https://link.springer.com/article/10.1007/s11069-021-04824-4>.

Olumuyiwa IO, Masengo FI (2018) Application of Nonparametric Trend Technique for Estimation of Onset and Cessation of Rainfall. *Air, Soil, and Water Research* 11:1-4. <http://doi.org/10.1177/1178622118790264>.

Omosho JB, Balogun AA, Ogunjobi K (2000) Predicting Monthly and seasonal rainfall, onset, and cessation of the rainy season in West Africa using only surface data. *International Journal of Climatology* 20(8):865 - 880. [https://doi.org/10.1002/1097-0088\(20000630\)20:8%3C865::AID - JOC505%3E3.0.CO;2-R](https://doi.org/10.1002/1097-0088(20000630)20:8%3C865::AID - JOC505%3E3.0.CO;2-R).

Ongoma V, Chen H (2016) Temporal and spatial variability of temperature and precipitation over East Africa from 1951 to 2010. *Meteorol Atmos Phys*. <https://doi.org/10.1007/s00703-016-0462-0>.

Opoku SK, Filho WL, Hubert F, Adejumo O (2021) Climate Change and Health Preparedness in Africa: Analysing Trends in Six African Countries. *International Journal of Environmental Research and Public Health* 18(9). <https://www.doi.org/10.3390/ijerph18094672>.

Pegram, G.G.S. and Clothier, A.N. (2001) 'High-resolution space-time modeling of rainfall: the "String of Beads" model', *Journal of Hydrology*, 241(1-2), pp. 26-41. 10.1016/S0022-1694(00)00373-5.

Partal T, Kahya E (2006) Trend analysis in Turkish precipitation data. *Hydrological Processes* 20(9):2011-2026. <http://dx.doi.org/10.1002/hyp.5993>.

Prichard TL, Verdegaaal PS (2001) Effects of water deficits upon winegrape yield and quality. *Water Management* 1-6. <https://ucanr.edu/sites/csnce/files/96234.pdf>.

Quenum GMLD, Nkrumah F, Klutse NAB, Sylla MB (2021) Spatiotemporal Changes in Temperature and Precipitation in West Africa. Part I: Analysis with the CMIP6 Historical Dataset. *Water* 13(24). <https://doi.org/10.3390/w13243506>.

RDB (2020) Agriculture. Rwanda Development Board Web. <https://rdb.rw/investment-opportunities/agriculture/>. Accessed 8 July 2021.

REMA (2011) Green Growth and Climate Resilience: National Strategy for Climate Change and Low Carbon Development. Rwanda Environment Management Authority Web. <https://www.rema.gov.rw>. Accessed 20 October 2021.

Rizwan M, Li X, Jamal K, Chen Y, Chauhdary JN, Zheng D, Anjum L, Ran Y, Pan X (2019) Precipitation variations under a changing climate from 1961-to 2015 in the source region of the Indus River. *Water* 11(7). <https://doi.org/10.3390/w11071366>.

Rwanyiziri G, Rugema J (2013) Climate Change Effects on Food Security in Rwanda: Case Study of Wetland Rice Production in Bugesera District. *Rwanda Journal, Series E: Agricultural Sciences* 1(1):35-51. <http://dx.doi.org/10.4314/rj.v1i1.3E>.

Safari B (2012) Trend Analysis of the Mean Annual Temperature in Rwanda during the Last Fifty-Two Years. *Journal of Environmental Protection* 3(6):538-551, <http://dx.doi.org/10.4236/jep.2012.36065>.

Safari B, Sebaziga JN, Siebert A (2022) Evaluation of CORDEX-CORE regional climate models in simulating rainfall variability in Rwanda. *International Journal of Climatology*, 1–29. <https://doi.org/10.1002/joc.7891>.

Safari B, Sebaziga JN (2023) Trends and Variability in Temperature and Related Extreme Indices in Rwanda during the Past Four Decades. *Atmosphere* 14, 1449. <https://doi.org/10.3390/atmos14091449>.

Sahin S, Cigizoglu HK (2010) Homogeneity analysis of Turkish meteorological data set. *Hydrol. Process.* 24 (8): 981–992. [http://refhub.elsevier.com/S2405-8440\(21\)02127-7/sref65](http://refhub.elsevier.com/S2405-8440(21)02127-7/sref65).

Sarkodie SA, Rufangura P, Jayaweera HMPC, Asantewaa OPA (2015) Situational Analysis of Flood and Drought in Rwanda. *International Journal of Scientific & Engineering Research* 6(8):960-970. <https://doi.org/10.6084/M9.FIGSHARE.3381463.V1>.

Sebaziga NJ, Ntirenganya F, Tuyisenge A, Iyakaremye V (2020) A Statistical Analysis of the Historical Rainfall Data Over Eastern Province in Rwanda. *East African Journal of Science and Technology* 10(1):33-52. <https://www.unilak.ac.rw/wp-content/uploads/2016/08/4.pdf>.

Sebaziga NJ, Safari B, Ngaina JN, Ntwali D, Mutai BK, Safari KA, Rwema M (2022) Rainfall variability and trends over Rwanda. *Journal of Climate Change and Sustainability* 4(1): 26-34. <https://doi.org/10.20987/jccs.04.06.2022>.

Sebaziga NJ, Twahirwa A, Kazora J, Rusanganwa F, Mugunga MM, Higirow S, Guhirwa S, Nyandwi JC, and Niyitegeka JMV (2023) Spatial and Temporal Analysis of Rainfall Variability and Trends for Improved Climate Risk Management in Kayonza District, Eastern Rwanda. *Advances in Meteorology* 2023:1-17. <https://doi.org/10.1155/2023/5372701>.

Sebaziga JN, Safari B, Ngaina JN, Ntwali D (2024) Spatial variability of seasonal rainfall onset, cessation, length and rainy days in Rwanda. *Theoretical and Applied Climatology*. <https://doi.org/10.1007/s00704-024-05086-3>.

Şen Z (2012) Innovative trend analysis methodology. *Journal of Hydrologic Engineering* 17(9):1042-1046. [http://dx.doi.org/10.1061/\(ASCE\)HE.1943-5584.0000556](http://dx.doi.org/10.1061/(ASCE)HE.1943-5584.0000556).

Seregina LS, Fink AH, Van der Linden R, Elagib NA, Pinto JG (2018) A new and flexible rainy season definition: Validation for the Greater Horn of Africa and application to rainfall trends. *International Journal of Climatology* 39(2):989 - 1012. <https://doi.org/10.1002/joc.5856>.

Siebert A, Dinku T, Vuguziga F, Twahirwa A, Kagabo MD, DelCorral J, Robertson AW (2019) Evaluation of ENACTS-Rwanda: A new multi-decade, high-resolution rainfall, and temperature data set—*Climatology*. *International Journal of Climatology* 34: 1262–1277. <https://doi.org/10.1002/joc.6010>.

Sintayehu DW (2018) Impact of climate change on biodiversity and associated key ecosystem in Africa: a systematic review. *Ecosystem health and sustainability* 4(9):225-239. <https://doi.org/10.1080/20964129.2018.1530054>.

Stern RD, Dennett MD, Garbutt DJ (1981) The start of the rains in West Africa. *Journal of Climatology* 1(1):59-68. <https://doi.org/10.1002/joc.3370010107>.

Suhaila J, Yusop Z (2018) Trend analysis and change-point detection of annual and seasonal temperature series in Peninsular Malaysia. *Meteorol. Atmos. Phys.* 130 (5):565–581. [http://refhub.elsevier.com/S2405-8440\(21\)02127-7/sref68](http://refhub.elsevier.com/S2405-8440(21)02127-7/sref68).

Sylla MB, Nikiema PM, Gibba P, Kebe I, Klutse NAB (2016) Chapter 3 Climate Change over West Africa: Recent Trends and Future Projections. Springer International Publishing Switzerland, pp. 25-40. http://dx.doi.org/10.1007/978-3-319-31499-0_3.

Taotao C, Guimin X, Lloyd TW, Wei C, Daocai C (2016) Trend and Cycle Analysis of Annual and Seasonal Precipitation in Liaoning, China. *Advances in Meteorology* 2016:1-15. <http://dx.doi.org/10.1155/2016/5170563>.

Todorovic M (2005) Crop water requirements. In *Water Encyclopedia: Surface and Agricultural Water* (Jay H. Lehr, Jack Keeley, Eds.), AW-59, John Wiley & Sons Publisher, pp. 557-558. <http://dx.doi.org/10.1002/047147844X.aw59>.

Ullah S, You Q, Ullah W, Ali A (2018) Observed changes in precipitation in China-Pakistan economic corridor during 1980-2016. *Atmospheric Research* 210:1-14. <https://doi.org/10.1016/j.atmosres.2018.04.007>.

Usman MT, Reason CJC (2004) Dry Spell Frequencies and Their Variability over Southern Africa. *Climate Research*, 26, 199-211. <https://doi.org/10.3354/cr026199>.

Uwimbabazi J, Jing Y, Iyakaremye V, Ullah I, Ayugi B (2022) Observed Changes in Meteorological Drought Events during 1981–2020 over Rwanda. *East Africa. Sustainability* 14(3):1-21. <https://doi.org/10.3390/su14031519>.

Warner K, Van de Logt P, Brouwer M, Van Bodegom AJ, Satijn B, Galema FM, Buit GL (2015) Climate change Profile: Rwanda' Netherlands Commission for Environmental Assessment and Dutch Sustainability Unit (DSU)Web. https://ees.kuleuven.be/klimos/toolkit/documents/687_CC_rwanda.pdf Accessed, 20 June 2021.

Zhang Y, Liang C (2020) Analysis of annual and seasonal precipitation variation in the Qinba Mountain area, China. *Scientific Reports* 10:1-13. <https://doi.org/10.1038/s41598-020-57743-y>.

Zhao J, Huang Q, Chang J, Liu D, Huang S, Shi X (2015) Analysis of temporal and spatial trends of hydro-climatic variables in the Wei River basin. *Environmental Research* 139:55-64. <https://doi.org/10.1016/j.envres.2014.12.028>.

Zwiers FW, Hegerl LV, Knutson GC, Kossin TR, Naveau J, Nicholls P, Schär N, Seneviratne CSI, Zhang X (2013) Challenges in estimating and understanding recent changes in the frequency and intensity of extreme climate and weather events. *Climate Science for Serving Society: Research, Modelling, and Prediction Priorities*: 339-389. http://dx.doi.org/10.1007/978-94-007-6692-1_13.

Xu ZX, Takeuchi K, Ishidaira H (2003) Monotonic trend and step changes in Japanese precipitation. *Journal of Hydrology* 279(1-4):144-150. [https://doi.org/10.1016/S0022-1694\(03\)00178-1](https://doi.org/10.1016/S0022-1694(03)00178-1).

Chapter 3 Trends and Variability of Temperatures in the Eastern Province of Rwanda

This Chapter reproduces the content of our published paper (<https://doi.org/10.1002/joc.8793>)

3.1 Introduction

During the last decades, several studies have indicated that the Earth's surface has experienced an increase in temperature in many parts of the world. The global average temperature increase, commonly referred to as global warming, has been observed since the Industrial Revolution, with significant warming recorded in recent decades (IPCC 2021). This warming is primarily driven by human-induced greenhouse gas emissions, with natural factors having a minimal impact on recent climate changes (IPCC 2021). The magnitude of the observed increase in temperature varies from one area to another, depending on several factors, including the topography, land use, and land cover (Vicente-Serrano 2007; Hansen et al. 2010; Revadekar et al. 2013). The global warming linked to climate change has led to significant changes in the climate system in many areas (IPCC 2022). Changes in sea level, precipitation patterns, and increases in the occurrence and intensity of extreme weather events such as floods and droughts constitute the most frequent impacts of climate change (IPCC 2023). These changes have caused considerable impacts worldwide on the environment, the economy, and society.

Studying temperature trends and variability has captured the attention of numerous researchers for a variety of reasons. Firstly, temperature changes are an indicator of climate change (Safeeq et al. 2013). Secondly, temperature changes have a significant impact on important sectors such as agriculture (Walther et al. 2002; FAO 2018; Safari and Sebaziga 2023), health (Ndenga et al. 2006; Carreras et al. 2015; Jang and Chun 2021), and food security (Meehl et al. 2000; Iqbal et al. 2016).

Africa is a continent noticeable by climatic contrasts and known for its ecological diversity, encompassing distinct geographical regions, each bearing unique climatic marks (Mahli and Wright 2004). It is the most vulnerable continent on Earth to the effects of climate change (IPCC 2007). This vulnerability, which is increasing in most African countries, is due to a range of factors that include limitations in adaptive and mitigation capacity, high dependence on ecosystem goods for livelihoods, and less developed agricultural production systems (Collier

et al. 2008; Dunning et al. 2016; WMO 2019; IPCC 2022). During recent decades, the East African region, including Rwanda, has experienced the effects of climate change, which have considerably affected the socio-economic well-being of the population and the environment (Herold 2017; Nicholson 2017; Vellinga and Milton 2018; Choi 2022). Drought is the most significant climate-induced stressor in East Africa, with its frequency, intensity, and duration increasing in recent years (Russo et al. 2016; Ayugi et al. 2019). This has resulted in water scarcity and agricultural production failures, to name a few, leading to famine and food poverty (Richardson et al. 2022). Furthermore, as the climate warms, health illnesses such as malaria are expected to affect a large number of people in East Africa (Zhou et al. 2004).

Rwanda, being part of the Eastern African region, has been subject to climate change and its impacts (Sebaziga et al. 2022; Rwema et al. 2025). Several studies have been conducted to analyse trends of temperature and variability in Rwanda using either station data or gridded data for different periods. Using station data, Safari (2012) analysed trends of annual mean temperatures over five sites distributed in the country during the period 1958-2010. An abrupt change was found around 1977-1979, followed by an increasing trend. The City of Kigali recorded the highest significant temperature increase of approximately 1.5 °C from the period following 1977-1979 to 2010. Ngarukiyimana et al. (2021), with station data, studied changes in maximum and minimum surface air temperature over 24 sites during 1961-2014 in Rwanda. Significant positive trends in both maximum and minimum temperatures were observed in most of the sites since the early 1980s. Haggag et al. (2016) examined observational data of air temperature and precipitation data from 6 sites in Rwanda during 1964-2010. A significant trend in temperature was observed in almost all sites, but no trend was found for rainfall. Using gridded time series of observed daily temperatures displayed on a network of 4 km resolution over the country during the period spanning the years 1983-2022, Safari and Sebaziga (2023) analysed trends and variabilities of mean seasonal temperatures. They found statistically significant positive trends of minimum temperature for the long dry season (i.e., June-July-August) and the short rainy season (i.e., September-October-November-December). The increase in cold days, alongside warm nights and warm days, was also found to be statistically significant.

Climate change has caused enormous impacts on infrastructure and agriculture, and livestock activities in Rwanda, particularly Eastern region (Uwimbabazi et al. 2022). The Eastern part of Rwanda plays an important role in the country's economy owing to its major contribution to

agricultural and livestock production (RAB 2020; NISR 2023A). However, this region has experienced climate-related hazards such as frequent and long periods of droughts and extreme rainfall impacting the society and the economy of the country (Munyaneza et al. 2011; Mikova et al. 2015; Sarkodie et al. 2015).

In most previous studies on Rwanda climate, the Eastern part has been treated as a uniform area, neglecting crucial distinctions in micro- and topoclimatology. Very limited studies have been done so far at a small scale in Rwanda. A recent study by Sebaziga et al. (2023) on a very small scale in the Eastern Province showed that microclimate conditions have a major influence in explaining trends and variations that occur temporally within this critical zone. The consideration of microclimate zones in climate variables analysis is important for the identification of changes and their extent within different zones.

Understanding temperature patterns and variability is crucial for informing policymakers and decision-makers in devising effective climate change mitigation and adaptation strategies. To this end, climate data-driven tools play a pivotal role in pinpointing areas most susceptible to the impacts of climate change. By leveraging such tools, decision-makers can strategically allocate resources to support the most vulnerable communities, enhancing their resilience and bolstering efforts to adapt to the challenges posed by climate change. The Eastern region needs to be studied carefully due to its particular climate characteristics, such as high temperature and particular topography. The spatial difference in temperature trends and variations that result from the difference in microclimatic conditions needs to be well understood.

This study aims to investigate air temperature trends and variations over the Eastern Province of Rwanda, through analysis of the identified optimal near-homogeneous zones. Data used in the present study were provided by the Rwanda Meteorology Agency. They consisted of a time series of daily rainfall and minimum (T_n), maximum (T_x), and mean (T) temperatures displayed on a grid of 4km resolution for rainfall and 5km for temperatures. This paper is structured as follows: after the introduction part, in Section 2, the methods and data are explained. In Section 3, results are presented and discussed in Section 4, and then go on to the conclusion in Section 5.

3.2 Data and Methods

3.2.1 Study area and data

Among the five provinces that compose Rwanda, the Eastern Province is the largest with 9,813 km² (see Figure 3.1a). It is also the first with a large part of national farming lands. Compared with other provinces, the Eastern Province was ranked number one after the 5th population and housing census of 2022, with the highest population (3,563,145) (representing 26.9 % of the total Rwandan population). On the other side, it remains the last in population density, with 433 inhabitants per km² (NISR 2023a). The climate over the Eastern Province is characterised by high annual mean temperature (above 20 °C), which varies with topography, alongside low annual rainfall of less than 1000 mm. Characterised by its lowland topography, with elevations typically below 1500 meters, the region features a gradual decline in altitude from West to East (see Figure 3.1b), with few noticeable hills or mountains, particularly in the Southeastern area (i.e., Kirehe district). This topographical profile creates an environment that is highly conducive to agriculture and cattle rearing, making it an ideal area for these activities. Currently, it plays an indispensable role in the country's economy through the production of staple food and animal production (MINAGRI 2023; NISR 2023b). Similar to other regions, the economic activities follow the two main rainy seasons available in Rwanda: March to May (MAM), and September to December (SOND) (Ntwali et al., 2016; Nicholson, 2018). In the agricultural context, the SOND corresponds to season A, while MAM corresponds to season B. The fluctuation in climate variables such as temperature and rainfall in the above seasons affects the production of important sectors, including agriculture.

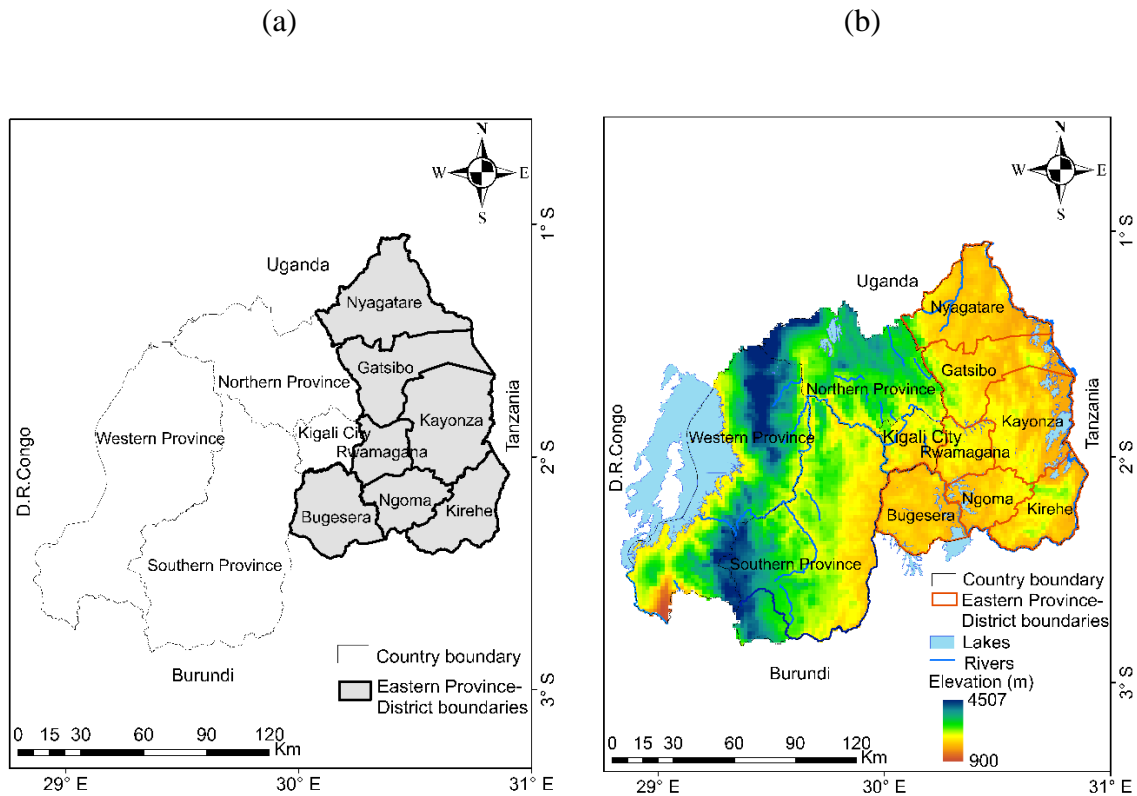


Figure 3.1 Geographical location of the study area. Panel (a) displays the study area highlighted in grey on the map of Rwanda, while panel (b) features a topographic map illustrating the area's elevation and terrain.

Daily rainfall and minimum, maximum, and mean temperatures data displayed on a grid cell of 4km resolution for rainfall and 5km for temperatures for the period 1983-2021 were obtained from the Rwanda Meteorology Agency (Meteo Rwanda 2023). The gridded datasets were reconstructed at Meteo Rwanda following the methodologies established by Dinku et al. (2014), Siebert et al. (2019), and Meteo Rwanda (2024). This process integrated station observations with satellite data, correcting for average climatological biases derived from records spanning 1981 to 1993. Additionally, interpolation and standard merging techniques were applied when station data were accessible, resulting in a comprehensive and dependable dataset suitable for further climatic research. Stringent quality control measures were implemented to ensure data integrity, which included verifying station coordinates, identifying outliers, and evaluating the homogeneity of time series data (Meteo Rwanda 2024). This dataset has been employed in numerous studies at both national and regional levels, including research conducted by Sebaziga et al. (2020), Uwimbabazi et al. (2022), Sebaziga et al. (2022), Safari and Sebaziga (2023), and Sebaziga et al. (2023).

3.2.2 Methods

a. Microclimatic zone identification

In this study, a clustering technique is used to identify microclimatic zones with respect to both annual mean rainfall and minimum and maximum temperature variables at each grid cell of the area of study. Clustering, sometimes called cluster analysis, is usually used to group data into structures (groups or clusters) that are more easily understood and manipulated without predefined classes. In this way, similar elements are found in each group, and at the same time, they show a distinct behavior concerning elements found in other groups. Cluster analysis and its applications are used in a wide range of domains spanning from linguistics, social sciences, and electrical engineering to atmospheric and climate sciences (Webb and Copsey 2011). Two categories of commonly used methods of clustering are found in literature (Theodoridis and Koutroumbas 2008): i) Hierarchical Clustering, also known as Hierarchical Cluster Analysis (Ward 1963; Székely and Rizzo 2005; Nielsen 2016; Fernández and Gómez 2020); ii) Partitioning Methods, including Self-Organizing Maps comprising a neural network-based model for data clustering (Kohonen, 2001); iii) and K-means (Alsabti et al. 1997; Shi et al. 2010; Trupti et al. 2013). The K-means method was opted to be used as it has been shown to be effective in producing good clustering results for many practical applications, especially in climatology (Yokoi et al. 2011; Carvalho et al. 2016; Kömüscü et al. 2022). A detailed description of the K-means method is given below.

Let's consider $X = \{x_i | i = 1, 2, \dots, n\}$ as a data set with n data points, k as the number of clusters, μ_k as the centroid of cluster C_k where $k = 1, 2, \dots, j$, the Euclidean distance is given by the formula

$$\text{Euclidean distance} = \sqrt{\sum |x_i - \mu_k|^2}. \quad (3.1)$$

Then each data point is assigned to the closest center (i.e., centroid). After having all data classified into some clusters, each center is updated by calculating the cluster average and placing it to become a new cluster center. The procedure is repeated until there is no change in the center of the clusters.

To identify the optimal number of clusters (k) after several runs of K-means, the Elbow plot method is used (Wickramasinghe et al. 2022). The approach requires running k-means multiple times by changing the number of clusters (k) and calculating the total within the sum of squares for each k value. Then, the obtained total within the sum of squares is plotted against k , which indicates the right number of clusters where there is a bend in the curve. This implies that with the optimal number of clusters, the clustering error is minimized. The total within-cluster variation is defined as the sum of squared Euclidean distances between points and their respective centroid, represented as:

$$W(C_k) = \sum_{x_i \in C_k} (x_i - \mu_k)^2, \quad (3.2)$$

where x_i is the i^{th} data point of cluster k (C_k), and μ_k is the mean value of points in cluster k . Hence, the clustering error function is:

$$\sum_{k=1}^k W(C_k) = \sum_{k=1}^k \sum_{x_i \in C_k} (x_i - \mu_k)^2. \quad (3.3)$$

To address the drawbacks of this approach related to both the selection and position of the initial cluster centers, several runs are recommended that vary in the initial positions of the cluster centers (Likas et al. 2003). A map of the clustered zones is then used to evaluate the number of clusters and reveal patterns of spatial organisation and cluster stability. The graphical map results for various values of k , specifically 2, 3, 4, and 5, were assessed to identify which k produces optimal, distinct zones without overlap, while also considering the climatological relevance of each value.

Microclimate zones were defined based on the identified optimal number of clusters, where each cluster corresponds to a unique microclimate zone. This approach was used by Sebaziga et al. (2023) in Rwanda on a small scale to identify four near-homogeneous zones of the Kayonza district in the Eastern Province. The same approach was used by Sebaziga et al. (2024), studying the spatial variability of seasonal rainfall onset, cessation, length, and rainy days in Rwanda. For each zone, a representative time series was constituted by considering the average of the time series of all grids located in the zone under consideration. The representative time series of each zone was then analysed using the dynamic linear model.

b. The dynamic linear model for trend analysis

The Mann-Kendall test and Sen's slope test are commonly used among the existing trend detection methods in environmental and climate data analysis. The Mann-Kendall test, which is a non-parametric approach, consists of testing a hypothesis based on the test's statistics to reveal if the data follow a monotonic trend. The magnitude of the trend is obtained from Sen's Slope test. The results of trend analysis using the Mann-Kendall test and Sen's slope test may be influenced by both autocorrelation and periodicity in the data if these factors are not addressed beforehand (Hipel and McLeod 1994; Sheng and Chun 2002; Pohlert 2023). With dynamic linear model methods, this restraint can be overcome, as it allows the inclusion of periodic components in the model and allows model correlation through autoregressive components in the model. In addition, it takes into account the uncertainties in the observation. It allows uncertainty quantification and provides credibility intervals, which improve the quality of the approach.

To study the trend in this study, a dynamic regression model based on the dynamic linear model (DLM) or state space model approach (Durbin and Koopman 2012) was used. The DLM model used here consists of two following main components: i) a smooth locally linear trend and ii) an autoregressive noise. The locally linear trend allows to model smooth changes in average temperature. The autoregressive term serves to model long-term correlations that are typical in climatic time series. The state-space approach is utilised in constructing all the components. To construct a dynamic linear model, it is necessary to conceptualise it as a general linear state-space model. This model is characterised by an observation equation and a state evolution equation, serving as the means to articulate its behavior and dynamics. Using notation similar in Durbin and Koopman (2012), these equations can be expressed as:

$$y_t = F_t x_t + v_t, \quad v_t \sim N(0, V_t), \quad (3.4)$$

$$x_t = G_t x_{t-1} + w_t, \quad w_t \sim N(0, W_t), \quad (3.5)$$

where y_t is a vector of length k of observations at time t , with $t = 1, \dots, T$, and x_t is a vector of length m of the system's unobserved states at time t . The observation operator, matrix F_t ($k \times m$), connects the hidden states to the observations, and the model evolution operator, matrix G_t ($m \times m$), describes the dynamics of the concealed states. Both uncertainties represented by observation uncertainty v_t and model error w_t are Gaussian, with V_t and W_t

representing observation uncertainty covariance and model error covariance, respectively. The time index t ranges from 1 to T , representing the length of the time series to be examined. In univariate time series analysis, k is set to 1. With multivariate data, the system matrices F_t , G_t , V_t , and W_t can be used to define correlations between the observed components. As this analysis involves a linear model, it is assumed that the operators F_t and G_t are linear. However, they may change over time.

In our case of a univariate temperature time series, the DLM model consists of two parts: one for the smooth background trend and one for the autoregressive error. The discussion begins with the trend, which consists of a local level and a local trend and has two hidden states $x_t = [\mu_t, \alpha_t]^T$, where μ_t is the mean level and α_t is the change in the level from time t to $t+1$. The Gaussian stochastic terms ε_{obs} , $\varepsilon_{\text{trend}}$, and $\varepsilon_{\text{level}}$ are used for observation error and for the random dynamics of the trend and level. This gives the model equations as follows:

$$y_t = \mu_t + \varepsilon_{\text{obs}}, \quad \varepsilon_{\text{obs}} \sim N(0, \sigma_{\text{obs}}^2), \quad (3.6)$$

$$\mu_t = \mu_{t-1} + \alpha_{t-1} + \varepsilon_{\text{level}}, \quad \varepsilon_{\text{level}} \sim N(0, \sigma_{\text{level}}^2), \quad (3.7)$$

$$\alpha_t = \alpha_{t-1} + \varepsilon_{\text{trend}}, \quad \varepsilon_{\text{trend}} \sim N(0, \sigma_{\text{trend}}^2). \quad (3.8)$$

Here in the state-space formulation of the trend process, it is observed that the matrices F_t , G_t , and V_t do not depend on time, and can be written as F_{trend} , G_{trend} , and V_t , with equations (3.4) and (3.5) becoming:

$$x_t = [\mu_t, \alpha_t]^T, \quad G_{\text{trend}} = \begin{bmatrix} 1 & 1 \\ 0 & 1 \end{bmatrix}, \quad F_{\text{trend}} = [1 \ 0], \quad (3.9)$$

$$W_{\text{trend}} = \begin{bmatrix} \sigma_{\text{level}}^2 & 0 \\ 0 & \sigma_{\text{trend}}^2 \end{bmatrix}, \quad \text{and } V_t = [\sigma_{\text{obs}}^2]. \quad (3.10)$$

In addition to the time-varying local state x_t , this model has three static parameters for the error variance $[\sigma_{\text{obs}}^2, \sigma_{\text{level}}^2, \sigma_{\text{trend}}^2]$.

By selecting appropriate levels of variance for both σ_{level}^2 and the mean state μ_t , a smoothly varying background level of the time series can be shaped, allowing for the detection of

temperature variations with enhanced precision. In our analysis, the σ_{level}^2 is set to be zero, and σ_{trend}^2 is estimated from the observations. This results in a captivating integrated random walk model for the estimated mean level μ_t (Durbin and Koopman 2012).

The DLM model defined by equations (3.9) and (3.10) is very efficient for modelling smooth changes in the temperature time series. To take into account possible long-term correlation in the data, which would manifest as correlated residuals, an additional DLM component was used for a first-order autoregressive model AR(1). For the term η_t , the first-order autoregressive model used can be stated as:

$$\eta_t = \rho\eta_{t-1} + \varepsilon_{\text{AR}}, \quad \varepsilon_{\text{AR}} \sim N(0, \sigma_{\text{AR}}^2), \quad (3.11)$$

where ρ is the autoregressive coefficient, and σ_{AR}^2 is innovation variance. In state-space form, this becomes:

$$G_{\text{AR}} = [\rho], \quad F_{\text{AR}} = [1], \quad W_{\text{AR}} = [\sigma_{\text{AR}}^2]. \quad (3.12)$$

Using the observations, both ρ and σ_{AR}^2 may be estimated.

The integration of selected individual model components into bigger model evolution and observation equations becomes the next phase in the DLM model creation:

$$G = \begin{bmatrix} G_{\text{trend}} & 0 \\ 0 & G_{\text{AR}} \end{bmatrix}, \quad F = [F_{\text{trend}} \quad F_{\text{AR}}], \quad (3.13)$$

$$W = \begin{bmatrix} W_{\text{trend}} & 0 \\ 0 & W_{\text{AR}} \end{bmatrix}. \quad (3.14)$$

After the previous steps, the focus shifts towards estimating the parameters of variance (i.e. σ_{trend}^2 and σ_{AR}^2) and other model components (such as the autoregressive coefficient ρ in the G_{AR} matrix) and estimating the model states using state-space Kalman filter techniques (Laine et al. 2014).

The estimation of the unknown parameter $\theta = [\sigma_{\text{trend}}^2, \sigma_{\text{AR}}^2, \rho]$ is based on Bayesian statistical analysis for which the Kalman filter is used for the likelihood evaluation (Durbin and Koopman 2012). The implementation involves using the Markov chain Monte Carlo (MCMC) simulation algorithm to estimate the posterior distribution of θ and to account for its uncertainty in the

trend analysis. Step-by-step details on the estimation procedure of θ with this approach can be found in Laine et al. (2014).

The DLM method was used by several authors in atmospheric and climate studies, including Petris (2010); Laine et al. (2014); Mikkonen et al. (2014), and Roininen et al. (2015), to mention a few. The advantages of this method are, among others, the ability to capture smooth varying behavior in the data, handle missing data, take into consideration uncertainties in the observations, and the fact that it does not require stationarity assumptions (Gamerman 2006; Petris 2010).

c. Goodness-of-Fit Test

Goodness-of-fit test statistics are used to verify if the distribution of experimental data follows a theoretical distribution. Several methods of fitting observational data with simulated data are found in the literature. They include i) the formal statistical tests (Razali and Wah 2011; Rahman et al. 2013; Ul Hassan et al. 2019), ii) graphical methods (Coles 2001), and iii) accuracy measure methods (Moriassi et al. 2007, Chen et al. 2017, Safari et al. 2022). In this study, graphical methods and accuracy methods have been used. For graphical methods, with the DLM model, two commonly used methods focus on residual distribution and residual autocorrelation analysis (Auger-Méthé et al. 2021). As commonly used and recommended for the DLM model (Durbin and Koopman 2012), the validation is made by studying the model residuals to see if the modeling assumptions are satisfied. The first check is that the residuals have to be normally distributed. This condition is examined through a particular assessment of the normal probability plot, the Q-Q plot, which compares the quantiles of observed residuals with the quantiles derived from the theoretical Gaussian distribution. To fulfill the normality condition, in the Normal Q-Q plot, the points should be mostly aligned with no sign of large outliers (Durbin and Koopman 2012; Laine et al. 2014). The second condition to be verified is the independence of residuals. The uncorrelated model residual is examined graphically from an estimated autocorrelation function plot (ACF) (Durbin and Koopman 2012). In this plot, the residuals have to show no significant autocorrelation, as all the coefficients have to fall in the 95 % confidence interval of a significant threshold. Once the two conditions are satisfied, then the fit agrees with the assumption, and the modeling results are consistent with the data.

For accuracy methods, three powerful statistical metrics commonly used to evaluate the performance of a regression model are considered: The Mean Absolute Error (MAE), the Root Mean Square Error (RMSE), and R-squared (R^2), known as the coefficient of determination (Boyle et al. 2000; Moriasi et al. 2007). MAE measures the average absolute difference between the predicted values and the actual target values (residuals). RMSE is the square root of the variance of the residuals. Both MAE and RMSE inform how accurate the model's prediction is, and give the amount of deviation from the actual values (Auger-Méthé et al. 2016). High values indicate that the model's performance is weak. The RMSE and the MAE were calculated using the one-step-ahead prediction and the observation. The RMSE and MAE can be interpreted to reveal how well the model can predict one-time unit ahead (e.g., one year). R^2 represents the proportion of the variance in the dependent variable that is explained by the model. It indicates how close the regression line (the predicted values plotted) is to the actual data values. The R^2 was calculated using the observation and smoother local mean estimate, which tells how much of the year-to-year variability of temperature is explained by the smooth background mean estimate. The R^2 obtained from the DLM component was also compared to the R^2 computed using the Linear model (LM). This comparison was to examine how DLM differs from LM in explaining the variance in our variable. For a linear model, the R^2 value lies between 0 and 1, where 0 indicates that this model does not fit the given data and 1 indicates that the model fits perfectly to the dataset provided. However, as DLM will produce a non-linear smooth curve as the mean estimate, this could produce even negative R^2 values in the cases where the DLM mean state component alone does not provide a good fit.

The computation in this paper was performed with the R statistical software (Core Team 2021) using packages DLM (Petris 2010), FME (Soetaert and Petzoldt 2010), and Bayesplot (Gabry et al. 2019). The ArcGIS software (ESRI 2021) was used to draw maps for near-homogeneous zones and the spatial distribution of the temperature means over the study area where the kriging method was applied for interpolation.

3.3 Results

3.3.1 Spatial Distributions of Long-Term Mean Temperature and Rainfall

Figure 3.2 illustrates the spatial distribution of seasonal mean temperature, including January to February (JF) in Figure 3.2a, March to May (MAM) in Figure 3.2b, June to August (JJA) in

Figure 3.2c, September to December (SOND) in Figure 3.2d, and the annual long-term mean temperature in Figure 3.2e, spanning from 1983 to 2021, across Eastern Rwanda. The Northwestern part indicates lower temperatures (17-18 °C) than the remaining parts of Eastern Rwanda (18-23 °C). T presents maximum values (19-23 °C) during the JJA (Figure 3.2c) mainly in the Central-east extended to the South. The part extending from the Southwest to the Northeast presents relatively high T values in all seasons and annually. The rainfall distribution across the region exhibits a gradual decline from West to East for annual totals, as well as during the MAM and SOND seasons, as illustrated in Supplementary Material Figure S1 for the period from 1981 to 2021. Notably, the figure reveals that only a small portion of the region's Northwestern and extreme Southwestern areas is characterised by significantly lower rainfall amounts during both the MAM and SOND rainy seasons, as well as throughout the annual period.

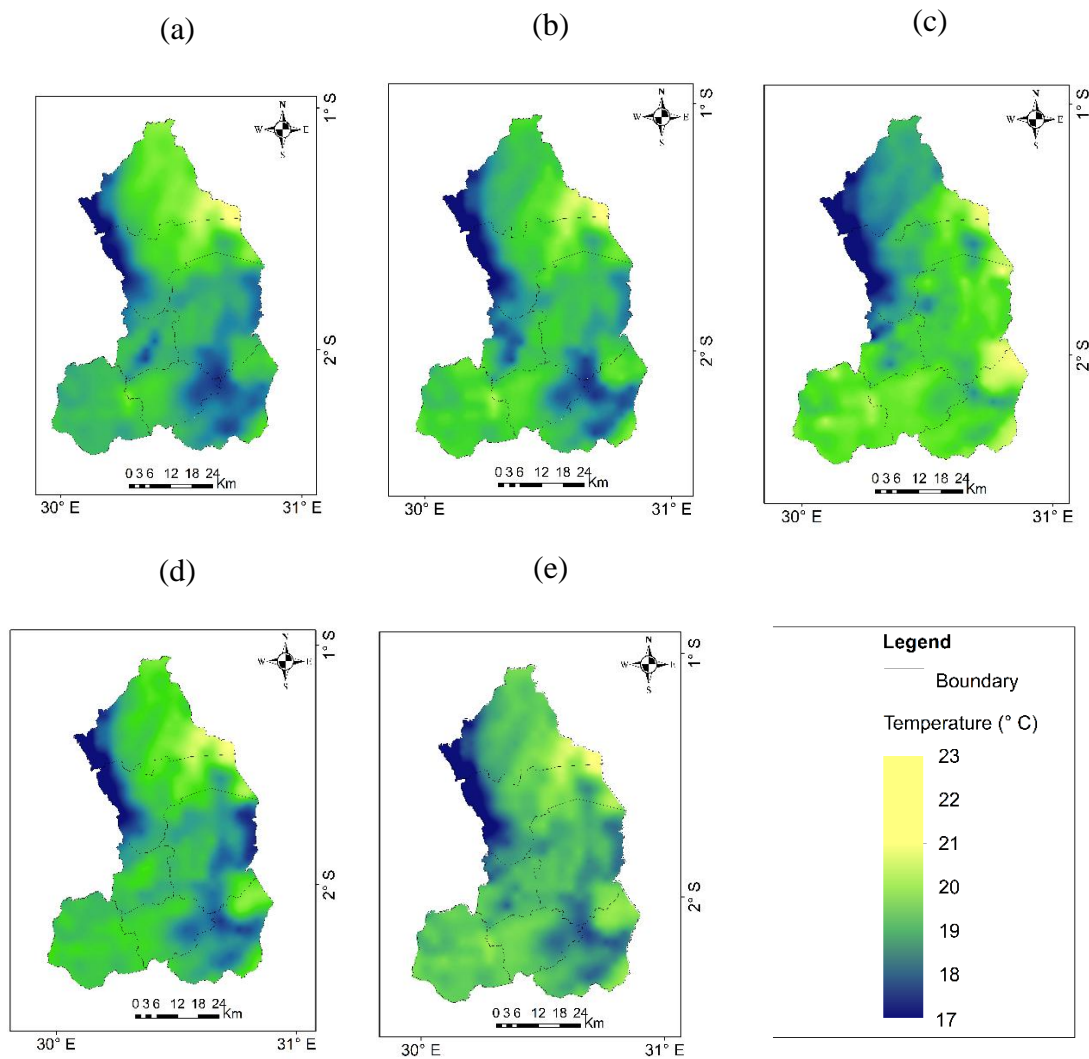


Figure 3.2 Spatial distribution of the long-term mean of Temperature (°C) over Eastern Rwanda for January-February (JF) (a), March-April-May (MAM) (b), June-July-August (JJA) (c), September-October-November-December (SOND) (d), and Annual (e) during the period of 1983–2021 (Source of data: Rwanda Meteorology Agency).

3.3.2 K-means clustering

Figure 3.3 presents the Elbow plot, which indicates that the optimal number of clusters is $k=3$. The clustering structure is further illustrated in the maps of clustered zones shown in Figure 3.4 for various values of k . As k increases, the regional partitioning expands, providing more detailed information about the study area. However, the interpretation becomes increasingly complex beyond a certain point, as additional clusters may not be distinct and can overlap significantly. With $k=3$, three clear clusters producing a distinct spatial partition of zones were

identified: zone one comprises 50 grid cells, zone two includes 353 grid cells, and zone three consists of 167 grid cells. When k increases to 4 or 5, a proliferation of clusters is observed; however, this leads to overlapping zones where elements from one zone are found within another. This overlap complicates interpretation and diminishes the clarity of the clustering results. In the following section and throughout the manuscript, the analysis focuses on the three distinct optimal zones of the Eastern Province, resulting from $k=3$.

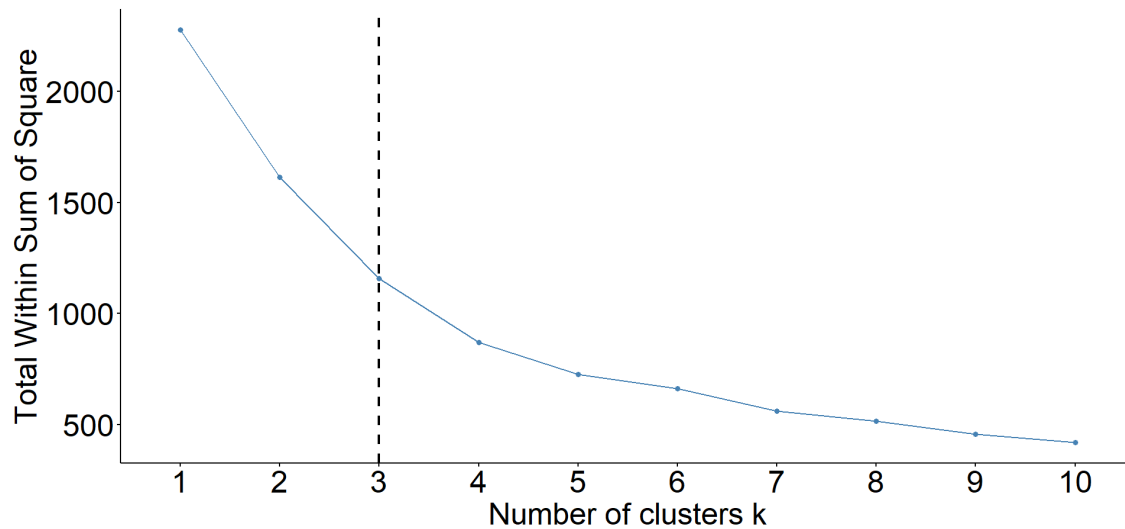


Figure 3.3 The Elbow plot shows the optimal cluster number with the vertical dotted line showing the Elbow joint corresponding to the chosen number of clusters ($k=3$).

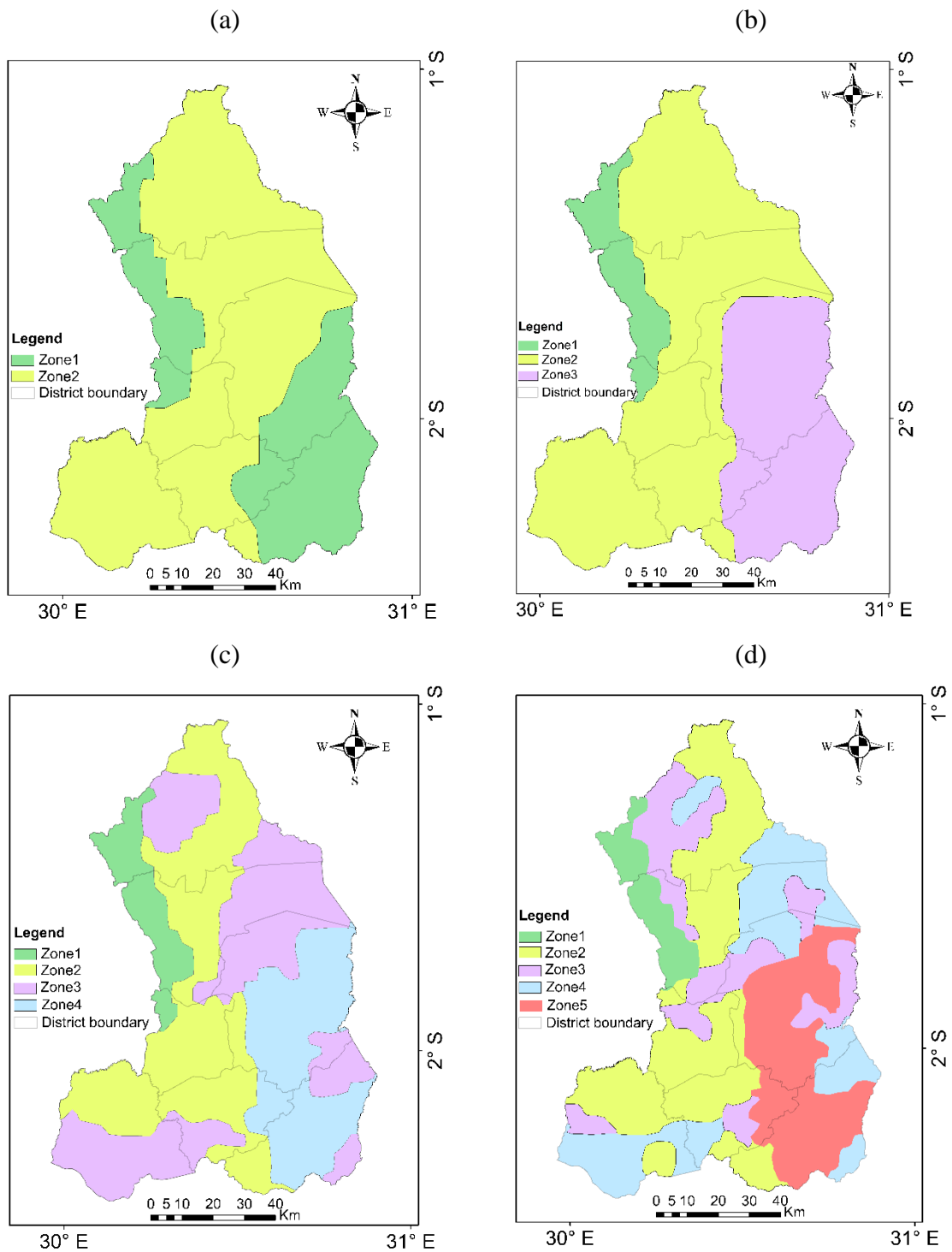


Figure 3.4 Maps of clustered zones by number of clusters (k). This figure shows the partition of Eastern Province for different cluster counts: (a) $k=2$, (b) $k=3$, (c) $k=4$, and (d) $k=5$. It demonstrates how the regional partitioning changes as the number of clusters increases, revealing patterns of spatial organisation and cluster stability.

3.3.3 Near Homogeneous zones

The spatial distribution of grid cells, each characterised by specific cluster class properties, produced a map displaying three distinct, nearly homogeneous zones within the Eastern Province. Figure 3.5 illustrates these near-homogeneous zones. Zone 1, named Northwestern, covers a small part extending from the central west to the northwest. It touches three districts: Nyagatare, Gatsibo, and Rwamagana. Zone 2, named Central, is the largest, extending from the Southwest to the Central and Northeast. It passes through all seven districts of the Eastern Province of Rwanda. Zone 3, named Southeastern, is located in part extending from the Southeast to the Central-eastern region, touching three districts: Kayonza, Ngoma, and Kirehe.

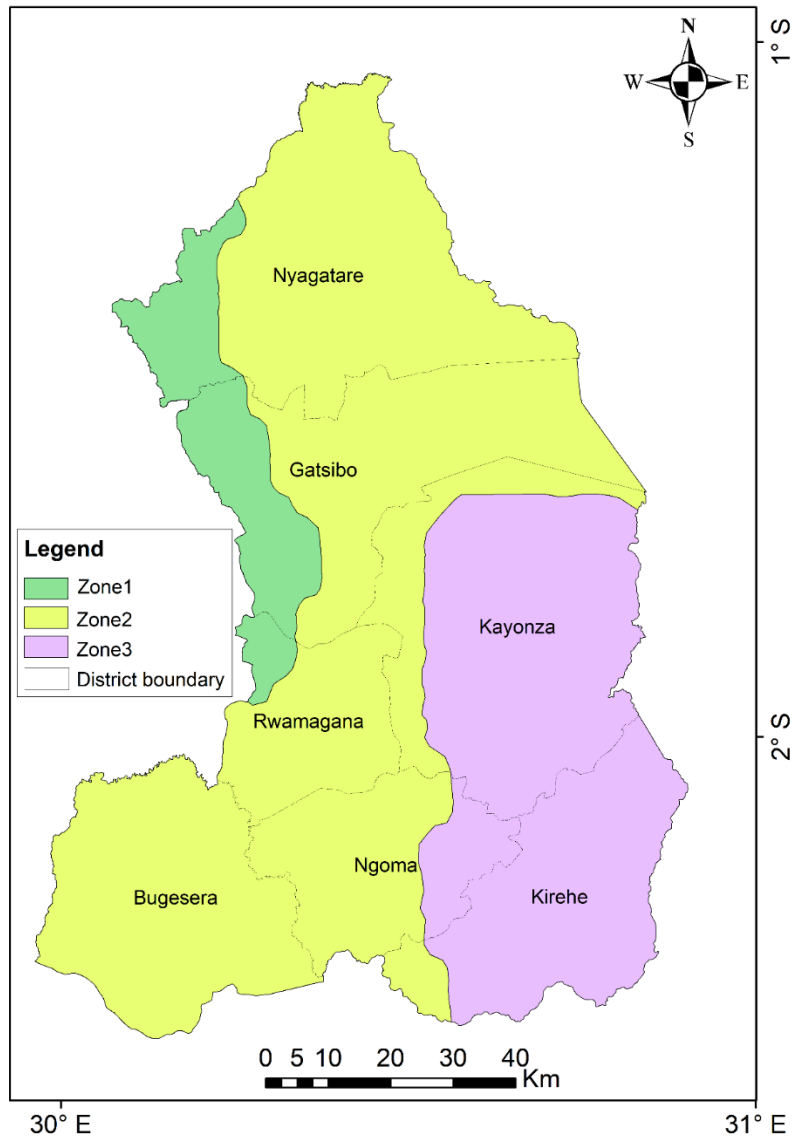


Figure 3.5 Climatic zone classification of the Eastern Province based on temperature and rainfall data for 1983-2021. The identified three near-homogeneous zones named Zone1: Northwestern, Zone2: Central, and Zone3: Southeastern are highlighted in green, yellow, and magenta, respectively.

3.3.4 Goodness-of-Fit

The validation diagnostic results for the Dynamic Linear Model (DLM) are detailed in the supplementary material. The empirical quantiles of the residuals plotted against their theoretical quantiles (Figure S2) demonstrate a strong adherence to the normality condition. Additionally, the autocorrelation function (ACF) plot of the residuals (Figure S3) reveals no significant autocorrelation, indicating independence among the residuals. Further analysis of

the prior and marginal posterior distributions (Figure S4) for three unknown model parameters (trend change standard deviation σ_{trend} , autoregressive standard deviation σ_{AR} , and autoregressive coefficient ρ) suggests that the posterior distributions are predominantly influenced by the data rather than the priors. Notably, the trend's standard deviation is assessed as relatively small, highlighting a preference for exploring smooth background variability. The autoregressive parameters also exhibit narrow posterior distributions compared to their priors, indicating precise data-driven estimations. Overall, these findings suggest a strong fit to the data. Accuracy metrics such as Mean Absolute Error (MAE), Root Mean Square Error (RMSE), and R-squared (\mathbf{R}^2) are also included in the supplementary material (see Tables S1, S2, S3, and S4). In all three zones and the Eastern Province, the computed error metrics for monthly and seasonal (annual) mean Tn demonstrate a robust model fit when compared to Tx and T. In most instances, the coefficient of determination (\mathbf{R}^2) from the DLM significantly exceeds that of the linear model (LM), further underscoring the effectiveness of our approach.

3.3.5 Trends and Variability in Temperatures

Table 3.2 and Figure 3.6, along with Figures S5-S8, illustrate the changes and non-linear trends in the averaged annual and seasonal means of Tx, Tn, and T series across Northwestern, Central, and Southeastern zones, as well as for the entire Eastern Province of Rwanda from 1983 to 2021. In the Eastern Province, the seasonal mean of Tn shows a greater increase (1.71-3.37 °C) compared to Tx and T across all seasons, with the most significant rise occurring in the JJA season at 3.37 °C [1.75-4.81]. The analysis of time-varying trends (see Figure S4) reveals notable nonlinearity in Tn, with no significant change observed from 1990 to 2010, followed by a marked warming trend thereafter. In terms of micro-climate zones, Tn increases during the JF season across all zones, with the highest change of 1.97 °C [0.90-3.14] recorded in the Northwestern zone, while the Southeastern zone exhibits the lowest change at 1.21 °C [-0.07-2.37]. Similar non-linear patterns are evident in all zones, particularly with a pronounced warming trend after 2010. During the MAM season, increases in Tn (0.93-3.11 °C) are observed across all zones, with the Northwestern zone experiencing the most significant rise. The same non-linear trend with strong warming after 2010 is noted in all zones. In the JJA season, Tn demonstrates a significant upward trend throughout the zones, with temperature changes ranging from 1.64 °C to 4.07 °C; the Northwestern zone is warming faster than the others. The SOND season also shows substantial changes in Tn, ranging from 1.57 °C to 3.42 °C, particularly notable in the Northwestern and Central zones. A time-varying analysis

indicates a consistent upward trend characterised by nonlinearity in Tn changes, with only slight fluctuations from 1983 to 2010, followed by a pronounced warming phase thereafter.

Table 3.1 Changes (in °C) and standard deviations of the averaged seasonal and annual mean of Tx, Tn, and T in Northwestern, Central, and Southeastern zones and the whole Eastern Province of Rwanda during the period 1983-2021

Northwestern zone						
	Tx		Tn		T	
Season	Change	SD	Change	SD	Change	SD
JF	1.29 [-0.24-2.74]	0.80	1.97 [0.90-3.14]	0.58	1.49 [0.31-2.64]	0.58
MAM	0.46 [-1.28-2.22]	0.73	3.11 [1.68-4.52]	0.88	1.63 [0.27-3.05]	0.66
JJA	0.99 [-0.26-2.28]	0.64	4.07 [2.26-6.08]	1.15	2.39 [0.89-3.90]	0.80
SOND	-0.00 [-0.02-0.02]	0.66	3.42 [1.54-5.22]	0.82	1.12 [-0.34-2.51]	0.54
Annual	0.46 [-1.03-1.98]	0.50	3.62 [1.92-5.29]	0.83	1.81 [0.45-3.08]	0.55
Central zone						
	Tx		Tn		T	
	Change	SD	Change	SD	Change	SD
JF	0.33 [-1.63-2.04]	0.85	1.81 [0.55-3.07]	0.55	1.001 [-0.43-2.31]	0.56
MAM	-0.21 [-1.95-1.50]	0.74	2.18 [0.99-3.49]	0.67	0.75 [-0.35-1.87]	0.52
JJA	0.67 [-0.52-1.84]	0.52	2.96 [1.60-4.39]	0.69	1.52 [0.53-2.56]	0.50
SOND	-0.65 [-2.17-0.91]	0.74	2.53 [0.80-4.40]	0.63	0.50 [-0.70-1.72]	0.50
Annual	-0.01 [-1.45-1.48]	0.48	2.70 [1.21-4.11]	0.59	1.06 [-0.06-2.08]	0.38

Southeastern zone						
	T_x		T_n		T	
	Change	SD	Change	SD	Change	SD
JF	1.42 [-0.39-3.14]	0.97	1.21 [-0.07-2.37]	0.51	1.24 [-0.05-2.51]	0.62
MAM	1.04 [-1.02-3.21]	0.88	0.93 [-0.11-2.01]	0.49	0.97 [-0.20-2.30]	0.57
JJA	1.01 [-0.51-2.44]	0.64	1.64 [0.38-2.73]	0.49	1.23 [0.26-2.25]	0.45
SOND	0.49 [-1.38-2.33]	0.79	1.57 [-0.03-3.20]	0.52	0.77 [-0.57-2.13]	0.54
Annual	1.07 [-0.56-2.78]	0.63	1.58 [0.29-2.85]	0.42	1.18 [0.08-2.21]	0.41
East						
	T_x		T_n		T	
	Change	SD	Change	SD	Change	SD
JF	0.88 [-1.02-2.74]	0.86	1.71 [0.66-2.83]	0.56	1.47 [0.28-2.62]	0.59
MAM	0.16 [-1.60-2.00]	0.74	2.37 [1.07-3.68]	0.70	1.69 [0.22-2.93]	0.57
JJA	0.85 [-0.27-1.97]	0.55	3.37 [1.75-4.81]	0.81	2.37 [0.94-3.68]	0.58
SOND	-0.37 [-2.17-1.42]	0.71	2.72 [1.10-4.46]	0.65	1.17 [-0.18-2.47]	0.52
Annual	0.30 [-1.31-1.71]	0.49	2.95 [1.64-4.45]	0.63	1.87 [0.61-3.19]	0.44

The average temperature (T_x) across the entire Eastern region shows a relatively low and non-significant increase of less than 1 °C during the JF, MAM, and JJA seasons. In contrast, there

is a decrease in SOND, with a change of $-0.37\text{ }^{\circ}\text{C}$ [-2.17 to 1.42]. The temporal change in T_x does not vary much over time when compared to T_n and T . When comparing the zones, the Southeastern zone exhibits the highest, though non-significant, positive change in T_x , ranging from 1.01 to $1.42\text{ }^{\circ}\text{C}$ during the JF, MAM, and JJA seasons. A decreasing trend in seasonal and annual mean T_x is observed only in the Northwestern zone (during SOND) and the Central zone (in MAM, SOND, and annually), with a more pronounced decline occurring after 2015 compared to earlier years.

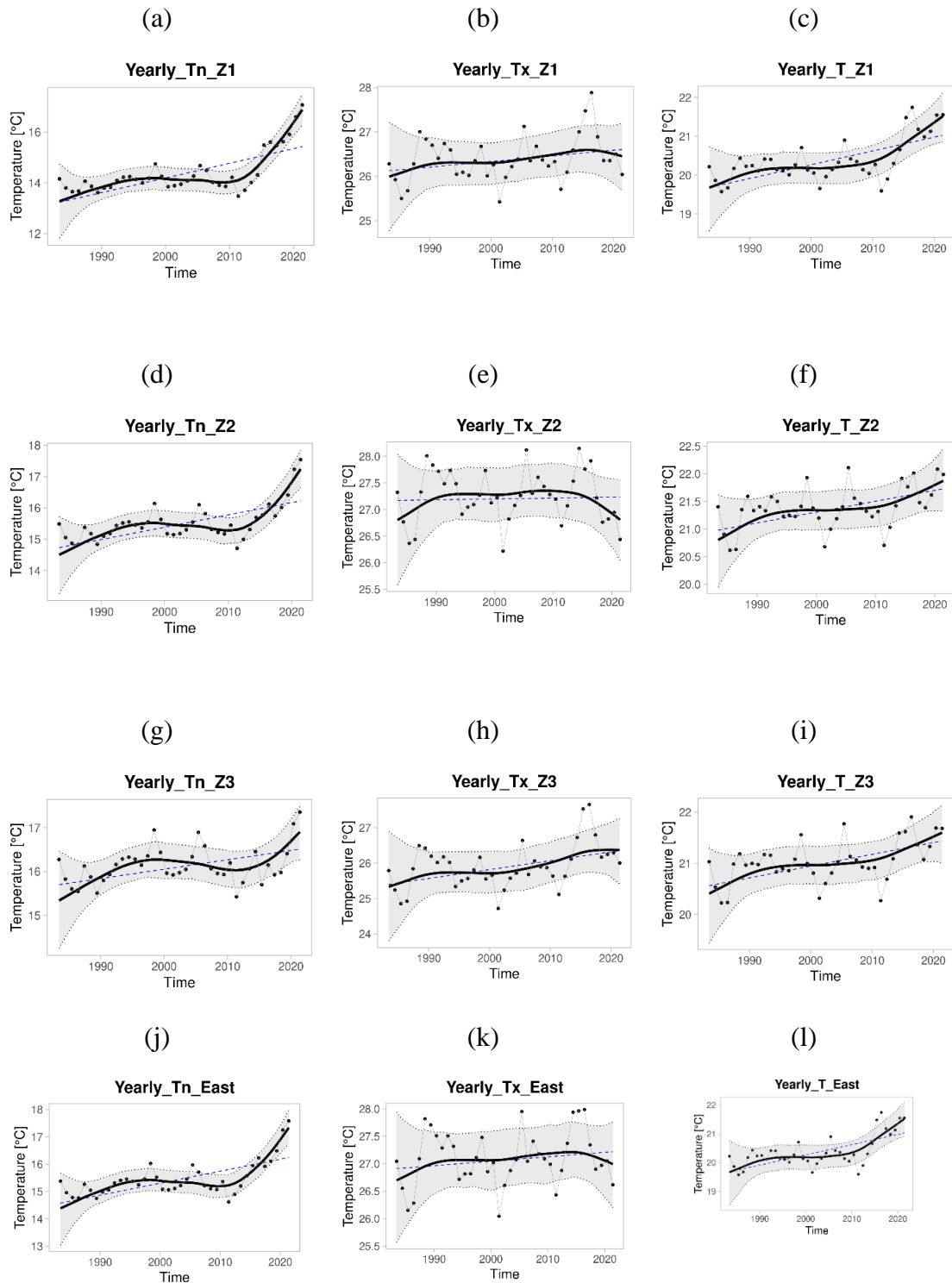


Figure 3.6 DLM fit for yearly average temperature during 1983-2021. The observed yearly average temperature (black dots) is displayed together with the background mean level μ_t (black solid line). The smooth black solid line represents the estimated temperature trend together with a 95 % probability envelope. The dashed blue line is the linear trend. The Z1, Z2, and Z3, respectively, stand for the Northwestern, Central, and Southeastern zones. The bottom panel in each column indicates the results obtained from the east.

In all zones and throughout the Eastern Province, the seasonal (annual) mean temperature (T) has been increasing, with the Northwestern zone experiencing a greater magnitude of change than the other zones and the overall region. Generally, the increases in monthly and seasonal (annual) mean T in the Northwestern zone, Central zone, and the entire Eastern Province can be attributed to rising monthly and seasonal (annual) minimum temperature (Tn). However, in the Southeastern zone, the increases observed during the JF and MAM seasons, as well as their respective monthly means, are primarily due to rising seasonal and monthly maximum temperature (Tx). Overall, the temporal changes in mean T indicate a strong influence of Tn, which aligns with its variation across months, seasons, and annually in most zones as well as in the entire region.

Throughout the Eastern Province and its three zones, the standard deviations for monthly and seasonal (annual) mean temperatures during the study period are generally low, typically less than 1 °C. This indicates that variations in these temperature measures are not significant. Across all zones, the magnitude of the standard deviation for maximum temperatures (Tx) during the study period was consistently greater than that for minimum temperatures (Tn) and overall temperatures (T) across all seasons and years.

Table S5 and Figures S9-S11 present the changes (trends) and standard deviations of the averaged monthly mean of Tx, Tn, and T in the Northwestern, Central, and Southeastern zones, as well as for the entire Eastern Province of Rwanda during the period 1983-2021. At the regional level of the Eastern Province, high increases in monthly mean Tn ranging between 2.19 °C [0.97-3.36] (in January) and 3.53 °C [2.01-5.09] (in November) are observed in January, March, and between May and November. The monthly mean T shows relatively low increases in almost all months except March and between June and August, with temperatures ranging between 2.17 °C [0.14-4.30] (in March) and 2.38 °C [0.99-3.69] (in July). Across all three zones, an increase in the individual monthly mean Tn is observed in all months.

3.4 Discussion

The identification of optimal number of cluster $k=3$ strikes a balance between detail and interpretability, allowing for meaningful distinctions among the clusters without overwhelming complexity. From a climatological perspective, $k=3$ effectively captures the observed patterns in spatial temperature distribution by delineating areas with low, moderate, and high temperatures. Additionally, it reflects the topographical differences across the region,

distinguishing between high-elevation zones and lowland areas. The analysis identified three distinct zones characterised by their unique topographical features and climatic conditions. Zone 1 (Northwestern) is situated near the central plateau in the northwest, nestled in the shadow of the Northern highlands. This region is marked by high elevations and cooler temperatures, as noted by Safari (2012). The elevation plays a significant role in shaping the local climate, leading to a distinct ecological environment that supports specific flora and fauna. Zone 2 (Central) encompasses areas of moderate elevation in the Eastern region, characterised by numerous lakes and the Eastern plain (Henniger 2013; Ekane et al. 2016). This zone's topography contributes to its unique hydrology and biodiversity. The presence of lakes not only influences local weather patterns but also provides critical habitats for various species. Zone 3 (Southeastern) extends into parts of Akagera National Park, featuring numerous inland lakes and relatively high hills, particularly in the Southeastern areas such as the Kirehe district. In the Eastern Province, mean temperatures vary with topography: areas of higher elevation tend to be cooler, while the lowlands experience warmer temperatures. This observation aligns with findings from Safari and Ndakize (2023), which indicate that temperatures in Rwanda decrease gradually with increasing elevation across all seasons. Verdoodt and Van Ranst (2003) indicate a similar pattern that temperature increases gradually from the West to the Eastern region. This relationship underscores how the country's hilly and mountainous terrain creates diverse microclimates that affect both temperature and precipitation patterns.

Increases in mean temperature have been observed across the Eastern Province in annual, seasonal, and monthly periods. The magnitude of these temperature changes varies significantly among different micro-climate zones, where distinct topographical features characterise each zone. Several studies have found that high-elevation regions are warming at an accelerated rate compared to moderate and low-elevation areas (Minder et al. 2018; Şevgin and Öztürk 2024; Zhao et al. 2024). However, other research, including work by Vuille and Bradley (2000), Pepin and Lundquist (2008), and Almazroui et al. (2013), has reported no significant correlation between warming rates and elevation. In all zones of Eastern Province, the change in T_n was increasing, and this increase in T_n was more pronounced in the Northwestern zone and Central zone compared to that of the T_x and T across various months, seasons, and years. In Northwestern zone, comprising mainly part of Nyagatare and Gatsibo districts in the northwest, the mean seasonal T_n changes are notably higher than in other zones across all seasons, exacerbating vulnerability to the impacts of the substantial increase in T_n

within this area. Several research efforts have linked the increased rate of minimum temperatures (T_n) relative to maximum temperatures (T_x) to factors such as soil properties, nighttime radiative cooling, and the stability of the surface layer (Ahmed et al. 2017; Chechin et al. 2019). An increase in temperature has been identified as a consequence of rising greenhouse gas levels (Kweku et al. 2018; Allabakash and Lim, 2022). The temperature trend in the Eastern Province exhibits a complex, non-linear pattern characterised by time-varying changes. Minimum temperatures (T_n) show an increasing trend, with a notable period of slight or no change from 1990 to 2010, followed by a phase of strong and continuous rise across all monthly, seasonal, and annual datasets. This significant non-linearity in T_n aligns with global warming trends, indicating that the rate of warming in recent decades has accelerated significantly compared to the average rate since the early 20th century. In fact, all ten of the warmest years recorded in history have occurred within the last decade (2014-2023)(NOAA 2024).

Factors including atmospheric and oceanic conditions (e.g., Sea Surface Temperatures), land cover changes, and locally based processes around a given site are major drivers of temperature variations over time and scales (Klutse et al. 2016). In the East Africa region, where Rwanda is situated, studies (Gu and Adler 2013; Dai 2016; Safari and Sebaziga 2023) have highlighted that temperature variability is generally linked to natural internal factors like the El Niño Southern Oscillation and the Inter-decadal Pacific Oscillation. Variations in temperature trends and magnitudes across different zones within the same region indicate the inadequacy of generalizing these patterns. Therefore, it is imperative to tailor adaptation and mitigation strategies to each specific zone. Developing customized coping and adaptation measures aligned with the experiences of each zone is crucial to effectively address the needs of vulnerable communities (Vervoort et al. 2014).

The observed significant positive trends in both maximum temperatures (T_x) and minimum temperatures (T_n) align with findings from Ngarukiyimana et al. (2021), who conducted a trend analysis of Rwanda's seasonal and annual T_x and T_n from 1961 to 2014, utilising data from 24 weather stations categorized into three elevation-based regions: R1 (1000-1500 m), R2 (1500-2000 m), and R3 (\geq 2000 m). Their study reported a notable warming trend in T_x and T_n across Rwanda at varying rates in the three regions, particularly since the early 1980s. Additionally, the temperature variations were distinct on both seasonal and annual scales. Notably, Ngarukiyimana et al. found that higher elevation zones (R3) are warming more

rapidly than lower elevation areas, with Tn increasing at a faster rate than Tx in R3, amounting to a total change of 1.46 °C vs. 0.38 °C during March to May, and 1.57 °C vs. 0.22 °C during October to December for 1961-2014. Similarly, the significant positive trends observed in both maximum temperatures and minimum temperatures are consistent with findings from Safari (2012), who conducted a trend analysis of Rwanda's mean annual temperature from 1958 to 2010 using data from five observatories. Safari (2012) identified a notable warming trend beginning after 1977-1979 to 2010, with the highest change of increase of approximately 1.5 °C in Kigali city. Our findings also resonate with the study conducted by Uwimbabazi et al. (2022), which examined trends in air surface temperature across Rwanda using data from 14 meteorological stations over the period from 1981 to 2020. This research reported a significant increasing change in surface air temperature during the MAM (0.76 °C), OND (0.80 °C), and annual (0.92 °C) time scales, noting that the last decade (2010–2020) experienced a sharp rise in temperatures across Rwanda. Furthermore, Safari and Ndakize (2023) indicate a statistically significant upward trend in Tn across Rwanda, with changes of 0.68 °C during the long dry season (JJA) and 0.80 °C during the short rainy season (SOND) from 1983 to 2022. Our study aligns with these findings, further supporting the evidence of increasing minimum temperatures in the region. Finally, in the equatorial region of Eastern Africa, where Rwanda is located, the Inter-Governmental Panel on Climate Change (IPCC 2014) has reported a significant increase in temperature since the early 1980s (Anyah and Qiu 2012). Specifically, reporting that Rwanda experienced an average temperature rise of 2.43 °C from 1961 to 2014. This notable increase is consistent with our findings, which also confirm a temperature rise in Eastern Rwanda.

The discrepancy in the observed trend magnitudes may be attributed to several factors, including the different datasets used, the varying number of stations and grids, and the length of time series analysed. Some studies did not include data from the past decade (2014-2023), which contains the ten warmest years on record (NOAA 2024). Additionally, our study focuses on the Eastern Province, which is the hottest region in Rwanda and exhibits a higher temperature magnitude compared to other areas of the country.

3.5 Conclusion

This study investigates the trends and variability of maximum, minimum, and mean temperatures across the Eastern Province of Rwanda and its derived near-homogeneous zones from 1983 to 2021, utilising a dynamic linear state-space model for trend analysis and standard

deviation for assessing variability. The K-means clustering method has been applied to derive near-homogeneous climatic zones by clustering rainfall and temperature data. As a clustering result, the Eastern Province is split into three distinct optimal zones: 1. Northwestern, 2. Central, and 3. Southeastern. The trend analysis reveals significant increases in both annual minimum and mean temperatures across the Eastern Province. Notably, the minimum temperature exhibited greater positive changes than both maximum and mean temperatures throughout all seasons, with the June-July-August season showing the most pronounced trend. The time-varying trends in minimum temperature indicate a marked nonlinearity, characterized by a stable temperature phase from 1990 to 2010, followed by accelerated warming post-2010. In terms of regional impacts, the Northwestern zone experienced substantial seasonal increases in minimum temperature, heightening its vulnerability to climate-related effects. Conversely, the Southeastern zone recorded significant rises in maximum temperature, which also escalates its susceptibility to the consequences of rising temperature compared to other regions. Furthermore, maximum temperatures demonstrated greater variability, as evidenced by higher standard deviation values across monthly, seasonal, and annual data in all zones, as well as at the scale of the Eastern Province.

Studying temperature changes across near-homogeneous climatic zones within Eastern Rwanda is crucial for identifying areas most susceptible to climate change impacts. This analysis provides valuable insights for policymakers to develop effective mitigation and adaptation strategies tailored to the specific needs of vulnerable communities. Additional research is necessary to investigate the factors contributing to observed temperature increases and understand the effects of climate change on key economic sectors like agriculture and livestock. Utilising various methodologies, future studies can explore microclimatic zones and changes specific to Eastern Rwanda.

Supporting information for Chapter 3

The additional information is provided, and the list of figures and tables included are:

Figure S1 Spatial distribution of MAM (a), SOND (b) and annual (c) mean rainfall for the period of 1981 to 2021.

Figure S2 Model diagnostic plot: Normal probability plot for the residuals.

Figure S3 Model diagnostic plot: Estimated autocorrelation function (ACF) plot of the DLM residuals.

Figure S4 Model diagnostic plot: Prior distributions (dashed line) and marginal posterior distributions (histogram) for three unknown model parameters: trend change standard deviation σ_{trend} , autoregressive standard deviation σ_{AR} , and autoregressive coefficient ρ .

Figure S5 DLM fit for JF (January-February) season average (T), minimum (Tn), and maximum (Tx) temperature during 1983-2021 in all zones.

Figure S6 DLM fit for MAM (March-April-May) season average (T), minimum (Tn), and maximum (Tx) temperature during 1983-2021 in all zones.

Figure S7 DLM fit for JJA (June-July-August) season average (T), minimum (Tn), and maximum (Tx) temperature during 1983-2021 in all zones.

Figure S8 DLM fit for SON (September-October-November-December) season average (T), minimum (Tn), and maximum (Tx) temperature during 1983-2021 in all zones.

Figure S9 DLM fit for January-December month average (T)(a), minimum (Tn)(b), and maximum (Tx)(c) temperature during 1983-2021 over the Northwestern zone.

Figure S10 DLM fit for January-December month average (T)(a), minimum (Tn)(b), and maximum (Tx)(c) temperature during 1983-2021 over the Central zone.

Figure S11 DLM fit for January-December monthly average (T)(a), minimum (Tn)(b), and maximum (Tx)(c) temperature during 1983-2021 over the Southeastern zone.

Table S1 Validation Metrics of DLM Model for Seasonal and Annual Mean Temperatures Across Zones.

Table S2 The comparison between DLM and LM models based on the coefficient of determination (R^2) computed using observations and smoother local mean estimates for DLM, and R^2 computed from LM using observations of seasonal and annual mean temperatures across zones.

Table S3 Validation Metrics of DLM Model for Monthly Mean Temperatures Across Zones.

Table S4 The comparison between DLM and LM models is based on the coefficient of determination (R^2) computed using observations and smoother local mean estimates for DLM, and R^2 computed from LM using observations of monthly mean temperatures across zones.

Table S5 Results of dynamic linear state space model: Changes (in °C), and standard deviations of the averaged monthly mean of Tx, Tn, and T in zones, as well as for the Eastern Province of Rwanda during the period 1983-2021.

Table S6 Linear Model’s results as trends (in °C/year), changes (in °C), and standard deviations of the averaged seasonal and annual mean of Tx, Tn, and T in zones, as well as for the Eastern Province of Rwanda during the period 1983-2021.

Table S7 Linear Model’s results as trends (in °C/year), changes (in °C), and standard deviations of the averaged monthly mean of Tx, Tn, and T in zones, as well as for the Eastern Province of Rwanda during the period 1983-2021.

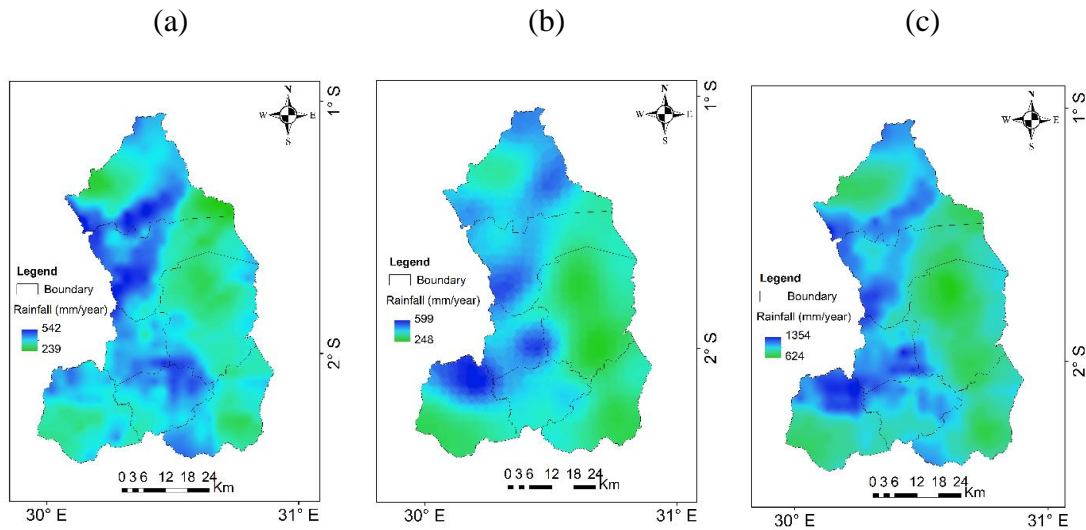


Figure S1 Spatial distribution of MAM (a), SON (b), and annual (c) mean rainfall for the period of 1981 to 2021.

1 Goodness-of-Fit

presents the plot of autocorrelation functions (ACF) for residuals in annual mean Tx, Tn, and T over the three zones of the Eastern Province. All the coefficients fall in the 95 % confidence interval illustrated by the dashed blue line representing the significant threshold for the annual mean Tx, Tn, and T in the three zones. This indicates that there is no significant autocorrelation, meaning that the residual is independent.

Figure S4 shows prior distributions and marginal posterior distributions for three unknown model parameters: trend change standard deviation σ_{trend} , autoregressive standard deviation σ_{AR} , and autoregressive coefficient ρ in annual mean Tn for Northwestern zone (Figure S4a), Tx for Northwestern zone (Figure S4b), T for Northwestern zone (Figure S4c), Tn for Central zone (Figure S4d), Tx for Central zone (Figure S4e), T for Central zone (Figure S4f), Tn for

Southeastern zone (Figure S4g), Tx for Southeastern zone (Figure S4h), T for Southeastern zone (Figure S4i). These parameters delineate the dynamic variability within the trend. Given the prior densities for each parameter together with the likelihood function, the posterior probability distributions are defined through MCMC analysis. In Figure S4, the prior distributions are depicted with dashed lines, while histograms represent the marginal posterior distributions. The MCMC results show that the posterior distributions of parameters are predominantly influenced by the data rather than the priors. The trend's standard deviation is assessed to be relatively small, indicating a preference for investigating smooth background variability. Additionally, the autoregressive parameters exhibit narrow posterior distributions compared to the prior, suggesting accurate data-derived estimations. This pattern was consistently observed across all analyses conducted for monthly, seasonal, and annual minimum, maximum, and mean temperatures across the zones.

Table S3 presents the assessment metrics of the DLM model, encompassing Mean Absolute Error (MAE), and Root Mean Square Error (RMSE). In

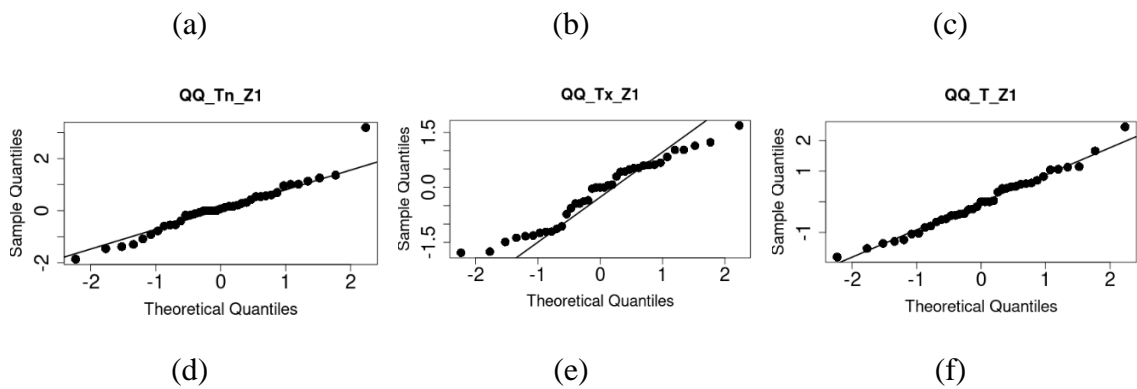
Table S4, we present the coefficient of determination (R^2) from DLM, and we also present the computed R^2 from LM. In the next section, the R^2 values obtained from DLM are presented together with the values obtained from LM in parentheses. Over the Northwestern zone, in the seasonal mean of Tn, the RMSE presents a moderate value in all seasons, while the annual mean of Tn presents a relatively low value of 0.36. The MAE shows a low value in JJA and SOND and moderate values for JF and MAM. A low MAE is observed in the annual mean of Tn (0.26). The R^2 of 0.41 (0.26), 0.79 (0.40), 0.85 (0.46), and 0.87 (0.38) are observed for JF, MAM, JJA, and SOND, respectively. The annual mean of Tn presents an R^2 of 0.85 (0.44). Over the Central zone, in the seasonal mean of Tn, the RMSE presents a moderate value in all seasons, corresponding to 0.57, 0.56, 0.44, and 0.43 for respectively, JF, MAM, JJA, and SOND. The annual mean of Tn presents an RMSE of 0.36. The MAE presents a moderate value corresponding to 0.44 and 0.46 for JF and MAM, and a low value of 0.34 and 0.33 in JJA and SOND, respectively. The annual mean of Tn presents a low MAE value of 0.28. The R^2 of 0.24 (0.19), 0.63 (0.29), 0.59 (0.36), and 0.75 (0.25) are observed for JF, MAM, JJA, and SOND, respectively. The annual mean of Tn presents an R^2 of 0.69 (0.33). In the Southeastern zone, the analysis reveals moderate RMSE values for seasonal mean Tn across all seasons, with corresponding low MAE values. However, R^2 values indicate very low values in JF, MAM, and JJA (<0.20), while for SOND and yearly, we get 0.50 (0.06) and 0.32 (0.11),

respectively. For seasonal mean Tx, RMSE values vary, showing moderate to high error rates across different seasons. Similarly, MAE also exhibits values ranging between 0.43 and 0.80 variability. R^2 values recorded were < 0.35 . Moderate RMSE and MAE values are observed for seasonal mean temperatures.

Table S5 summarizes the validation diagnostics of the DLM model, including MAE and RMSE for monthly mean temperatures.

Table S6 presents the R^2 from both DLM and LM. Over the three zones, MAE and RMSE present high and moderate values in the monthly mean Tx, Tn, and T in most months. The R^2 shows a high value (>0.50) in most of the monthly mean Tn of the Northwestern zone and Central zone and a low value for monthly mean Tx and T in most of the months in all zones.

In general, in all three zones and the Eastern Province, the computed error metrics for monthly and seasonal (annual) mean Tn indicate a good model fit compared to Tx and T. In most cases, we found that the coefficient of determination (R^2) from DLM was far greater than that of LM. The data structure was among the major problems that challenged the model. Dataset issues include high variation in data, large differences between data values (i.e. year), abrupt change, and short dataset length. To confirm the data structure in each zone, we further examined the data distribution of sampled stations available in the respective zone to compare observed features, and the observed data behavior from stations was similar to the zonal datasets.



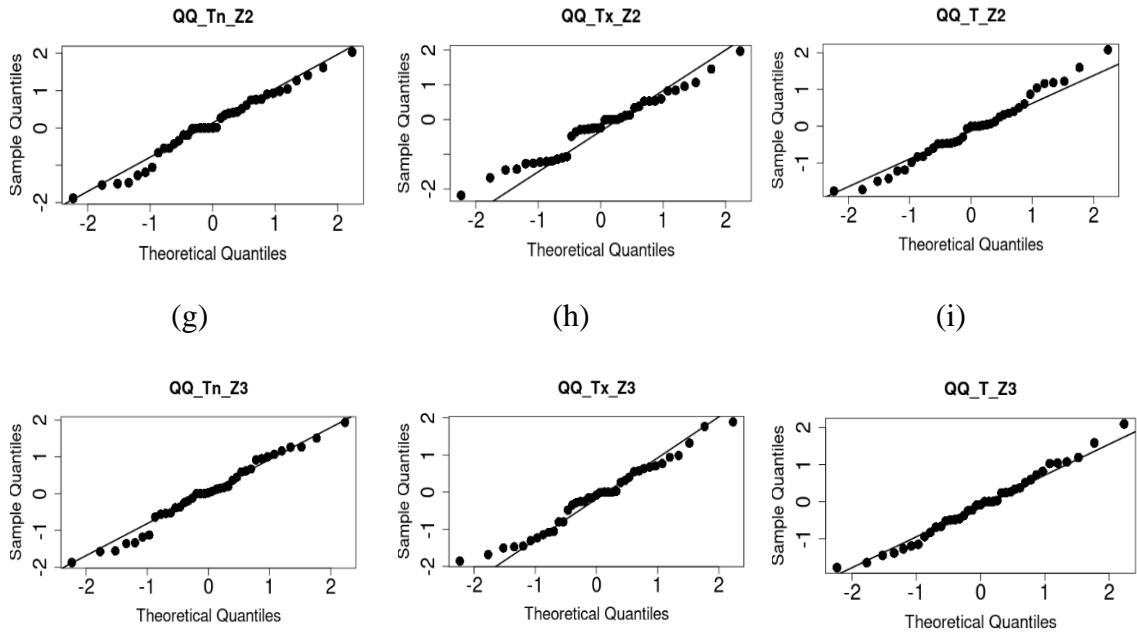
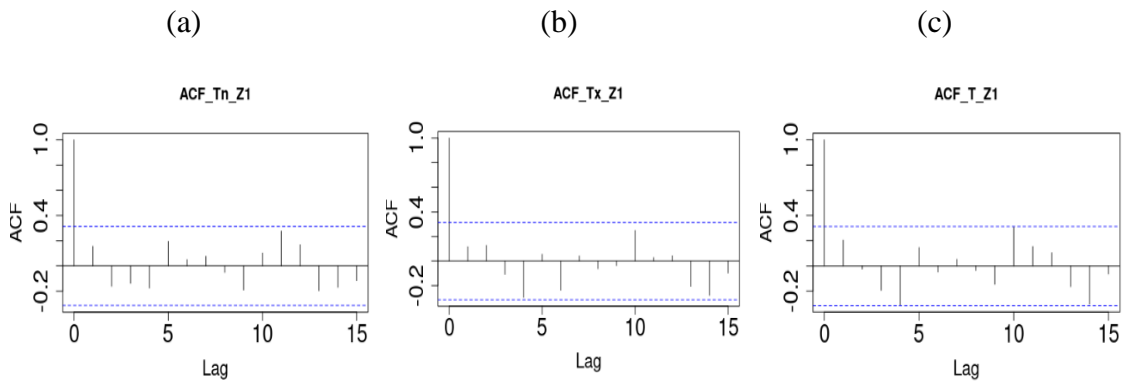


Figure S2 Normal probability plot for the residuals in annual mean Tn for Northwestern zone (a), Tx for Northwestern zone (b), T for Northwestern zone (c), Tn for Central zone (d), Tx for Central zone (e), T for Central zone (f), Tn for Southeastern zone (g), Tx for Southeastern zone (h), T for Southeastern zone (i).



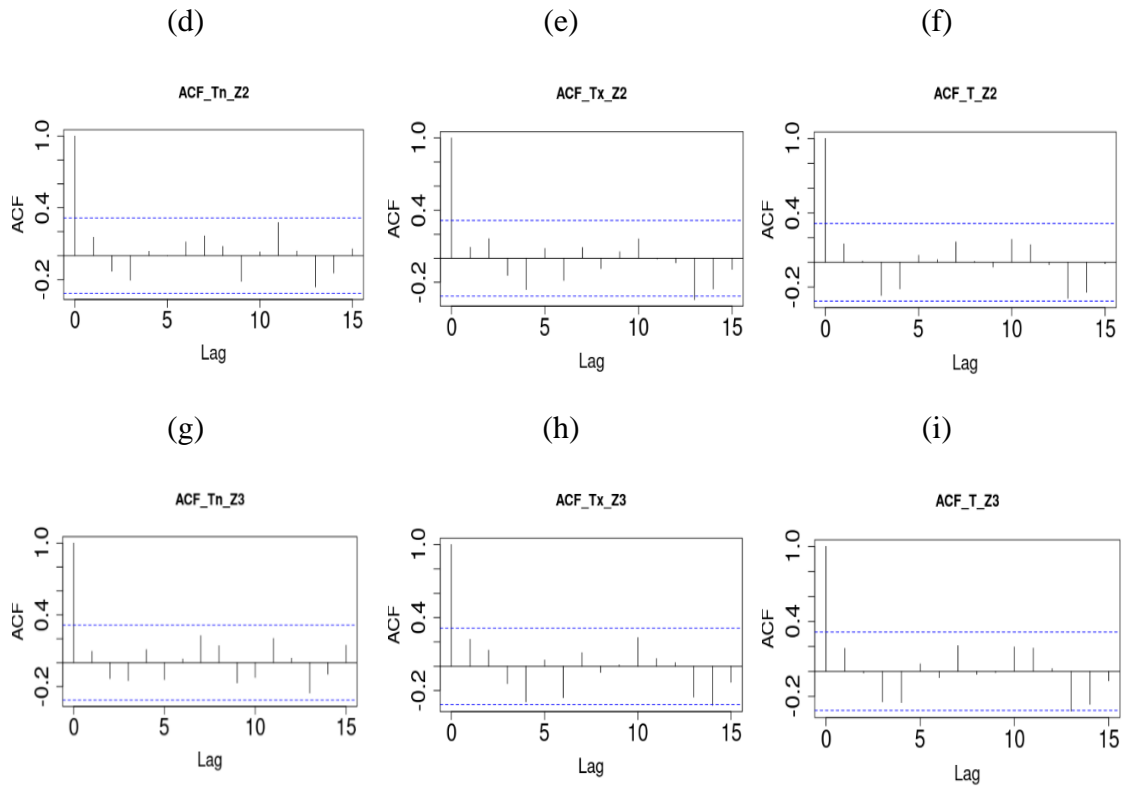
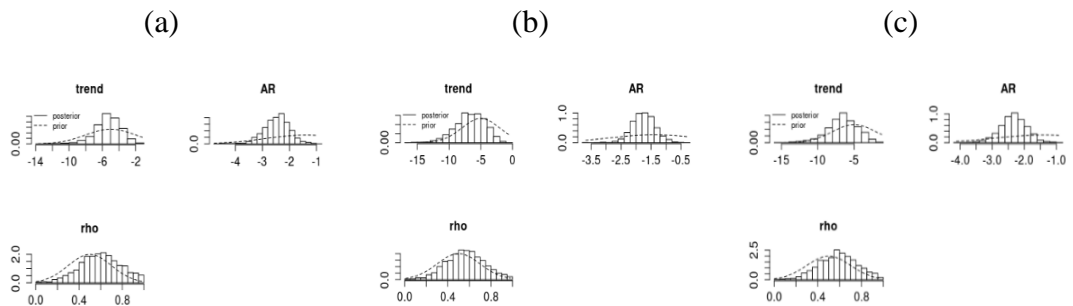


Figure S3 Estimated autocorrelation function (ACF) plot of the DLM residuals in annual mean Tn for Northwestern zone (a), Tx for Northwestern zone (b), T for Northwestern zone (c), Tn for Central zone (d), Tx for Central zone (e), T for Central zone (f), Tn for Southeastern zone (g), Tx for Southeastern zone (h), T for Southeastern zone (i).



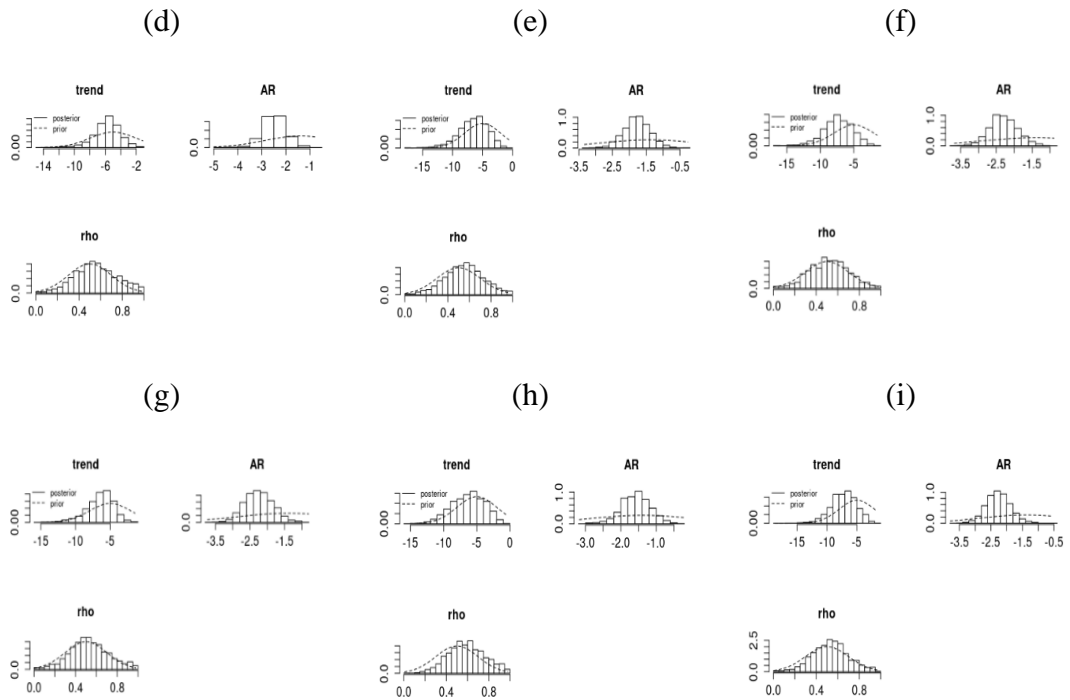
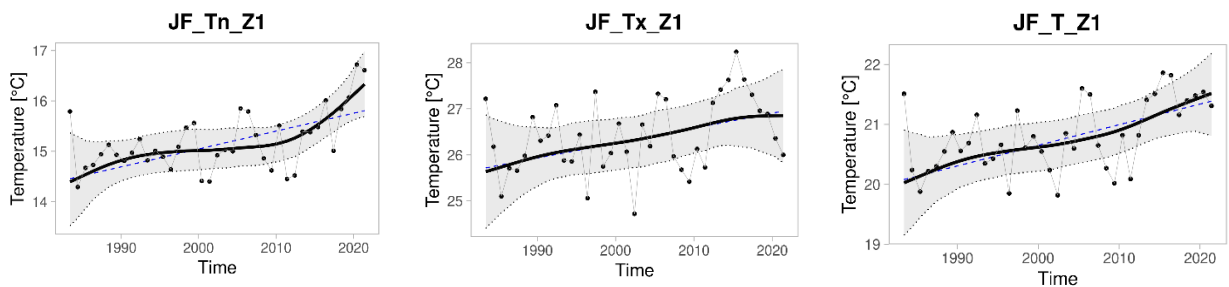


Figure S4 Prior distributions (dashed line) and marginal posterior distributions (histogram) for three unknown model parameters: trend change standard deviation σ_{trend} , autoregressive standard deviation σ_{AR} , and autoregressive coefficient ρ in annual mean Tn for Northwestern zone (a), Tx for Northwestern zone (b), T for Northwestern zone (c), Tn for Central zone (d), Tx for Central zone (e), T for Central zone (f), Tn for Southeastern zone (g), Tx for Southeastern zone (h), T for Southeastern zone (i).



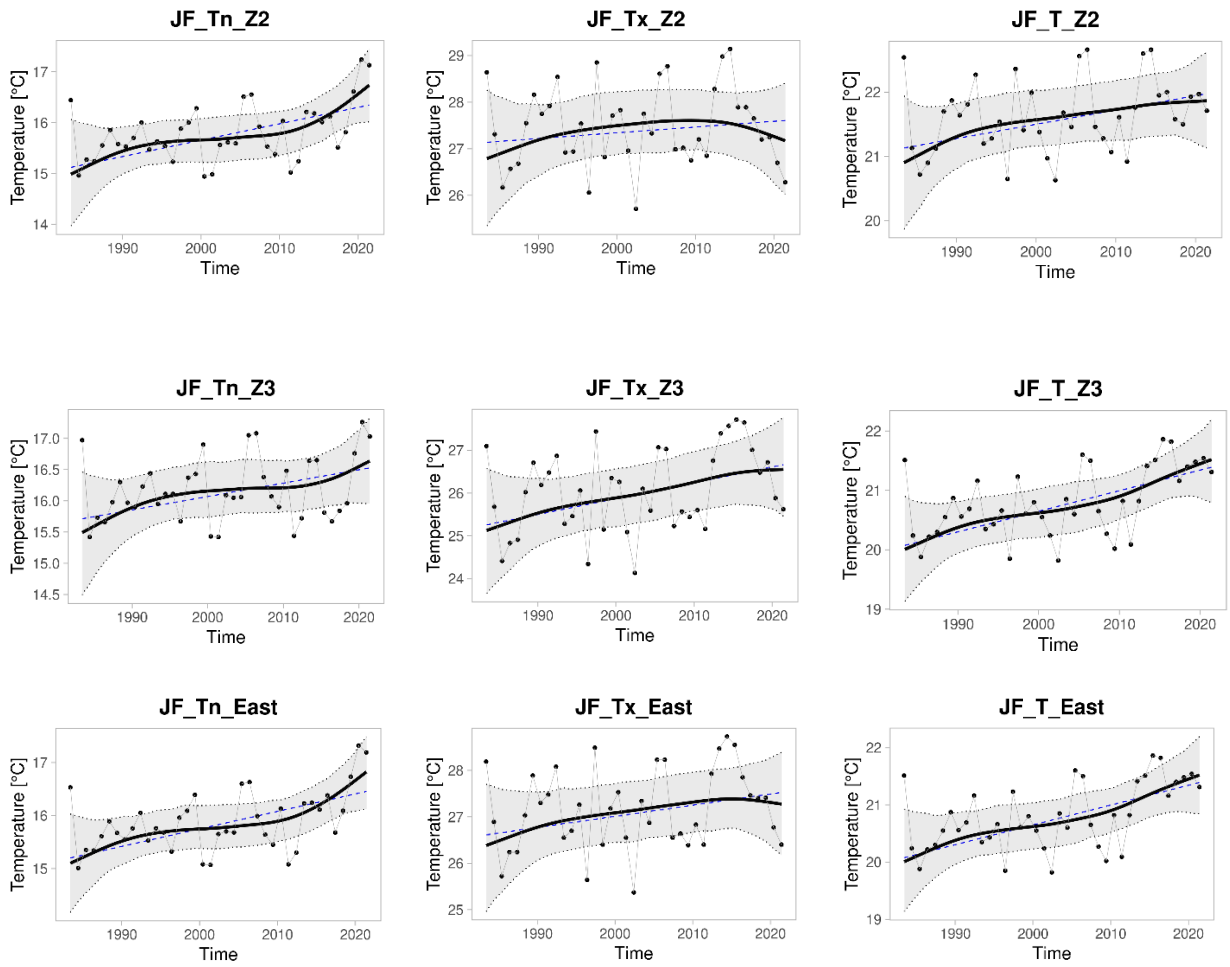
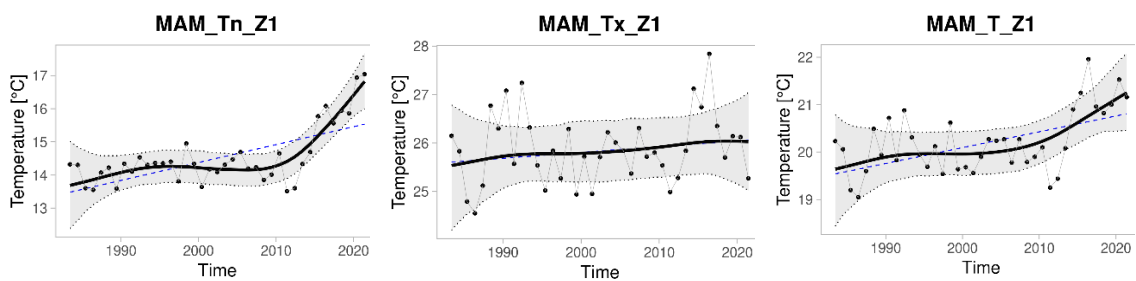


Figure S5 DLM fit for JF (January-February) season average (T), minimum (Tn), and maximum (Tx) temperature during 1983-2021. The observed yearly average temperature (black dots) is displayed together with the background mean level μ_t (black solid line). The smooth black solid line represents the estimated temperature trend together with a 95 % probability envelope. The dashed blue line is the linear trend. The Z1, Z2, and Z3, respectively, stand for the Northwestern, Central, and Southeastern zones. The bottom panel in each column indicates the results obtained from the East.



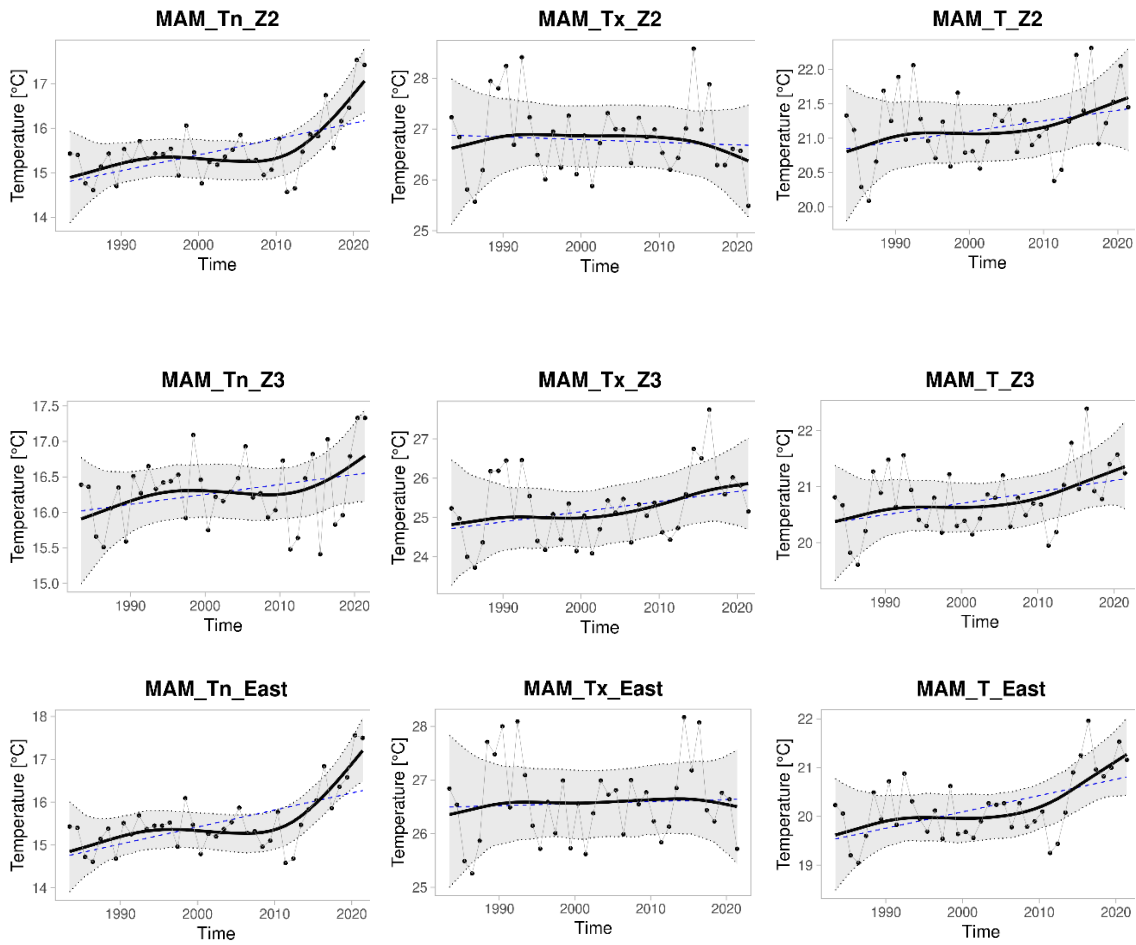
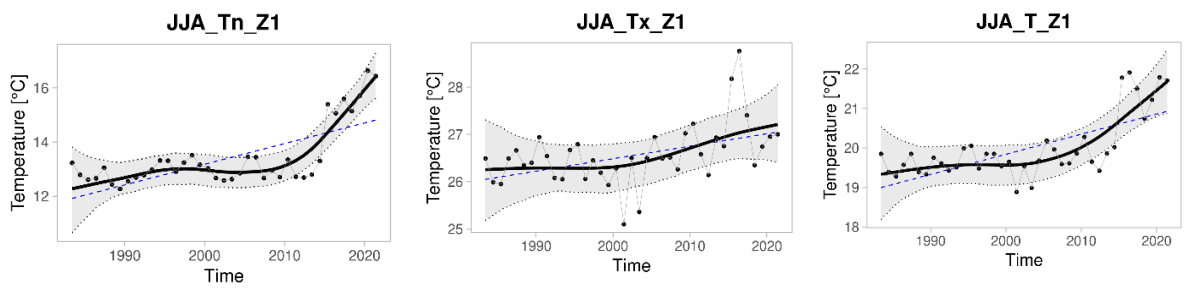


Figure S6 DLM fit for MAM (March-April-May) season average (T), minimum (Tn), and maximum (Tx) temperature during 1983-2021. The observed yearly average temperature (black dots) is displayed together with the background mean level μ_t (black solid line). The smooth black solid line represents the estimated temperature trend together with a 95 % probability envelope. The dashed blue line is the linear trend. The Z1, Z2, and Z3, respectively, stand for the Northwestern, Central, and Southeastern zones. The bottom panel in each column indicates the results obtained from the East.



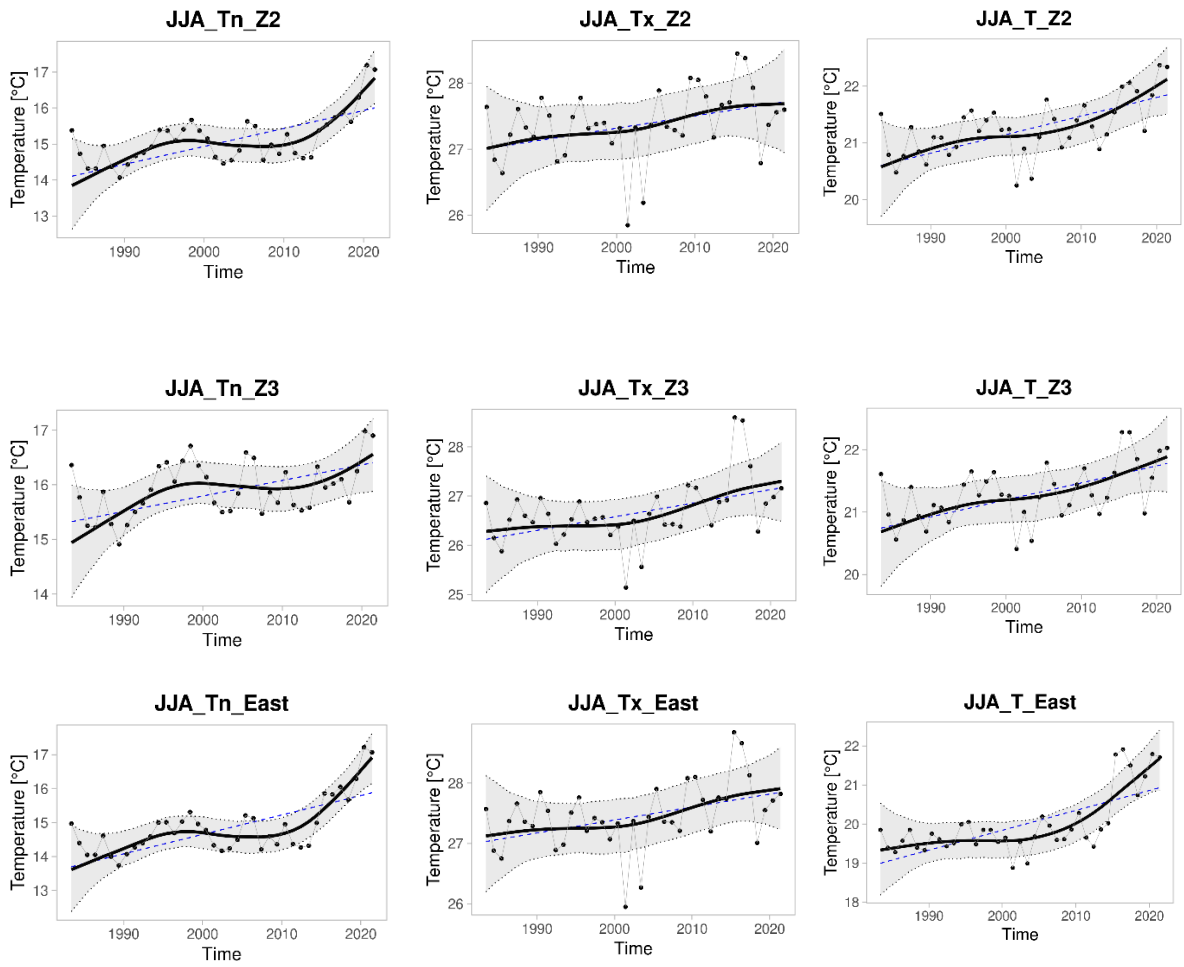
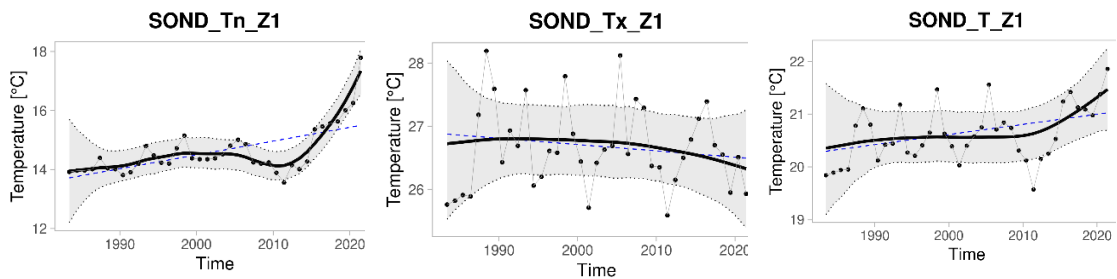


Figure S7 DLM fit for JJA (June-July-August) season average (T), minimum (Tn), and maximum (Tx) temperature during 1983-2021. The observed yearly average temperature (black dots) is displayed together with the background mean level μ_t (black solid line). The smooth black solid line represents the estimated temperature trend together with a 95 % probability envelope. The dashed blue line is the linear trend. The Z1, Z2, and Z3, respectively, stand for the Northwestern, Central, and Southeastern zones. The bottom panel in each column indicates the results obtained from the East.



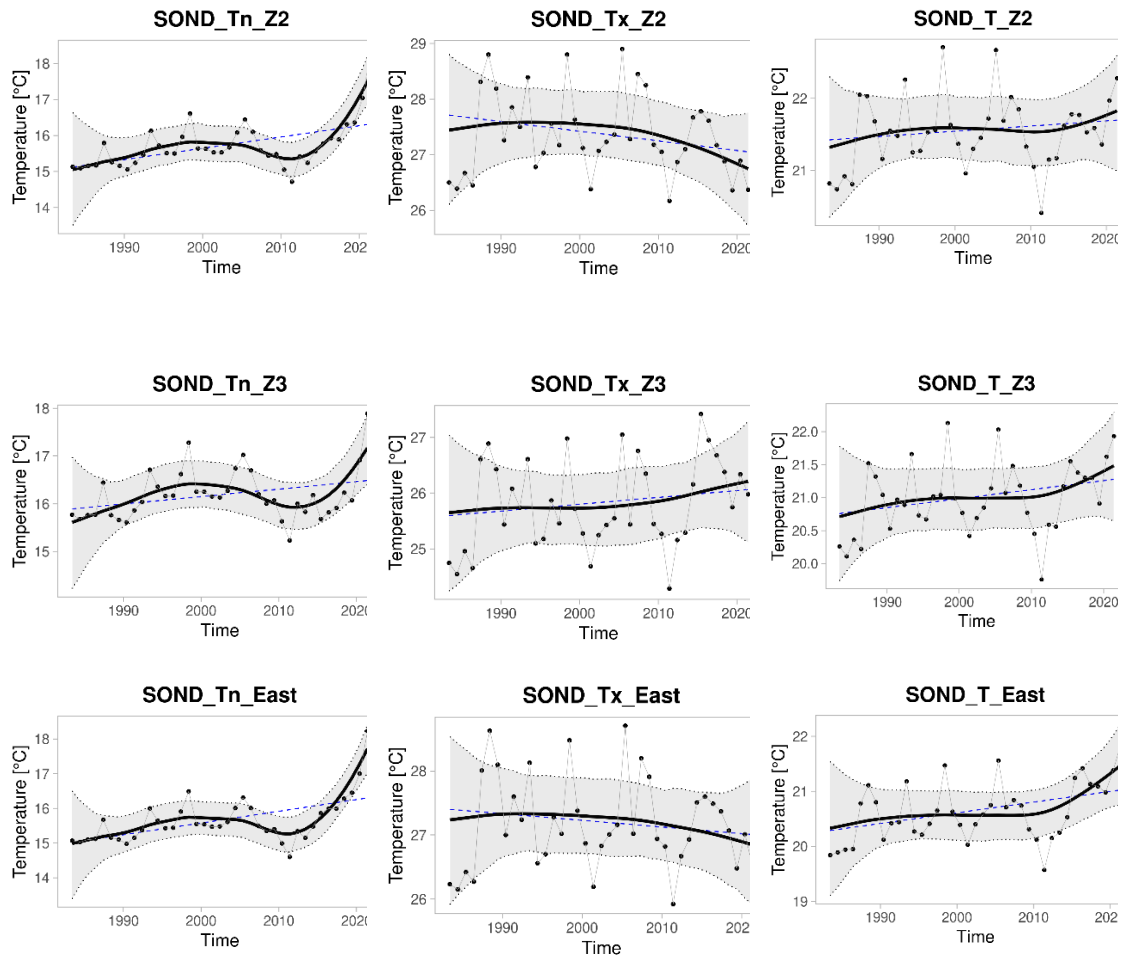
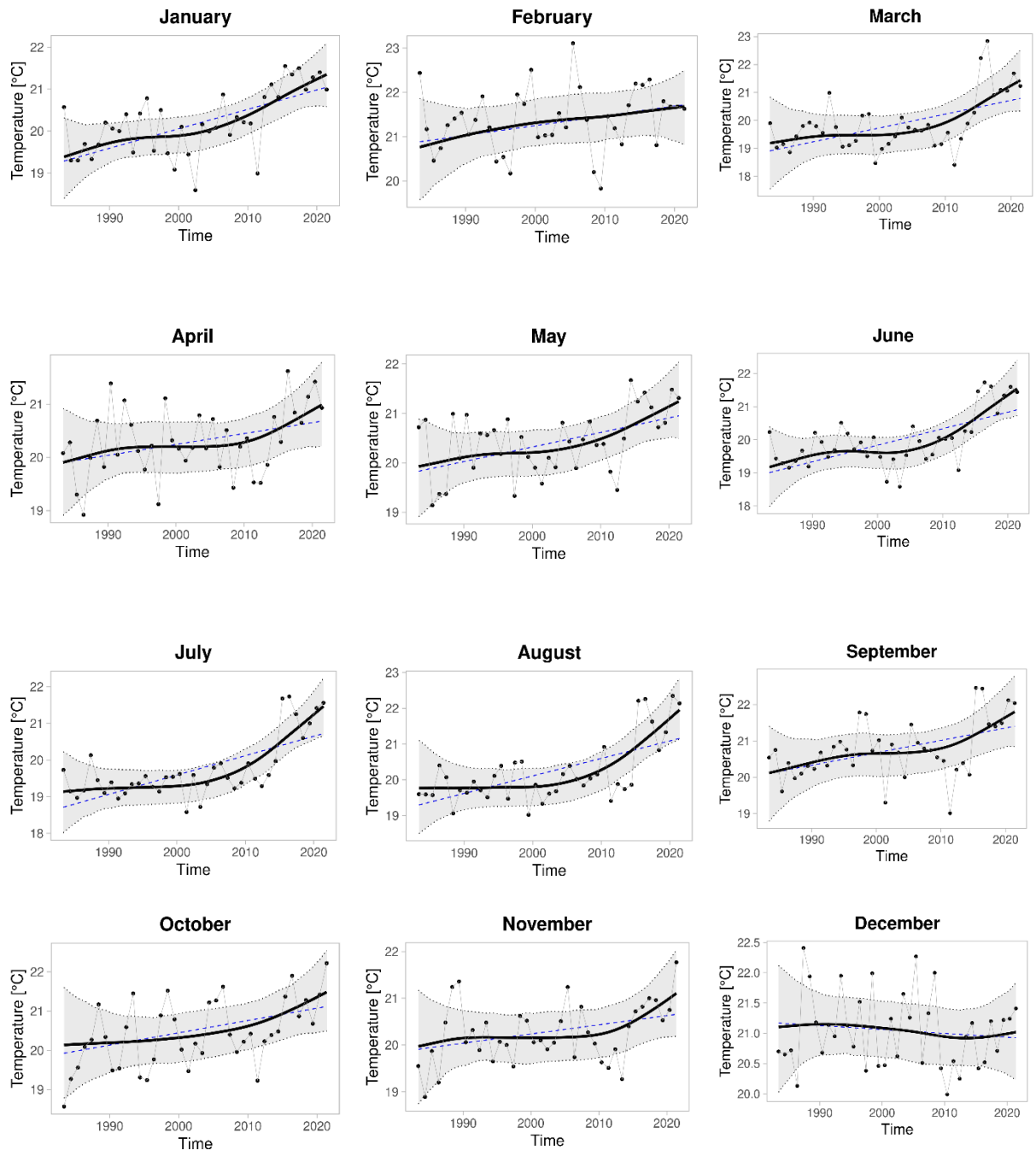
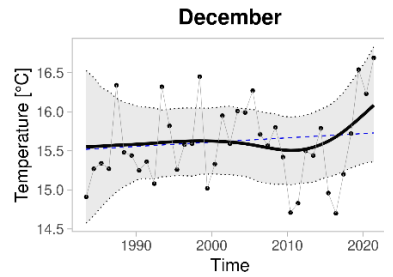
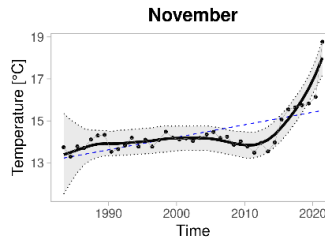
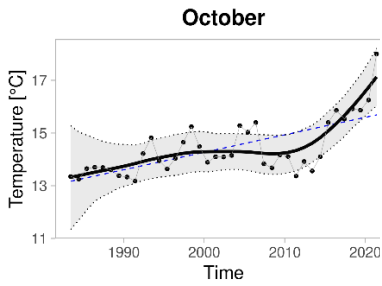
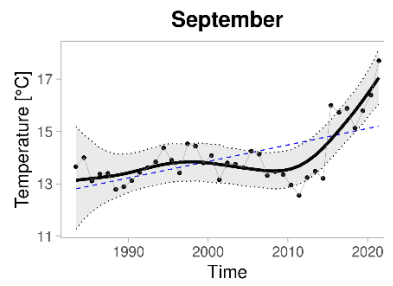
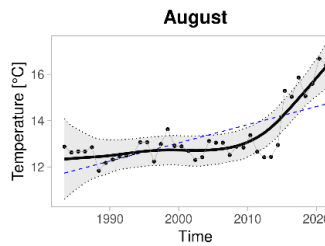
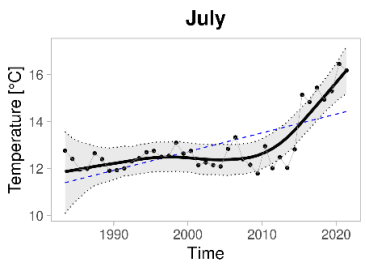
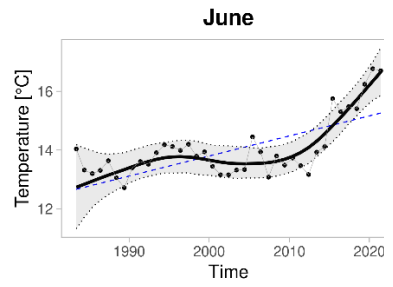
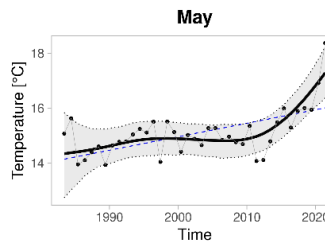
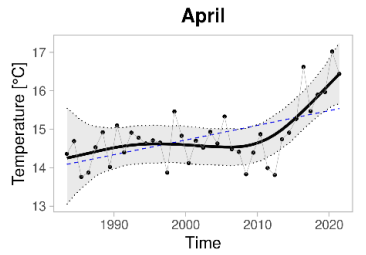
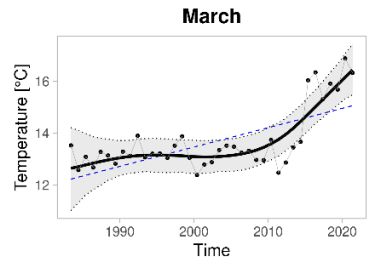
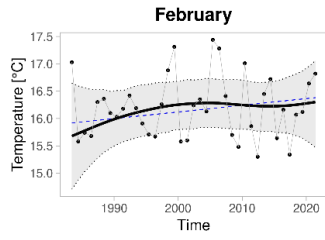
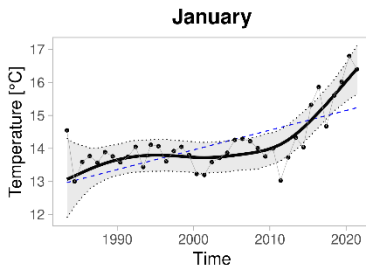


Figure S8 DLM fit for SOND (September-October-November-December) season average (T), minimum (Tn), and maximum (Tx) temperature during 1983-2021. The observed yearly average temperature (black dots) is displayed together with the background mean level μ_t (black solid line). The smooth black solid line represents the estimated temperature trend together with a 95 % probability envelope. The dashed blue line is the linear trend. The Z1, Z2, and Z3, respectively, stand for the Northwestern, Central, and Southeastern zones. The bottom panel in each column indicates the results obtained from the East.

(a)



(b)



(c)

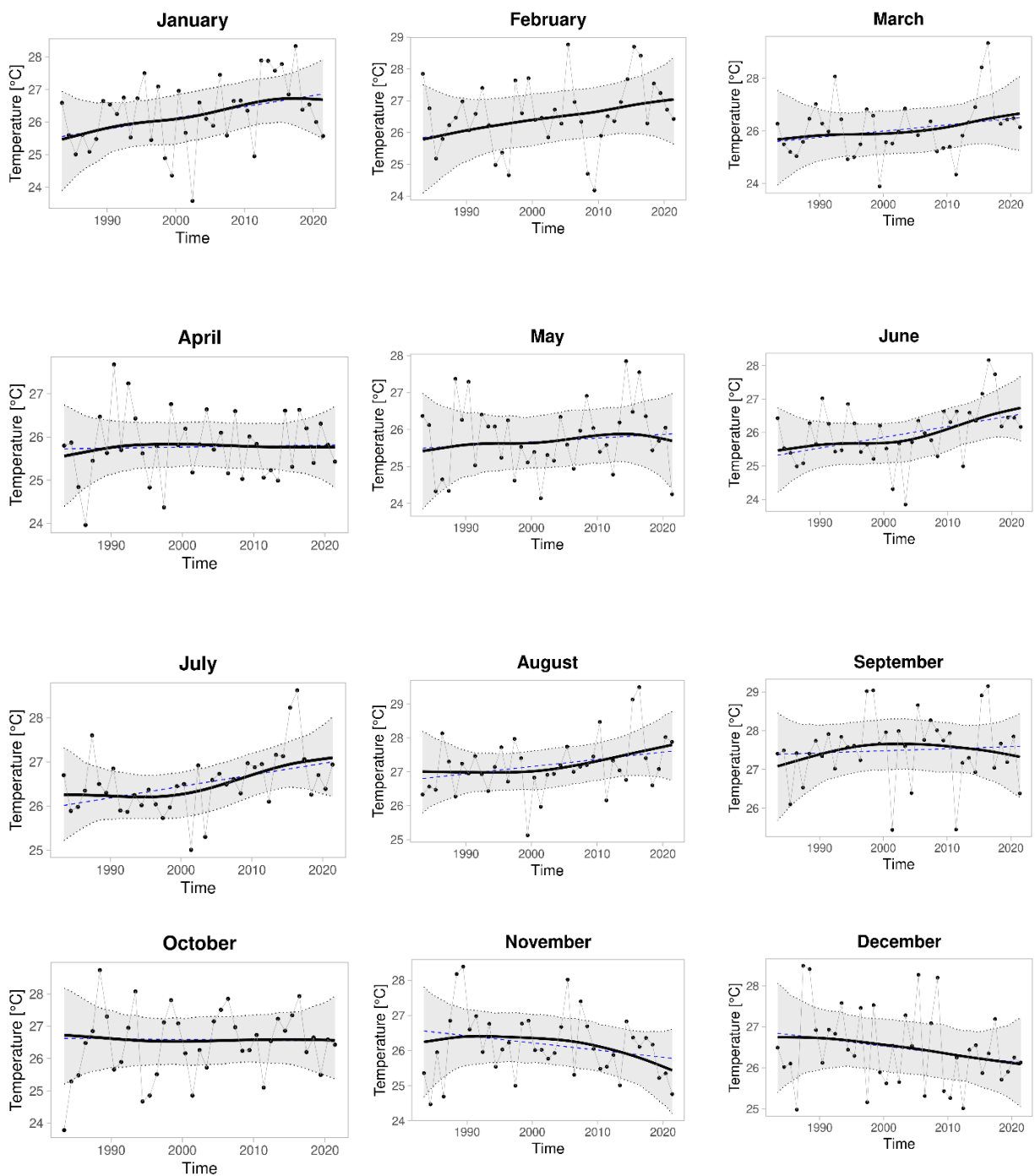
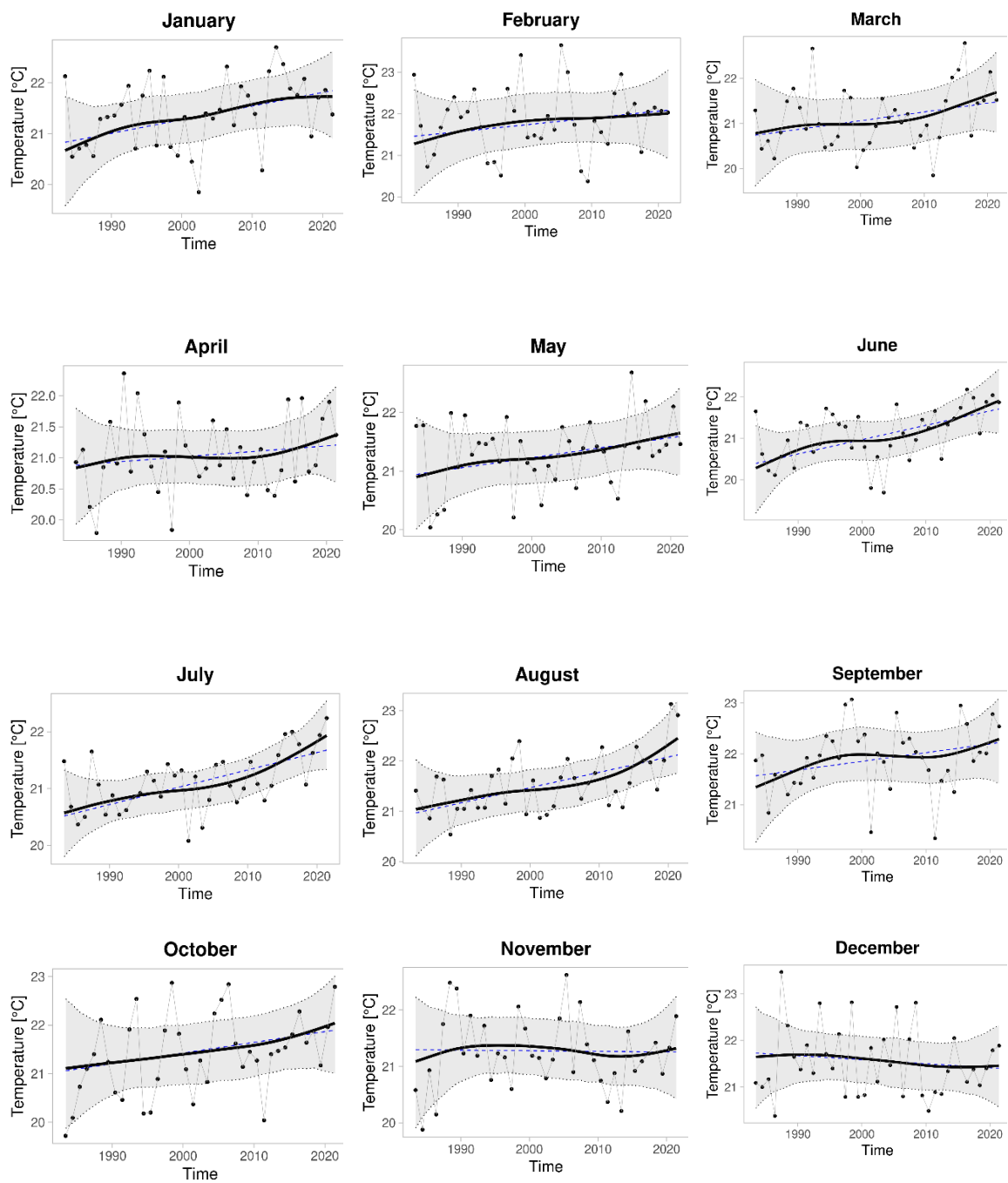
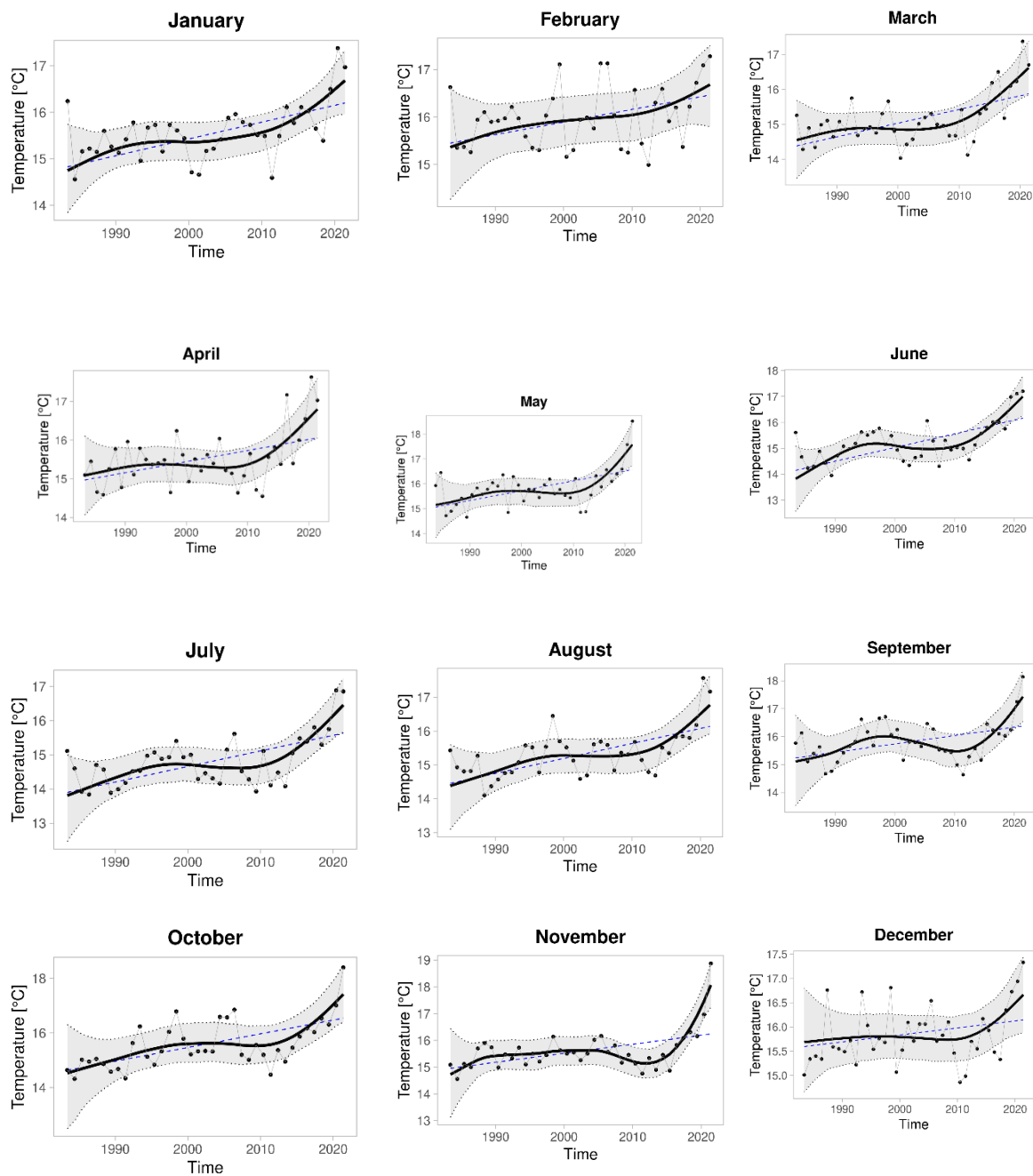


Figure S9 DLM fit for January-December month average (T)(a), minimum (Tn)(b), and maximum (Tx)(c) temperature during 1983-2021. The observed yearly average temperature (black dots) is displayed together with the background mean level μ_t (black solid line). The smooth black solid line represents the estimated temperature trend together with a 95 % probability envelope. The dashed blue line is the linear trend. The Z1 stands for Northwestern zone.

(a)



(b)



(c)

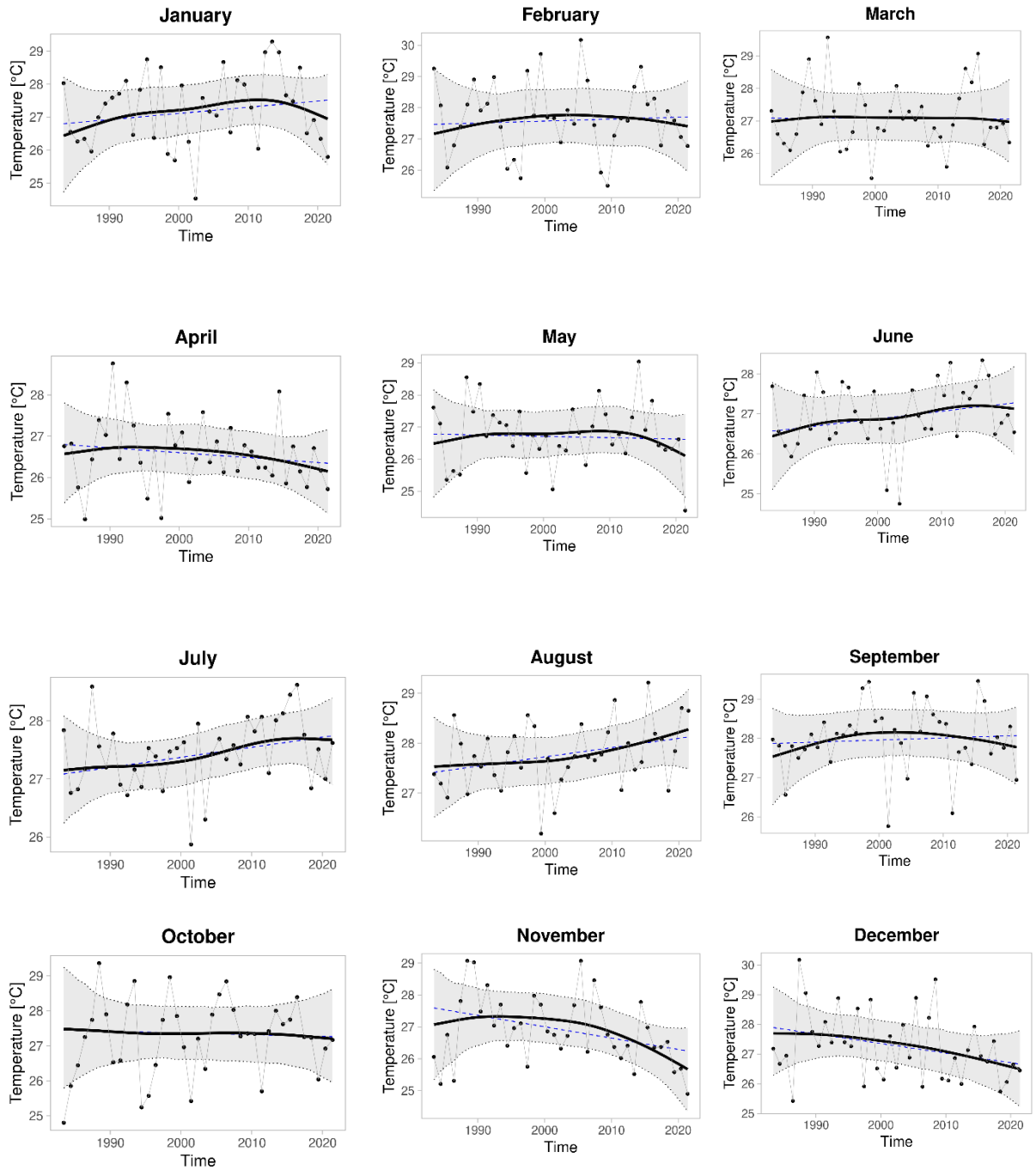
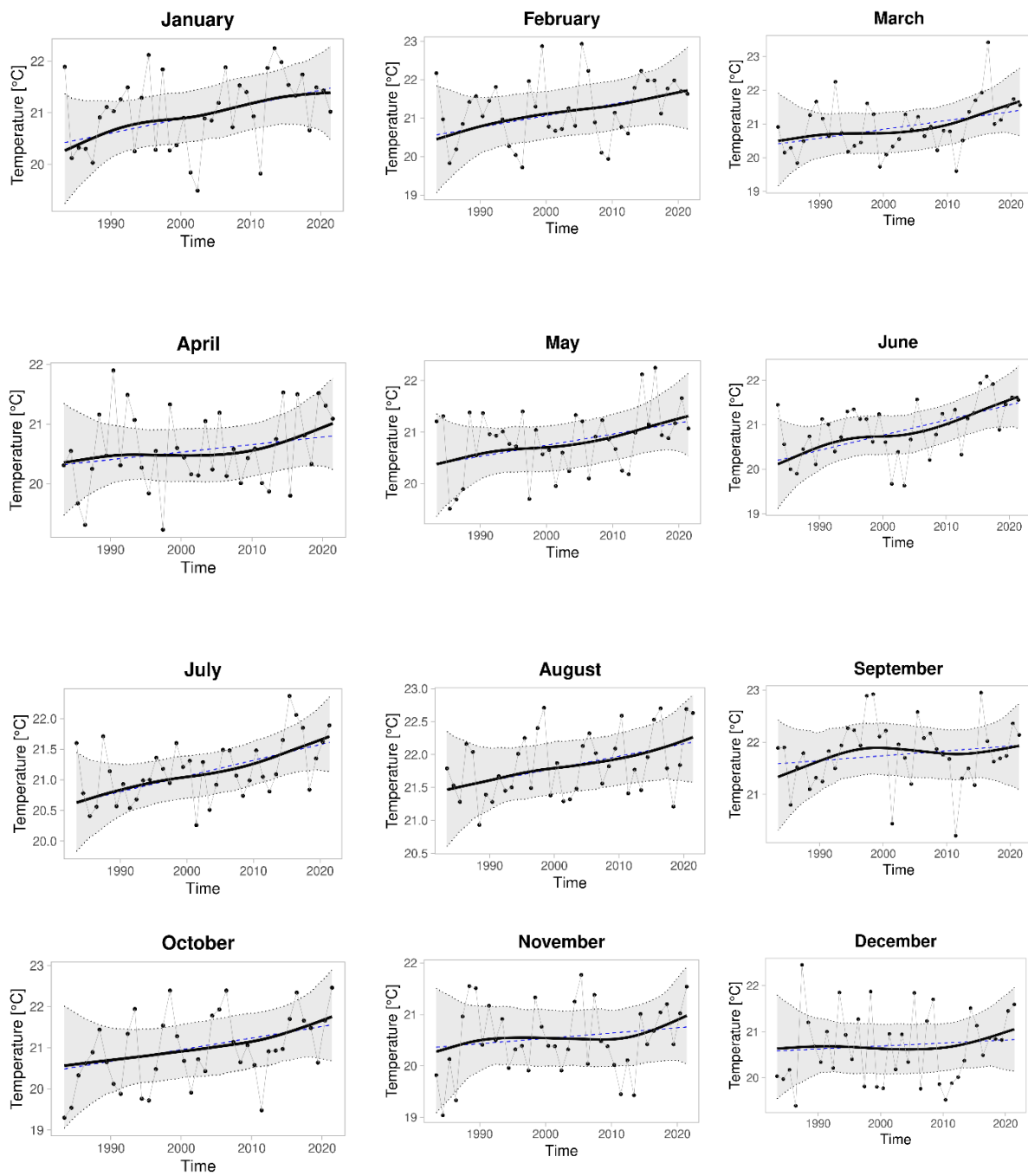
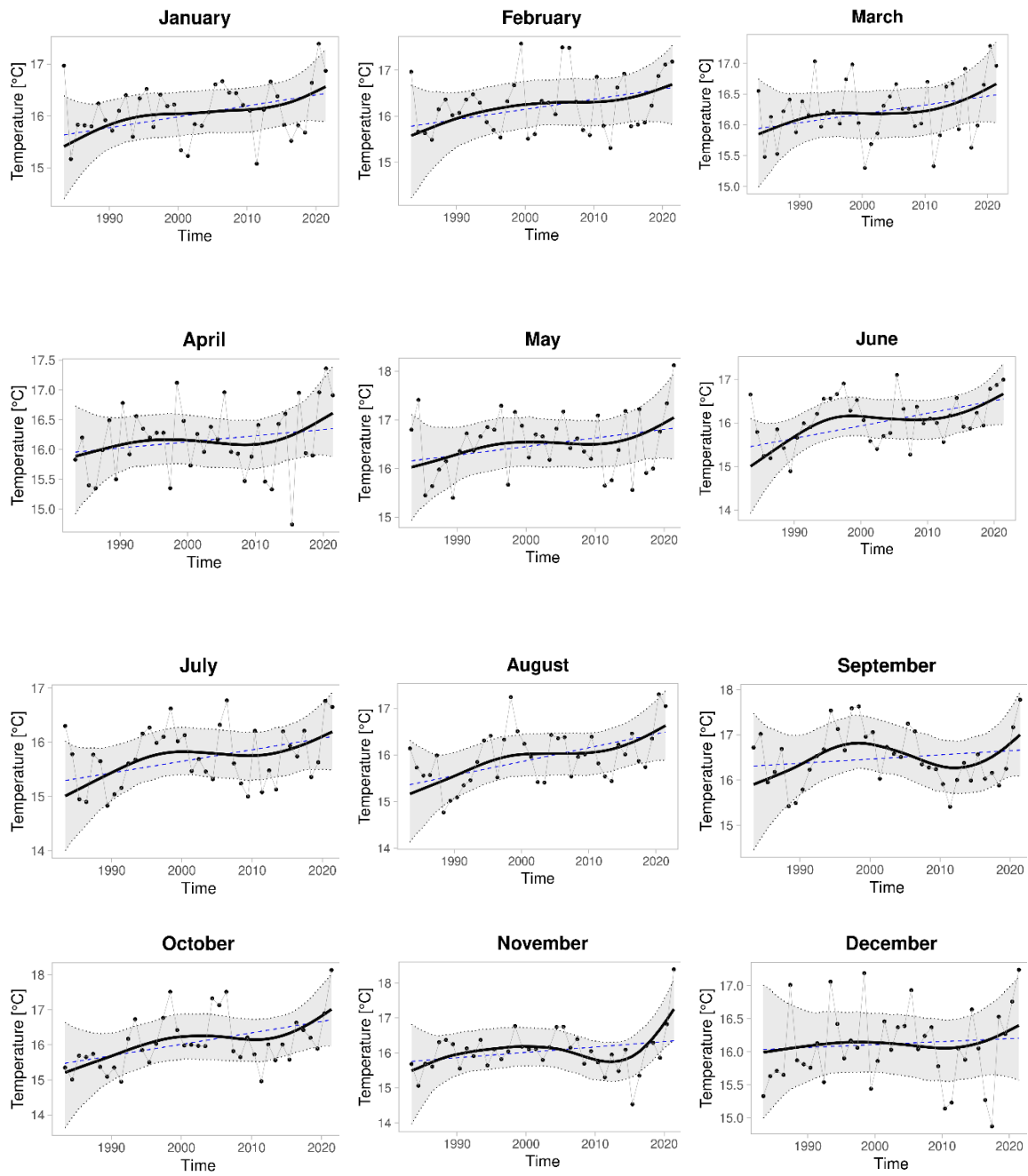


Figure S10 DLM fit for January-December month average (T)(a), minimum (Tn)(b), and maximum (Tx)(c) temperature during 1983-2021. The observed yearly average temperature (black dots) is displayed together with the background mean level μ_t (black solid line). The smooth black solid line represents the estimated temperature trend together with a 95 % probability envelope. The dashed blue line is the linear trend. The Z2 stands for Central zone.

(a)



(b)



(c)

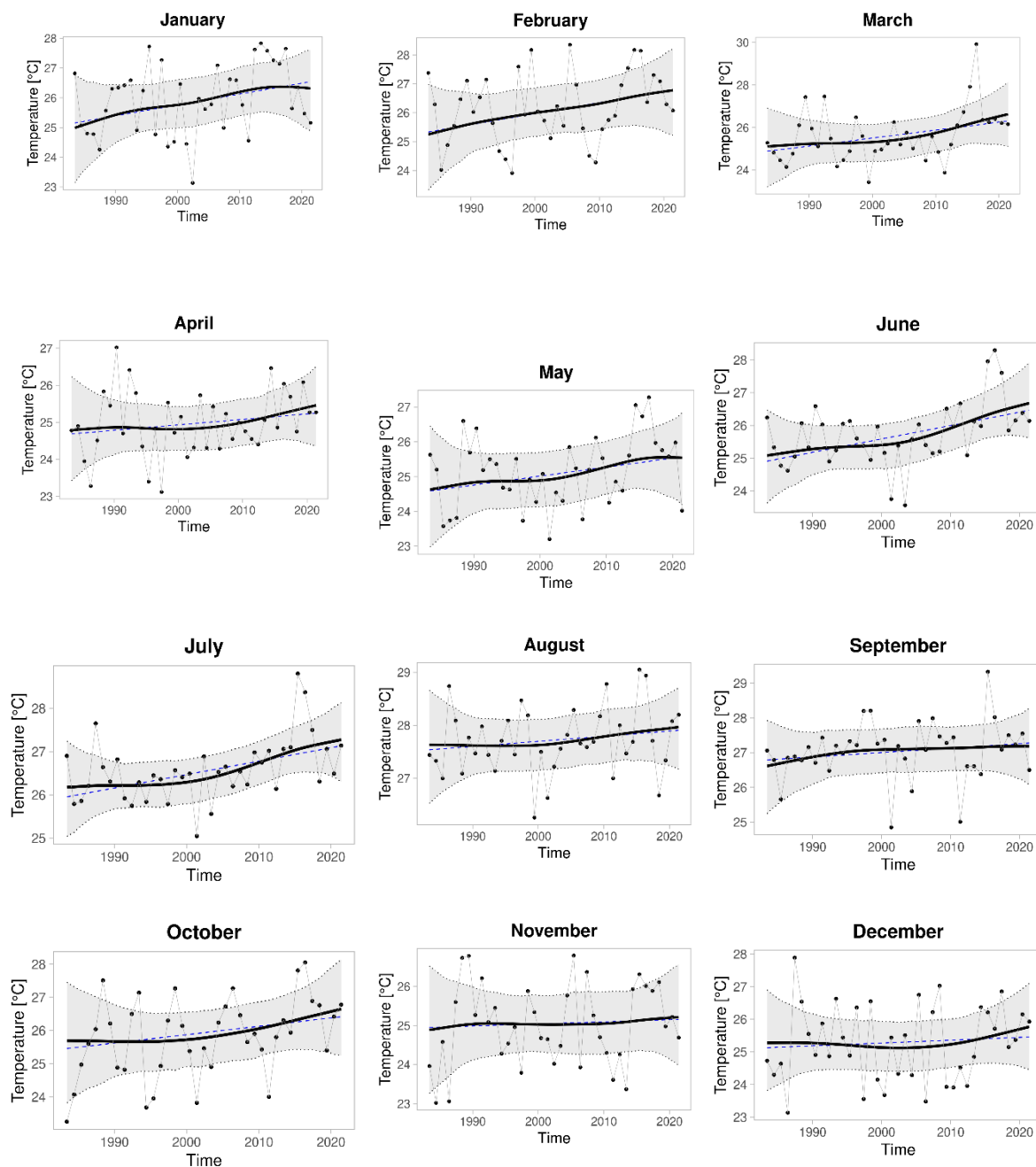


Figure S11 DLM fit for January-December month average (T)(a), minimum (Tn)(b), and maximum (Tx)(c) temperature during 1983-2021. The observed yearly average temperature (black dots) is displayed together with the background mean level μ_t (black solid line). The smooth black solid line represents the estimated temperature trend together with a 95 % probability envelope. The dashed blue line is the linear trend. The Z3 stands for Southeastern zone.

Table S3 Validation Metrics of DLM Model for Seasonal and Annual Mean Temperatures Across Zones

Northwestern zone						
	Tx		Tn		T	
Season	RMSE	MAE	RMSE	MAE	RMSE	MAE
JF	0.84	0.68	0.56	0.46	0.51	0.42
MAM	0.87	0.69	0.55	0.44	0.62	0.51
JJA	0.62	0.50	0.51	0.35	0.49	0.36
SOND	0.73	0.56	0.42	0.29	0.48	0.38
Annual	0.48	0.41	0.36	0.26	0.36	0.30
Central zone						
	Tx		Tn		T	
Season	RMSE	MAE	RMSE	MAE	RMSE	MAE
JF	0.96	0.75	0.57	0.44	0.58	0.47
MAM	0.90	0.72	0.56	0.46	0.63	0.52
JJA	0.57	0.42	0.44	0.34	0.42	0.33
SOND	0.82	0.64	0.43	0.33	0.56	0.44
Annual	0.48	0.39	0.36	0.28	0.36	0.29
Southeastern zone						
	Tx		Tn		T	
Season	RMSE	MAE	RMSE	MAE	RMSE	MAE
JF	1.02	0.80	0.58	0.45	0.63	0.50
MAM	0.92	0.76	0.61	0.49	0.66	0.53
JJA	0.62	0.45	0.45	0.35	0.42	0.34
SOND	0.88	0.70	0.47	0.36	0.58	0.47
Annual	0.53	0.43	0.38	0.30	0.37	0.30
East						
	Tx		Tn		T	
Season	RMSE	MAE	RMSE	MAE	RMSE	MAE
JF	0.95	0.75	0.57	0.45	0.51	0.42

MAM	0.90	0.73	0.55	0.45	0.62	0.51
JJA	0.58	0.44	0.44	0.35	0.49	0.35
SOND	0.81	0.62	0.42	0.32	0.48	0.37
Annual	0.48	0.40	0.34	0.27	0.36	0.30

Table S4 Validation Metrics for Dynamic Linear Model (DLM) and Linear Model (LM) applied to seasonal and annual mean temperatures across zones. The comparison between DLM and LM models is based on the coefficient of determination (R^2) computed using observations and smoother local mean estimates for DLM, and R^2 computed from LM using observations.

Northwestern zone						
	DLM			LM		
	Tx	Tn	T	Tx	Tn	T
Season	R^2	R^2	R^2	R^2	R^2	R^2
JF	0.12	0.41	0.27	0.11	0.26	0.26
MAM	0.05	0.79	0.45	0.03	0.40	0.26
JJA	0.31	0.85	0.72	0.20	0.46	0.45
SOND	0.03	0.87	0.34	0.00	0.38	0.20
Annual	0.17	0.85	0.62	0.08	0.44	0.40
Central zone						
	Tx	Tn	T	Tx	Tn	T
Season	R^2	R^2	R^2	R^2	R^2	R^2
JF	0.05	0.24	0.03	0.00	0.19	0.06
MAM	0.05	0.63	0.14	0.01	0.29	0.07
JJA	0.16	0.59	0.43	0.11	0.36	0.35
SOND	0.11	0.75	0.12	0.02	0.25	0.04
Annual	0.15	0.69	0.26	0.00	0.33	0.19
Southeastern zone						
	Tx	Tn	T	Tx	Tn	T
Season	R^2	R^2	R^2	R^2	R^2	R^2
JF	0.09	0.02	0.10	0.10	0.06	0.13
MAM	0.21	0.17	0.22	0.11	0.06	0.13
JJA	0.29	0.17	0.26	0.19	0.14	0.26

SOND	0.09	0.50	0.18	0.08	0.06	0.1
Annual	0.30	0.32	0.32	0.18	0.11	0.24
East						
	Tx	Tn	T	Tx	Tn	T
Season	R ²	R ²	R ²	R ²	R ²	R ²
JF	0.02	0.29	0.26	0.04	0.22	0.26
MAM	0.03	0.68	0.50	0.00	0.33	0.26
JJA	0.24	0.72	0.72	0.16	0.42	0.45
SOND	0.04	0.78	0.35	0.00	0.28	0.20
Annual	0.12	0.74	0.62	0.03	0.38	0.39

Table S5 Validation Metrics of DLM Model for Monthly Mean Temperatures Across Zones

Northwestern zone						
	Tx		Tn		T	
Month	RMSE	MAE	RMSE	MAE	RMSE	MAE
January	1.14	0.91	0.63	0.49	0.66	0.51
February	1.12	0.87	0.61	0.53	0.73	0.57
March	1.04	0.77	0.73	0.54	0.78	0.57
April	1.03	0.83	0.71	0.58	0.78	0.63
May	1.24	0.92	0.86	0.62	0.87	0.62
June	0.87	0.72	0.50	0.36	0.57	0.46
July	0.75	0.58	0.63	0.45	0.54	0.39
August	0.97	0.74	0.61	0.42	0.69	0.48
September	1.14	0.83	0.75	0.54	0.86	0.58
October	1.11	0.85	0.65	0.49	0.76	0.61
November	1.24	0.90	0.57	0.37	0.81	0.60
December	1.26	0.97	0.57	0.42	0.82	0.65
Central zone						
	Tx		Tn		T	
Month	RMSE	MAE	RMSE	MAE	RMSE	MAE
January	1.22	0.97	0.62	0.46	0.74	0.61
February	1.28	1.00	0.67	0.58	0.84	0.65

March	1.07	0.82	0.67	0.52	0.75	0.59
April	1.07	0.83	0.73	0.59	0.81	0.65
May	1.23	0.93	0.86	0.63	0.88	0.64
June	0.89	0.71	0.52	0.38	0.59	0.47
July	0.73	0.56	0.56	0.45	0.50	0.37
August	0.82	0.61	0.54	0.40	0.57	0.44
September	1.04	0.71	0.69	0.53	0.79	0.53
October	1.13	0.85	0.71	0.57	0.81	0.66
November	1.34	1	0.59	0.48	0.89	0.67
December	1.54	1.19	0.65	0.47	1.01	0.78
Southeastern zone						
	Tx		Tn		T	
Month	RMSE	MAE	RMSE	MAE	RMSE	MAE
January	1.27	1.00	0.59	0.45	0.79	0.64
February	1.36	1.05	0.67	0.56	0.85	0.66
March	1.21	0.94	0.66	0.50	0.8	0.61
April	1.08	0.86	0.74	0.60	0.84	0.67
May	1.17	0.91	0.98	0.73	0.89	0.67
June	0.90	0.70	0.51	0.40	0.56	0.45
July	0.78	0.59	0.59	0.48	0.51	0.37
August	0.82	0.62	0.54	0.42	0.57	0.45
September	1.04	0.68	0.70	0.56	0.77	0.52
October	1.14	0.89	0.73	0.59	0.82	0.69
November	1.39	1.05	0.67	0.54	0.92	0.72
December	1.61	1.26	0.69	0.51	1.04	0.82
East						
	Tx		Tn		T	
Month	RMSE	MAE	RMSE	MAE	RMSE	MAE
January	1.23	0.99	0.59	0.43	0.66	0.51
February	1.26	0.99	0.65	0.56	0.73	0.56
March	1.12	0.86	0.68	0.52	0.78	0.57
April	1.09	0.86	0.69	0.57	0.79	0.63

May	1.22	0.92	0.87	0.62	0.87	0.62
June	0.87	0.69	0.49	0.37	0.57	0.46
July	0.71	0.56	0.57	0.45	0.54	0.39
August	0.84	0.63	0.53	0.41	0.69	0.48
September	1.06	0.73	0.69	0.54	0.86	0.58
October	1.13	0.85	0.69	0.55	0.76	0.61
November	1.34	1.02	0.56	0.43	0.81	0.60
December	1.49	1.18	0.62	0.46	0.82	0.65

Table S6 Validation Metrics for Dynamic Linear Model (DLM) and Linear Model (LM) applied to monthly mean temperatures across zones. The comparison between DLM and LM models is based on the coefficient of determination (R^2) computed using observations and smoother local mean estimates for DLM, and R^2 computed from LM using observations.

Northwestern zone						
	DLM			LM		
	Tx	Tn	T	Tx	Tn	T
Month	R^2	R^2	R^2	R^2	R^2	R^2
January	0.15	0.74	0.48	0.11	0.41	0.37
February	0.02	0.00	0.02	0.05	0.00	0.03
March	0.10	0.78	0.49	0.06	0.43	0.27
April	0.02	0.63	0.24	0.00	0.31	0.12
May	0.04	0.64	0.28	0.01	0.30	0.19
June	0.24	0.80	0.62	0.14	0.43	0.37
July	0.26	0.83	0.71	0.16	0.44	0.45
August	0.15	0.83	0.62	0.12	0.47	0.41
September	0.05	0.76	0.32	0.00	0.32	0.20
October	0.02	0.73	0.27	0.04	0.45	0.28
November	0.10	0.88	0.25	0.03	0.37	0.13
December	0.06	0.18	0.04	0.05	0.03	0.01
Central zone						
	Tx	Tn	T	Tx	Tn	T
Month	R^2	R^2	R^2	R^2	R^2	R^2

January	0.08	0.37	0.10	0.02	0.25	0.10
February	0.02	0.11	0.04	0.00	0.09	0.01
March	0.01	0.58	0.15	0.00	0.30	0.08
April	0.06	0.500	0.08	0.02	0.21	0.02
May	0.07	0.54	0.07	0.01	0.24	0.06
June	0.07	0.57	0.28	0.03	0.35	0.22
July	0.12	0.56	0.37	0.07	0.30	0.30
August	0.13	0.52	0.38	0.11	0.32	0.29
September	0.06	0.54	0.14	0.00	0.12	0.06
October	0.02	0.57	0.14	0.02	0.34	0.16
November	0.22	0.76	0.09	0.08	0.19	0.00
December	0.11	0.27	0.03	0.09	0.11	0.01
Southeastern zone						
	Tx	Tn	T	Tx	Tn	T
Month	R ²	R ²	R ²	R ²	R ²	R ²
January	0.10	0.08	0.08	0.08	0.05	0.10
February	0.04	0.02	0.04	0.06	0.04	0.07
March	0.20	0.11	0.22	0.13	0.05	0.13
April	0.09	0.16	0.11	0.04	0.04	0.05
May	0.14	0.12	0.13	0.08	0.04	0.10
June	0.27	0.13	0.27	0.18	0.12	0.23
July	0.28	0.10	0.21	0.18	0.06	0.21
August	0.05	0.24	0.15	0.03	0.18	0.14
September	0.04	0.28	0.09	0.02	0.00	0.01
October	0.12	0.34	0.19	0.16	0.16	0.21
November	0.04	0.43	0.12	0.02	0.04	0.03
December	0.05	0.09	0.06	0.01	0.02	0.02
East						
	Tx	Tn	T	Tx	Tn	T
Month	R ²	R ²	R ²	R ²	R ²	R ²
January	0.07	0.46	0.48	0.04	0.29	0.37
February	0.01	0.09	0.01	0.01	0.09	0.03

March	0.07	0.65	0.48	0.04	0.35	0.27
April	0.04	0.56	0.24	0.01	0.25	0.12
May	0.04	0.53	0.28	0.00	0.24	0.19
June	0.12	0.65	0.61	0.06	0.39	0.37
July	0.21	0.67	0.71	0.13	0.36	0.45
August	0.13	0.69	0.61	0.11	0.43	0.41
September	0.05	0.58	0.32	0.02	0.17	0.20
October	0.03	0.57	0.26	0.04	0.35	0.28
November	0.13	0.81	0.27	0.05	0.25	0.13
December	0.06	0.27	0.04	0.05	0.09	0.01

Table S7 Results of dynamic linear state space model: Changes (in °C), and standard deviations of the spatially averaged monthly mean of Tx, Tn, and T in Northwestern, Central, and Southeastern zones, as well as for the Eastern Province of Rwanda during the period 1983-2021.

Northwestern zone						
	Tx		Tn		T	
Month	Change Trend	SD	Change Trend	SD	Change Trend	SD
January	1.28 [-0.67-3.32]	1.04	3.33 [2.03-4.77]	0.89	1.97 [0.57-3.26]	0.76
February	1.29 [-0.94-3.71]	1.05	0.60 [-0.68-1.77]	0.56	1.03 [-0.58-2.59]	0.70
March	0.99 [-1.33-3.15]	1.02	3.81 [1.83-5.96]	1.19	2.25 [0.29-4.44]	0.98
April	0.22 [-1.27-1.80]	0.76	2.19 [0.69-3.57]	0.77	1.03 [-0.18-2.41]	0.64
May	0.24 [-1.86-2.17]	0.92	2.92 [1.22-4.52]	0.84	1.35 [0.01-2.81]	0.65
June	1.30 [-0.45-2.96]	0.84	3.93 [2.28-5.66]	1.01	2.39 [1.00-3.86]	0.81
July	0.93 [-0.45-2.24]	0.69	4.22 [2.30-6.28]	1.26	2.33 [0.96-3.67]	0.83
August	0.77 [-0.78-2.51]	0.82	3.97 [2.11-5.88]	1.23	2.22 [0.57-3.64]	0.88

September	0.26 [-1.39-1.94]	0.86	3.90 [1.60-6.14]	1.12	1.65 [-0.07-3.15]	0.79
October	-0.30 [-2.36-1.86]	1.06	3.79 [1.43-6.05]	1.04	1.26 [-0.59-3.10]	0.85
November	-0.76 [-2.60-1.03]	0.92	4.61 [2.58-6.55]	1.00	1.10 [-0.33-2.66]	0.64
December	-0.67 [-2.37-1.06]	0.94	0.56 [-0.65-1.75]	0.51	-0.08 [-1.26-1.18]	0.61
Central zone						
	T_x		T_n		T	
	Change Trend	SD	Change Trend	SD	Change Trend	SD
January	0.51 [-1.73-2.47]	1.09	1.89 [0.73-3.16]	0.59	1.06 [-0.17-2.54]	0.67
February	0.36 [-1.97-2.82]	1.12	1.29 [-0.18-2.77]	0.63	0.73 [-0.93-2.49]	0.78
March	-0.03 [-2.08-1.93]	0.94	2.02 [0.55-3.37]	0.72	0.95 [-0.57-2.38]	0.68
April	-0.41 [-2.12-1.17]	0.81	1.70 [0.35-3.03]	0.70	0.52 [-0.58-1.67]	0.59
May	-0.42 [-2.67-1.55]	0.96	2.45 [1.06-4.18]	0.75	0.76 [-0.45-2.08]	0.59
June	0.72 [-0.87-2.13]	0.79	3.17 [1.76-4.65]	0.77	1.54 [0.28-2.75]	0.63
July	0.49 [-0.75-1.68]	0.59	2.57 [1.16-3.93]	0.73	1.32 [0.37-2.29]	0.50
August	0.73 [-0.63-1.99]	0.64	2.43 [0.71-3.82]	0.70	1.41 [0.21-2.54]	0.57
September	0.26 [-1.44-1.79]	0.82	2.29 [0.47-4.15]	0.71	0.98 [-0.41-2.33]	0.63
October	-0.33 [-2.42-1.95]	1.09	2.99 [0.96-5.20]	0.87	0.88 [-0.91-2.53]	0.82
November	-1.44 [-3.48-0.81]	1.07	3.34 [1.71-5.11]	0.72	0.22 [-1.18-1.78]	0.64

December	-1.14 [-3.30-0.95]	1.13	0.95 [-0.43-2.20]	0.59	-0.20 [-1.62-1.29]	0.72
Southeastern zone						
	Tx		Tn		T	
	Change Trend	SD	Change Trend	SD	Change Trend	SD
January	1.27 [-1.23-3.73]	1.17	1.13 [-0.13-2.40]	0.51	1.08 [-0.20-2.48]	0.71
February	1.59 [-0.95-3.81]	1.20	1.14 [-0.25-2.47]	0.61	1.27 [-0.53-3.06]	0.81
March	1.45 [-1.06-4.03]	1.22	0.87 [-0.18-1.97]	0.49	1.23 [-0.30-3.02]	0.75
April	0.66 [-1.02-2.35]	0.86	0.69 [-0.50-1.94]	0.58	0.67 [-0.62-1.95]	0.64
May	0.78 [-1.46-2.99]	1.00	0.99 [-0.38-2.34]	0.63	0.89 [-0.46-2.21]	0.62
June	1.61 [-0.38-3.54]	0.95	1.70 [0.48-2.99]	0.54	1.44 [0.17-2.73]	0.61
July	1.09 [-0.23-2.37]	0.72	1.19 [-0.08-2.49]	0.54	1.03 [0.08-2.03]	0.48
August	0.32 [-1.04-1.64]	0.62	1.48 [0.16-2.67]	0.57	0.75 [-0.34-1.91]	0.48
September	0.57 [-1.13-2.12]	0.83	1.07 [-0.73-2.91]	0.61	0.65 [-0.63-1.85]	0.60
October	0.94 [-1.46-3.27]	1.19	1.84 [-0.06-3.55]	0.75	1.17 [-0.77-2.89]	0.86
November	0.35 [-1.87-2.33]	1.03	1.77 [0.30-3.32]	0.61	0.64 [-0.84-2.15]	0.67
December	0.42 [-1.57-2.39]	1.15	0.39 [-0.92-1.85]	0.58	0.42 [-1.00-1.83]	0.76
East						
	Tx		Tn		T	
	Change Trend	SD	Change Trend	SD	Change Trend	SD
January	0.85 [-1.42-3.30]	1.10	2.19 [0.97-3.36]	0.62	1.99 [0.69-3.29]	0.69

February	0.95 [-1.29-3.22]	1.10	1.32 [-0.08-2.69]	0.61	0.98 [-0.64-2.57]	0.78
March	0.78 [-1.35-3.27]	1.04	2.42 [1.03-3.67]	0.82	2.17 [0.14-4.30]	0.82
April	-0.28 [-1.94-1.52]	0.82	1.92 [0.69-3.16]	0.70	1.09 [-0.12-2.36]	0.61
May	-0.06 [-2.08-2.03]	0.93	2.37 [0.84-3.80]	0.74	1.32 [0.04-2.68]	0.59
June	0.89 [-0.79-2.46]	0.79	3.31 [1.74-4.81]	0.81	2.32 [0.87-3.72]	0.66
July	0.71 [-0.58-2.05]	0.61	3.14 [1.39-4.84]	0.86	2.38 [0.99-3.69]	0.59
August	0.71 [-0.60-2.00]	0.66	3.03 [1.50-4.67]	0.84	2.21 [0.64-3.75]	0.64
September	0.52 [-1.117-2.35]	0.83	2.59 [0.66-4.49]	0.78	1.70 [0.16-3.27]	0.68
October	-0.02 [-2.29-2.44]	1.10	2.77 [0.60-4.72]	0.87	1.39 [-0.28-3.26]	0.84
November	-1.04 [-3.01-0.92]	1.03	3.53 [2.01-5.09]	0.75	1.23 [-0.25-2.73]	0.63
December	-0.81 [-2.79-1.03]	1.09	0.85 [-0.45-2.23]	0.57	-0.11 [-1.33-1.09]	0.71

Table S8 Linear Model's results as trends (in °C/year), changes (in °C) and standard deviations of the spatially averaged seasonal and annual mean of Tx, Tn, and T in Northwestern, Central, and Southeastern zones, as well as for the Eastern Province of Rwanda during the period 1983-2021.

Northwestern zone						
	Tx		Tn		T	
Season	Change Trend	SD	Change Trend	SD	Change Trend	SD
JF	0.03 [0.00-0.05]	0.80	0.03 [0.01-0.04]	0.58	0.03 [0.01-	0.58

	1.17		1.17		0.04]	
					1.17	
MAM	0.01 [-0.01-0.03] 0.39	0.73	0.05 [0.02-0.07] 1.95	0.88	0.03 [0.01-0.05] 1.17	0.66
JJA	0.03 [0.01-0.04] 1.17	0.64	0.07 [0.04-0.09] 2.73	1.15	0.05 [0.03-0.06] 1.95	0.80
SOND	-0.00 [-0.02-0.02] -0.00	0.66	0.04 [0.03-0.06] 1.56	0.82	0.02 [0.01-0.04] 0.78	0.54
Annual	0.01 [-0.00-0.03] 0.39	0.50	0.05 [0.03-0.07] 1.95	0.83	0.03 [0.02-0.04] 1.17	0.55
Central zone						
	T_x		T_n		T	
	Change Trend	SD	Change Trend	SD	Change Trend	SD
JF	0.00 [-0.02-0.03] 0.19	0.85	0.02 [0.01-0.04] 0.78	0.55	0.01 [-0.00-0.03] 0.39	0.56
MAM	-0.01 [-0.03-0.02] -0.39	0.74	0.03 [0.02-0.05] 1.17	0.67	0.01 [-0.00-0.03] 0.39	0.52
JJA	0.02 [0.00-0.03] 0.78	0.52	0.04 [0.02-0.05] 1.56	0.69	0.03 [0.01-0.04] 1.17	0.50
SOND	-0.01 [-0.03-0.01] -0.39	0.74	0.03 [0.01-0.04] 1.17	0.63	0.01 [-0.01-0.02] 0.39	0.50
Annual	-0.00 [-0.01-0.01] -0.00	0.48	0.03 [0.01-0.04] 1.17	0.59	0.02 [0.01-0.03] 0.78	0.38
Southeastern zone						
	T_x		T_n		T	
	Change	SD	Change	SD	Change	SD

	Trend		Trend		Trend	
JF	0.03 [0.00-0.05] 1.17	0.97	0.01 [-0.00-0.03] 0.39	0.51	0.02 [0.00-0.04] 0.78	0.62
MAM	0.03 [0.00-0.05] 1.17	0.88	0.01 [-0.00-0.02] 0.39	0.49	0.02 [0.00-0.03] 0.78	0.57
JJA	0.02 [0.01-0.04] 0.78	0.64	0.02 [0.00-0.03] 0.78	0.49	0.02 [0.01-0.03] 0.78	0.45
SOND	0.02 [-0.00-0.04] 0.78	0.79	0.01 [-0.00-0.03] 0.39	0.52	0.02 [0.00-0.03] 0.78	0.54
Annual	0.02 [0.01-0.04] 0.78	0.63	0.01 [0.00-0.02] 0.39	0.42	0.02 [0.01-0.03] 0.78	0.41
East						
	T_x		T_n		T	
	Change Trend	SD	Change Trend	SD	Change Trend	SD
JF	0.02 [-0.01-0.04] 0.78	0.86	0.02 [0.01-0.04] 0.78	0.56	0.03 [0.01-0.05] 1.17	0.59
MAM	0.00 [-0.02-0.03] 0.19	0.74	0.03 [0.02-0.05] 1.17	0.70	0.03 [0.01-0.05] 1.17	0.57
JJA	0.02 [0.00-0.03] 0.78	0.55	0.05 [0.03-0.06] 1.95	0.81	0.05 [0.02-0.06] 1.95	0.58
SOND	-0.00 [-0.02-0.02] -0.00	0.71	0.03 [0.01-0.05] 1.17	0.65	0.02 [0.01-0.04] 0.78	0.52
Annual	0.01 [-0.01-0.02] 0.39	0.49	0.03 [0.02-0.05] 1.17	0.63	0.03 [0.02-0.04] 1.17	0.44

Table S9 Linear Model's results as trends (in °C/year), changes (in °C) and standard deviations of the spatially averaged monthly mean of Tx, Tn, and T in Northwestern, Central, and Southeastern zones, as well as for the Eastern Province of Rwanda during the period 1983-2021.

Northwestern zone						
	Tx		Tn		T	
Month	Change Trend	SD	Change Trend	SD	Change Trend	SD
January	0.03 [0.00-0.06] 1.17	1.04	0.05 [0.03-0.07] 1.95	0.89	0.04 [0.02-0.06] 1.56	0.76
February	0.02 [-0.01-0.05] 0.78	1.05	0.00 [-0.01-0.02] 0.19	0.56	0.01 [-0.01-0.03] 0.39	0.70
March	0.02 [-0.01-0.05] 0.78	1.02	0.07 [0.04-0.10] 2.73	1.19	0.04 [0.02-0.07] 1.56	0.98
April	0.00 [-0.02-0.02] 0.00	0.76	0.04 [0.02-0.06] 1.56	0.77	0.02 [0.00-0.04] 0.78	0.64
May	0.01 [-0.02-0.03] 0.39	0.92	0.04 [0.02-0.06] 1.56	0.84	0.02 [0.01-0.04] 0.78	0.65
June	0.03 [0.01-0.05] 1.17	0.84	0.06 [0.04-0.08] 2.34	1.01	0.04 [0.02-0.06] 1.56	0.81
July	0.02 [0.01-0.04] 0.78	0.69	0.07 [0.05-0.10] 2.73	1.26	0.05 [0.03-0.07] 1.95	0.83
August	0.03 [0.00-0.05] 1.17	0.82	0.07 [0.04-0.10] 2.73	1.23	0.05 [0.03-0.07] 1.95	0.88
September	0.01 [-0.02-0.03] 0.39	0.86	0.06 [0.03-0.08] 2.34	1.12	0.03 [0.01-0.05] 1.17	0.79
October	0.02 [-0.01-0.05] 0.78	1.06	0.06 [0.04-0.08] 2.34	1.04	0.04 [0.02-0.06] 1.56	0.85
November	-0.01 [-0.04-0.01] -0.39	0.92	0.05 [0.03-0.08] 1.95	1.00	0.02 [0.00-0.04] 0.78	0.64
December	-0.02 [-0.04-0.01] -0.78	0.94	0.01 [-0.01-0.02] 0.39	0.51	-0.01 [-0.02- 0.01] -0.39	0.61

Central zone						
	T_x		T_n		T	
	Change Trend	SD	Change Trend	SD	Change Trend	SD
January	0.01 [-0.02-0.04] 0.39	1.09	0.03 [0.01-0.04] 1.17	0.59	0.02 [0.00-0.04] 0.78	0.67
February	-0.01 [-0.04-0.03] -0.39	1.12	0.02 [-0.00-0.03] 0.78	0.63	0.01 [-0.02-0.03] 0.39	0.78
March	-0.00 [-0.03-0.03] -0.00	0.94	0.03 [0.02-0.05] 1.17	0.72	0.02 [-0.00-0.04] 0.78	0.68
April	-0.01 [-0.04-0.01] -0.39	0.81	0.03 [0.01-0.05] 1.17	0.70	0.01 [-0.01-0.03] 0.39	0.59
May	-0.01 [-0.03-0.02] -0.39	0.96	0.03 [0.01-0.05] 1.17	0.75	0.01 [-0.00-0.03] 0.39	0.59
June	0.01 [-0.01-0.04] 0.39	0.79	0.04 [0.02-0.06] 1.56	0.77	0.03 [0.01-0.04] 1.17	0.63
July	0.01 [-0.00-0.03] 0.39	0.59	0.03 [0.02-0.05] 1.17	0.73	0.02 [0.01-0.04] 0.78	0.50
August	0.02 [0.00-0.03] 0.78	0.64	0.03 [0.02-0.05] 1.17	0.70	0.03 [0.01-0.04] 1.17	0.57
September	0.01 [-0.02-0.03] 0.39	0.82	0.02 [0.00-0.04] 0.78	0.71	0.01 [-0.00-0.03] 0.39	0.63
October	0.02 [-0.01-0.04] 0.78	1.09	0.04 [0.02-0.06] 1.56	0.87	0.03 [0.01-0.05] 1.17	0.82
November	-0.03 [-0.06-0.00] -1.17	1.07	0.03 [0.01-0.05] 1.17	0.72	0.00 [-0.01-0.02] 0.19	0.64
December	-0.03 [-0.06-0.00] -1.17	1.13	0.02 [0.00-0.03] 0.78	0.59	-0.01 [-0.03- 0.01] -0.39	0.72
Southeastern						
	T_x		T_n		T	
	Change Trend	SD	Change Trend	SD	Change Trend	SD

January	0.03 [-0.00-0.06] 1.17	1.17	0.01 [-0.00-0.03] 0.39	0.51	0.02 [-0.00-0.04] 0.78	0.71
February	0.03 [-0.01-0.06] 1.17	1.20	0.01 [-0.01-0.03] 0.39	0.61	0.02 [-0.00-0.04] 0.78	0.81
March	0.04 [0.00-0.07] 1.56	1.22	0.01 [-0.00-0.02] 0.39	0.49	0.02 [0.00-0.04] 0.78	0.75
April	0.01 [-0.01-0.04] 0.39	0.86	0.01 [-0.01-0.03] 0.39	0.58	0.01 [-0.00-0.03] 0.39	0.64
May	0.02 [-0.00-0.05] 0.78	1.00	0.01 [-0.01-0.03] 0.39	0.63	0.02 [0.00-0.03] 0.78	0.62
June	0.03 [0.01-0.06] 1.17	0.95	0.02 [0.00-0.03] 0.78	0.54	0.03 [0.01-0.04] 1.17	0.61
July	0.03 [0.01-0.05] 1.17	0.72	0.01 [-0.00-0.03] 0.39	0.54	0.02 [0.01-0.03] 0.78	0.48
August	0.01 [-0.01-0.03] 0.39	0.62	0.02 [0.01-0.04] 0.78	0.57	0.02 [0.00-0.03] 0.78	0.48
September	0.01 [-0.01-0.03] 0.39	0.83	-0.00 [-0.02-0.02] -0.00	0.61	0.01 [-0.01-0.02] 0.39	0.60
October	0.04 [0.01-0.07] 1.56	1.19	0.02 [0.01-0.05] 0.78	0.75	0.03 [0.01-0.06] 1.17	0.86
November	0.01 [-0.01-0.04] 0.39	1.03	0.01 [-0.01-0.03] 0.39	0.61	0.01 [-0.01-0.03] 0.39	0.67
December	0.01 [-0.02-0.04] 0.39	1.15	0.01 [-0.01-0.02] 0.39	0.58	0.01 [-0.01-0.03] 0.39	0.76
East						
	Tx		Tn		T	
	Change Trend	SD	Change Trend	SD	Change Trend	SD
January	0.02 [-0.01-0.05] 0.78	1.10	0.02 [0.01-0.04] 0.78	0.62	0.04 [0.02-0.06] 1.56	0.69
February	0.01 [-0.02-0.04] 0.39	1.10	0.02 [-0.00-0.03] 0.78	0.61	0.01 [-0.01-0.03] 0.39	0.78
March	0.02 [-0.01-0.05] 0.78	1.04	0.04 [0.02-0.06] 0.78	0.82	0.04 [0.02-0.07] 0.78	0.82

	0.78		1.56		1.56	
April	-0.01 [-0.03-0.02] -0.39	0.82	0.03 [0.01-0.05] 1.17	0.70	0.02 [0.00-0.04] 0.78	0.61
May	0.00 [-0.03-0.03] 0.00	0.93	0.03 [0.01-0.05] 1.17	0.74	0.02 [0.01-0.04] 0.78	0.59
June	0.02 [-0.00-0.04] 0.78	0.79	0.04 [0.02-0.06] 1.56	0.81	0.04 [0.02-0.06] 1.56	0.66
July	0.02 [0.00-0.04] 0.78	0.61	0.05 [0.03-0.07] 1.95	0.86	0.05 [0.03-0.07] 1.95	0.59
August	0.02 [0.00-0.04] 0.78	0.66	0.05 [0.03-0.07] 1.95	0.84	0.05 [0.03-0.07] 1.95	0.64
September	0.01 [-0.01-0.03] 0.39	0.83	0.03 [0.01-0.05] 1.17	0.78	0.03 [0.01-0.05] 1.17	0.68
October	0.02 [-0.01-0.05] 0.78	1.10	0.04 [0.02-0.06] 1.56	0.87	0.04 [0.02-0.06] 1.56	0.84
November	-0.02 [-0.05-0.01] -0.78	1.03	0.03 [0.01-0.05] 1.17	0.75	0.02 [0.00-0.04] 0.78	0.63
December	-0.02 [-0.05-0.01] -0.78	1.09	0.02 [-0.00-0.03] 0.78	0.57	-0.01 [-0.02- 0.01] -0.39	0.71

References

- Abera, W., Tamene, L., Tibebe, D., Adimassu, Z., Kassa, H., Hailu, H., Mekonnen, K., Desta, G., Sommer, R. and Verchot, L. (2020) Characterizing and evaluating the impacts of national land restoration initiatives on ecosystem services in Ethiopia. *Land Degrad. Dev.*, 31, 37-52. <http://doi.org/10.1002/ldr.3424>.
- Ahmed, K., Shahid, S., Ali, R.O., Bin Harun, S. and Wang, X.J., (2017) Evaluation of the performance of gridded precipitation products over Balochistan Province, Pakistan. *Desalin. Water Treat.*, 79, 73-86. <https://doi.org/10.5004/dwt.2017.20859>.

Allabakash, S. and Lim, S. (2022) Anthropogenic influence of temperature changes across East Asia using CMIP6 simulations. *Sci. Rep.*, 12, 11896. <https://doi.org/10.1038/s41598-022-16110-9>.

Almazroui, M., Islam, M. N. and Jones, P. D. (2013) Urbanization effects on the air temperature rise in Saudi Arabia. *Clim. Change*, 120, 109-122. <https://link.springer.com/article/10.1007/s10584-013-0796-2>.

Alsabti, K., Ranka, S. and Singh, V. (1997) An efficient k-means clustering algorithm. *Electrical Engineering and Computer Science*, 43. <https://surface.syr.edu/eecs/43>.

Anyah, R.O. and Qiu, W., (2012) Characteristic 20th and 21st century precipitation and temperature patterns and changes over the Greater Horn of Africa. *International Journal of Climatology*, 32(3), 347-363. <https://doi.org/10.1002/joc.2270>.

Auger-Méthé, M. et al. (2016) State-space models dirty little secrets: even simple linear Gaussian models can have estimation problems. *Scientific Reports*, 6, 26677. <https://doi.org/10.1038/srep26677>.

Auger-Méthé, M., Newman, K., Cole, D., Empacher, F., Gryba, R., King, A. A., Leos-Barajas, V., Mills Flemming, J., Nielsen, A., Petris, G. and Thomas, L. (2021) A guide to state-space modeling of ecological time series. *Ecological Monographs*, 91(4):e01470. <https://doi.org/10.1002/ecm.1470>.

Ayugi, B., Tan, G., Niu, R., Dong, Z., Ojara, M., Mumo, L., Babaousmail, H. and Ongoma, V. (2020) Evaluation of Meteorological Drought and Flood Scenarios over Kenya, East Africa. *Atmosphere*, 11, 307. <https://doi.org/10.3390/atmos11030307>.

Boyle, D.P., Gupta, H.V. and Sorooshian, S. (2000) Toward improved calibration of hydrologic models: Combining the strengths of manual and automatic methods. *Water Resources Res.*, 36(12), 3663-3674. <https://doi.org/10.1029/2000WR900207>.

- Carreras, H., Zanobetti, A. and Koutrakis, P. (2015) Effect of daily temperature range on respiratory health in Argentina and its modification by impaired socio-economic conditions and PM10 exposures. *Environ. Pollut.*, 206, 175-182. <https://doi.org/10.1016/j.envpol.2015.06.037>.
- Carvalho, M.J., Melo-Gonçalves, P., Teixeira, J.C. and Rocha, A. (2016) Regionalization of Europe based on a K-Means Cluster Analysis of the climate change of temperatures and precipitation. *Physics and Chemistry of the Earth, Parts A/B/C*, 94, 22-28. <https://doi.org/10.1016/j.pce.2016.05.001>.
- Cechin, D.G., Makhotina, I.A., Lüpkes, C. and Makshtas, A.P. (2019) Effect of wind speed and leads on clear-sky cooling over Arctic Sea ice during polar night. *J. Atmos. Sci.*, 76, 2481-2503. <https://doi.org/10.1175/JAS-D-18-0277.1>.
- Chen, X., Shao, Q., Xu, C.-Y., Zhang, J., Zhang, L. and Ye, C. (2017) Comparative Study on the Selection Criteria for Fitting Flood Frequency Distribution Models with Emphasis on Upper-Tail Behavior. *Water* 9 (5), 320. <https://doi.org/10.3390/w9050320>.
- Choi, Y.W., Campbell, D.J. and Eltahir, E.A.B. (2022) Near-term regional climate change in East Africa. *Clim. Dyn.*, 61, 961-978. <https://doi.org/10.1007/s00382-022-06591-9>.
- Coles, S., (2001) *An Introduction to Statistical Modeling of Extreme Values*. Springer-Verlag, London, Springer, London. ISBN 978-1-4471-3675-0. <https://doi.org/10.1007/978-1-4471-3675-0>.
- Collier, P., Conway, G. and Venables, T. (2008) Climate Change and Africa. *Oxford Review of Economic Policy*, 24(2), 337-353. <http://oxrep.oxfordjournals.org/>.
- Core Team (2021) *R: A language and environment for statistical computing*. R Foundation for Statistical Computing, Vienna, Austria. <https://www.R-project.org/>.
- Dai, A. (2016) Future Warming Patterns Linked to Today's Climate Variability. *Sci. Rep.*, 6, 6-11. <https://doi.org/10.1038/srep19110>.
- Dinku, T., Hailemariam, K., Maidment, R., Tarnavsky, E. and Connor, S. (2014) Combined use of satellite estimates and rain gauge observations to generate high-quality historical

rainfall time series over Ethiopia. *International Journal of Climatology*, 34, 2489-2504.
<https://doi.org/10.1002/joc.3855>.

Dunning, C.M., Black, E.C.L. and Allan, R.P. (2016) The onset and cessation of seasonal rainfall over Africa. *Journal of Geophysical Research: Atmospheres*, 121(19), 11, 405- 424.
<https://doi.org/10.1002/2016JD025428>.

Durbin, T.J. and Koopman, S.J. (2012) *Time series analysis by state space methods*. 2nd edition, Oxford statistical science series, Oxford University Press, Oxford, 346 Pages.
<https://www.scribd.com/doc/55179464/Time-Series-Analysis-by-State-Space-Methods-by-Durbin-and-Koopman#>.

Ekane, N. (2016) *Sanitation and Hygiene: Policy, Stated Beliefs, and Actual Practice*. Stockholm Environment Institute. <https://doi.org/10.13140/RG.2.1.2250.8569>.

ESRI. (2021). *ArcGIS (Version 10.4)*. Redlands, CA: Environmental Systems Research Institute, Inc. <https://www.esri.com>.

FAO. (2018) *Tracking Adaptation in Agricultural Sectors: Climate Change Adaptation Indicators*. Food and Agriculture Organization of the United Nations, Rome, Italy.
<https://doi.org/10.18356/87fe25de-en>.

Fernández, A. and Gómez, S. (2020) Versatile linkage: a family of space-conserving strategies for agglomerative hierarchical clustering. *Journal of Classification*, 37(3), 584-597.
<https://doi.org/10.1007/s00357-019-09339-z>.

Gabry, J., Simpson, D., Vehtari, A., Betancourt, M. and Gelman, A. (2019) Visualization in Bayesian workflow. *Journal of the Royal Statistical Society Series A*, 182(2), 389-402.
<https://doi.org/10.1111/rssa.12378>.

Gamerman, D. (2006) *Markov chain Monte Carlo—stochastic simulation for Bayesian inference*. 2nd edition, Chapman & Hall, London, 342 Pages.
<https://www.routledge.com/Markov-Chain-Monte-Carlo-Stochastic-Simulation-for-Bayesian-Inference/Gamerman-Lopes/p/book/9781584885870>.

Gu, G. and Adler, R.F. (2013) Interdecadal variability/long-term changes in global precipitation patterns during the past three decades: Global warming and/or Pacific decadal variability? *Clim. Dyn.*, 40, 3009-3022. <https://doi.org/10.1007/s00382-012-1443-8>.

Haggag, M., Kalisa, J.C. and Abdeldayem, A.W. (2016) Projections of precipitation, air temperature, and potential evapotranspiration in Rwanda under changing climate conditions. *African Journal of Environmental Science and Technology*, 10(1), 18– 33. <https://doi.org/10.5897/ajest2015.1997>.

Hansen, J., Ruedy, R., Sato, M. and Lo, K. (2010) Global surface temperature change. *Review of Geophysics*, 48(4), 1-29. <https://doi.org/10.1029/2010RG000345>.

Hatfield, J.L. and Prueger, J.H. (2015) Temperature extremes: Effect on plant growth and development. *Weather Clim. Extrem.*, 10: 4-10. <http://doi.org/10.1016/j.wace.2015.08.001>.

Henninger, S.M. (2013) Does the global warming modify the local Rwandan climate?. *Natural Science*, 5(1A), 124-129. <http://dx.doi.org/10.4236/ns.2013.51A019>.

Herrero, M., Addison, J., Bedelian, C., Carabine, E., Havlik, P., Henderson, B., Van De Steeg, S.J. and Thornton, P. (2016) Climate change and pastoralism: Impacts, consequences and adaptation. *Rev. Sci. Tech. Loie*, 35: 417-433. <http://doi.org/10.20506/rst.35.2.2533>.

Herold, N., Alexander, L., Green, D. and Donat, M. (2017) Greater increases in temperature extremes in low versus high-income countries *Environ. Res. Lett.*, 12, 10-13. <https://doi.org/10.1088/1748-9326/aa5c43>.

Hipel, K.W. and McLeod, A.I. (1994) *Time Series Modelling of Water Resources and Environmental Systems*. Elsevier Science, Amsterdam. <https://www.perlego.com/book/1856325/time-series-modelling-of-water-resources-and-environmental-systems-pdf>.

IPCC. (2007) Climate Change 2007: Synthesis Report. Contribution of Working Groups I, II, and III to the Fourth Assessment Report of the Intergovernmental Panel on Climate Change, [Core Writing Team, Pachauri, R.K and Reisinger, A. (eds.)]. IPCC, Geneva, Switzerland. <http://dx.doi.org/10.1017/CBO9780511546013>.

IPCC. (2014) Africa. In: Climate Change 2014: Impacts, Adaptation, and Vulnerability. Part B: Regional Aspects. Contribution of Working Group II to the Fifth Assessment Report of the Intergovernmental Panel on Climate Change. Cambridge University Press, Cambridge, United Kingdom and New York, NY, USA, 1199-1265. https://www.ipcc.ch/site/assets/uploads/2018/02/WGIIAR5-Chap22_FINAL.pdf.

IPCC. (2021) Summary for Policymakers. In: Climate Change 2021: The Physical Science Basis. Masson-Delmotte, V., Zhai, P., Pirani, A., Connors, S.L., Pean, C., Berger, S., Caud, N., Chen, Y., Yelekci, L.O., Yu, R. and Zhou, B. (eds), Contribution of Working Group I to the Sixth Assessment Report of the Intergovernmental Panel on Climate Change. Cambridge University Press. In Press. <https://www.ipcc.ch/report/sixth-assessment-report-working-group-i/>.

IPCC. (2022) Climate Change 2022: Impacts, Adaptation, and Vulnerability. Contribution of Working Group II to the Sixth Assessment Report of the Intergovernmental Panel on Climate Change [H.-O. Pörtner, D.C. Roberts, M. Tignor, E.S. Poloczanska, K. Mintenbeck, A. Alegría, M. Craig, S. Langsdorf, S. Löschke, V. Möller, A. Okem, B. Rama (eds.)], Cambridge University Press, Cambridge, UK and New York, NY, USA. <https://doi.org/10.1017/9781009325844>.

IPCC. (2023) Summary for Policymakers. In: Climate Change 2023: Synthesis Report. Contribution of Working Groups I, II, and III to the Sixth Assessment Report of the Intergovernmental Panel on Climate Change, [Core Writing Team, H. Lee and J. Romero (eds.)]. IPCC, Geneva, Switzerland, 1-34. <https://doi.org/10.59327/IPCC/AR6-9789291691647.001>.

Iqbal, M. A., Penas, A., Cano-Ortiz, A., Kersebaum, K.C., Herrero, L. and del Río, S. (2016) Analysis of recent changes in maximum and minimum temperatures in Pakistan. *Atmospheric Research*, 168, 234-249. <https://doi.org/10.1016/J.ATMOSRES.2015.09.016>.

Jang, J.Y. and Chun, B.C. (2021) Effect of diurnal temperature range on emergency room visits for acute upper respiratory tract infections. *Environ. Health Prev. Med.*, 26, 55. <https://doi.org/10.1186/s12199-021-00974-w>.

Kew, S.F., Philip, S.Y., Hauser, M., Hobbins, M., Wanders, N., van Oldenborgh, G.J., van der Wiel, K., Veldkamp, T.I.E., Kimutai, J., Funk, C., et al. (2021) Impact of precipitation and increasing temperatures on drought trends in eastern Africa. *Earth Syst. Dyn.*, 12, 17-35. <https://doi.org/10.5194/esd-12-17-2021>.

Kohonen, T. (2001) *Self-Organizing Maps*. Springer, Heidelberg. <https://doi.org/10.1007/978-3-642-56927-2>.

Klutse, N.A.B., Sylla, M.B., Diallo, I., Sarr, A., Dosio, A., Diedhiou, A., Kamga, A., Lamptey, B., Ali, A., Gbobaniyi, E.O., et al. (2016) Daily characteristics of West African monsoon rainfall in CORDEX regional climate models. *Theor. Appl. Climatol.*, 123: 369-386. <http://doi.org/10.1007/s00704-014-1352-3>.

Kömüščü, A.Ü., Turgu, E. and DeLiberty, T. (2022) Dynamics of precipitation regions of Turkey: A clustering approach by K-means methodology in respect of climate variability. *Journal of Water and Climate Change*, 13(10), 3578–3606. <https://doi.org/10.2166/wcc.2022.186>.

Kweku, D. W., Bismark, O., Maxwell, A., Desmond, K. A., Danso, K. B., Oti-Mensah, E. A., et al. (2018). Greenhouse effect: greenhouse gases and their impact on global warming. *Journal of Scientific research and reports*, 17(6), 1-9. <https://doi.org/10.9734/JSRR/2017/39630>.

Laine, M., Latva-Pukkila, N. and Kyrölä, E. (2014) Analysing time-varying trends in stratospheric ozone time series using the state space approach. *Atmospheric Chemistry and Physics*, 14, 9707-9725. <https://doi.org/10.5194/acp-14-9707-2014>.

Likas, A., Vlassis, N. and Verbeek, J. (2003) The global k-means clustering algorithm. *Pattern Recognition*, 36(2), 451-461. [https://doi.org/10.1016/S0031-3203\(02\)00060-2](https://doi.org/10.1016/S0031-3203(02)00060-2).

Lim, Y.H., Hong, Y.C. and Kim, H. (2012) Effects of diurnal temperature range on cardiovascular and respiratory hospital admissions in Korea. *Sci. Total Environ.*, 15-417-418. <https://doi.org/10.1016/j.scitotenv.2011.12.048>.

Malhi, Y. and Wright, J. (2004) Spatial Patterns and Recent Trends in the Climate of Tropical Rainforest Regions. *Philosophical Transactions of Royal Society London Series B*, 359, 311-329. <http://dx.doi.org/10.1098/rstb.2003.1433>.

Maure, G.A., Pinto, I., Ndebele-Murisa, M.R., Muthige, M., Lennard, C., Nikulin, G., Dosio, A. and Meque, A.O. (2018) The southern African climate under 1.5 °C and 2 °C of global warming as simulated by CORDEX regional climate models. *Environ. Res. Lett.*, 13, 065002. <http://doi.org/10.1088/1748-9326/aab190>.

Meehl, G.A., Karl, T., Easterling, D.R., Changnon, S., Pielke, R., Changnon, D.Jr., Evans, J., Groisman, P.Y., Knutson, T.R., Knukel, K.E., et al. (2000) An introduction to trends in extreme weather and climate events: Observations, socioeconomic impacts, terrestrial ecological impacts, and model projections. *Bulletin of the American Meteorological Society*, 81(3), 413-416. [http://dx.doi.org/10.1175/1520-0477\(2000\)081%3C0413:AITTIE%3E2.3.CO;2](http://dx.doi.org/10.1175/1520-0477(2000)081%3C0413:AITTIE%3E2.3.CO;2).

Meteo Rwanda (2023) Climatology of Rwanda. Rwanda Meteorology Agency. Available at: <https://www.meteorwanda.gov.rw/> (Accessed: 4 June 2023).

Meteo Rwanda (2024) Dataset Documentation. Rwanda Meteorology Agency. Available at: <http://maproom.meteorwanda.gov.rw/maproom/Summary/index.html#tabs-2>. (Accessed: 31 July 2024).

Mikkonen, S., Laine, M., Mäkelä, H. M., Gregow, H., Tuomenvirta, H., Lahtinen, M. and Laaksonen, A. (2014) Trends in the average temperature in Finland, 1847–2013. *Stochastic*

Environmental Research and Risk Assessment, 29, 1521-1529.
<https://doi.org/10.1007/s00477-014-0992-2>.

Mikova, K., Makupa, E. and Kayumba, J. (2015) Effect of Climate Change on Crop Production in Rwanda. *Earth Sciences*, 4(3), 120-128. <https://doi.org/10.11648/j.earth.20150403.15>.

MINAGRI (2023) Annual Report 2022-2023. Republic of Rwanda, Ministry of Agriculture and Animal Resources. <https://www.minagri.gov.rw/publications/reports>.

Minder, J. R., Letcher, T. W. and Liu, C. (2018) The character and causes of elevation-dependent warming in high-resolution simulations of Rocky Mountain climate change. *J. Clim.*, 31(6), 2093-2113. <https://doi.org/10.1175/JCLI-D-17-0321.1>.

Moriasi, D.N., Arnold, J. G., Van Liew, M. W., Bingner, R. L., Harmel, R. D. and Veith, T. L. (2007) Model Evaluation Guidelines for Systematic Quantification of Accuracy in Watershed Simulations. *American Society of Agricultural and Biological Engineers*, 50(3), 885-900. <http://dx.doi.org/10.13031/2013.23153>.

Muneza, L. (2016) Droughts and Floodings Implications in Agriculture Sector in Rwanda: Consequences of Global Warming. In *The Nature, Causes, Effects and Mitigation of Climate Change on the Environment*; IntechOpen: London, UK, 2016; p. 11. <https://doi.org/10.5772/intechopen.98922>.

Munyaneza, O., Ndayisaba, C., Wali, U.G., Mulungu, D.M.M. and Dulos, S.O. (2011) Integrated flood and drought Management for Sustainable Development in Kagera River. *Nile Basin Water Science & Engineering Journal*, 4(1), 60-70. https://www.nilebasin-journal.com/pdf_ReadDownload.php?type=download&file=557_20091933.pdf.

Mupangwa, W., Chipindu, L., Ncube, B., Mkuhlani, S., Nhantumbo, N., Masvaya, E., Ngwira, A., Moeletsi, M., Nyagumbo, I. and Liben, F. (2023) Temporal Changes in Minimum and Maximum Temperatures at Selected Locations of Southern Africa. *Climate* 11(4), 84. <https://doi.org/10.3390/cli11040084>.

Ndenga, B., Githeko, A., Omukunda, E., Munyekenye, G., Atieli, H., Wamai, P. et al. (2006) Population dynamics of malaria vectors in western Kenya highlands. *Journal of Medical Entomology*, 43(2), 200-206. [https://doi.org/10.1603/0022-2585\(2006\)043\[0200:pdomvi\]2.0.co;2](https://doi.org/10.1603/0022-2585(2006)043[0200:pdomvi]2.0.co;2).

Ngarukiyimana, J.P, Fu Y., Sindikubwabo, C., Nkurunziza, I.F., Ogou, F.K., Vuguziga, F., Ogwang, B.A. and Yang, Y. (2021) Climate Change in Rwanda: The Observed Changes in Daily Maximum and Minimum Surface Air Temperatures during 1961–2014. *Frontiers in Earth Sciences*, 9, 1-18. <https://doi.org/10.3389/feart.2021.619512>.

Nicholson, S.E. (2017) Climate and climatic variability of rainfall over eastern Africa. *Reviews of Geophysics (in French)*, 55(3), 590-635. <https://doi.org/10.1002/2016RG000544>.

Nicholson, S.E. (2018) The ITCZ and the seasonal cycle over equatorial Africa *Bulletin of American Meteorological Society*, 99(2), 337-348. <https://doi.org/10.1175/BAMS-D-16-0287.1>.

Nielsen, F. (2016) *Introduction to HPC with MPI for Data Science*. Springer, ISBN 978-3-319-21903-5. <https://link.springer.com/book/10.1007/978-3-319-21903-5>.

NISR. (2023a) *The Fifth Rwanda Population and Housing Census, Main Indicators Report*, February 2023. National Institute of Statistics of Rwanda, Kigali, Rwanda. <http://www.statistics.gov.rw>.

NISR. (2023b) *Seasonal Agriculture Survey: Season A 2023 Report*. Republic of Rwanda, National Institute of Statistics of Rwanda, Kigali, Rwanda. <https://www.statistics.gov.rw/publication/1930>.

NOAA National Centers for Environmental Information (2024) *Annual 2023 Global Climate Report*. Available at: <https://www.ncei.noaa.gov/access/monitoring/monthly-report/global/202313> (Accessed: 19 October 2024).

Ntwali, D., Ogwang, B.A. and Ongoma, V. (2016) The impacts of topography on spatial and temporal rainfall distribution over Rwanda based on WRF model. *Atmospheric and Climate Sciences*, 6(2), 145-157. <https://doi.org/10.4236/acs.2016.62013>.

Parthasarathi, T., Firdous, S., Mariya, D.E., et al. (2022) Effects of High Temperature on Crops. *Advances in Plant Defense Mechanisms*. IntechOpen. Available at: <http://dx.doi.org/10.5772/intechopen.105945>.

Petris, G. (2010) An R package for dynamic linear models. *Journal of Statistical Software*, 36(12), 1-16. <https://doi.org/10.18637/jss.v036.i12>.

Pohlert, T. (2023) Non-Parametric Trend Tests and Change-Point Detection, R-package trend. Available at: <https://cran.r-project.org/web/packages/trend/vignettes/trend.pdf> (Accessed: 1 June 2023).

Pepin, N. C., and Lundquist, J. D. (2008) Temperature trends at high elevations: patterns across the globe. *Geophys. Res. Lett.*, 35(14). <https://doi.org/10.1029/2008GL034026>.

RAB. (2020) Rwanda Irrigation Master Plan, Kigali. Republic of Rwanda, Rwanda Agriculture and Animal Resources Development Board. https://www.minagri.gov.rw/fileadmin/user_upload/Minagri/Publications/Policies_and_strategies/Rwanda_Irrigation_Master_Plan.pdf.

Rahman, A.S., Rahman, A., Zaman, M.A., Haddad, K., Ahsan, A. and Imteaz, M. (2013) A study on selection of probability distributions for at-site flood frequency analysis in Australia. *Nat Hazards* 69, 1803-1813. <https://doi.org/10.1007/s11069-013-0775-y>.

Razali, N. M. and Wah, Y. B. (2011) Power Comparisons of Shapiro-Wilk, Kolmogorov-Smirnov, Lilliefors and Anderson-Darling Tests. *Journal of Statistical Modeling and Analytics*, 2(1), 21-33. <https://www.nrc.gov/docs/ML1714/ML17143A100.pdf>.

Revadekar, J.V., Hameed, S., Collins, D., Manton, M., Sheikh, M., Borgaonkar, H. P., et al. (2013) Impact of altitude and latitude on changes in temperature extremes over South Asia during 1971–2000. *International Journal of Climatology*, 33(1), 199-209. <http://dx.doi.org/10.1002/joc.3418>.

Richardson, K., Calow, R., Pichon, F., New, S. and Osborne, R. (2022) Climate Risk Report for the East Africa Region. Met Office, ODI, FCDO: Cape Town, South Africa, 2022. <https://reliefweb.int/organization/odi>.

Roininen, L., Laine, M. and Ulich, T. (2015) Time-varying ionosonde trend: Case study of Sodankylä hmF2 data 1957–2014. *Journal of Geophysical Research: Space Physics*, 120(8), 6851-6859. <https://doi.org/10.1002/2015JA021176>.

Rwema, M., Sylla, M.B., Safari, B., Roininen, L. and Laine, M. (2025) Trends analysis and change point detection in precipitation time series over the Eastern Province of Rwanda during 1981-2021. *Theoretical and Applied Climatology*, 156, 98. <https://doi.org/10.1007/s00704-024-05317-7>.

Russo, S., Marchese, A.F., Sillmann, J. and Immé, G. (2016) When will unusual heat waves become normal in a warming Africa? *Environ. Res. Lett.*, 11, 054016. <https://doi.org/10.1088/1748-9326/11/5/054016>.

Rust, J.M. and Rust, T. (2013) Climate change and livestock production: A review with emphasis on Africa. *South Afr. J. Anim. Sci.*, 43, 255. <http://doi.org/10.4314/sajas.v43i3.3>.

Safari, B. (2012) Trend Analysis of the Mean Annual Temperature in Rwanda during the Last Fifty-Two Years. *Journal of Environmental Protection*, 3(6), 538-551. <http://dx.doi.org/10.4236/jep.2012.36065>.

Safari, B., Sebaziga, J.N. and Siebert, A. (2022) Evaluation of CORDEX-CORE regional climate models in simulating rainfall variability in Rwanda. *International Journal of Climatology*, 43(2), 1112-1140. <https://doi.org/10.1002/joc.7891>.

Safari, B. and Sebaziga, J.N. (2023) Trends and Variability in Temperature and Related Extreme Indices in Rwanda during the Past Four Decades. *Atmosphere*, 2023, 14, 1449. <https://doi.org/10.3390/atmos14091449>.

Safeeq, M., Mair, A. and Fares, A. (2013) Temporal and spatial trends in air temperature on the Island of Oahu, Hawaii. *International Journal of Climatology*, 33(13), 2816-2835. <https://doi.org/10.1002/joc.3629>.

Sarkodie, S.A., Rufangura, P., Jayaweera, H.M.P.C. and Asantewaa, O.P.A. (2015) Situational Analysis of Flood and Drought in Rwanda. *International Journal of Scientific & Engineering Research*, 6(8), 960-970. <https://doi.org/10.6084/M9.FIGSHARE.3381463.V1>.

Sebaziga, N.J., Ntirenganya, F., Tuyisenge, A. and Iyakaremye, V. (2020) A Statistical Analysis of the Historical Rainfall Data Over Eastern Province in Rwanda. *East African Journal of Science and Technology*, 10(1), 33-52. <https://www.unilak.ac.rw/wp-content/uploads/2016/08/4.pdf>.

Sebaziga, N.J., Safari, B., Ngaina, J.N., Ntwali, D., Mutai, B.K., Safari, K.A. and Rwema, M. (2022) Rainfall variability and trends over Rwanda. *Journal of Climate Change and Sustainability*, 4(1), 26-34. <https://doi.org/10.20987/jccs.04.06.2022>.

Sebaziga, N.J., Twahirwa, A., Kazora, J., Rusanganwa, F., Mugunga, M.M., Higiuro, S., Guhirwa, S., Nyandwi, J.C. and Niyitegeka, J.M.V. (2023) Spatial and Temporal Analysis of Rainfall Variability and Trends for Improved Climate Risk Management in Kayonza District, Eastern Rwanda. *Advances in Meteorology*, 2023, 1-17. <https://doi.org/10.1155/2023/5372701>.

Sebaziga, J. N., Safari, B., Ngaina, J. N. and Ntwali, D. (2024) Spatial variability of seasonal rainfall onset, cessation, length and rainy days in Rwanda. *Theoretical and Applied Climatology*, 155, 7591-7608. <https://doi.org/10.1007/s00704-024-05086-3>.

Şevgin, F. and Öztürk, A. (2024) Variation of temperature increase rate in the Northern Hemisphere according to latitude, longitude and altitude: the Turkey example. *Scientific Reports*, 14(1), 18207. <https://doi.org/10.1038/s41598-024-68164-6>.

Shah, F., Huang, J., Cui, K., Nie, L., Shah, T., Chen, C. and Wang, K. (2011) Impact of high-temperature stress on rice plant and its traits related to tolerance. *J. Agric. Sci.*, 149, 545-556. <http://doi.org/10.1017/S0021859611000360>.

Sheng, Y. and Chun, W. (2002) Applicability of prewhitening to Eliminate the Influence of Serial Correlation on the Mann-Kendall Test. *Water Resources Research*, 38(6) 1068. <https://doi.org/10.1029/2001WR000861>.

Shi, N., Liu, X. and Guan, Y. (2010) Research on k-means Clustering Algorithm: An Improved k-means Clustering Algorithm. *Computer Society*. <https://doi.org/10.1109/IITSI.2010.74>.

Siebert, A., Dinku, T., Vuguziga, F., Twahirwa, A., Kagabo, M.D., DelCorral, J. and Robertson, A.W. (2019) Evaluation of ENACTS-Rwanda: A new multi-decade, high-resolution rainfall, and temperature data set—Climatology. *International Journal of Climatology*, 34, 1262-1277. <https://doi.org/10.1002/joc.6010>.

Soetaert, K. and Petzoldt, T. (2010) Inverse Modeling, Sensitivity, and Monte Carlo Analysis in R Using Package FME. *Journal of Statistical Software*, 33(3), 1-28. <https://doi.org/10.18637/jss.v033.i03>.

Székely, G.J. and Rizzo, M.L. (2005) Hierarchical clustering via Joint Between-Within Distances: Extending Wards Minimum Variance Method. *Journal of Classification*, 22(2), 151-183. <https://doi.org/10.1007/s00357-005-0012-9>.

Theodoridis, S. and Koutroumbas, K. (2008) *Pattern Recognition*. 4th Edition. Academic Press, Cambridge. ISBN: 9781597492720. [https://darmanto.akakom.ac.id/pengenalanpola/Pattern%20Recognition%204th%20Ed.%20\(2009\).pdf](https://darmanto.akakom.ac.id/pengenalanpola/Pattern%20Recognition%204th%20Ed.%20(2009).pdf).

Trupti, M.K. and Prashant, R.M. (2013) Review on determining the number of Cluster in K-Means Clustering. *International Journal of Advance Research in Computer Science and Management Studies*, 1(6), 90-95. <http://www.ijarcsms.com/>.

Ul Hassan, M., Hayat, O. and Noreen, Z. (2019) Selecting the best probability distribution for at-site flood frequency analysis; a study of Torne River. *SN Appl. Sci.* 1, 1629. <https://doi.org/10.1007/s42452-019-1584-z>.

Uwimbabazi, J., Jing, Y., Iyakaremye, V., Ullah, I. and Ayugi, B. (2022) Observed Changes in Meteorological Drought Events during 1981–2020 over Rwanda, East Africa. *Sustainability*, 14, 1519. <https://doi.org/10.3390/su14031519>.

Vellinga, M. and Milton, S. (2018) Drivers of interannual variability of the East African "Long Rains". *Quarterly Journal of the Royal Meteorological Society*, 144(1), 861-876. <https://doi.org/10.1002/qj.3263>.

Vervoort, J.M., Thornton, P.K., Kristjanson, P., Förch, W., Ericksen, P.J., Kok, K., Ingram, J.S., Herrero, M., Palazzo, A., Helfgott, A.E., et al. (2014) Challenges to scenario-guided adaptive action on food security under climate change. *Glob. Environ. Chang.*, 4(28), 383-394. <http://doi.org/10.1016/j.gloenvcha.2014.03.001>.

Vicente-Serrano, S.M. (2007) Evaluating the Impact of Drought Using Remote Sensing in a Mediterranean, Semi-arid Region. *Natural Hazards*, 40, 173-208. <https://doi.org/10.1007/s11069-006-0009-7>.

Vuille, M. and Bradley, R. S. (2000) Mean annual temperature trends and their vertical structure in the tropical Andes. *Geophys. Res. Lett.*, 27(23), 3885-3888 <https://doi.org/10.1029/2000GL011871>.

Walther, G.R., Post, E., Convey, P., Menzel, A., Parmesan, C., Beebee, T.J.C., Fromentin, J.M., Hoegh Guldberg, O. and Bairlein, F. (2002) Ecological responses to recent climate change. *Nature*, 416, 389-395. <https://doi.org/10.1038/416389a>.

Ward, J.H. (1963) Hierarchical Grouping to Optimize an Objective Function. *Journal of the American Statistical Association*, 58(301), 236-244. <https://doi.org/10.2307/2282967>.

Wang, Z., Zhou, Y., Luo, M., Yang, H., Xiao, S., Huang, X., Ou, Y., Zhang, Y., Duan, X., Hu, W., et al. (2020) Association of diurnal temperature range with daily hospitalization for exacerbation of chronic respiratory diseases in 21 cities. China. *Respir. Res.* 2020, 21, 251. <https://doi.org/10.1186/s12931-020-01517-7>.

Webb, A.R. and Copsey, K.D. (2011) *Statistical Pattern Recognition*. 3rd Edition. John Wiley & Sons, Hoboken. <https://doi.org/10.1002/9781119952954>.

Wickramasinghe, A., Muthukumarana, S., Loewen, D. and Schaubroeck, M. (2022) Temperature clusters in commercial buildings using k-means and time series clustering. *Energy Informatics*, 5(1), 2-14. <https://doi.org/10.1186/s42162-022-00186-8>.

WMO. (2019) World Meteorological Organization Commission for Climatology. In *State of the Climate in Africa 2019: Report WMO-No.1253*. World Meteorological Organisation, Geneva, Switzerland, 2020. <https://library.wmo.int/idurl/4/57196>.

Verdoodt, A. and Van Ranst, E. (2003) Land evaluation for agricultural production in the tropics. A large-scale land suitability classification for Rwanda. Ghent University. Laboratory of Soil Science. <https://api.semanticscholar.org/CorpusID:131005551>.

Yokoi et al. (2011) Application of cluster analysis to climate model performance metrics. *Journal of Applied Meteorology and Climatology*, 50, 1666-1675. https://www.mri-jma.go.jp/Dep/clg/hendo/paper/paper_7.pdf.

Zhao, P., He, Z., Ma, D., Wang, W. and Qian, L. (2024) Temperature trends and its elevation-dependent warming over the Qilian Mountains. *J. Mt. Sci.*, 21, 500-510. <https://doi.org/10.1007/s11629-023-8449-z>.

Zhou, G., Minakawa, N., Githeko, A.K. and Yan, G. (2004) Association between climate variability and malaria epidemics in the East African highlands. *Proc. Natl. Acad. Sci., USA*, 101, 2375-2380. <https://doi.org/10.1073/pnas.0308714100>.

Chapter 4 Climate-induced drought characteristic estimate in the Eastern region of Rwanda

4.1 Introduction

Rising temperatures combined with increased variability in rainfall patterns, shaped by geographic location, atmospheric circulation, and seasonal fluctuations, have contributed to drought becoming a frequent phenomenon in recent decades. This research examines the characteristics and progression of drought events in Rwanda's Eastern Province over the period from 1981 to 2021. The study focuses on three relatively homogeneous microclimatic zones and utilizes monthly rainfall data along with the Standardized Precipitation Index (SPI) calculated over 3-month (SPI-3) and 6-month (SPI-6) intervals. The SPI is a widely adopted metric for assessing drought severity based solely on precipitation, making it particularly suitable for regions like eastern Rwanda, where rainfall is the chief driver of hydrological dynamics. By using SPI, it becomes possible to better understand drought impacts such as soil moisture depletion and reduced agricultural productivity, thereby contributing to more informed water resource management and climate-responsive planning (Ntale and Gan 2003; Hasan, Dongkai, and Al-Shibli 2023).

The choice of SPI at 3-month and 6-month scales is deliberate, as these timescales effectively represent both short-term and medium-term drought conditions (Edwards, McKee, et al. 1997). The 3-month SPI enables timely detection of short-term precipitation deficits that primarily affect soil moisture and streamflow, crucial factors for crop growth and everyday water availability. Meanwhile, the 6-month SPI captures longer-term moisture deficits that influence reservoir storage and groundwater recharge. Combining these two indices provides a comprehensive perspective on drought development and severity across the study area. This analysis not only quantifies the frequency, duration, and intensity of drought episodes but also examines their temporal patterns, thereby offering a detailed assessment of drought risk in Eastern Rwanda.

4.2 Methodology

4.2.1 Drought index calculation with SPI

To assess and measure drought severity linked to climate variability in the Eastern Province, this study employs the Standardized Precipitation Index (SPI), which emphasizes fluctuations in precipitation (McKee et al. 1993; Pramudya and Onishi 2018). This index is particularly useful in regions such as eastern Rwanda, where rainfall critically influences hydrological conditions, providing a reliable means to relate precipitation deficits to drought impacts like reduced soil moisture and decreased crop yields. Key components of the SPI calculation involve characterizing the cumulative probability distribution, which is modeled using the gamma function $\gamma(\alpha)$ as

$$G(x) = \int_0^x f(x)dx = \frac{1}{\beta^\alpha \gamma(\alpha)} \int_0^x x^{\alpha-1} e^{-\frac{x}{\beta}} dx \quad (4.1)$$

where x is the precipitation amount, while α and β represent shape and scale parameters, respectively (Thom 1958). In the presence of dry conditions (i.e., $x = 0$), the value of the cumulative probability density is used as

$$H(x) = q + (1 - q) * G(x) \quad (4.2)$$

where q is the probability of $x = 0$, which is obtained by dividing the number of zeros (m) by the sample size (n) as (m/n). The SPI index values are then calculated as

$$Z = SPI = \begin{cases} -\left(t - \frac{c_0 + c_1 t + c_2 t^2}{1 + d_1 + d_2 t^2 + d_3 t^3}\right), \text{ where, } t = \left(\ln\left(\frac{1}{(H(x))^2}\right)\right)^{1/2}, \text{ for } 0 < H(x) \leq 0.5 \\ \left(t - \frac{c_0 + c_1 t + c_2 t^2}{1 + d_1 + d_2 t^2 + d_3 t^3}\right), \text{ where, } t = \left(\ln\left(\frac{1}{(1 - H(x))^2}\right)\right)^{1/2}, \text{ for } 0.5 < H(x) \leq 1.0 \end{cases} \quad (4.3)$$

The constants used in the calculation are fixed at $c_0=2.515517$, $c_1=0.802853$, $c_2=0.010328$, $d_1=1.432788$, $d_2=0.189269$, $d_3=0.001308$ (McKee et al. 1993). This methodology has been widely applied in various studies, including those by Ntale and Gan (2003) and Rahman and

Lateh (2016), among others. The computations in this study were carried out using the R statistical software, specifically utilizing the “SPEI” package, version 1.7 (Beguería and Vicente-Serrano 2017).

4.3 Results

4.3.1. Incidence and Categories of Drought Events

Across all three microclimatic zones, near-normal conditions represented by SPI values between -0.99 and 0.99 dominated both the 3-month and 6-month timescales, accounting for 68–72% of all events (Table 4.1). Following these, moderate wet and moderate dry conditions were the next most frequent, with both severely and extremely wet or dry events occurring less regularly. Notably, extremely dry events, which indicate the most severe drought conditions, comprised between 2% and 4% of events depending on the zone and timescale. For example, SPI-3 analysis showed extremely dry events at 3.47% in the Northwestern zone, 2.24% in the Central zone, and 2.86% in the Southeastern zone. At the 6-month scale, these percentages ranged from 2.04% to 3.67%, underscoring the spatial variability in drought risk.

Table 4.1 Frequency of different drought categories in 3-month and 6-month SPI from 1981-2021 in three micro-climate zones of the Eastern Province.

	SPI Values	SPI-3			SPI-6		
		Zone1	Zone2	Zone3	Zone1	Zone2	Zone3
Extremely wet	≥ 2	8	6	8	7	11	13
Severely wet	1.99 to 1.5	23	26	20	26	20	17
Moderate wet	1.49 to 1	47	46	55	45	42	44
Near-Normal	0.99 to -0.99	342	334	342	346	336	353
Moderate dry	-1 to -1.49	34	44	34	40	46	34
Severely dry	-1.50 to -1.99	19	23	17	9	22	8
Extremely dry	≤ -2	17	11	14	14	10	18

4.3.2. Drought Episodes, Duration, and Severity

The analysis of drought episodes revealed significant differences between zones (Table 4.2). At the 3-month timescale, the Central zone stood out as the most drought-prone, experiencing 18 episodes with a cumulative duration of 62 months and a total severity of -104.80 . In

contrast, the Northwestern zone and Southeastern zone each recorded 12 episodes, with durations of 50 and 42 months and severities of -92.78 and -78.84 , respectively. The pattern was similar at the 6-month scale, where the Central zone again led with 14 episodes, 70 months of drought, and a severity of -111.68 , while the Northwestern zone and the Southeastern zone had 12 and 10 episodes, respectively. The year 2017 was particularly notable, as it marked the most severe drought across all zones and timescales, with the lowest SPI values recorded throughout the study period.

Table 4.2 Drought quantities for the 1981–2021 period

	SPI Values	SPI-3			SPI-6		
		Zone1	Zone2	Zone3	Zone1	Zone2	Zone3
Episode	≤ -1 & 2 months	12	18	12	12	14	10
Duration (months)		50	62	42	58	70	54
Severity (total)		-92.78	-104.80	-78.84	-99.41	-111.68	-98.48

4.3.3. Temporal Distribution and Evolution of Droughts

Examining the temporal evolution of drought events with SPI-3 (Figure 4.1) and SPI-6 (Figure 4.2), two major dry periods were identified: an early period from 1982 to 1992/1994 and a more recent period from 2011 to 2021. Between these dry spells, the mid-years (1993–2010) were generally dominated by wetter conditions, although occasional dry months did occur. The most extreme drought peaks, with SPI values below -3.5 , were observed in 2017 across all zones, highlighting this year as a critical point of climate stress. Over the entire study period, the number of negative SPI values, indicative of drought, decreased until the late 1990s, but then began to increase from the mid-2000s onward. This trend suggests a recent acceleration in both the frequency and severity of drought events across the Eastern Province.

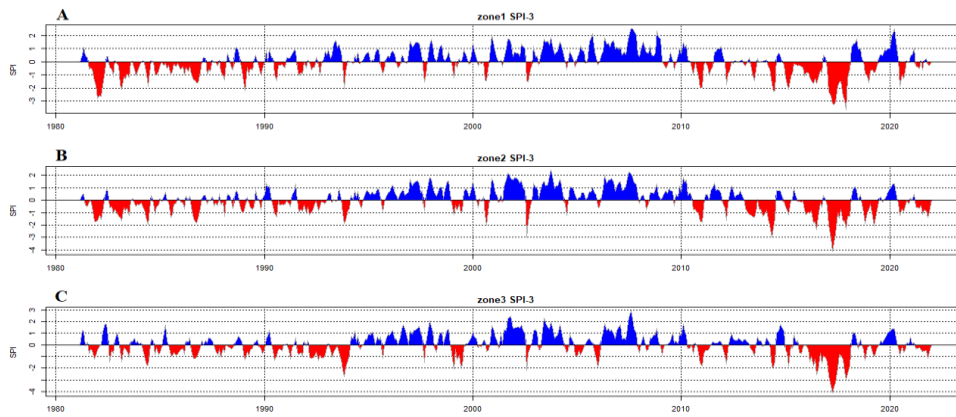


Figure 4.1 Temporal variation of the Standardized Precipitation Index (SPI-3) from 1981 to 2021 across three micro-climate zones in the Eastern Province of Rwanda: (a) Northwestern zone: Zone 1 SPI-3, (b) Central zone: Zone 2 SPI-3, and (c) Southeastern zone: Zone 3 SPI-3. Red bars indicate periods of drought, while blue bars represent wet conditions.

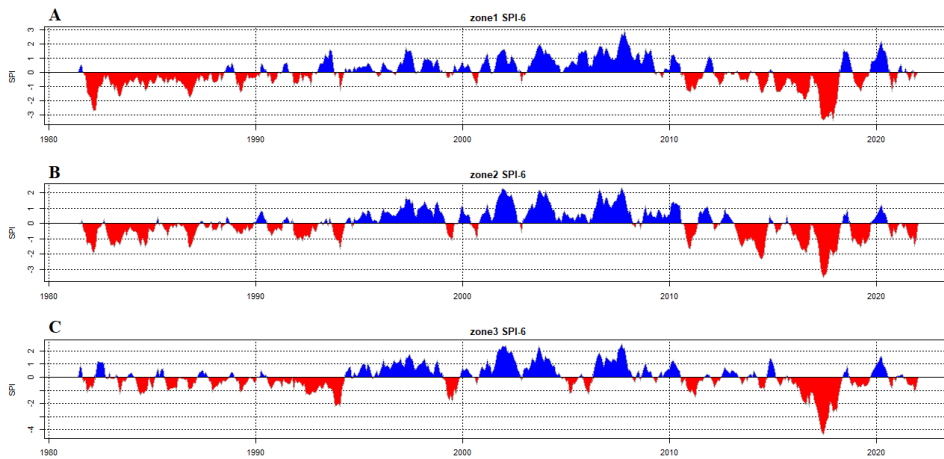


Figure 4.2 Temporal variation of the Standardized Precipitation Index (SPI-6) from 1981 to 2021 across three micro-climate zones in the Eastern Province of Rwanda: (a) Northwestern zone: Zone 1 SPI-6, (b) Central zone: Zone 2 SPI-6, and (c) Southeastern zone: Zone 3 SPI-6. Red bars indicate periods of drought, while blue bars represent wet conditions.

4.3.4 Comparison of First and Last 21 Years

A comparison of the first and last 21 years of the study period reveals a clear intensification of drought conditions. In most zones and at both timescales, the latter period (2001–2021) experienced more drought episodes, longer durations, and greater severity than the earlier period (1981–2001) (Figure 4.3). For instance, in Zone 1 at the 3-month scale, both periods had 7 episodes, but the last period was marked by longer duration (33 vs. 26 months) and higher

severity (-57.37 vs. -46.37). Zone 2 consistently showed more severe drought metrics in the recent period, reinforcing the trend of increasing drought risk over time.

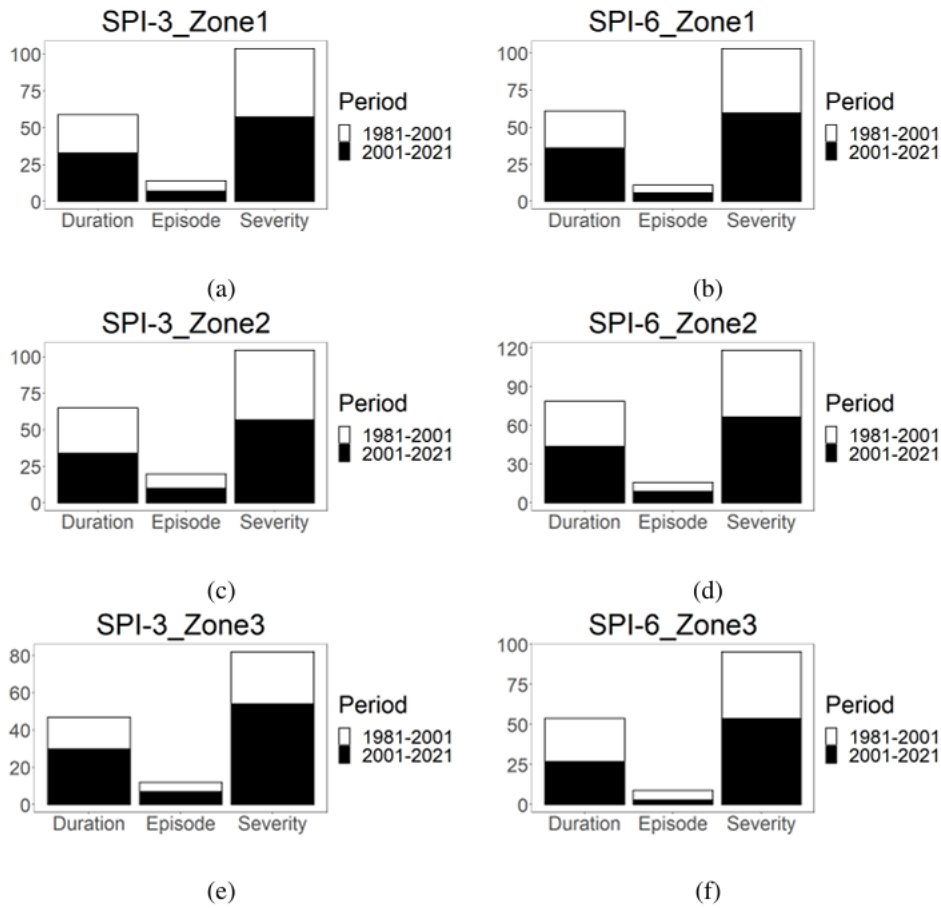


Figure 4.3 Comparison of drought characteristics (episode, duration (in the month), and severity) of the periods 1981-2001 and 2001-2021 using the Standardized Precipitation Index (SPI-3 and SPI-6) across three micro-climate zones in the Eastern Province of Rwanda: (a–b) Zone 1, (c–d) Zone 2, and (e–f) Zone 3. Black bars represent data from the period 2001–2021, while the white bars indicate the period from 1981–2001.

4.4 Discussion

The marked variation in drought frequency across the three zones highlights the spatial complexity of drought risk within Eastern Rwanda. Zone 2's higher incidence of drought events compared to Zones 1 and 3 suggests that local climatic and environmental factors may intensify drought vulnerability in this area. Conversely, the greater occurrence of extreme short-term droughts in Zone 1 and prolonged extreme droughts in Zone 3 indicates distinct

temporal dynamics and impacts, likely driven by variations in topography, soil characteristics, and land use. These spatial differences warrant tailored drought preparedness strategies adapted to zone-specific risk profiles.

Our findings are consistent with previous studies (Rwanyiziri and Rugema 2013; Muneza 2022; Uwimbabazi et al. 2022), which similarly pointed to Eastern Rwanda as a hotspot for climate-related hazards, particularly drought. The escalation of drought frequency and severity over recent decades raises concerns about increasing water scarcity and food insecurity across the region. This trend underscores the urgent need to strengthen adaptive capacity among vulnerable farming communities, many of whom rely heavily on rainfed agriculture that is sensitive to shifts in precipitation patterns.

Temporal analysis revealed two critical drought-prone periods within the 1981–2021 timeframe: an early period marked by a gradual reduction in dry conditions followed by a wetter phase, and a more recent decade characterized by a resurgence and intensification of drought episodes. This recent uptick aligns with broader climate change projections for East Africa, indicating increased drought risk due to warming temperatures and altered rainfall regimes (Kew et al. 2021; IPCC 2023). The extreme drought event in 2017, identified as the most severe across all zones and time scales, serves as a poignant example of the type of climate extremes the region may face more frequently in the future.

To address worsening droughts in eastern Rwanda, it is essential to adopt innovative management strategies that combine improved monitoring, water infrastructure, drought-resistant crops, and community early warnings, alongside blending traditional and scientific knowledge.

References

Beguéría, S., Vicente-Serrano, S.M., (2017). SPEI: calculation of the standardised precipitation-evapotranspiration index.

Hasan, N. A., Dongkai, Y., and Al-Shibli, F. (2023). SPI and SPEI drought assessment and prediction using TBATS and ARIMA models, Jordan. *Water* 15(20), p. 3598.

Edwards, D. C., McKee, T. B., et al. (1997). Characteristics of 20th century drought in the United States at multiple time scales.

IPCC, (2023). Climate Change 2022 – Impacts, Adaptation and Vulnerability: Working Group II Contribution to the Sixth Assessment Report of the Intergovernmental Panel on Climate Change, 1st ed. Cambridge University Press. <https://doi.org/10.1017/9781009325844>.

Kew, S.F., Philip, S.Y., Hauser, M., Hobbins, M., Wanders, N., Van Oldenborgh, G.J., Van Der Wiel, K., Veldkamp, T.I.E., Kimutai, J., Funk, C., Otto, F.E.L., (2021). Impact of precipitation and increasing temperatures on drought trends in eastern Africa. *Earth Syst. Dyn.* 12, 17–35. <https://doi.org/10.5194/esd-12-17-2021>.

McKee, T.B., Doesken, N.J. and Kleist, J. (1993) ‘The Relationship of Drought Frequency and Duration to Time Scales’, Eighth Conference on Applied Climatology, Anaheim, California, 17-22 January 1993, pp. 179-184. https://www.droughtmanagement.info/literature/AMS_Relationship_Drought_Frequency_Duration_Time_Scales_1993.pdf.

Muneza, L., (2022). Droughts and Floodings Implications in Agriculture Sector in Rwanda: Consequences of Global Warming, in: A. Harris, S. (Ed.), *The Nature, Causes, Effects and Mitigation of Climate Change on the Environment*. IntechOpen. <https://doi.org/10.5772/intechopen.98922>.

Ntale, H.K. and Gan, T.Y. (2003) ‘Drought Indices and their Application to East Africa’, *International Journal of Climatology*, 23(11), pp. 1335-1357. <https://doi.org/10.1002/joc.931>.

Pramudya, Y. and Onishi, T. (2018) ‘Assessment of the Standardized Precipitation Index (SPI) in Tegal City, Central Java, Indonesia’, 2018 IOP Conference Series: Earth Environmental Sciences, 129(2018). <https://doi.org/10.1088/1755-1315/129/1/012019>.

Rahman, M. R. and Lateh, H., (2016) ‘Meteorological drought in Bangladesh: assessing, analysing and hazard mapping using SPI, GIS, and monthly rainfall data’, *Environmental Earth Sciences*, 75(1026). <http://dx.doi.org/10.1007/s12665-016-5829-5>.

Rwanyiziri, G. and Rugema, J. (2013) 'Climate Change Effects on Food Security in Rwanda: Case Study of Wetland Rice Production in Bugesera District', *Rwanda Journal, Series E: Agricultural Sciences*, 1(1), pp. 35-51. <http://dx.doi.org/10.4314/rj.v1i1.3E>.

Uwimbabazi, J., Jing, Y., Iyakaremye, V., Ullah, I., Ayugi, B., (2022). Observed Changes in Meteorological Drought Events during 1981–2020 over Rwanda, East Africa. *Sustainability* 14, 1519. <https://doi.org/10.3390/su14031519>.

Chapter 5 Understanding Farmers' Knowledge, Perceptions, and Adaptation Strategies to Climate Change in Eastern Rwanda

This Chapter reproduces the content of our published paper (<https://doi.org/10.3390/su17156721>)

5.1 Introduction

Increasing greenhouse gases in the Earth's atmosphere owing to human activities such as the burning of fossil fuels and deforestation, together with natural activities since the mid-20th century, have resulted in a global average temperature increase (IPCC 2014; Mind'je et al. 2019). The rise in the Earth's temperature, known as global warming, influences climate and weather patterns from global to local scales. The existing consequences of climate change that have been identified include frequent and intense droughts, downpours, floods, hurricanes, storms, water scarcity, severe wildfires, melting polar ice, sea level rise, and declining biodiversity (IPCC 2023). Those consequences have impacted most of the critical sectors of life, ranging from agriculture, food production, water resources, energy, health and public health systems, transportation, infrastructure, ecosystems, and biodiversity (Pecl et al. 2017).

People worldwide experience climate change impacts in various ways, with varying severity based on geographic location and primary economic activities. Agriculture remains a crucial sector supporting a significant portion of the population in Africa, a continent with many developing nations. Most agricultural activities are rain-dependent, increasing their vulnerability to climate change effects (Christian 2010; Zougmore et al. 2018). Changes in temperature and rainfall patterns owing to climate change have posed significant challenges for agricultural communities across the African continent, with the severity of these challenges varying from region to region and country to country.

In East Africa, many people in this region, especially those in the agriculture sector, are impacted by climate change through protracted droughts, floods, and water scarcity, which put them at risk of food insecurity (Nahayo et al. 2019). Rwanda, one of the East African nations, has been previously studied, revealing changes in temperature and rainfall during important seasons over the years. These changes include the observed decline in seasonal and annual total rainfall (Rwanyiziri and Rugema 2013; Ntirenganya 2018; Sebaziga et al. 2020; Jonah et al. 2021) and increasing temperature (Safari 2012; Mohammed, Jean and Ahmad 2016;

Ngarukiyimana et al. 2021) in many parts of the country. In studies including those by Sebaziga et al. (2020) and Rwema et al. (2025), focusing on Rwanda's Eastern Province, which is the largest under agricultural production, scholars have noted a decrease in seasonal rainfall, while a high increase in temperature was also recorded over this region (Safari and Sebaziga 2023).

Increased temperatures and decreased rainfall often resulted in diminished water availability for rainfed agriculture, increasing the likelihood of droughts and intensifying pressure on agricultural water resources (Kew et al. 2021). Over the past few decades, Eastern Rwanda has experienced recurring deficits in rainfall, leading to severe and prolonged droughts. Consequently, water scarcity and food insecurity have escalated in this area (Muneza 2022; Uwimbabazi et al. 2022), leading to diverse experiences among farmers. Repeated exposure to climate-related hazards influences individuals' perceptions (Wolfe et al. 2006), prompting the development of various adaptation and mitigation strategies to address the perceived impacts. Factors, including knowledge, beliefs, and perceptions, play a crucial role in developing and adopting adaptation strategies. It is imperative to understand climate change comprehensively by exploring its physical mechanisms and considering individual behaviors in response to the occurring changes.

Previous studies conducted in Eastern Rwanda have predominantly centered on climatic mechanisms, particularly analyzing trends and variabilities in annual and seasonal temperature and rainfall patterns (Rwanyiziri and Rugema 2013; Sebaziga et al. 2020; Rwema et al. 2025). Studying the climate aspect is very important for several reasons: it promotes a better understanding of patterns and dynamics of climate systems. It also reveals long-term trends in climate variables, which further explain significant implications for vital sectors such as agriculture, water resources, and health. Furthermore, analyzing historical data enables the construction of models and projections for future climate conditions, which is crucial for decision-makers to take appropriate actions to adapt to and mitigate the potential impact of climate change. However, very little attention has been paid to exploring the variations in behaviors among individuals, particularly farmers, concerning their perceptions, experiences, and knowledge of climate change across the Eastern Province. This information helps identify the knowledge gaps and misconceptions, allowing for tailored educational efforts (Adomah Bempah and Olav Øyhus 2017) in vulnerable communities.

Studying how individuals perceive and experience climate change is also instrumental in assessing their behavioral responses and identifying barriers to adaptation and sustainable behaviors (Messner and Meyer 2006). Additionally, engaging with local and indigenous knowledge provides valuable insights into climate change impacts at local and regional levels. This knowledge complements historical data, informs policy decisions, and contributes to more context-specific responses. This study aims to explore farmers' knowledge and perceptions of climate change, its impacts, and the adaptation strategies employed in the Eastern Province of Rwanda. Additionally, it seeks to identify the key factors influencing farmers' decisions to adopt specific adaptation measures. To accomplish this, we analyzed data gathered from interviews with farmers across five districts in Eastern Rwanda. To guide this investigation, we address the following research questions:

- To what extent do farmers in Eastern Rwanda perceive and respond to climate change?
- What are the key socioeconomic determinants of their adaptation strategies?

These questions help frame the study's focus on understanding both the perceptions and adaptive responses of farmers, providing insights that are relevant for policy and practice.

The remaining part of this manuscript is structured as follows: The second section gives details of the methods used for data collection and analysis in the study. The third section presents the findings, which are discussed further in the fourth section. Lastly, the fifth section provides conclusions and offers recommendations.

5.2 Materials and Methods

5.2.1. Study Area

This study is conducted in the Eastern Province of Rwanda, the largest (9,813,000,000 m²) of the five provinces. Its administrative borders connect this province to three countries: Uganda to the North, Tanzania to the East, and Burundi to the South. It is subdivided into seven districts: Bugesera, Gatsibo, Kayonza, Kirehe, Ngoma, Nyagatare, and Rwamagana (see Figure 5.1). Geographically, the Eastern Province is located approximately between longitudes 29.9° and 30.9° E and latitudes 1.1° and 2.3° S. The region's topography features lowland areas with altitudes below 1500 m, characterized by a high annual mean temperature exceeding 293.15 K and low annual rainfall of less than 1000 mm. With the largest population (i.e., 3,563,145), the region's economy mainly relies on agriculture and livestock. The Eastern region experiences four seasons throughout the year, including two rainy seasons and two dry seasons. The

primary rainy seasons occur from March to May (MAM) and from September to December (SOND), with April and November serving as the peak months for these seasons, respectively. Conversely, the dry seasons take place from January to February (JF) and from June to August (Meteo Rwanda 2023).

Most agricultural practices in this area rely on rainfall and align with the two rainy seasons (Ntwali, Ogwang and Ongoma 2016; Nicholson 2018). The main crops in Eastern Rwanda include maize, beans, sorghum, rice, cassava, and bananas. As in other parts of the country, the high dependence on rainfall increases vulnerability to the adverse impacts of changes and variability in rainfall and temperature (Kew et al. 2021). Over the past few decades, drought has emerged as a significant challenge in this region, leading to decreased agricultural and livestock production, exacerbating food insecurity among a substantial portion of the population (Muneza 2022; Uwimbabazi et al. 2022). From the Northern to the Southern regions of the Eastern Province, farmers have extensive insights to share, particularly about climate change, its impacts, and various adaptation strategies. The farmers participating in this study were recruited from five of the seven districts in the Eastern Province: Nyagatare, Gatsibo, Kayonza, Ngoma, and Kirehe (see Figure 5.1).

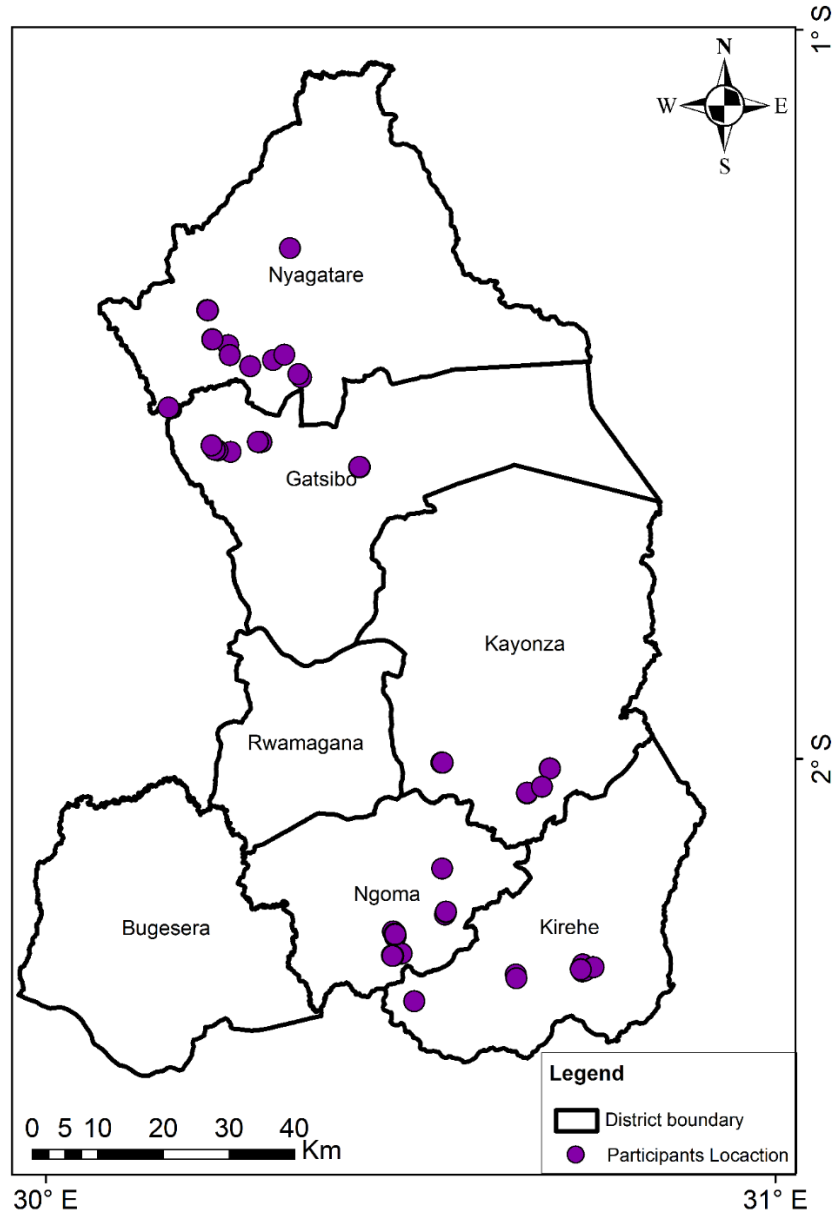


Figure 5.1 Eastern Province map with the surveyed participants’ location highlighted with purple dots.

5.2.2. Sample(s)

The total number of 638,806 agricultural households from seven districts of the Eastern Province (NISR 2023) was considered to be the population size. With Yamane’s formula (Slovin, Sushka and Polonchek 1993), we estimated the size of the sample to be 204 heads of households at a 93% confidence level, which implies allowing a margin error of 7%.

$$n = \frac{N}{(1+Ne^2)}, \quad (5.1)$$

where n = Sample size, N = Total population, and e = Margin of error.

While a 95% confidence level would have necessitated a substantially larger sample of approximately 400 farmers, practical constraints related to time and resources required adjustment. Although this reduction in confidence level may marginally affect estimate precision, the final sample of 204 respondents was deemed sufficient to yield robust and meaningful findings within the study's logistical parameters.

Multistage sampling was used to select respondent farmers from the Eastern Province. Five of the seven districts in the Eastern Province were chosen purposely to ensure representation from the North, Central, and Southern regions. In the North, we included the Nyagatare and Gatsibo districts; in the Central area, we included the Kayonza district; and in the South, we included the Ngoma and Kirehe districts (See Figure 5.1). Sectors from each district were selected systematically, mainly based on agricultural activities, farmers' availability, and accessibility. From each sector, with the assistance of sector agronomists, we purposely selected cells based on farmers' availability. In each cell, the Executive Secretary or Socio-Economic Development Officer (SEDO) assisted in identifying exemplary farmers who, due to their extensive knowledge of and active participation in local farmer groups, were able to provide a comprehensive and prompt list of potential respondents. To reduce selection bias, respondents were then randomly selected from this list, ensuring a representative sample of the farming community within each cell.

The distribution of respondent farmers from the districts to cells, as shown in Table 5.1, indicates the number of respondent farmers per district as follows: Nyagatare (33), Gatsibo (35), Kayonza (36), Ngoma (74), and Kirehe (26). The higher number of respondents from the Ngoma district reflects a proportional allocation based on the relative size of agricultural households in each district, with districts having larger agricultural populations receiving a correspondingly larger share of the sample. This approach was used to ensure that the sample accurately represents the population distribution across the study area and helps reduce sampling bias that could arise if all districts were sampled equally, regardless of their size.

Table 5.1 Farmers' distribution in districts, sectors, and cells.

Zone	District	Sector	Cell		
North	Nyagatare (33)	Nyagatare (1)	Nyagatare (1)		
		Gatunda (9)	Nyamirembe (9)		
		Mukama (6)	Gihengeri (1), Rugarama (5)		
		Mimuri (4)	Mimuri (2), Rugari (2)		
		Katabagemu (13)	Barija (3), Nyakigando (9), Ryaruganzu (1)		
	Gatsibo (35)	Ngarama (10)	Nyarubungo (9), Cyigashi (1)		
		Nyagihanga (14)	Gitinda (14)		
		Kabarore (11)	Nyabikiri (10), Nyabikenke (1)		
		Central	Kayonza (36)	Ndego (10)	Byimana (7), Kiyovu (3)
				Kabare (12)	Rubumba (10), Cyarubare (1), Karubimba (1)
South	Ngoma (74)	Kabarondo (14)	Cyabajwa (14)		
		Mutenderi (24)	Karwema (19), Kibare (5)		
		Kazo (29)	Kinyonzo (29)		
	Kirehe (26)	Murama (21)	Sakara (19), Rurenge (1), Mvumba (1)		
		Nyamugali (10)	Nyamugali (7), Kiyanzi (3)		
		Kigina (11)	Gatarama (11)		
		Musaza (5)	Mubuga (4), Nganda (1)		

5.2.3. Data Type and Data Collection Approach

The meteorological data analyzed included rainfall through derived seasonal rainfall variables such as seasonal rainfall amount, onset and cessation, and seasonal duration, along with minimum (T_n), maximum (T_x), and average (T) temperatures at both annual and seasonal levels. The rainfall and temperature datasets were obtained from the Rwanda Meteorology Agency (Meteo Rwanda 2024).

To define the onset and cessation of the rainy season, we adopted established agroclimatic criteria originally proposed by Stern et al. (Stern, Dennett and Garbutt 1981), Omotosho et al. (Omotosho, Balogun and Ogunjobi 2000), and others, as applied and adapted by Rwema et al.

(Rwema et al. 2025). Specifically, the onset of rain was identified as the first day when a total rainfall of at least 20 mm accumulated over a 5-day period, with at least 3 consecutive rainy days (≥ 1 mm/day), and no dry spell exceeding 7 consecutive days within the subsequent 21 days. The cessation of rain was defined as the first day after which precipitation remained below 0.5 times the evapotranspiration for at least 10 consecutive days. The season duration was calculated as the difference in days between the cessation and onset dates.

The farmers' data were based on recorded responses from interviews conducted in November 2023 with farmers from the Eastern Province of Rwanda. A semi-structured questionnaire (see Supporting Information SII) featuring a combination of open-ended and closed-ended questions was prepared and used for data collection. While some sections, such as socioeconomic characteristics, primarily used closed-ended questions (e.g., gender, group membership), other sections employed a mix of both closed-ended and open-ended questions to capture richer information. For example, in the knowledge of weather and climate change section, respondents were first asked closed-ended questions (e.g., "Have you heard about weather and climate?"), followed by open-ended questions to explore their understanding in more detail. Similarly, sections on perceptions, adaptation strategies, and barriers to adaptation included mainly open-ended questions, often allowing multiple responses to better capture the complexity of farmers' experiences. Below are example questions and measurement scales used for each section:

- Section 1: Socioeconomic characteristics

Example questions:

- "How old are you?" (Open numerical response)
- "What is your gender?" (Male/Female)
- "Do you belong to any farmer group/cooperative?" (Yes/No)

- Section 2: Knowledge of weather and climate change

Example questions:

- "Have you heard about the weather and climate?" (Yes/No)
- "If yes, what do you know about weather and climate?" (Open-ended)

- Section 3: Perceptions regarding climate change and its impacts

Example questions:

- "Do you agree when they say the climate has changed?" (Yes/No)

- “What change have you observed?” (Open-ended)

- Section 4: Adaptation strategies

Example questions:

- “What do you do to adapt to the impacts of climate change?” (Open-ended, multiple responses)

- “What adaptation strategies have you found to be most effective?” (Open-ended)

- Section 5: Barriers to adaptation

Example question:

- “What are the main barriers/challenges you have faced in implementing adaptation strategies?” (Open-ended, multiple responses)

This structured questionnaire design ensures comprehensive coverage of key topics relevant to farmers’ experiences with climate change and adaptation. The questionnaire was refined and incorporated into smartphones and tablets using the Open Data Kit (ODK) Collect (GetODK, San Diego, CA, USA), version v2023.3.0 (Tikito and Souissi 2021) for efficient field data collection. We applied an in-depth interview technique involving intensive individual interviews with 204 farmers from the Eastern Province. Depending on the respondent’s understanding, the interview lasted between 3600 and 5400 s. Informed consent was obtained verbally from all participants.

To further clarify the research approach, a conceptual framework (Figure 5.2) has been included to visually represent the logical flow of the study. This framework outlines how farmers’ socioeconomic characteristics and knowledge inform their perceptions and observed impacts of climate change, which in turn influence their adaptation strategies and the barriers they face. By linking each section of the questionnaire to the broader research objectives, the diagram enhances the clarity and structure of the paper. This approach aligns with established frameworks in climate change research that emphasize the progression from exposure and knowledge to perception, response, and constraints, thereby facilitating a comprehensive understanding of adaptation processes.

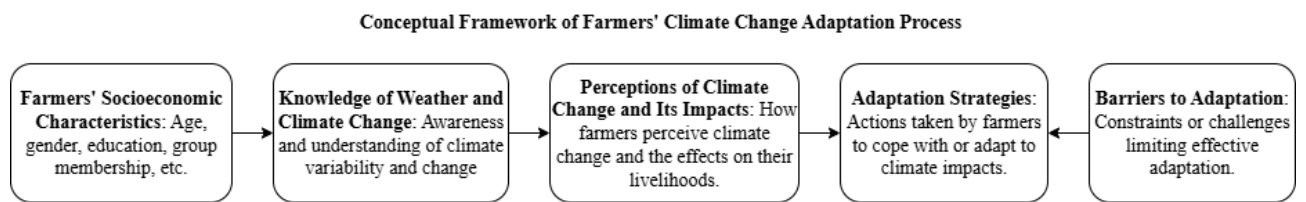


Figure 5.2 Conceptual framework illustrating the process of farmers' climate change adaptation. The framework shows how socioeconomic characteristics and knowledge of weather and climate change influence farmers' perceptions and observed impacts, which in turn shape adaptation strategies. Barriers to adaptation are also depicted as factors that constrain or modify the effectiveness of these strategies.

a. Climate Data Analysis

To analyze rainfall events, we applied the non-parametric Regional Kendall test (Helsel and Frans 2006). This test enhances the Mann–Kendall test (Mann 1945; Kendall 1975) by enabling the simultaneous analysis of trends across multiple locations while accounting for spatial correlation among datasets. It is robust against non-normal distributions and is less influenced by missing data and outliers (Partal and Kahya 2006). This enhanced capacity allows for the identification of region-wide patterns and trends, considering the interrelationships among different monitoring stations or regions. The Regional Kendall test has been widely employed to determine whether there is an increasing or decreasing trend over time in environmental and climatic data (Chen et al. 2016; Margaritidis 2021). The magnitude of the trend was quantified using the non-parametric Sen's Slope estimator, which is reliable and resistant to the influence of outliers (Xu, Takeuchi and Ishidaira 2003; Sebaziga et al. 2020; Rwema et al. 2025). Seasonal and annual changes in minimum, maximum, and mean temperatures are calculated using a dynamic linear state-space model. This model effectively captures overall changes and temporal patterns by connecting hidden states that evolve over time to observed measurements while accounting for random fluctuations (Gamerman and Lopes 2006; Petris 2010; Durbin and Koopman 2012; Laine, Latva-Pukkila and Kyrölä 2014). The construction procedure for a DLM model and estimations of model states and parameters can be found in Rwema et al. (Rwema et al. 2025), which utilizes a similar DLM model to investigate trends in air temperature across nearly homogeneous zones of the Eastern Province of Rwanda.

b. Farmers' Field Data Analysis

After collecting field data, we processed and analyzed the dataset using Microsoft Excel 2016 (Microsoft Corporation, Redmond, WA, USA), version 16.0.4266.1001, 64-bit and IBM SPSS

Statistics (IBM Corp., Armonk, NY, USA), version 28.0.0 (IBM 2021) for a comprehensive statistical evaluation. All responses were anonymized to protect participants' identities. The analysis primarily employed descriptive statistics, including frequencies, means, and percentages. A Chi-square test was conducted to explore whether a significant association exists between gender and adaptation strategies. The binary logistic model was used to examine how socioeconomic factors influence farmers' choice of adaptation strategies. As farmers utilized multiple adaptation strategies in combination, it was recommended to use a logistic regression approach to identify the determinants of farmers' choices regarding adaptation strategies (Batungwanayo et al. 2023). This approach allows for the assessment of adoption choices by categorizing the dependent variables into a binary choice: either adopted or not adopted. The binary logistic model can be expressed as:

$$Y_{ij}^* = a + \sum_k \beta_k X_k + \varepsilon_{ij}, \quad (5.2)$$

where Y_{ij}^* is the dependent variable (hidden) for a farmer i who adopts strategy j . The X_k represents independent variables (k factors that influence the farmer's decision). The a and β_k are, respectively, the intercept and the coefficient of the model, while ε_{ij} is the error term. From Equation (2), the condition for Y_{ij} is set to be

$$Y_{ij} = \begin{cases} 1 & \text{if } Y_{ij}^* > 0 \\ 0 & \text{otherwise,} \end{cases} \quad (5.3)$$

where Y_{ij} is the dependent variable (observed), indicating that the farmer i will (will not) adopt strategy j as $Y_{ij} = 1$. Therefore, the conditional probability that $Y_{ij} = 1$ is defined as:

$$\begin{aligned} \Pr(Y_{ij} = 1|x) &= \Pr(Y_{ij}^* > 0|x) = \frac{\exp(\beta_k X_k)}{1 + \exp(\beta_k X_k)} \\ &= G(\beta_k X_k), \end{aligned} \quad (5.4)$$

here, x denotes the particular value of the independent variable X_k for a specific observation being evaluated for its conditional probability, and where G is the binomial distribution (Fernihough 2011).

To obtain the marginal effects that explain the significance and the magnitude of the relationship between dependent variables (i.e., adaptation strategies) and independent variables (i.e., factors influencing farmers' choices), the derivative of Equation (4) with respect to X_k is required.

$$\frac{\partial G(\beta_k X_k)}{\partial X_k} = \Pr(Y_{ij} = 1|x) \cdot (1 - \Pr(Y_{ij} = 1|x)) \cdot \beta_k. \quad (5.5)$$

Then, the coefficients in Equation (5) are explained concerning marginal effects on odds ratios (Funk *et al.*, 2020). With $p_i = \Pr(Y_{ij} = 1|x)$ as the probability that a farmer i adopts the adaptation strategy j , the odds ratio is $\frac{p_i}{1-p_i}$, the ratio of the probability of adopting to the probability of not adopting (Lever, Krzywinski and Altman 2016).

$$\begin{aligned} \text{Odds} &= \frac{p_i}{1-p_i} = \frac{\frac{\exp(\beta_k X_k)}{1 + \exp(\beta_k X_k)}}{1 - \frac{\exp(\beta_k X_k)}{1 + \exp(\beta_k X_k)}} \\ &= \exp(\beta_k X_k); \ln \frac{p_i}{1-p_i} = \beta_k X_k, \end{aligned} \quad (5.6)$$

Various scholars, including Acquah-de Graft (Acquah 2011), Asekun-Olarinmoye *et al.* (Asekun-Olarinmoye *et al.* 2014), Kabir *et al.* (Kabir *et al.* 2016), Mubalama *et al.* (2020), Balasha *et al.* (2023), and Batungwanayo *et al.* (Batungwanayo 2023), have employed this approach to examine the factors influencing farmers' decisions regarding adaptation measures.

The model was validated using the Omnibus and Hosmer and Lemeshow tests, which assess its robustness by comparing the predictors with a model that includes only an intercept. Accordingly, it follows an asymptotic Chi-square distribution, with degrees of freedom determined by the difference between the number of variables in the predictor model and the intercept-only model (Abid *et al.* 2015). The Omnibus test should yield a significant p-value (<0.05), while the Hosmer and Lemeshow test should produce an insignificant p-value (>0.05). To evaluate the model's accuracy, we utilize the classification method, which compares the predicted scores from the model's independent variables against their actual responses recorded in the data. Consequently, the model's accuracy reflects the proportion of correctly estimated positive and negative events relative to the total number of events (Lever, Krzywinski and Altman 2016). Higher percentages indicate effective performance.

5.3. Results

5.3.1. Changes in Temperature and Rainfall Events in Eastern Province

The investigation of temperature trends has revealed a significant positive increase in annual mean temperature over Eastern Rwanda (Table 5.2). The mean annual maximum temperature showed no significant change. The mean seasonal minimum temperature demonstrated a

notable positive change across all seasons, suggesting that the observed rise in both seasonal and annual mean temperatures is mainly attributed to increasing minimum temperatures. Rainfall amounts in the Eastern Rwanda region exhibit non-significant decreasing and increasing trends during the March to May and September to December seasons, respectively (Table 5.3). The onset of the rainy season has changed significantly, starting earlier than in the past. The length of the seasons indicates an increase across the region in both periods, with a significant change noted for the September to December season.

Table 5.2 Displays changes (in °C/decade) with a 95% confidence interval in brackets [] for the averaged seasonal and annual means of Tx, Tn, and T in the Eastern Province of Rwanda from 1983 to 2021.

1983–2021			
Season	T _x	T _n	T
JF	0.22 [−0.26–0.70]	0.44 [0.17–0.73]	0.38 [0.07–0.67]
MAM	0.04 [−0.41–0.51]	0.61 [0.27–0.94]	0.433 [0.06–0.75]
JJA	0.22 [−0.07–0.51]	0.86 [0.45–1.23]	0.61 [0.24–0.94]
SOND	−0.09 [−0.56–0.36]	0.70 [0.28–1.14]	0.30 [−0.05–0.63]
Annual	0.08 [−0.34–0.44]	0.76 [0.42–1.14]	0.48 [0.16–0.82]

Table 5.3 Slope value of identified trends for rainfall events at the Eastern regional scale. The * in the results indicates that significant regional trends are observed at a 95% confidence level.

1981–2021				
Season	Rainfall Amount mm/Day/Year	Onset Days/Year	Cessation Days/Year	Season Duration Days/Year
MAM	−0.01	−0.21	0.00	0.21
SOND	0.00	−0.21 *	0.00	0.23 *

5.3.2. Socioeconomic Characteristics of Respondent Farmers

Table 5.4 presents the socioeconomic characteristics of 204 respondent farmers (heads of household) in the Eastern Province of Rwanda. A total of 57% of the respondents were male and 43% were female. The mean age of the respondents was 44 years, and they had a mean farming experience of 22 years. The mean duration of working on a farm per day was 20,160

s. The respondents exhibited a low level of education, with the majority (61%) having attended only primary school, and 17% reporting no formal education.

The farm sizes ranged from 200 to 10,000 m² for 71% of respondents, from 11,000 to 20,000 m² for 20%, and from 21,000 m² and above for 10% of respondents, with an average size of 13,000 m². Of the respondents, 48% exclusively farm on hillsides, 15% solely farm in wetlands, and 38% engage in farming activities in both hillsides and wetlands. The majority (53%) of respondents utilized inherited land for agriculture, while 17% relied on privately rented land, and 30% of respondents utilized both inherited and rented land.

The primary farming objective for the majority (68%) of the respondents was to generate income while meeting home consumption needs. Meanwhile, 30% focused solely on home consumption, and 2% aimed solely at generating income. Most respondents primarily cultivated maize (90%) and beans (89%) as their main crops. While carrying out agricultural practices, 64% of respondents are also engaged in livestock breeding, while 36% do not engage in livestock activities. A total of 37% of respondents were members of at least one farmer group, while 63% did not belong to any group. A total of 79% of respondents reported exchanging agricultural information with fellow farmers, while 21% did not. The majority (51%) of respondents lacked access to weather information, while 49% primarily accessed it through radio broadcasts. More than half (58%) of the respondents had access to banking services and had bank accounts, while 42% were not linked to any banking institution. The average household size was five people.

Table 5.4 Socioeconomic characteristics of respondents (*n* = 204).

Variables	Category	Frequency	Percentage (%)	Mean
Gender	Female	88	43	
	Male	116	57	
Age	20–34	48	24	43.66
	35–49	98	48	
	50–64	48	24	
	65–80	10	5	
Farming Experience (years)	1–20	96	47	22.18
	21–40	97	48	

	41–60	10	5	
Time on farm per day (unit is s)	≤14,400	21	10	
	18,000–28,800	167	82	20,880
	≥32,400	16	8	
	None	34	17	
Education	Primary	124	61	
	Secondary_level_1_(Senior_3)	22	11	
	Secondary_level_2_(Senior_6)	17	8	
	Technical_vocation	6	3	
	University	1	0.5	
Farm size (unit is m ²)	0–10,000	144	71	
	11,000–20,000	40	20	13,000
	>20,000	20	10	
Farm location	Hillside	97	48	
	Wetland	30	15	
	Both	77	38	
Farm ownership status	Owner	108	53	
	Tenant	34	17	
	Both	62	30	
Farming goals	Home consumption	62	30	
	Income	4	2.0	
	Both (Income and home consumption)	138	68	
Main crops	Maize	184	90	
	Beans	181	89	
	Cassava	63	31	
Livestock ownership	Yes	131	64	
	No	73	36	
Group membership	Yes	76	37	
	No	128	63	
Exchanging info	Yes	161	79	

	No	43	21	
Access to weather info	Yes	99	49	
	No	105	51	
Access to bank services	Yes	119	58	
	No	85	42	
Household size	1–5	136	67	
	6–10	65	32	5
	11–15	3	1.5	

5.3.3. Farmers’ Knowledge of Weather and Climate Change

The climate variables linked to farmers’ indigenous knowledge of critical agricultural indicators, such as the onset and cessation of rainy seasons, are presented in Table 5.5. As many as 35% of respondent farmers reported that they could predict/forecast the seasonal onset based on cloud features. For example, one farmer explained: “*As the onset of rainy season approaches, we begin to observe dark clouds circulating in the sky and experience very cold mornings while the nights grow warmer*” (farmer number 178). A total of 19% of respondent farmers claimed to have knowledge linked to the wind direction and patterns prevalent over the region. For instance, one farmer stated: “*We recognize that the onset of the rainy season is near when, around the 5th of September, we begin to experience strong winds, which we interpret as a precursor to rainfall, and we use to say that the wind is going to fetch rain, when these winds return around the 5th to 10th of October, they bring rain*” (farmer number 181). A total of 13% of respondents claim to possess knowledge related to temperature patterns. For instance, one respondent mentioned: “*One of the signs of the onset of the rainy season is that we begin to experience warmer nights, accompanied by observable changes in cloud formations in the sky*” (farmer number 84).

The farmer’s knowledge regarding the rainy seasonal cessation (Table 5.5) was mainly linked to rainfall patterns, including rainfall distribution, rainfall amount, rainfall frequency, and rainfall duration in the region. Of the respondent farmers, 46% reported that they could predict/forecast the cessation of a rainy season based on rainfall distribution. One respondent explained: “*We can tell that the rain is about to stop when we start experiencing reduced rainfall, often localized to some part of our region without extending to the whole region*”

(farmer number 116). A total of 18% of respondent farmers claimed to have knowledge linked to the quantity of rainfall. For instance, one respondent noted: *“We know that the cessation of the rainy season is near when we start experiencing reduced rainfall, which is not equivalent to the number of clouds we observed before. Sometimes, we even observe cloud formations in the sky, but they do not result in rainfall”* (farmer number 13). A total of 17% of farmers surveyed asserted that they knew about the rainfall duration. For example, one farmer explained: *“We can tell that the rain is about to stop when it starts falling for a short duration and becomes localized. It may rain in one area for a brief period, then move to another part of the region in a similar manner”* (farmer number 176). Knowledge related to rainfall frequency was reported by 11% of respondent farmers. For instance, one respondent farmer explained: *“When the seasonal rainfall is about to cease, its frequency starts to decrease. For example, it might rain on a Tuesday and then not rain again until Sunday. After Sunday, there might be another week-long gap before it rains again, continuing like this until it stops completely”* (farmer number 43).

Table 5.5 Climate indicators associated with farmers’ knowledge about rainy season onset and cessation ($n = 204$).

	Onset Skills			Cessation Skills	
	Frequency	Percentage		Frequency	Percentage
Cloud	72	35	Rainfall distribution	93	46
Wind	38	19	Rainfall amount	36	18
Temperature	27	13	Rainfall duration	35	17
Lightning	12	6	Rainfall frequency	22	11
Do not know	32	16	Cloud	16	8
			Temperature	13	6
			Wind	4	2
			Do not know	25	12

Figure 5.3 illustrates the participants’ perspectives on the causes of climate change. The majority (55%) attributed climate change to deforestation, 16% cited industrial effluents, and another 16% pointed to carbon emissions by developed countries. Additionally, 10% associated climate change with the black smoke of vehicles, while 9% linked it to the destruction of the environment. A smaller percentage (2%) attributed climate change to natural

causes or ‘God’s Plan,’ and another 2% mentioned the ocean as a factor. Notably, 32% of respondents indicated uncertainty about the cause of climate change.

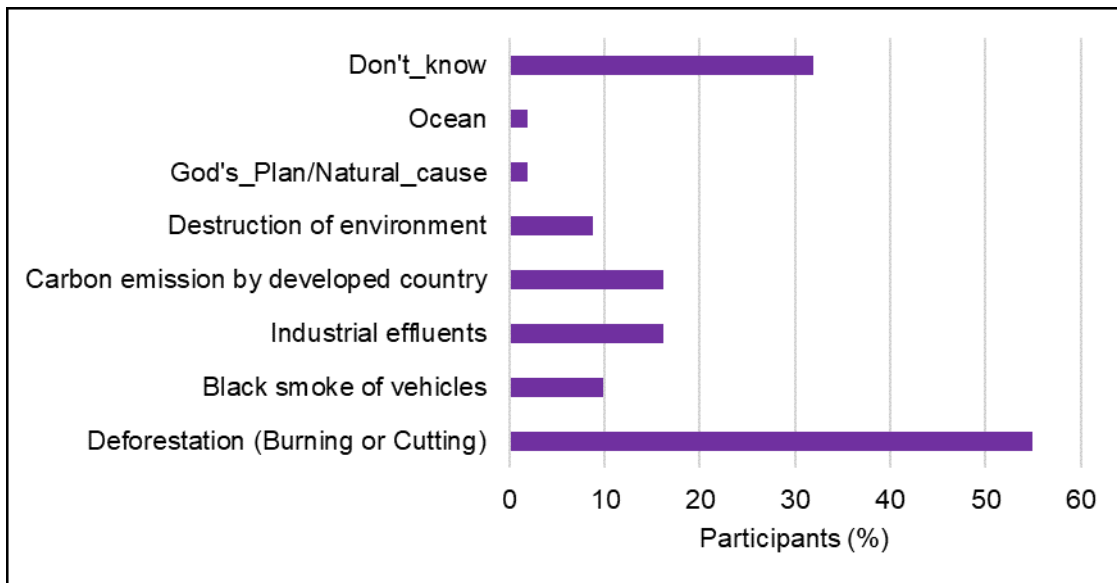


Figure 5.3 Farmers’ knowledge about causes or reasons for climate change ($n = 204$).

5.3.4. Respondent Farmers’ Perceptions of Climate Change

The perceived changes in temperature and drought among farmers are shown in Figure 5.4. Of the respondent farmers, 54% reported perceiving an increase in temperature, 47% noticed an increase in the frequency of droughts, and 41% observed an increase in the duration of droughts.

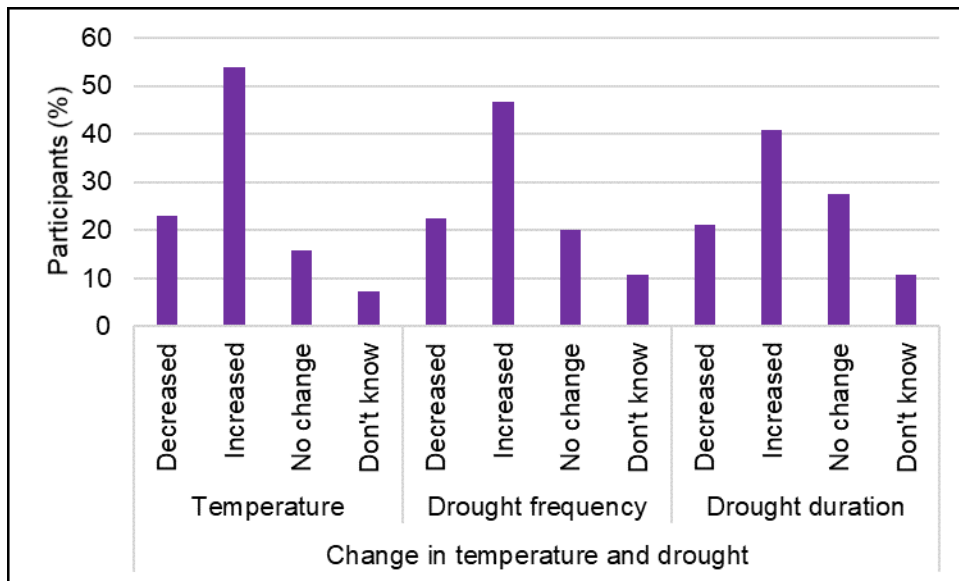


Figure 5.4 Respondent farmers’ perception of change in temperature and drought pattern ($n = 204$).

Figure 5.5 presents the farmers’ perceptions of changes in the MAM season rainfall pattern. The majority (53%) of the respondent farmers perceived a delayed onset of the MAM rainy season and an early cessation (58%), leading to a reduction in the length of the rainy season (53%) and a decrease in the amount of seasonal rainfall (49%). Figure 6 shows the perceived changes in the SON/D season’s rainfall pattern. Similarly, to the perceived change in the MAM season, as many as 39% of respondents perceived a delayed onset of the SON/D rainy season and early cessation (39%), resulting in a reduction in the length of the rainy season (41%) and a decrease in the amount of seasonal rainfall (37%).

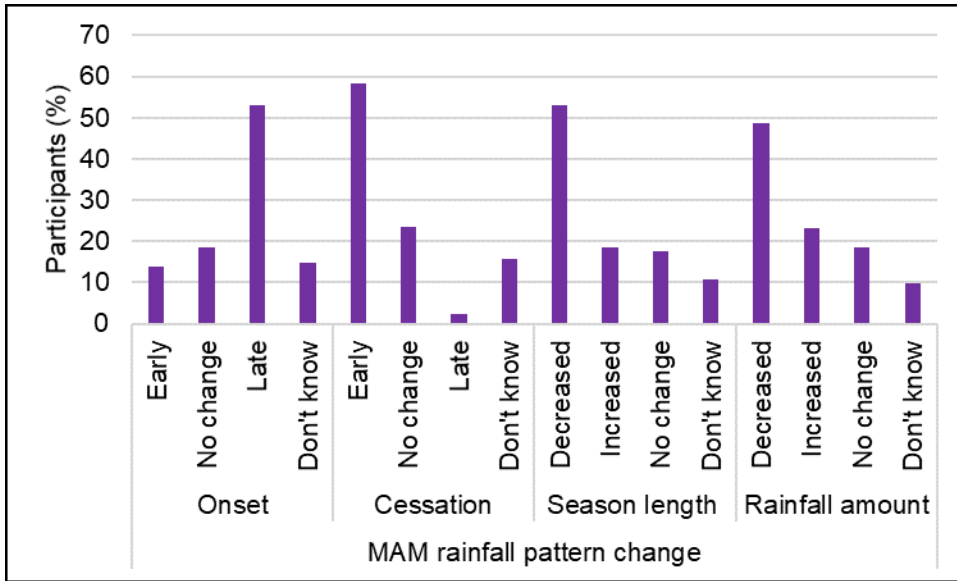


Figure 5.5 Respondent farmers' perceptions of change in the MAM season rainfall pattern.

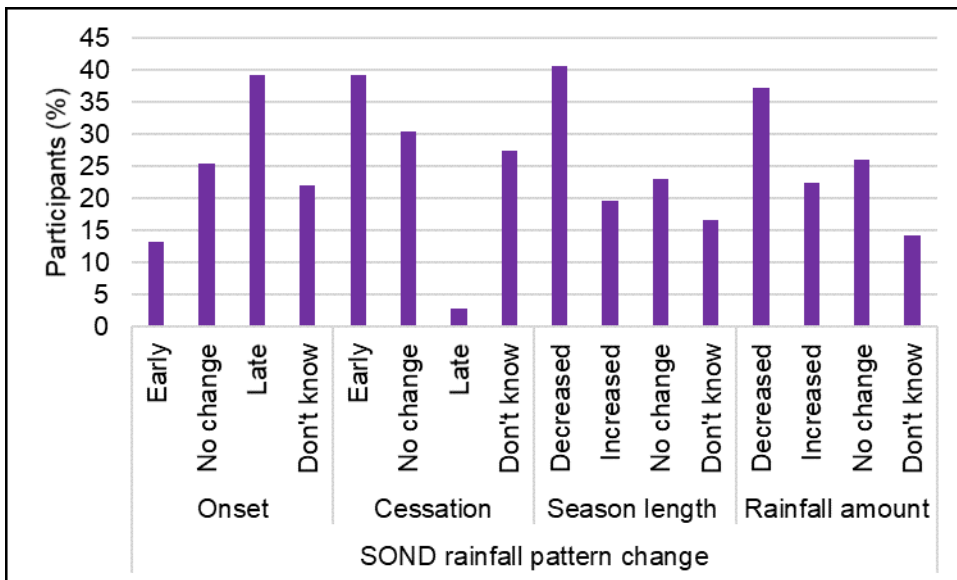


Figure 5.6 Respondent farmers' perceptions of change in the SON/D season rainfall pattern.

5.3.5. Respondent Farmers' Perceptions of the Impacts of Climate Change

Figure 5.7 illustrates the perceived impacts of climate change among the respondent farmers. The most commonly reported impact was crop failure, experienced by 56% of farmers. Other significant impacts included reduced crop yields (20%), food shortages affecting families (24%) and livestock (7%), income loss (6%), increased poverty (11%), migration (2%), and

higher food costs (1%). Additionally, 2% of farmers reported that climate variability disrupted their agricultural calendars.

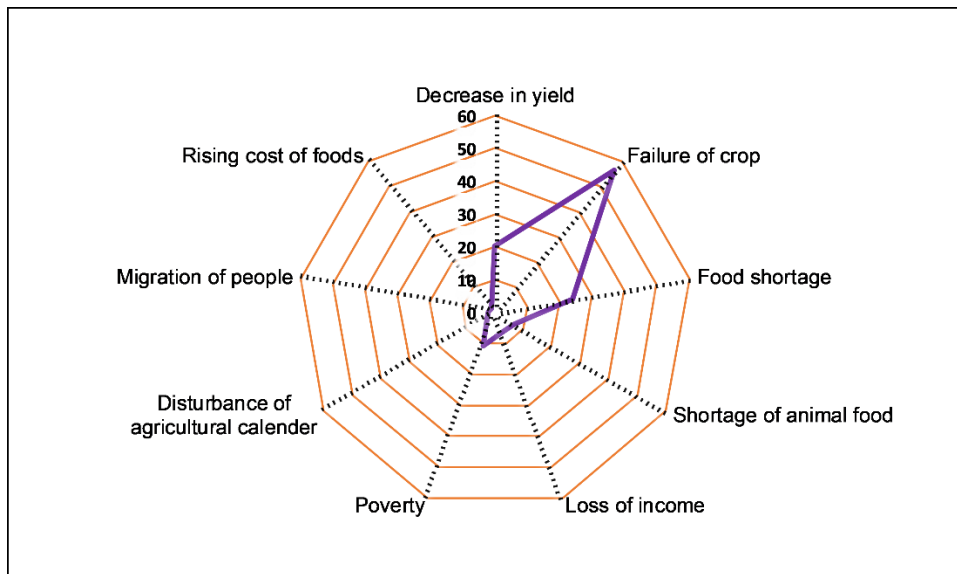


Figure 5.7 Percentage (%) of respondent farmers who perceived the impacts of climate change ($n = 204$).

5.3.6. Climate Change Adaptation Strategies

Various adaptation strategies that were applied by the respondent farmers in response to the perceived impact of climate change are presented in Table 5.6. As many as 40% of respondents reported agroforestry/planting trees, changing crop varieties (23%), application of fertilizers (23%), and changing planting dates (26%). The adoption of soil conservation (25%), use of irrigation (21%), focusing on wetlands (10%), mulching (4%), and use of pesticides (7%) were also the measures employed among the farmers.

Table 5.6 Climate change adaptation strategies adopted by respondent farmers ($n = 204$).

Adaptation Strategies	Frequency	Percentage
Agroforestry/Planting trees (PT)	81	40
Changing crop varieties (CCV)	47	23
Application of fertilizer (organic and inorganic) (AF)	47	23
Changing planting dates (CPD)	54	26

Soil conservation (SC)	50	25
Focus on wetland (FWL)	21	10
Use irrigation (UI)	43	21
Mulching (M)	9	4
Use of pesticides (UP)	15	7
Planting grass (PG)	11	5

5.3.7. Barrier to the Effective Adaptation to Climate Change

Table 5.7 presents the farmers' responses when they were asked about barriers hindering their adaptation to climate change. Of the farmer respondents, 28% cited insufficient financial capacity, 18% reported inadequate agricultural skills, and 21% indicated a lack of appropriate material for adaptation. Additionally, 12% mentioned the absence of timely weather information, 20% reported shortages of farm inputs when needed, and 2% noted challenges linked to the location of their farm. Moreover, 7% reported a lack of water sources near their farms, while 3% and 2% cited the high cost of agricultural inputs and materials, respectively.

Table 5.7 Barriers to the effective adaptation of climate change by respondent farmers ($n = 204$).

Barriers	Frequency	Percentage
Lack of finance	58	28
Inadequate info	39	19
Lack of material	43	21
Lack of weather info	24	12
Shortage of farm inputs	40	20
Lack of water	14	7
High cost of input	7	3
Land location	4	2
High cost of material	4	2

5.3.8. Socioeconomic Factors Influencing Farmers' Choice of Adaptation Strategies

Binary logistic models were used to identify the relationship between socioeconomic factors and the three most essential adaptation strategies that the farmers highlighted to be the most effective: agroforestry/planting trees (PT), changing crop varieties (CCV), and application of

fertilizer (AF). The validation diagnostics of the regression logistic models are presented in Table 5.8. In general, with the Omnibus test of the model coefficients (test of model fit), all the models indicated good fits, confirming their ability to make predictions. It indicated chi-square values ranging between 29.940 and 45.219 and significant p -values ($<\alpha = 5\%$). The results from the Hosmer and Lemeshow test (test of model fit) also confirmed how goodness-of-fit the models were, with the Chi-square values varying between 2.590 and 9.611 and no significant p -values ($>\alpha = 5\%$). Furthermore, Nagelkerke's R-squared values varying between 0.208 and 0.301 were observed. Overall, the accuracy rate of all the models was reasonable ($>66\%$). All these confirm how models were able to correctly determine how socioeconomic factors influence the farmers' choice of particular adaptation strategies for dealing with climate change impacts.

Table 5.8 Analysis of the models' significance and goodness of fit.

Omnibus Tests of Model Coefficients			
Models	Chi-square	Degree of freedom(df)	p -value
Agroforestry/Planting trees (PT)	34.026	15	0.003
Changing crop varieties (CCV)	29.94	15	0.012
Application of fertilizer (Organic and inorganic) (AF)	45.219	15	0.000
Hosmer and Lemeshow Test			
	Chi-square	Degree of freedom(df)	p -value
Agroforestry/Planting trees (PT)	5.316	8	0.723
Changing crop varieties (CCV)	2.59	8	0.957
Application of fertilizer	9.611	8	0.293

(organic and inorganic)				
(AF)				
Model Summary				
	-2 Log likelihood	Cox and Snell R Square	Nagelkerke R Square	Model correctness (%)
Agroforestry/Planting trees (PT)	240.068	0.154	0.208	66.7
Changing crop varieties (CCV)	190.278	0.137	0.207	77.5
Application of fertilizer (Organic and inorganic) (AF)	174.999	0.199	0.301	82.4

The binary logistic regression results are presented in Table 5.9. The table presents the relationship between socioeconomic factors (predictors) and selected adaptation strategies using odds ratios (OR) with a 95% confidence interval (Table 5.9). While there were notable positive correlations among various variables examined, only those that showed statistical significance were interpreted. Engaging in farming activities in both hillsides and wetlands indicated a positive relationship with adaptation strategies of changing crop varieties and applying fertilizer. Notably, a significant positive relationship was observed in the adaptation strategy of applying fertilizer with an OR of 1.926 and a 95% confidence interval ranging from 1.225 to 3.028, meaning that farmers engaged in both hillside and wetland farming are approximately 1.9 times more likely to apply fertilizer as an adaptation strategy compared to those who do not farm in both areas.

Farming to fulfill home consumption needs and generate an income from the market exhibited a positive correlation with adopting agroforestry/planting trees and changing crop varieties as adaptation strategies. Remarkably, farmers aiming to meet home consumption and generate a market income were significantly more motivated to adopt the agroforestry/planting trees adaptation strategy compared to others, with an observed OR of 1.668 and a 95% confidence interval of 1.099–2.531. Membership in farmer groups/cooperatives showed a positive correlation with all adaptation strategies, significantly influencing the changing of crop varieties and the application of fertilizer as measures for adaptation. Farmers belonging to a

group or cooperative were 2.740 times more likely to change crop varieties as an adaptation strategy than those not affiliated with any farmer group, with a 95% confidence interval ranging from 1.206 to 6.226. Similarly, farmers belonging to a group or cooperative were 3.926 times more likely to apply fertilizer as an adaptation strategy than those not affiliated with any farmer group, with a 95% confidence interval of 1.556–9.906. Access to bank services is significantly associated with lower odds of fertilizer application (OR = 0.286, with a 95% confidence interval of 0.116–0.706), suggesting that farmers with bank access are less likely to use fertilizer as an adaptation strategy compared to those without bank access.

Table 5.9 Logistic regression results: odds ratio (OR) and 95% confidence interval showing socioeconomic factors influencing farmers' choice of selected adaptation strategies.

Variables	PT	CCV	AF
Gender	0.700 [0.345–1.418]	0.477 [0.205–1.109]	0.408 [0.167–1.000]
Age	0.965 [0.915–1.017]	0.963 [0.904–1.026]	1.009 [0.951–1.070]
Education level	1.037 [0.717–1.502]	0.963 [0.629–1.474]	1.013 [0.635–1.616]
Farmer experience(years)	1.019 [0.969–1.072]	1.036 [0.977–1.099]	1.002 [0.946–1.061]
Time spent/day (Hours)	1.007 [0.810–1.252]	0.843 [0.647–1.099]	0.751 [0.553–1.020]
Farm size (ha)	0.885 [0.690–1.134]	1.013 [0.780–1.314]	0.773 [0.498–1.201]
Farm location	0.739 [0.513–1.064]	1.052 [0.697–1.587]	1.926 * [1.225–3.028]
Land-holding status	1.158 [0.803–1.670]	1.324 [0.867–2.022]	1.008 [0.638–1.591]
Farming goal	1.668 * [1.099–2.531]	1.245 [0.745–2.083]	0.770 [0.460–1.288]
Livestock ownership	1.979 [0.965–4.060]	1.250 [0.530–2.948]	1.674 [0.679–4.128]
Farmer group membership	1.587 [0.776–3.245]	2.740 * [1.206–6.226]	3.926 * [1.556–9.906]
Exchanging info	2.024 [0.770–5.320]	3.167 [0.810–12.375]	1.118 [0.321–3.895]
Access to weather info (Radio)	1.234 [0.639–2.384]	1.272 [0.592–2.732]	2.271 [0.978–5.276]
Access to bank services	0.703 [0.344–1.437]	0.494 [0.216–1.127]	0.286 * [0.116–0.706]

Household size (Individuals)	1.043 [0.893–1.218]	1.009 [0.846–1.205]	0.994 [0.818–1.208]
Constant	0.261	0.203	0.403

* shows significant levels at 0.05.

5.4. Discussion

In this discussion, both male and female farmers in this study have on average over 22 years of farming experience, indicating that both genders have been equally exposed to the adverse effects of climate change in Eastern Rwanda over the past two decades. This shared experience highlights the widespread and long-term impact of climate change on farming communities in the region. Moreover, the predominance of small-scale mixed farming, which combines crop cultivation and livestock rearing on plots averaging less than 1.3 hectares, reflects the structural constraints typical of Rwandan agriculture, as also documented by NISR (NISR 2023). Such land fragmentation may limit the adoption of resource-intensive adaptation measures, reinforcing the need for strategies tailored to smallholder realities. Additionally, the low educational attainment observed, with most respondents having only primary education or none, aligns with national statistics (NISR 2023) but raises critical concerns about the capacity to engage with complex adaptation interventions that require technical knowledge or access to extension services (IRDP 2020). This educational limitation likely constrains the effectiveness of climate adaptation strategies. Taken together, these socioeconomic characteristics highlight the multifaceted challenges facing farmers and suggest that adaptation policies must consider gender inclusivity, land size constraints, and educational support to enhance resilience effectively.

Turning to the knowledge systems, the reliance of respondent farmers on indigenous knowledge to predict local weather patterns highlights the enduring importance of traditional ecological understanding in agricultural decision-making. Their specific indicators, such as dark clouds, wind direction, and nocturnal lightning, reflect a nuanced, place-based knowledge system shaped by long-term observation and experience. This finding aligns with numerous studies across East Africa that document how farmers continue to use indigenous knowledge as a critical tool for agricultural planning and climate adaptation (Kijazi et al. 2013; Radeny et al. 2019). However, while indigenous knowledge remains valuable, its accuracy in forecasting weather is increasingly challenged by the unpredictability introduced by climate change, which disrupts historical patterns and reduces the reliability of traditional indicators (Nkomwa et al.

2014). This uncertainty underscores the need for integrating indigenous knowledge with scientific meteorological data, combining the contextual sensitivity of local observations with the predictive power of modern technology. Such integration has been shown to enhance farmers' adaptive capacity by providing more reliable and timely climate information, thereby improving resilience to environmental variability (Ziervogel and Opere 2010; Kalanda-Joshua et al. 2011; Kolawole et al. 2014; Nkuba et al. 2020). Consequently, this study not only confirms the persistence and value of indigenous knowledge but also emphasizes the importance of developing hybrid knowledge systems tailored to the evolving challenges faced by smallholder farmers.

Building on the previous findings, farmers demonstrated a clear awareness of the drivers of climate change, with deforestation identified as the most frequently cited cause, followed by industrial effluents and carbon emissions from developed countries. In addition, further factors such as vehicle emissions, environmental degradation, natural causes, and oceanic influences were also mentioned, reflecting a multifaceted understanding of climate change origins. This level of awareness suggests that farmers recognize the critical role of environmental conservation, particularly forest protection, in mitigating climate impacts. Such knowledge is significant because it can influence local engagement in sustainable practices and community-led conservation efforts. These findings align with studies from Bangladesh (Kabir et al. 2016) and Nigeria (Asekun-Olarinmoye et al. 2014), which similarly report that small-scale farmers possess meaningful, if sometimes partial, knowledge about climate change causes. Together, these insights underscore the potential for leveraging existing farmer awareness in designing targeted climate education and mitigation programs that build on local perceptions to enhance effectiveness.

Furthermore, a substantial majority (85%) of respondent farmers acknowledged that the climate has changed, reflecting a widespread awareness of shifting environmental conditions. However, their ability to articulate the underlying causes or mechanisms of these changes varied, suggesting differences in climate literacy or access to information. Many farmers specifically reported temperature increases, as well as greater frequency and duration of droughts, which are critical stressors for rainfed agriculture. Concurrently, perceptions of declining rainfall amounts and fewer rainy days during key seasons, along with shifts in the timing of rainy season onset and cessation for both the March–May (MAM) and September–December (SOND) seasons, highlight a nuanced understanding of seasonal variability.

Importantly, these farmers' perceptions are strongly supported by multiple climatological studies in Rwanda that document rising temperatures and declining rainfall trends over recent decades (Safari 2012; Mohammed, Jean and Ahmad 2016; Ngarukiyimana et al. 2021; Safari and Sebaziga 2023). In particular, research focused on the Eastern Province confirms a marked decrease in seasonal rainfall (Sebaziga et al. 2020), especially during the MAM season in southern areas (Rwema et al. 2025), alongside a pronounced upward trend in temperature (Safari and Sebaziga 2023). Similar evidence from Butera et al. (Butera, Kim and Choi 2022), who studied rice farmers in the same region, further corroborates the observed temperature increases reported by participants. The combined effect of rising temperatures and diminishing rainfall has been linked to the intensification of severe and prolonged drought events in Eastern Rwanda (Sarkodie et al. 2016; Muneza 2022; Uwimbabazi et al. 2022), thereby underscoring the tangible impacts of climate change on local agroecosystems. While the majority of farmers demonstrated awareness and willingness to adopt adaptation measures, a minority who did not perceive any climate change represents a critical group requiring targeted education and outreach to improve their understanding of climate risks and adaptive options.

Given the study's focus on farmers in the Eastern Province, a region highly vulnerable to climate change impacts such as drought (Uwimbabazi et al. 2022), it is unsurprising that participants consistently reported experiencing crop failures, reduced yields, and food shortages. Moreover, these observations, coupled with reports of increased crop diseases, decreased land fertility, and disrupted farming calendars, underscore the multifaceted and tangible challenges climate change poses to agricultural livelihoods in this region. While these impacts align with documented consequences of changing temperatures and rainfall patterns at local and regional scales (Brevik 2013; Bele, Sonwa and Tiani 2014; Balasha et al. 2023; Batungwanayo et al. 2023), the convergence of farmer perceptions with scientific findings highlights the value of local knowledge as a reliable indicator of climate stress. However, the farmers' heavy reliance on seasonal rainfall (Harvey et al. 2014) further amplifies their vulnerability, emphasizing the urgent need for adaptive strategies that can sustain agricultural productivity amid climatic uncertainty (Menike and Arachchi 2016; Balasha et al. 2023).

Turning to the question of responsibility for adaptation, the finding that only 5% of farmers viewed themselves as solely responsible, 19% assigned responsibility to the government, and the majority (75%) perceived it as a shared obligation reveals a nuanced understanding of the collective nature of climate adaptation. This distribution likely reflects recognition that

effective adaptation requires both individual initiative and systemic support, especially given the high costs associated with technologies like irrigation. Such a shared responsibility perspective aligns with the broader literature emphasizing the critical role of policy and institutional support in empowering smallholder farmers to adapt effectively. Furthermore, the reported adoption of agroforestry, changing crop varieties, and fertilizer application as key adaptation strategies demonstrates farmers' proactive engagement with climate challenges. The prominence of changing crop varieties and fertilizer use is expected, given their direct impact on the productivity of staple crops like maize and beans, which dominate the Eastern Province's agricultural landscape (Abera, Debele and Wegary 2017; Azeem 2018; Mubalama et al. 2020). Notably, the recognition of agroforestry as the most sustainable adaptation strategy reflects farmers' awareness of its long-term benefits for soil conservation, biodiversity, and socioeconomic well-being, reinforcing findings from Murthy et al. (Murthy et al. 2016) and supporting the promotion of ecosystem-based adaptation approaches.

Consistent with findings from other regions where climate change threatens agriculture, smallholder farmers in the study area employed multiple adaptation strategies simultaneously to mitigate climate impacts (Balasha et al. 2023; Batungwanayo et al. 2023; Olana Jawo et al. 2023). This multifaceted approach reflects the recognition that combining different strategies enhances overall effectiveness and resilience, as supported by the adaptation literature advocating for integrated practices rather than isolated interventions (Rajan, Manjet and Solanke 2017). Nevertheless, farmers face significant barriers that constrain their adaptive capacity. Key challenges identified include limited financial resources, inadequate access to climate and agricultural information, and shortages of appropriate technology and farm inputs. Moreover, the high cost of these inputs and technologies further exacerbates these constraints, limiting farmers' ability to implement necessary adaptations. These barriers are consistent with those reported at both the Eastern Province level and nationally in Rwanda (World Bank 2015; Butera, Kim and Choi 2022), and mirror common obstacles encountered by smallholder farmers across Sub-Saharan Africa (Bryan et al. 2009; Juana, Kahaka and Okurut 2013; Sani 2016; Mubalama et al. 2020; Olana Jawo et al. 2023).

Despite these challenges, Rwanda's government has demonstrated political commitment to enhancing agricultural resilience through targeted programs such as "Nkunganire" and "Hinga Urishingiwe", which support farmers cultivating key crops including tea, coffee, maize, and beans (World Bank 2015; MoE 2017; IRDP 2020). Specifically, the Nkunganire program

facilitates access to essential inputs for vulnerable populations while improving supply chain coordination (IRDP 2020), whereas Hinga Urishingiwe provides insurance coverage against climate-induced crop losses caused by extreme weather events (World Bank 2015). Encouraging farmer participation in these initiatives is crucial to leverage available resources and interventions aimed at sustainably strengthening resilience. This highlights the importance of aligning policy support with on-the-ground adaptation needs to overcome persistent barriers and promote effective climate-smart agriculture.

Regarding the factors influencing farmers' choice of adaptation strategies, we found that farmers working simultaneously in challenging environments such as hillsides and wetlands tend to adopt more adaptive practices, like changing crop types and increasing fertilizer use. The significant odds ratio for fertilizer application suggests that this strategy is particularly important and more commonly used among these farmers to cope with environmental or climatic challenges. Moreover, having the goal of meeting family needs and generating a market income positively and significantly influenced agroforestry/planting trees as an adaptation strategy. This finding agrees with studies indicating different socioeconomic benefits of agroforestry at farm and household levels (Murthy et al. 2016). Additionally, farmer group membership was also discovered to positively influence farmers to implement all three adaptation strategies, particularly changing crop variety and applying fertilizers, which showed a significant correlation. This is likely because group meetings provide farmers with opportunities to exchange information and share their experiences, enabling them to advise each other on the most effective adaptation measures implemented on their farms (Verhofstadt and Maertens 2014; Murthy et al. 2016; Manda et al. 2020; Habiyaemye et al. 2023).

Broadly, this study analyzes farmers' indigenous knowledge, perceptions of climate change impacts, adaptation strategies, barriers to adaptation, and socioeconomic factors influencing adaptation in Rwanda's Eastern Province. Notably, the indigenous knowledge held by farmers, including observations of cloud formations, wind patterns, and rainfall characteristics, constitutes an invaluable resource for climate adaptation. Leveraging this knowledge alongside scientific data could enhance the timeliness and accuracy of weather forecasts and adaptation advice. Therefore, integrating indigenous knowledge into climate services and extension programs presents a promising pathway to strengthen farmers' resilience to climate variability and change. Future research should focus on validating indigenous knowledge for seasonal prediction and exploring its integration with scientific methods to enhance forecasting

accuracy. Additionally, studies are needed to quantify losses from perceived impacts and assess the effectiveness of adaptation strategies. Prioritizing the incorporation of indigenous knowledge into farmers' decision-making processes, while considering the full range of adaptation strategies in relation to socioeconomic factors, will be critical for future research.

While our study included a substantial number of both male and female farmers, it was not specifically designed or powered to conduct detailed statistical comparisons between gender groups. Consequently, gender-differentiated analyses were beyond the scope of this research. However, we acknowledge that exploring differences in perceptions and adaptation strategies by gender could provide valuable insights. Therefore, we recommend that future studies with larger and more targeted samples investigate gender-specific experiences and responses to climate change in greater depth. In a similar vein, our analytical approach modeled each adaptation strategy independently using separate binary logistic regressions, which assumes that farmers' choices are uncorrelated. Nevertheless, adaptation decisions are often interdependent, with farmers adopting multiple complementary or substitutive strategies simultaneously. Ignoring these correlations may lead to biased estimates and limit the understanding of the complexity of farmers' decision-making processes. Hence, future research should consider joint modeling approaches, such as multivariate probit or count-based models, to better capture the interplay among adaptation strategies and provide more comprehensive insights into farmers' adaptive behavior.

5.5. Conclusions

In summary, the present study examined farmers' indigenous knowledge, perceptions of changes in the climate system, impacts of perceived changes, adaptation strategies employed by farmers, barriers constraining these adaptation strategies, and the socioeconomic determinants of adaptations to climate change in the Eastern Province of Rwanda. Specifically, data collected at the household level from interviews with farmers in five districts of Eastern Rwanda were analyzed, along with meteorological data from 1981 to 2021. Notably, it was observed that farmers have indigenous knowledge regarding meteorological indicators, which they use for predicting/forecasting important agricultural events such as rainy seasonal onset and cessation. Furthermore, most farmers were aware of climate change and perceived an increase in temperature and a decrease in seasonal rainfall, which corresponded to the observed change in meteorological data. Moreover, farmers identified deforestation as the most

significant cause of climate change. In terms of impacts, respondent farmers reported that the most significant consequences were crop failures, reduced yield, and food shortages.

Regarding adaptation, farmers were adopting various adaptation strategies such as agroforestry/planting trees, changing crop varieties and planting dates, application of fertilizers, soil conservation, and use of irrigation. Among these strategies, the most valuable strategies identified by farmers were agroforestry, changing crop varieties, and application of fertilizers, and their adoption was highly influenced by socioeconomic factors, including farm location, farming goal, and farmer group membership. However, findings also showed that the significant barriers that hindered farmers from adapting to climate change included limited financial capacity, lack of information (both climate and agriculture), and lack of technology and farm inputs when needed.

Recommendations drawn from this study include the following:

1. Climate research highlights significant shifts in temperature and rainfall patterns across the Eastern Province. While many farmers accurately recognize these changes in alignment with scientific findings, a considerable portion of them remain unaware or misinformed. This lack of awareness can impede the successful adoption of adaptation strategies, as understanding the nature of climate change and its implications is critical for fostering resilience. To address this challenge, it is essential for stakeholders, including government authorities, farmers, and community organizations, to take concerted action to mitigate the impacts of climate change in Eastern Rwanda. Priority should be given to capacity-building programs that educate farmers on the observed climatic shifts, their consequences, and the importance of adopting effective adaptation, mitigation, and prevention strategies. Enhancing farmers' knowledge and awareness will contribute to building resilience and promoting sustainable agricultural practices in the region.
2. We recommend that stakeholders establish a participatory framework that actively involves farmers in decision-making processes. This study reveals that farmers not only recognize climate change but also possess a deep understanding of their local climate conditions, which is vital for strengthening their resilience. Their localized knowledge is an invaluable resource that must be integrated into adaptation planning. Excluding farmers from these discussions could lead to the development of strategies that fail to address their most critical needs, thereby undermining the effectiveness and sustainability of adaptation efforts.

3. The study highlights that farmers encounter numerous challenges, particularly those linked to financial constraints. To address this, stakeholders must strengthen their collaboration with farmers to gain a deeper understanding of these difficulties. This approach will enable the development of support programs and solutions that are both cost-effective and aligned with farmers' financial realities. Efforts to improve the financial capacity of farmers are especially crucial for fostering resilience and sustainable agricultural practices in Eastern Rwanda.

4. Since adaptation methods like agroforestry have been widely embraced by farmers, it is vital for the government and other stakeholders to prioritize selecting tree species that are best suited to the soil and climatic conditions of Eastern Rwanda. Adopting this targeted approach can maximize the benefits of agroforestry, strengthening farmers' resilience by improving health, nutrition, and financial stability, all of which are influenced by the choice of tree species planted.

Beyond the scope of this study, further research endeavors could focus on validating indigenous knowledge for seasonal prediction and investigating its integration with scientific methodologies to bolster forecasting precision. Additionally, there is a need for studies to quantify the losses incurred due to perceived impacts and evaluate the efficacy of implemented adaptation strategies. Exploring the incorporation of indigenous knowledge into farmers' decision-making processes within the study area would also yield valuable insights. Given that the examination of the relationship between socioeconomic factors and adaptation strategies did not encompass all available options, future studies may seek to expand upon this investigation by exhaustively documenting the full spectrum of adaptation strategies as reported by farmers.

SI1: Supporting information for chapter 5: Questionnaire

Section 1: Socioeconomic characteristic of Farmers

1. Respondent's address:

Name(optional):	Province:	District:	Sector:	Cell:	Village:
-----------------	-----------	-----------	---------	-------	----------

2. How old are you?
3. What is your gender? (**Male or Female**)
4. What is your highest level of education?
5. How many years have you been farming?
6. How many Ares of land does your household own?
7. What is the status of the land your household uses in farming? (**owned or tenant**)
8. Where are your farms located?
9. What is the average time you spend on the farm per day?
10. What is the main crop your household grows?
11. What is your main farming goal? (**Home consumption/income/Both**)
12. How many members does your household have?
13. How many members of your household do help you in faming activities?
14. Does your household own livestock? **Yes/No**
15. If **yes**, what is the number of small and large livestock?
16. Do you belong to any farmer group/cooperative? **Yes/No**
17. Do you exchange farming information with fellow farmers outside your household?
18. Do you have access to weather/climate information?
19. Do you have a bank account?

Section 2: Farmers' knowledge of climate/weather and climate change

1. Have you heard about the weather and climate? **Yes/No**
2. If **yes**, what do you know about weather and climate?
3. Do you know the seasons we have in Rwanda? **Yes/No**
4. If **yes**, how many seasons do we have?
5. If **yes**, can you differentiate the dry and rainy seasons in terms of their names?
6. If **yes**, can you specify the start and end times of the above seasons?

7. In which rain season do we have more rainfall?
8. In which month of MAM (Itumba) and SON (Umuhindo) season do we have more rainfall?
9. How many days on average do you have rainfall in the MAM and SON seasons?
10. What do you know about the start of the rainy season (Onset)?
11. What do you know about the end of the rainy season (Cessation)?
12. How can you describe a good year/season that makes you harvest more?
13. How can you describe a bad year/season that makes you harvest less?
14. Which year can be recorded as the worst in your farming experience?
15. In which season of the above year did you suffer most (season MAM or SON or both)?
16. What was the characteristic of that year made it worse?
17. What do you understand when they say “climate change”?
18. What do you know about the cause of climate change? (**Multiple responses**)

Section 3: Changes in climate pattern

1. Do you agree when they say the climate has changed? **Yes/No**
2. If **yes**, what change have you observed?
3. Have you noticed any change in mean temperature? **Yes/No/Don't know**
4. If **yes**, how has the mean temperature changed?
5. Changes in MAM and SON seasons' variables:

MAM	SON
Have you noticed any change in MAM rainfall amounts? Yes/No/Don't know If yes , what changes were observed?	Have you noticed any change in SON rainfall amounts? Yes/No/Don't know If yes , what changes were observed?
Have you noticed any change in MAM rainy days? Yes/No/Don't know If yes , what changes were observed? Have you noticed any change in MAM onset days? Yes/No/Don't know	Have you noticed any change in SON rainy days? Yes/No/Don't know If yes , what changes were observed? Have you noticed any change in SON onset days? Yes/No/Don't know

<p>If yes, what changes were observed?</p>	<p>If yes, what changes were observed?</p>
<p>Have you noticed any change in MAM cessation days? Yes/No/Don't know</p> <p>If yes, what changes were observed?</p>	<p>Have you noticed any change in SOND cessation days? Yes/No/Don't know</p> <p>If yes, what changes were observed?</p>
<p>Have you noticed any change in the frequency of MAM Light rain?</p> <p>Yes/No/Don't know</p> <p>If yes, what changes were observed?</p>	<p>Have you noticed any change in the frequency of SOND Light rain?</p> <p>Yes/No/Don't know</p> <p>If yes, what changes were observed?</p>
<p>Have you noticed any change in the frequency of MAM Moderate rain?</p> <p>Yes/No/Don't know</p> <p>If yes, what changes were observed?</p>	<p>Have you noticed any change in the frequency of SOND Moderate rain?</p> <p>Yes/No/Don't know</p> <p>If yes, what changes were observed?</p>
<p>Have you noticed any change in the frequency of MAM Heavy rain?</p> <p>Yes/No/Don't know</p> <p>If yes, what changes were observed?</p>	<p>Have you noticed any change in the frequency of SOND Heavy rain?</p> <p>Yes/No/Don't know</p> <p>If yes, what changes were observed?</p>

6. What change that is significantly affecting your practices?
7. Which seasons do you think changed more due to climate change? (season MAM or SOND or both)
8. Have you noticed any change in drought frequency? **Yes/No/Don't know**
9. If **yes**, what changes were observed?

Section 4: Perception of Climate Change Impacts

1. What climate change impacts have you observed/faced in your farming practices? (**Multiple responses**)
2. What is the significant impact of climate change that makes you suffer the most?
3. From your experience, which sector do you perceive is more affected by climate change in the eastern province? (e.g., Agriculture, Livestock, Health...)
4. Why do you think it is the most affected?

Section 5: Climate Change Adaptation Strategies

1. What do you do to adapt to the impacts of climate change (adaptation strategies)? (**Multiple responses**)
2. What adaptation strategies have you found to be most effective in coping with the impacts of climate change on your farming practices?
3. From your experience, which sector do you perceive is more resilient to climate change over the eastern province? (e.g. Agriculture, Livestock, Health...)
4. Why do you think it is the most resilient?
5. Who should be responsible for climate change adaptation? (**Government/Citizen/Both**)
6. Do you receive information on climate change and its impacts? **Yes/No**
7. If **yes**, through which channel do you receive information on climate change and its impacts?
8. What communication channels do you prefer to receive weather and climate change information?
9. Do you have access to or receive information on the season forecast from Meteo Rwanda?
Yes/No
10. If **yes**, are the season forecasts you receive accurate?
11. If **not accurate**, which information mismatches most of the time? (e.g. onset, cessation, rainfall amount, rainy days...)
12. Do you think the forecast is given at the right time? **Yes/No**
13. If **not**, when it can be released?
14. Did you receive any training on agriculture or weather and climate information?
15. If yes, What the training received were about?

Section 6: Barriers/Challenges to Climate Change Adaptations

1. What are the main barriers/challenges you have faced in implementing adaptation strategies?
(Multiple responses)

Section 7: Priority Intervention Desired by Farmers

1. In your opinion, what interventions would be most effective in addressing the impacts of climate change on agriculture in your region?

References

Abera, T., Debele, T., & Wegary, D. (2017). Effects of Varieties and Nitrogen Fertilizer on Yield and Yield Components of Maize on Farmers Field in Mid Altitude Areas of Western Ethiopia. *International Journal of Agronomy*, 2017, 1–13. <https://doi.org/10.1155/2017/4253917>.

Abid, M., Scheffran, J., Schneider, U. A., & Ashfaq, M. (2015). Farmers' perceptions of and adaptation strategies to climate change and their determinants: The case of Punjab province, Pakistan. *Earth System Dynamics*, 6(1), 225–243. <https://doi.org/10.5194/esd-6-225-2015>.

Acquah, H. D.-G. (2011). Farmers perception and adaptation to climate change: A willingness to pay analysis. <http://ir.ucc.edu.gh/jspui/handle/123456789/4312>.

Adomah Bempah, S., & Olav Øyhus, A. (2017). The role of social perception in disaster risk reduction: Beliefs, perception, and attitudes regarding flood disasters in communities along the Volta River, Ghana. *International Journal of Disaster Risk Reduction*, 23, 104–108. <https://doi.org/10.1016/j.ijdr.2017.04.009>.

Asekun-Olarinmoye, E., Bamidele, J. O., Odu, O. O., Olugbenga-Bello, A. I., Abodunrin, O., Adebimpe, W., Oladele, Adeomi, A. A., Adeoye, & Ojofeitimi. (2014). Public perception of climate change and its impact on health and environment in rural southwestern Nigeria. *Research and Reports in Tropical Medicine*, 1. <https://doi.org/10.2147/RRTM.S53984>.

Azeem, K. (2018). The Impact of Different P Fertilizer Sources on Growth, Yield and Yield Component of Maize Varieties. *Agricultural Research & Technology: Open Access Journal*, 13(3). <https://doi.org/10.19080/ARTOAJ.2018.13.555881>.

Balasha, A. M., Munyahali, W., Kulumbu, J. T., Okwe, A. N., Fyama, J. N. M., Lenge, E. K., & Tambwe, A. N. (2023). Understanding farmers' perception of climate change and adaptation practices in the marshlands of South Kivu, Democratic Republic of Congo. *Climate Risk Management*, 39, 100469. <https://doi.org/10.1016/j.crm.2022.100469>.

Batungwanayo, P. (2023). Confronting climate change and livelihood: Smallholder farmers' perceptions and adaptation strategies in northeastern Burundi. *Reg. Environ. Change*, 23(47). <https://doi.org/10.1007/s10113-022-02018-7>.

Batungwanayo, P., Habarugira, V., Vanclooster, M., Ndimubandi, J., F. Koropitan, A., & Nkurunziza, J. D. D. (2023). Confronting climate change and livelihood: Smallholder farmers' perceptions and adaptation strategies in northeastern Burundi. *Regional Environmental Change*, 23(1), 47. <https://doi.org/10.1007/s10113-022-02018-7>.

Bele, M. Y., Sonwa, D. J., & Tiani, A. M. (2014). Local Communities Vulnerability to Climate Change and Adaptation Strategies in Bukavu in DR Congo. *The Journal of Environment & Development*, 23(3), 331–357. <https://doi.org/10.1177/1070496514536395>.

Brevik, E. (2013). The Potential Impact of Climate Change on Soil Properties and Processes and Corresponding Influence on Food Security. *Agriculture*, 3(3), 398–417. <https://doi.org/10.3390/agriculture3030398>.

Bryan, E., Deressa, T. T., Gbetibouo, G. A., & Ringler, C. (2009). Adaptation to climate change in Ethiopia and South Africa: Options and constraints. *Environmental Science & Policy*, 12(4), 413–426. <https://doi.org/10.1016/j.envsci.2008.11.002>.

Butera, T., Kim, T. K., & Choi, S. H. (2022). Determinant Factors of Rice Farmers' Selection of Adaptation Methods to Climate Change in Eastern Rwanda. *Korean J. Org. Agric.*, 30(2), 241–253.

Chen, T., Xia, G., Wilson, L. T., Chen, W., & Chi, D. (2016). Trend and Cycle Analysis of Annual and Seasonal Precipitation in Liaoning, China. *Advances in Meteorology*, 2016, 1–15. <https://doi.org/10.1155/2016/5170563>.

Christian, E. (2010). Climate Change and Global Warming: Implications for Sub-Saharan Africa. *Lwati: A Journal of Contemporary Research*, 7(1). <https://doi.org/10.4314/lwati.v7i1.61069>.

Durbin, T. J., & Koopman, S. J. (2012). Time Series Analysis by State Space Methods by Durbin and Koopman | PDF | Normal Distribution | Estimation Theory. Scribd. <https://www.scribd.com/doc/55179464/Time-Series-Analysis-by-State-Space-Methods-by-Durbin-and-Koopman>.

Fernihough, A. (2011). Simple logit and probit marginal effects in R, Working paper series. UCD Center for Economic Research, University of Dublin, Ireland. <http://www.ucd.ie/t4cms/WP1122.pdf>.

Funk, C., Raghavan Sathyan, A., Winker, P., & Breuer, L. (2020). Changing climate - Changing livelihood: Smallholder's perceptions and adaption strategies. *Journal of Environmental Management*, 259, 109702. <https://doi.org/10.1016/j.jenvman.2019.109702>.

Gamerman, D., & Lopes, H. F. (2006). *Markov chain Monte Carlo: Stochastic simulation for Bayesian inference* (2nd ed). Taylor & Francis.

Habiyaremye, N., Mtimet, N., Ouma, E. A., & Obare, G. A. (2023). Cooperative membership effects on farmers' choice of milk marketing channels in Rwanda. *Food Policy*, 118, 102499. <https://doi.org/10.1016/j.foodpol.2023.102499>.

Harvey, C. A., Rakotobe, Z. L., Rao, N. S., Dave, R., Razafimahatratra, H., Rabarijohn, R. H., Rajaofara, H., & MacKinnon, J. L. (2014). Extreme vulnerability of smallholder farmers to agricultural risks and climate change in Madagascar. *Philosophical Transactions of the Royal Society B: Biological Sciences*, 369(1639), 20130089. <https://doi.org/10.1098/rstb.2013.0089>.

Helsel, D. R., & Frans, L. M. (2006). Regional Kendall Test for Trend. *Environmental Science & Technology*, 40(13), 4066–4073. <https://doi.org/10.1021/es051650b>.

IBM. (2021). SPSS Statistics for Windows (Version 28.0.0) [Computer software]. <https://www.ibm.com/docs/en/spss-statistics/28.0.0>.

IPCC. (2014). Climate Change 2013 – The Physical Science Basis: Working Group I Contribution to the Fifth Assessment Report of the Intergovernmental Panel on Climate Change. Cambridge University Press. <https://doi.org/10.1017/CBO9781107415324>.

IPCC. (2023). Climate Change 2021 – The Physical Science Basis: Working Group I Contribution to the Sixth Assessment Report of the Intergovernmental Panel on Climate Change (1st ed.). Cambridge University Press. <https://doi.org/10.1017/9781009157896>.

IRD. (2020). Determinants of inorganic fertilizers and improved seeds along with extension services support for agricultural productivity in Rwanda. Final policy issues and recommendations. Institute of Research and Dialogue for Peace. <https://irdp.rw/wp-content/uploads/IRD%20Agri%20Final%20Policy%20brief%20Final.pdf>.

Jonah, K., Wen, W., Shahid, S., Ali, Md. A., Bilal, M., Habtemicheal, B. A., Iyakaremye, V., Qiu, Z., Almazroui, M., Wang, Y., Joseph, S. N., & Tiwari, P. (2021). Spatiotemporal variability of rainfall trends and influencing factors in Rwanda. *Journal of Atmospheric and Solar-Terrestrial Physics*, 219, 105631. <https://doi.org/10.1016/j.jastp.2021.105631>.

Juana, J., Kahaka, Z., & Okurut, F. (2013). Farmers' Perceptions and Adaptations to Climate Change in Sub-Sahara Africa: A Synthesis of Empirical Studies and Implications for Public Policy in African Agriculture. *Journal of Agricultural Science*, 5(4), p121. <https://doi.org/10.5539/jas.v5n4p121>.

Kabir, M. I., Rahman, M. B., Smith, W., Lusha, M. A. F., Azim, S., & Milton, A. H. (2016). Knowledge and perception about climate change and human health: Findings from a baseline survey among vulnerable communities in Bangladesh. *BMC Public Health*, 16(1), 266. <https://doi.org/10.1186/s12889-016-2930-3>.

Kalanda-Joshua, M., Ngongondo, C., Chipeta, L., & Mpembeka, F. (2011). Integrating indigenous knowledge with conventional science: Enhancing localised climate and weather forecasts in Nessa, Mulanje, Malawi. *Physics and Chemistry of the Earth, Parts A/B/C*, 36(14–15), 996–1003. <https://doi.org/10.1016/j.pce.2011.08.001>.

Kendall, M. G. (1975). Rank correlation methods, 4th edn. Charles Griffin & Company Limited. [http://refhub.elsevier.com/S1364-6826\(21\)00091-2/opt98UitOxCu](http://refhub.elsevier.com/S1364-6826(21)00091-2/opt98UitOxCu).

Kew, S. F., Philip, S. Y., Hauser, M., Hobbins, M., Wanders, N., Van Oldenborgh, G. J., Van Der Wiel, K., Veldkamp, T. I. E., Kimutai, J., Funk, C., & Otto, F. E. L. (2021). Impact of precipitation and increasing temperatures on drought trends in eastern Africa. *Earth System Dynamics*, 12(1), 17–35. <https://doi.org/10.5194/esd-12-17-2021>.

Kijazi, A. L., Chang'a, L. B., Liwenga, E. T., & Nindi, S. J. (2013). The use of indigenous knowledge in weather and climate prediction in Mahenge and Ismani wards, Tanzania. *Journal of Geography and Regional Planning*, 6(7), 274–279. <https://doi.org/10.5897/JGRP2013.0386>.

Kolawole, O. D., Wolski, P., Ngwenya, B., & Mmopelwa, G. (2014). Ethno-meteorology and scientific weather forecasting: Small farmers and scientists' perspectives on climate variability in the Okavango Delta, Botswana. *Climate Risk Management*, 4–5, 43–58. <https://doi.org/10.1016/j.crm.2014.08.002>.

Laine, M., Latva-Pukkila, N., & Kyrölä, E. (2014). Analysing time-varying trends in stratospheric ozone time series using the state space approach. *Atmospheric Chemistry and Physics*, 14(18), 9707–9725. <https://doi.org/10.5194/acp-14-9707-2014>.

Lever, J., Krzywinski, M., & Altman, N. (2016). Logistic regression. *Nature Methods*, 13(7), 541–542. <https://doi.org/10.1038/nmeth.3904>.

Manda, J., Khonje, M. G., Alene, A. D., Tufa, A. H., Abdoulaye, T., Mutenje, M., Setimela, P., & Manyong, V. (2020). Does cooperative membership increase and accelerate agricultural technology adoption? Empirical evidence from Zambia. *Technological Forecasting and Social Change*, 158, 120160. <https://doi.org/10.1016/j.techfore.2020.120160>.

Mann, H. B. (1945). Nonparametric Tests Against Trend. *Econometrica*, 13(3), 245. <https://doi.org/10.2307/1907187>.

Margaritidis, A. K. (2021). Site and Regional Trend Analysis of Precipitation in Central Macedonia, Greece. *Computational Water, Energy, and Environmental Engineering*, 10(02), 49–70. <https://doi.org/10.4236/cweee.2021.102004>.

Menike, L. M. C. S., & Arachchi, K. A. G. P. K. (2016). Adaptation to Climate Change by Smallholder Farmers in Rural Communities: Evidence from Sri Lanka. *Procedia Food Science*, 6, 288–292. <https://doi.org/10.1016/j.profoo.2016.02.057>.

Messner, F., & Meyer, V. (2006). Flood damage, vulnerability and risk perception—Challenges for flood damage research. In J. Schanze, E. Zeman, & J. Marsalek (Eds.), *Flood Risk Management: Hazards, Vulnerability and Mitigation Measures* (Vol. 67, pp. 149–167). Springer Netherlands. https://doi.org/10.1007/978-1-4020-4598-1_13.

Meteo Rwanda. (2023). *Climatology of Rwanda*. <https://www.meteorwanda.gov.rw/>.

Meteo Rwanda. (2024). Dataset Documentation. <http://maproom.meteorwanda.gov.rw/maproom/Summary/index.html#tabs-2>.

Mind'je, R., Li, L., Amanambu, A. C., Nahayo, L., Nsengiyumva, J. B., Gasirabo, A., & Mindje, M. (2019). Flood susceptibility modeling and hazard perception in Rwanda. *International Journal of Disaster Risk Reduction*, 38, 101211. <https://doi.org/10.1016/j.ijdr.2019.101211>.

MoE. (2017). *Strategic Programme for Climate Resilience (SPCR) Rwanda*. <http://www.fonerwa.org/sites/default/files/2021-06/SPCR.pdf>.

Mohammed, H., Jean, C. K., & Ahmad, W. A. (2016). Projections of precipitation, air temperature and potential evapotranspiration in Rwanda under changing climate conditions. *African Journal of Environmental Science and Technology*, 10(1), 18–33. <https://doi.org/10.5897/AJEST2015.1997>.

Mubalama, L. K., Masumbuko, D. M., Mweze, D. R., Banswe, G. T., & Mirindi, P. A. (2020). Farmers' Perceptions towards Climate Change, and Meteorological Data in Kahuzi-Biega National Park Surroundings, Eastern DR. Congo. *International Journal of Innovative Research and Development*, 9(6). <https://doi.org/10.24940/ijird/2020/v9/i6/JUN20055>.

Muneza, L. (2022). Droughts and Floodings Implications in Agriculture Sector in Rwanda: Consequences of Global Warming. In S. A. Harris (Ed.), *The Nature, Causes, Effects and Mitigation of Climate Change on the Environment*. IntechOpen. <https://doi.org/10.5772/intechopen.98922>.

- Murthy, I. K., Dutta, S., Varghese, V., & Kumar, P. (2016). Impact of Agroforestry Systems on Ecological and Socio-Economic Systems: A Review. *Glob. J. Sci. Front. Res.*, 16(5), 15–28.
- Nahayo, L., Nsengiyumva, J. B., Mupenzi, C., Mind'je, R., & Nyesheja, E. M. (2019). Climate Change Vulnerability in Rwanda, East Africa. *International Journal of Geography and Geology*, 8(1), 1–9. <https://doi.org/10.18488/journal.10.2019.81.1.9>.
- Ngarukiyimana, J. P., Fu, Y., Sindikubwabo, C., Nkurunziza, I. F., Ogou, F. K., Vuguziga, F., Ogwang, B. A., & Yang, Y. (2021). Climate Change in Rwanda: The Observed Changes in Daily Maximum and Minimum Surface Air Temperatures during 1961–2014. *Frontiers in Earth Science*, 9, 619512. <https://doi.org/10.3389/feart.2021.619512>.
- Nicholson, S. E. (2018). The ITCZ and the Seasonal Cycle over Equatorial Africa. *Bulletin of the American Meteorological Society*, 99(2), 337–348. <https://doi.org/10.1175/BAMS-D-16-0287.1>.
- NISR. (2023). 5th Population and Housing Census, Main Indicators Report. National Institute of Statistics Rwanda. <http://www.statistics.gov.rw>.
- Nkomwa, E. C., Joshua, M. K., Ngongondo, C., Monjerezi, M., & Chipungu, F. (2014). Assessing indigenous knowledge systems and climate change adaptation strategies in agriculture: A case study of Chagaka Village, Chikhwawa, Southern Malawi. *Physics and Chemistry of the Earth, Parts A/B/C*, 67–69, 164–172. <https://doi.org/10.1016/j.pce.2013.10.002>.
- Nkuba, M. R., Chanda, R., Mmopelwa, G., Kato, E., Mangheni, M. N., & Lesolle, D. (2020). Influence of Indigenous Knowledge and Scientific Climate Forecasts on Arable Farmers' Climate Adaptation Methods in the Rwenzori region, Western Uganda. *Environmental Management*, 65(4), 500–516. <https://doi.org/10.1007/s00267-020-01264-x>.
- Ntirenganya, F. (2018). Analysis of Rainfall Variability in Rwanda for Small-scale Farmers Coping Strategies to Climate Variability. *East African J Sci Technol*, 8(1), 75–96.

Ntwali, D., Ogwang, B. A., & Ongoma, V. (2016). The Impacts of Topography on Spatial and Temporal Rainfall Distribution over Rwanda Based on WRF Model. *Atmospheric and Climate Sciences*, 06(02), 145–157. <https://doi.org/10.4236/acs.2016.62013>.

Olana Jawo, T., Teutscherová, N., Negash, M., Sahle, K., & Lojka, B. (2023). Smallholder coffee-based farmers' perception and their adaptation strategies of climate change and variability in South-Eastern Ethiopia. *International Journal of Sustainable Development & World Ecology*, 30(5), 533–547. <https://doi.org/10.1080/13504509.2023.2167241>.

Omosho, J. B., Balogun, A. A., & Ogunjobi, K. (2000). Predicting monthly and seasonal rainfall, onset and cessation of the rainy season in West Africa using only surface data. *International Journal of Climatology*, 20(8), 865–880. [https://doi.org/10.1002/1097-0088\(20000630\)20:8<865::AID-JOC505>3.0.CO;2-R](https://doi.org/10.1002/1097-0088(20000630)20:8<865::AID-JOC505>3.0.CO;2-R).

Partal, T., & Kahya, E. (2006). Trend analysis in Turkish precipitation data. *Hydrological Processes*, 20(9), 2011–2026. <https://doi.org/10.1002/hyp.5993>.

Pecl, G. T., Araújo, M. B., Bell, J. D., Blanchard, J., Bonebrake, T. C., Chen, I.-C., Clark, T. D., Colwell, R. K., Danielsen, F., Evengård, B., Falconi, L., Ferrier, S., Frusher, S., Garcia, R. A., Griffis, R. B., Hobday, A. J., Janion-Scheepers, C., Jarzyna, M. A., Jennings, S., ... Williams, S. E. (2017). Biodiversity redistribution under climate change: Impacts on ecosystems and human well-being. *Science*, 355(6332), eaai9214. <https://doi.org/10.1126/science.aai9214>.

Petris, G. (2010). An R Package for Dynamic Linear Models. *Journal of Statistical Software*, 36(12). <https://doi.org/10.18637/jss.v036.i12>.

Radeny, M., Desalegn, A., Mubiru, D., Kyazze, F., Mahoo, H., Recha, J., Kimeli, P., & Solomon, D. (2019). Indigenous knowledge for seasonal weather and climate forecasting across East Africa. *Climatic Change*, 156(4), 509–526. <https://doi.org/10.1007/s10584-019-02476-9>.

Rajan, P., Manjet, P., & Solanke, K. (2017, December 20). Organic Mulching- A Water Saving Technique to Increase the Production of Fruits and Vegetables – Current Agriculture Research Journal. <http://www.agriculturejournal.org/volume5number3/organic-mulching-a-water-saving-technique-to-increase-the-production-of-fruits-and-vegetables/>.

Rwanyiziri, G., & Rugema, J. (2013). Climate Change Effects on Food Security in Rwanda: Case Study of Wetland Rice Production in Bugesera District. *Rwanda J. Agric. Sc.*, 1(1), 35–51.

Rwema, M., Safari, B., Laine, M., Sylla, M. B., & Roininen, L. (2025). Trends and Variability of Temperatures in the Eastern Province of Rwanda. *International Journal of Climatology*, e8793. <https://doi.org/10.1002/joc.8793>.

Rwema, M., Sylla, M. B., Safari, B., Roininen, L., & Laine, M. (2025). Trend analysis and change point detection in precipitation time series over the Eastern Province of Rwanda during 1981–2021. *Theoretical and Applied Climatology*, 156(2), 98. <https://doi.org/10.1007/s00704-024-05317-7>.

Safari, B. (2012). Trend Analysis of the Mean Annual Temperature in Rwanda during the Last Fifty Two Years. *Journal of Environmental Protection*, 3(6), 538–551. <https://doi.org/10.4236/jep.2012.36065>.

Safari, B., & Sebaziga, J. N. (2023). Trends and Variability in Temperature and Related Extreme Indices in Rwanda during the Past Four Decades. *Atmosphere*, 14(9), 1449. <https://doi.org/10.3390/atmos14091449>.

Sani, S. (2016). Farmers' Perception, Impact and Adaptation Strategies to Climate Change among Smallholder Farmers in Sub-Saharan Africa: A Systematic Review. *Journal of Resources Development and Management*, 26(0), 1.

Sarkodie, S., Rufangura, P., Herath MPC Jayaweera, & Owusu, P. A. (2016). Situational Analysis of Flood and Drought in Rwanda. 1773839 Bytes. <https://doi.org/10.6084/M9.FIGSHARE.3381463.V1>.

Sebaziga, N. J., Ntirenganya, F., Tuyisenge, A., & Iyakaremye, V. (2020). A Statistical Analysis of the Historical Rainfall Data Over Eastern Province in Rwanda. *East Afr. J. Sc. Technol.*, 10(1), 33–52.

Slovin, M. B., Sushka, M. E., & Polonchek, J. A. (1993). The Value of Bank Durability: Borrowers as Bank Stakeholders. *The Journal of Finance*, 48(1), 247–266. <https://doi.org/10.1111/j.1540-6261.1993.tb04708.x>.

Stern, R. D., Dennett, M. D., & Garbutt, D. J. (1981). The start of the rains in West Africa. *Journal of Climatology*, 1(1), 59–68. <https://doi.org/10.1002/joc.3370010107>.

Tikito, I., & Souissi, N. (2021). ODK-X: From A Classic Process To A Smart Data Collection Process. *International Journal of Interactive Mobile Technologies (iJIM)*, 15(13), 28. <https://doi.org/10.3991/ijim.v15i13.22945>.

Uwimbabazi, J., Jing, Y., Iyakaremye, V., Ullah, I., & Ayugi, B. (2022). Observed Changes in Meteorological Drought Events during 1981–2020 over Rwanda, East Africa. *Sustainability*, 14(3), 1519. <https://doi.org/10.3390/su14031519>.

Verhofstadt, E., & Maertens, M. (2014). Smallholder cooperatives and agricultural performance in Rwanda: Do organizational differences matter? *Agricultural Economics*, 45(S1), 39–52. <https://doi.org/10.1111/agec.12128>.

Wolfe, J. M., Kluender, K. R., Levi, D. M., Bartoshuk, L. M., Herz, R. S., Klatzky, R. L., Lederman, S. J., & Merfeld, D. M. (2006). Sensation & perception. <https://scholar.google.com/citations?user=QO9ARccAAAAJ&hl=en&oi=sra>.

World Bank. (2015). Climate-Smart Agriculture in Rwanda. CSA Country Profiles for Africa, Asia, and Latin America and the Caribbean Series. World Bank. <https://climateknowledgeportal.worldbank.org/sites/default/files/2019-06/CSA%20RWANDA%20NOV%2018%202015.pdf>.

Xu, Z. X., Takeuchi, K., & Ishidaira, H. (2003). Monotonic trend and step changes in Japanese precipitation. *Journal of Hydrology*, 279(1–4), 144–150. [https://doi.org/10.1016/S0022-1694\(03\)00178-1](https://doi.org/10.1016/S0022-1694(03)00178-1).

Ziervogel, G., & Opere, A. (2010). Integrating meteorological and indigenous knowledge-based seasonal climate forecasts for the agricultural sector: Lessons from participatory action research in sub-Saharan Africa. <https://idl-bnc-idrc.dspacedirect.org/items/a4b47199-a1ba-4047-a1e4-32ef2bc48c00>.

Zougmore, R. B., Partey, S. T., Ouédraogo, M., Torquebiau, E., & Campbell, B. M. (2018). Facing climate variability in sub-Saharan Africa: Analysis of climate-smart agriculture

opportunities to manage climate-related risks. *Cahiers Agricultures*, 27(3), 34001.
<https://doi.org/10.1051/cagri/2018019>.

Chapter 6 Conclusion and Future Directions

6.1. Conclusion

This dissertation provides a thorough assessment of climate trends and farmers' perceptions in Rwanda's Eastern Province, including detailed analyses of rainfall and temperature patterns, drought dynamics, and farmer knowledge and adaptation strategies. The climate trend analysis highlights contrasting yet significant changes across the province: seasonal rainfall shows spatial variability, with a notable decrease in the March-May rainy season in the south and an overall extension of the September-December season due to earlier start dates. Temperature patterns have significantly shifted, with consistent increases in minimum and average temperatures across all zones, especially after 2010. These climatic changes result in diverse impacts across microclimatic zones, influencing local drought frequency and severity. Drought occurrence varies across regions and time, with the Central zone experiencing the highest drought frequency, while the Northwestern and Southeastern zones display unique short- and long-term drought patterns. The intensification of drought over the past two decades worsens risks to water supply and food security, given the region's dependency on rainfed agriculture. Meanwhile, an examination of farmers' perceptions shows strong awareness of climate change, especially regarding rising temperatures and declining rainfall, which aligns with meteorological data. Farmers adopt various strategies such as agroforestry, changing crop varieties, and soil conservation, influenced by socioeconomic factors like location and group membership. However, challenges such as limited finances, lack of information, and poor access to inputs restrict the wider adoption of effective practices. Notably, farmers' indigenous knowledge, particularly in predicting seasonal rainfall, is a valuable asset for building resilience. Promoting participatory approaches that combine local knowledge with scientific research can help develop more appropriate and sustainable adaptation measures. Overall, these findings highlight the complex and changing nature of climate risks in Eastern Rwanda and the essential need for integrated, multi-scale approaches to climate adaptation. Recognizing both physical climate changes and the social responses of farmers provides a solid basis for designing targeted interventions that enhance resilience in the region.

6.2. Limitations and Directions for Future Research

While this research improves understanding of climate trends and adaptive capacities in Eastern Rwanda, several limitations should be recognized. Relying on precipitation-based indices such as the Standardized Precipitation Index (SPI) mainly captures meteorological drought but might miss critical hydrological and agricultural drought aspects related to soil moisture and groundwater. Data gaps, especially from 1994 to 2010 when station data were limited and satellite estimates were heavily used, could impact the accuracy of change point detection in climate trends. Cross-validation with independent datasets and alternative methods could boost confidence in these results. Future research should aim to include additional drought indices, higher-resolution hydrological and soil moisture data, and utilize advanced regional climate models to better project and understand future drought and temperature scenarios under different climate pathways. Moreover, expanding studies on farmers' indigenous knowledge, including validation and integration with scientific forecasts, could enhance the precision and acceptance of early warning systems. A thorough investigation of socioeconomic barriers to adaptation is also necessary to develop more inclusive and effective support programs. Lastly, measuring the economic and ecological impacts of drought and adaptation strategies would provide essential insights for policy-making and resilience efforts.